

Evaluation of the biophysical performance upon the integration of helper components into cationic niosomes for the treatment of both retinal and brain diseases by gene therapy approach



Universidad del País Vasco Euskal Herriko Unibertsitatea

Nuseibah Hasan Flayyeh Al Qtaish

Vitoria-Gasteiz, 2023

**Evaluation of the biophysical performance upon the
integration of helper components into cationic niosomes
for the treatment of both retinal and brain diseases by
gene therapy approach**

NanoBioCel group

Laboratory of Pharmaceutics, School of Pharmacy

University of the Basque Country UPV/EHU

Nuseibah Hasan Flayyeh Al Qtaish

Vitoria-Gasteiz, 2023

Acknowledgements for the financial support

This doctoral thesis has been supported by the Basque Country Government (Department of Education, University and Research, Consolidated Groups IT907-16). Additional funding was provided by the CIBER of Bioengineering, Biomaterials and Nanomedicine (CIBER-BBN); the intellectual and technical assistance from the ICTS “NANBIOSIS”, more specifically the Drug Formulation Unit (U10) of the Networking Research Centre of Bioengineering, Biomaterials and Nanomedicine (CIBER-BBN); initiative of the Carlos III Health Institute (ISCIII).

Acknowledgments to research groups

Authors would like to thank Hatim S.AIKhatib /department of Pharmaceutics and Industrial Pharmacy in the Faculty of Pharmacy /the University of Jordan (FP-UJ), and Walhan Alshaer /the Cell Therapy Center (CTC) /University of Jordan for the intellectual and technical support during the international internship. Authors also acknowledge SGIker (UPV/EHU) for technical and human support. Authors acknowledge Rocio Arranz, access to the cryoEM CNB-CSIC facility in the context of the CRIOMECCORR project (ESFRI-2019-01-CSIC-16) and Noelia Zamareño Francisco Javier Chichón for technical and human support for cryoEM.

Acknowledgements to the editorials

Authors thank the editorials for granting permission to reuse the published articles in this thesis. The published versions can be accessed at the following links:

- Al Qtaish, N et al. (2020). Niosome-Based Approach for In Situ Gene Delivery to Retina and Brain Cortex as Immune-Privileged Tissues. *Pharmaceutics*, 12(3), 198.
<https://doi.org/10.3390/pharmaceutics12030198> (Appendix 1)
- Al Qtaish, N et al. (2021). Sphingolipid extracts enhance gene delivery of cationic lipid vesicles into retina and brain. *European journal of pharmaceutics and biopharmaceutics*, 169, 103–112.
<https://doi.org/10.1016/j.ejpb.2021.09.011> (Appendix 2)
- Nuseibah AL Qtaish, et al. (2022). Nanodiamond Integration into Niosomes as an Emerging and Efficient Gene Therapy Nanoplatfrom for Central Nervous System Diseases *ACS Applied Materials & Interfaces* 14 (11), 13665-13677 DOI: 10.1021/acsami.2c02182

<https://pubs.acs.org/doi/full/10.1021/acsami.2c02182> (Appendix 3)

- Long-term biophysical stability of nanodiamonds combined with lipid nanocarriers for non-viral gene delivery to the retina (Under review).

International Journal of Pharmaceutics (Appendix 4)

ACKNOWLEDGMENTS

Numerous people over the years have helped me get here, so there are many people I need to thank:

Words cannot express my gratitude to my dearest supervisor Prof. Dr. Jose Luis Pedraz for giving me the opportunity to work on this thesis in his laboratory and for providing guidance and feedback throughout this project. I am extremely grateful because you took me on as a student and kept faith in me over the years. I am extremely thankful to my supervisor Prof. Dr. Gustavo Puras for offering advice and encouragement from the initial step of research. I'm proud of my time working with you.

I would like to express my special thanks to Idoia and Ilia, for their time and efforts provided throughout the years. Your useful advice and suggestions were really helpful to me during the project's completion. I would like also to thank Tania and Myriam who have given much time and effort to aid in the experimental work. Thank you for your patience and friendship. I am also grateful to my lab-mates, the group of NanoBioCel, thank you for your wonderful patience, continual support and warm humor. I am lucky to have made such great friends.

I cannot begin to express my gratitude to my parents, Hasan and Aysheh, without whom I would never have enjoyed so many opportunities. You have smiled with me during the highs of my life and cried with me through the lows. Thank you for all of the love, support, encouragement and prayers you have sent my way along this journey. To my brothers, sisters and all my family, thank you for your unconditional love and support, that has meant the world to me, I hope that I have made you proud. To my son, Seraj, you are my inspiration to achieve my dream. Without you, I would not be where I am today. You have made me stronger, better and more fulfilled than I could have ever imagined. I love you to the moon and back. I would also like to thank my dog and my cat for all the entertainment and emotional support.

Carmen and Agustin, There is no way I could ever thank you enough for being my "second" family in Vitoria. You may not be my family by blood, but you are my family by choice. You have loved me through every circumstance that came my way as one of your own, and for that, I could

not be more thankful. I have been shown an example of true, unconditional love, and it will never be forgotten.

I would also like to express my gratitude to this lovely country, Spain, and its wonderful people, I thank them for respecting people regardless of their color, gender, beliefs, education, status, race or religion, and I thank them for respecting women and supporting them to become stronger. I would also like to express my gratitude to the city of Vitoria-Gasteiz, the government of the Basque country and Spanish embassy in Jordan for all the facilities during my stay in Spain. I also express my gratitude to Jordan, my wonderful homeland, for everything it has provided me during my life, and I send my best wishes to it.

Thank You Very Much!

Glossary

ARPE-19: a human retinal pigment epithelial cell

ASO: antisense oligonucleotide

BBB: blood brain barrier

BRB: blood retinal barrier

BOB: blood-ocular-barrier

BSA: bovine serum albumin

BSCFB: blood-cerebrospinal fluid barrier

CCF: cross-correlation function

CME: clathrin-mediated endocytosis

CNS: central nervous system

CRISPR: clustered regularly interspaced short palindromic repeats

CvME: caveolae-mediated endocytosis

DAPI: 4',6-diamidino-2-phenylindole

DCM: dichloromethane

DLS: dynamic light scattering

DNA: deoxyribonucleic acid

DOTMA: 1,2-di-O-octadecenyl-3-trimethylammonium propane

DSB: double-strand break

EGFP: enhanced green fluorescent protein

EDTA: ethylenediaminetetraacetic acid

FITC: fluorescence isothiocyanate

FITC-pEGFP: fluorescence isothiocyanate labeled pCMS-EGFP

HEK-293: human embryonic kidney

HR: homologous recombination

LDV: Laser Doppler Velocimetry

MFI: mean fluorescence intensity

mRNA: messenger RNA

NHEJ: non-homologous end joining

NLS: nuclear localization signal

NPC: nuclear pore complexes

o/w: oil in water

PBS: phosphate buffered saline

pDNA: plasmid DNA

pEGFP: plasmid encoding enhanced green fluorescent protein

PS: phosphatidylserine

RISC: RNA-induced silencing complex

RME: receptor-mediated endocytosis

RNA: ribonucleic acid

RNP: Ribonucleoprotein Particle

SC DNA: supercoiled DNA

SD: standard deviation

SDS: sodium dodecyl sulfate

SV40: simian virus 40

TALEN: transcription activator-like effector nuclease

TEM: transmission electron microscopy

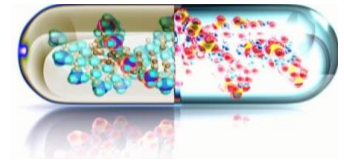
XLMTM: X-linked myotubular myopathy

ZFN: zinc finger nuclease

Index

Chapter 1. Introduction	21
1. State of the art	23
2. Methodology	34
2.1. Preparation of formulations and complexes	34
2.2. Physicochemical characterization of formulations and complexes	36
2.2.1. Size, dispersity, superficial charge and morphology	36
2.2.2. Gel retardation assay	37
2.2.3. Endosomal escape of the complexes from the late endosome	37
2.3. <i>In vitro</i> assays	37
2.3.1. Cell culture and <i>in vitro</i> transfection assays	37
2.3.2. Cellular uptake	39
2.3.3. Intracellular trafficking	39
2.4. <i>In vivo</i> assays	40
2.4.1. Animal model	40
2.4.2. Transfection assays of complexes in rat primary retinal and neuronal cell cultures	40
2.4.3. Subretinal, intravitreal and brain administration	41
2.5. Statistical analysis	41
3. Hypothesis and objectives	42
4. Results and discussion	44
5. Bibliography	71
Chapter 2. Conclusions	77
Chapter 3. Appendices I Published articles	81
Appendix 1. Niosome-Based Approach for In Situ Gene Delivery to Retina and Brain Cortex as Immune-Privileged Tissues	83
Appendix 2. Sphingolipid extracts enhance gene delivery of cationic lipid vesicles into retina and brain	131
Appendix 3. Nanodiamond Integration into Niosomes as an Emerging and Efficient Gene Therapy Nanoplatfor for Central Nervous System Diseases	159
Appendix 4. Long-term biophysical stability of nanodiamonds combined with lipid nanocarriers for non-viral gene delivery to the retina	197
Chapter 4. Resumen	219

Chapter 1



INTRODUCTION

1. State-of-the-art

Since the discovery of the gene as the fundamental unit of heredity, the ability to make site-specific alterations to the human genome has been a medical goal. Thus, gene therapy was defined as the ability to correct genetic mutations or produce site-specific changes for therapeutic purposes. This therapy was became possible by advances in genetics and bioengineering, which enabled the construction of vectors for the delivery of extrachromosomal material to target cells [1]. Gene therapy has the potential to treat a wide range of hereditary disorders. The development of nanoparticles with a unique features using advanced technologies is the initial step in delivering medications and genes to specific targets. Yet, this nanoparticle-mediated gene delivery faces significant obstacles because of its reproducibility and host cell toxicity [2].

Gene therapy involves the administration of specific genetic material (i.e., DNA or RNA) via a "vector" that permits the foreign genetic material to enter the target cells. Some gene therapies use modified forms of natural viruses as vectors, as they are an efficient way of transferring DNA or RNA into a cell. The gene therapy agent can be delivered into the body (*in vivo* gene therapy) or used to repair cells extracted from the body (*ex vivo* gene therapy), which are then reinfused. Replacement gene therapy gives a working copy of the damaged genes, to enhance the availability of a disease-modifying gene, or inhibit the production of a damaged gene. Gene therapy aims to eliminate or stop the proliferation of malignant cells to treat cancer. New “gene editing” technologies are designed to alter chromosomal DNA and correct genetic defects [3].

Concepts about gene therapy first appeared in the 1960s and 1970s, as genetically marked cell lines were being developed and methods of cell transformation by papovaviruses polyoma and SV40 were being clarified. Employing cloned genes, scientists demonstrate that foreign genes may cure genetic defects and disease phenotypes in mammalian cells. Effective retroviral vectors and other gene transfer techniques have enabled convincing demonstrations of efficient phenotypic correction *in vitro* and *in vivo* [4]. Viral vectors were used to have further development, since the early 1990s. Employing genetic engineering methods, DNA is inserted at random into the host genome throughout these processes. As for viral vectors, they have their own set of limitations due to their complexity, being potentially immunogenic, and difficulty in production.

Genome editing tools, such as zinc-finger nucleases (ZFNs), transcription activator-like effector nucleases (TALENs), and the more recently developed clustered regularly interspaced palindromic repeats/CRISPR-associated-9 (CRISPR/Cas9) technologies, were developed in the 2000s and induce genome modifications at specific target sites [5]. A wide range of disorders, including hereditary diseases and malignancies, have been treated using novel therapeutic options thanks to genome editing tools. Thus, gene therapy has become a focus of medical research. However, gene therapy creates significant ethical issues because it modifies the genetic background [6].

Vectors for gene transfer

Vectors are vehicles that transport genetic material to different cells, tissues, and organs. The ideal vector and delivery mechanism are determined by the target cells and the properties of the vector, as well as the duration of expression and the amount of genetic material included into the vector [7]. Successful delivery of therapeutic genes and adequate gene expression are required for clinically effective gene therapy. Viruses are vehicles that efficiently deliver their genes into the host cells. This characteristic made them desirable for therapeutic gene delivery. The viral vectors are evolved from RNA and DNA viruses that process genomes and host ranges. Certain viruses have been employed as vectors for gene delivery due to their capacity to transport foreign genes and their ability to successfully deliver these genes with efficient gene expression. This is why viral vectors derived from retroviruses, adenovirus, adeno-associated virus, herpesvirus, and poxvirus are used in many clinical gene therapy trials [8].

Retrovirus vectors are among the most commonly used types, as these vectors have excellent gene transfer efficiency and promote high expression of therapeutic genes. For in situ treatment, retroviruses are ideal candidates due to their ability to penetrate the nuclear pores of mitotic cells and transfect dividing cells [9]. The increasing number of clinical trials that use DNA virus vectors such as adenovirus, adeno-associated virus, or herpesvirus demonstrates the importance of these vectors for efficient gene delivery. For both *in vivo* and *ex vivo* applications, a wide range of viral vector systems have been developed [8]. There is a subclass of retroviruses known as lentiviruses. Unlike other retroviruses, lentiviruses can infect nondividing cells. Their great affinity for neural stem cells indicates that lentiviruses can be utilized extensively for *ex vivo* gene transfer in the central nervous system, with no significant immune responses and no undesired side effects [9].

Until recently, AAV gene treatment had a great record of success. However, the terrible deaths of three children during a trial to treat X-linked myotubular myopathy (XLMTM) using an AAV8 vector that promotes the expression of functional MTM1 have recently destroyed this unmatched safety record. The deaths of the three children are being widely researched, and the trial is now on hold [10].

Recent clinical trials have focused on the possible risks of using viruses to transport and integrate DNA into host cells in gene therapy. However, findings suggest that efficient, long-term gene expression can be done without the need of viruses. Additionally, recent developments provide non-viral methods for long-term gene expression. DNA can be targeted to specific genomic sites without deleterious effects, and transgenes can be maintained as small episomal plasmids or artificial chromosomes. A great number of non-viral vector products have entered clinical trials due to improvements in efficiency, specificity, gene expression duration, and safety [11]. Non-viral vectors are a simpler, less expensive, and, most importantly, safer alternative to viral vectors for gene transfer. In addition, they can be manufactured on a large scale with great reproducibility and acceptable costs, they are generally stable during storage, they can be administered repeatedly without or with minimal immunological response [12].

***In vivo* gene therapy**

Once a drug candidate demonstrates efficacy in *in vitro* experiments, drug development can be advanced by using *in vivo* models. Preclinical studies use animals to evaluate a drug candidate's safety, efficacy, and delivery. For example, anti-tumor drug candidates that showed promise in prior *in vitro* experiments are frequently screened using mouse models implanted with tumor cells. The goal of *in vivo* genetic engineering is to genetically modify somatic cells in order to treat genetic diseases, correct or disrupt mutated disease-causing genes, promote endogenous regeneration, and tackle cancer. The recent approval of several *in vivo* gene therapy products reveals that *in vivo* genetic engineering has demonstrated great potential as a novel therapeutic treatment for an ever-growing number of diseases [13]. To study and develop new drugs, many *in vivo* experimental models have been developed, but only a few accurately reproduce the physiologic responses that would occur in humans. Inbred mouse strains are most usually employed. Although hamsters and rats (primary tests), dogs and nonhuman primates (secondary and tertiary tests) have also been used [14].

***Ex vivo* gene therapy**

New advances in *ex vivo* gene therapy have pushed the field closer to the promise envisioned. These gains are largely due to vector technologies that can transduce cells without genotoxicity and improved cell treatment processes [15]. In an *ex vivo* delivery method, cells are extracted from the patient's own body (autologous) or other healthy people (allogeneic or donor). The transformed cells are then modified using genetic engineering tools outside the body, purified, enriched, and/or activated before being transplanted back into the patient. These altered cells then replicate and spread in the body. The *ex vivo* technique permits the delivery of a gene or genes to a specific cell subpopulation without damaging other cells or organs; nevertheless, the vectors used must be capable of integrating genetic material into the genome for long-term clinical efficacy. Most *ex vivo* therapies use autologous cells, with few exceptions. Autologous cells are less likely to cause immunological reactions than allogeneic cells [16].

Gene editing

Genome editing tools based on engineered or bacterial nucleases have enabled the direct targeting and modification of genomic sequences in almost all eukaryotic cells. Genome editing has demonstrated tremendous potential in a variety of domains, including basic research, applied biotechnology, and biomedical research. Which has enabled us to develop more specific cellular and animal models of pathogenic processes, and improved our understanding of how genetics affects disease. Recent advances in the development of programmable nucleases, such as zinc-finger nucleases (ZFNs), transcription activator-like effector nucleases (TALENs), and clustered regularly interspaced short palindromic repeat (CRISPR)–Cas-associated nucleases, have greatly accelerated the transition from concept to clinical practice of gene editing [17]. The edition mechanism consists of a double-strand break (DSB), achieved by different techniques that are classed in two groups depending on the usage or not of a homologous DNA sequence as a template, repair through non-homologous end joining (NHEJ) and homologous recombination (HR) that requires a homologous DNA sequence [18].

Biological barriers

Gene delivery systems need to be capable of overcoming biological barriers in order to be active at the site of action. For *ex vivo* gene delivery systems, only intracellular obstacles can limit

their final performance. While in the case of *in vivo* experimentation, the delivery process to the site of action may also be effected by additional extracellular barriers. The route of administration and the organ to be treated can have a large impact on the efficacy of the treatment [19].

Extracellular barriers

Regardless of how vectors are administered *in vivo*, it will invariably come into touch with the extracellular environment. Multiple variables in the extracellular environment can cause vector clearance and/or destruction before it ever reaches the target organ. It has been demonstrated that intravenously administered naked DNA has a short serum half-life, ranging from 1.2 to 21 minutes depending on the DNA's topology. Endo and exonuclease activity in the plasma is believed to be responsible for this. Intramuscular injections of plasmid DNA have resulted in similar degradation. However, DNA that is able to evade nucleases is also exposed to proteins and cells in the external environment. In addition, DNA delivery vehicles also come into contact with blood cells, which is an essential consideration. Erythrocytes, leukocytes, macrophages, and platelets have negative surface charges, permitting electrostatic interactions with cationic vectors.

The activation of the immune system is yet another extracellular barrier that should be considered. Although immune activation has been most commonly linked with viral gene delivery, it has been demonstrated that some non-viral approaches can also produce an immunological response [20]. Physicochemical characteristics such as zeta potential, particle size distribution, polydispersity index, or hydrophobicity/hydrophilicity balance can also contribute to immune system compatibility in the case of genetic material delivered by non-viral vectors [21]. In addition, biomacromolecules can be phagocytosed by macrophages, the bacterial origin of their components can provoke cellular and humoral immune responses, which can affect their final performance and safety profile after administration [22]. Moreover, the time needed to reach therapeutic concentrations by the transfection process, can be even more difficult if immune-privileged organs like the brain and eye are the target. Nanoparticles should efficiently cross the blood-brain barrier and blood-retinal barrier to reach the target cells in the brain and eye, respectively [23, 24]. Figure 1 shows a basic schematic representation of extracellular barriers.

Intracellular barriers

As extracellular barriers have been crossed, biomacromolecules still need to reach significant concentrations at cytoplasmic or even nuclear levels, ideally only on the target cells, in order to be biologically active. Nanomaterials should have appropriate biological and physical features to improve uptake by cytoplasmic membranes. The internalization pathway has two subtypes, phagocytosis and pinocytosis. Non-viral vectors can use multiple uptake pathways together to enter cells, although some lead to degradation if uptake is higher than treatment efficiency [23]. There are different mechanisms of endocytosis that are generally classified as follows: Main energy-dependent uptake pathways of the cell. Macropinocytosis forms macropinosomes that could finally join the early endosomes. Clathrin-mediated endocytosis (CME) and caveolin mediated endocytosis (CVME) are the main receptor-mediated endocytosis (RME) processes [25]. The interaction of an agonist with its receptor triggers the formation of clathrin-coated endocytic vesicles. The vesicle internalizes, loses its clathrin coat, and unites with other vesicles to create an early endosome, which later fuses with a lysosome [26]. Caveolin vesicles are generated and connect with other caveolin vesicles, resulting in multicaveolar structures called caveosomes that fuse with early endosomes in a bidirectional way. From this point, the vesicular structures can move to the smooth endoplasmic reticulum or to the Golgi-trans network depending on the cell type [27]. It has considered that CME, CvME, and macropinocytosis are associated with lysosomes, where the acidic pH destroys DNA. Thus, the transfection process is strongly affected. As the 'end-point' of the endocytic pathway, lysosomes have a highly acid lumen with hydrolases/lipases for protein/lipid degradation and recycling of external and intracellular components [28].

In order to prevent the breakdown of vectors and genetic material, endosomal escape is required prior to endosomal-lysosomal fusion. For siRNA to reach the RNA-induced silencing complex (RISC), as well as for ASOs to reach the target mRNA, nanoparticles need to move fast and properly through the cytosol. The nuclear membrane's impermeability is a challenge for plasmids, RNPs, and some ASOs that target pre-RNA [29, 30]. Due to restricted diffusion through nuclear pore complexes (NPC) at the nuclear membrane, nuclear localization is more difficult than intracellular localization [31]. Passive diffusion allows only very small NPs of less than 50 kDa and less than 10 nm in size to enter the nucleus, while macromolecules larger than 50 kDa can

only enter via the nuclear localization signal (NLS) sequence-mediated active transport [32,33]. Once within the nucleus, or even earlier during cytoplasmic trafficking, biomacromolecules must be split from gene delivery systems, to gain entry into the target cell's transcriptional machinery and cause the desired biological function [34]. Figure 1 shows a basic schematic representation of intracellular barriers.

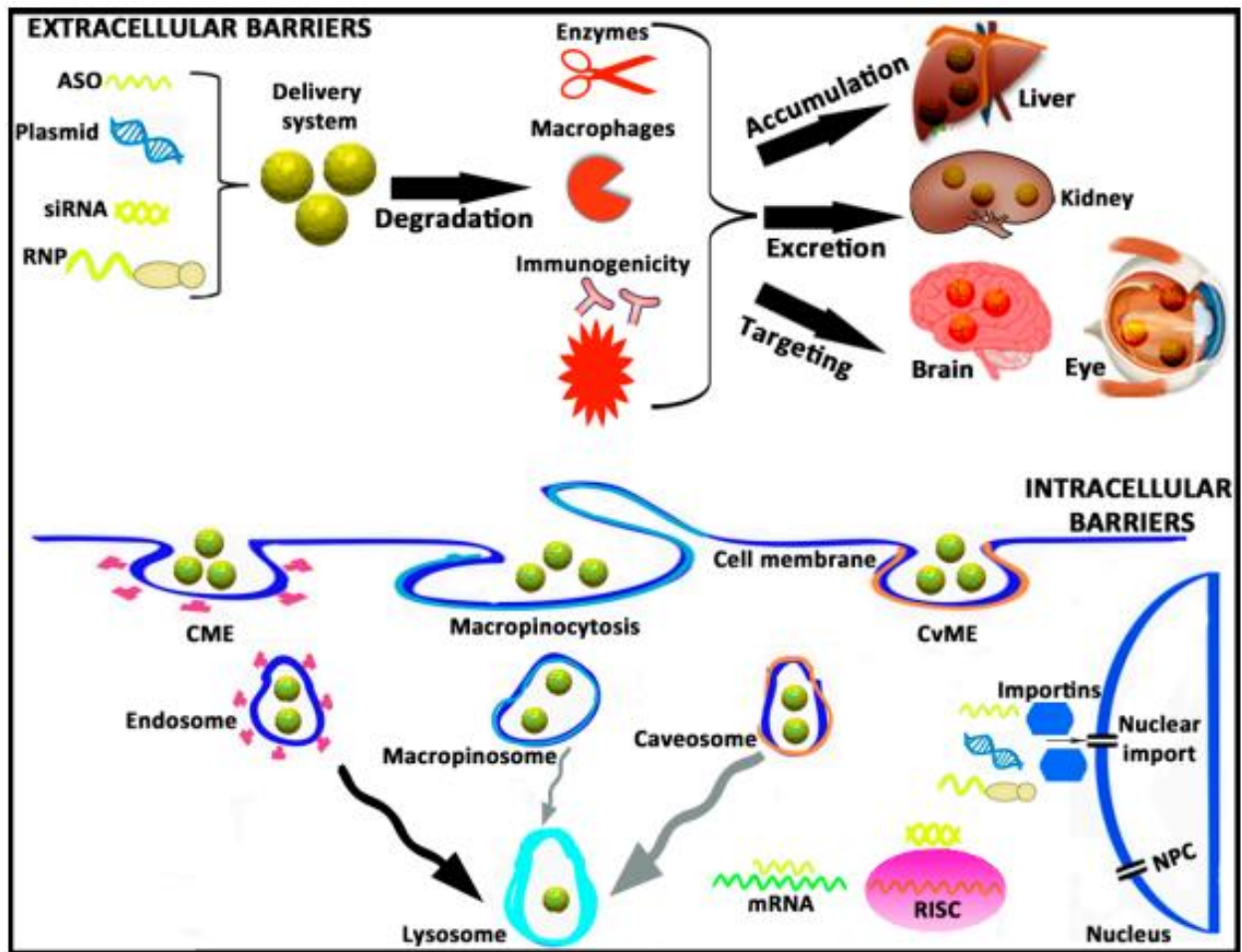


Figure 1: A basic schematic showing extracellular and intracellular hurdles that genetic material faces during transfection. ASO, antisense oligonucleotide; siRNA, small interfering RNA; RNP, ribonucleoprotein; CME, clathrin-mediated endocytosis; CvME, caveolae-mediated endocytosis; RISC, RNA-induced silencing complex; mRNA, messenger RNA; NPC, nuclear pore complex. Copyright 2019, Elsevier B.V and Al Qtaish N et al [35].

Non-viral gene delivery systems

The most essential considerations in gene therapy are the introduction of the gene into the cell and the improvement of transfection efficiency. Due to their hydrophilic properties and large size, naked DNA molecules can't enter the cell. Moreover, nuclease enzymes can also break them up easily. So, the main challenge in gene therapy is developing physical mechanisms to assure gene transfer of vectors and transmitted gene to the target cells [36]. In an effort to provide an alternative to systems based on viruses, non-viral gene delivery methods have been developed. Physical or chemical preparations classify non-viral systems. In a broad sense, the concept "physical techniques" refers to the process of delivering the gene by increasing the permeability of the cell membrane by use of external physical force. The terms "microinjection", "electroporation", "gene gun", "ultrasound" and "hydrodynamic applications" refer to some of the most frequent types of physical methods. Chemical methods, on the other hand, involve the utilization of natural or manufactured carriers in order to transport genes into cells. As gene delivery systems, this method takes use of polymers, liposomes, dendrimers, and cationic lipid systems [37].

Niosome nanoparticles for gene delivery

Understanding the basic structural units of niosome may help determine which substances can form niosome as well as how drugs can be loaded into niosome. Niosomes are bilayer structured non-ionic surfactant vesicles, hydrophilic heads are orientated toward an aqueous solution, while hydrophobic heads are orientated toward an organic solution, and therefore niosomes can deliver both hydrophobic and hydrophilic drugs [38]. Niosomes are a suitable alternative to liposomes. The drug-loaded niosome can give a higher degree of tissue-specific targeting and sustained drug release to the target. Niosomes are biodegradable, biocompatible, and non-immunogenic. They have an extended shelf life, display great stability, and provide the regulated and/or sustained administration of encapsulated molecules to a target site [39]. As Gene delivery system, niosomes consist of three components: non-ionic surfactants, cationic lipids, and, if necessary, "helper" components [40]. As carriers for genes or hydrophilic/hydrophobic medicines, non-ionic surfactants are safe, with affordable cost and they are necessary to stabilize emulsions, preventing the formation of particle aggregates [41]. In addition to non-ionic surfactants, niosomes contain one or more cationic lipids, permitting nucleic acids to be complexed

to cationic niosomes by simple electrostatic interactions [42]. Cationic lipids have become known as one of the most versatile tools for the delivery of DNA, RNA and many other therapeutic molecules, and are especially attractive because they can be easily designed, synthesized and characterized. Most of cationic lipids share the common structure of cationic head groups and hydrophobic portions with linker bonds between both domains. The linker bond is an important determinant of the chemical stability and biodegradability of cationic lipid, and further governs its transfection efficiency and cytotoxicity [43]. Regarding the helper components, it has been suggested that they are responsible for improving the physicochemical properties of the emulsion and gene delivery [44]. However, the mechanisms that are involved in these advancements in cationic niosome formulations for gene delivery applications have not been fully understood, and additional research that is more in-depth is required [45].

Different methods, including ether injection, sonication, and microfluidics, are used to form niosomes [46]. The solvent-evaporation method is an easy way to prepare niosomes. In this procedure, the non-ionic surfactant is introduced to the aqueous phase, while cationic lipids and "helper" components have been dissolved in a small volume of organic phase. An emulsion is formed after a brief duration of sonication. The organic solvent in such an emulsion can be evaporated by leaving it under magnetic agitation for some time, which will result in the resuspension of the niosome vesicles into the aqueous phase [47]. Schematic of niosome components and solvent evaporation process is shown in the figure 2.

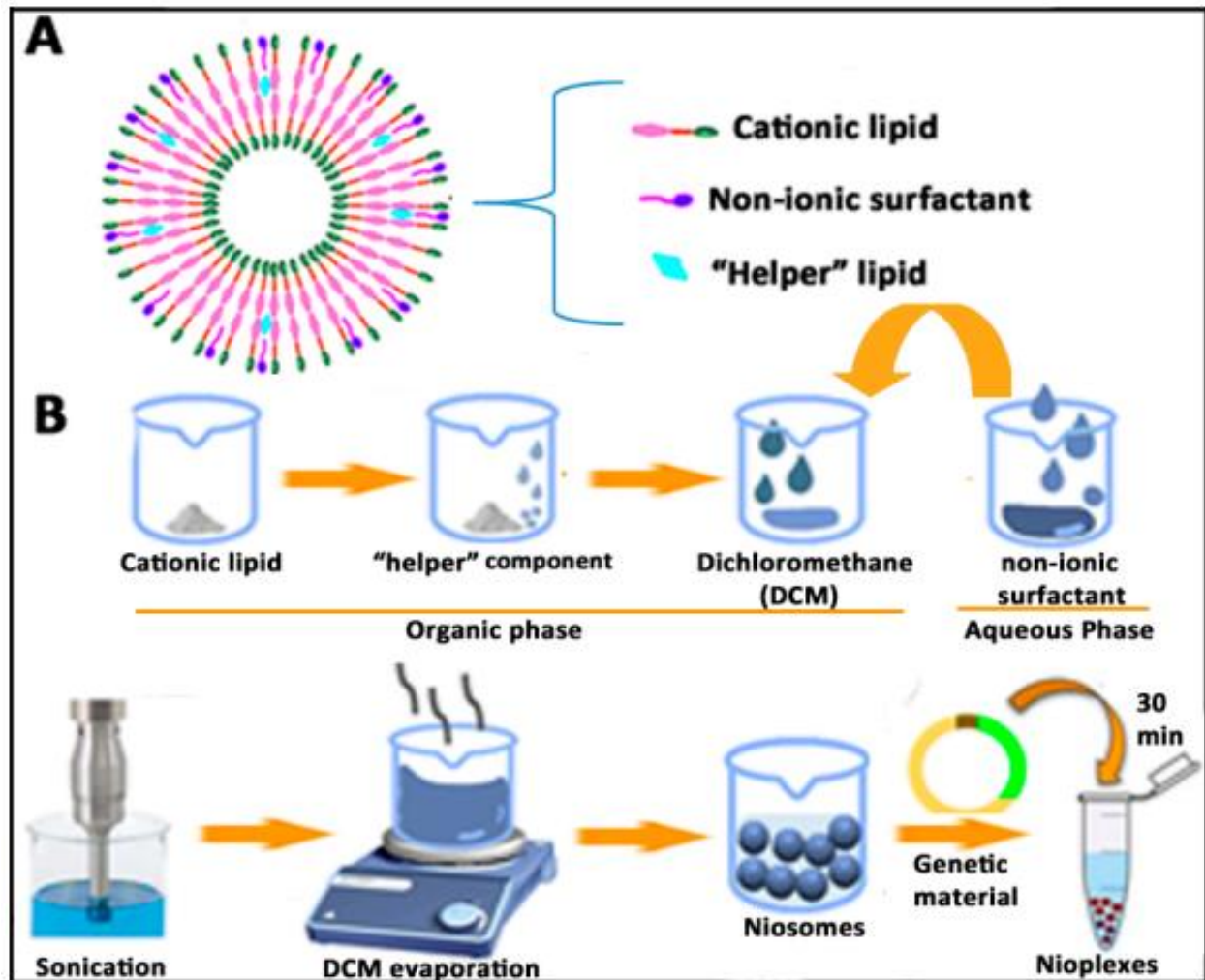


Figure 2: A) Bilayer structure of niosomes and disposition of components. B) Schematic representation of the solvent evaporation method for the elaboration of niosomes and corresponding nioplexes. Copyright 2019, Elsevier B.V and Al Qtaish N et al [35].

The related nioplexes can be obtained once the niosomes have been prepared, and then a solution containing the appropriate genetic material is added to a colloidal suspension of the niosomes. As a result of electrostatic interactions between the positively charged amine groups of the cationic lipids and negatively charged phosphate groups of the nucleic acid, nioplexes are obtained [48].

Gene delivery to the eye

In the past two decades, gene therapy has made big progress in treating inherited and previously incurable diseases. The goal among all gene therapy approaches is to modify the expression of proteins by the target cells through an inserted foreign DNA fragment into host cells.

The eye is a good target for genetic therapy since it is immune-privileged, easily accessible, and affected by inherited illnesses. The retina is suggested for gene therapy because it can be easily visualized; it lacks lymphatic veins and an outer blood network, and its cells do not proliferate after birth, therefore, transgenic expression is not affected [49]. Gene delivery strategies for eye diseases extend from eye drops and ointments to mucoadhesive systems, polymers, liposomes, and ocular implants. Most of these technologies were designed for front-of-the-eye ophthalmic therapy [50]. When the systemic delivery method is employed to target the eye, non-viral vector/DNA complexes need to be able to pass across the blood-ocular-barrier (BOB) in order to reach the ocular tissue. The BOB has tight epithelial connections, making this difficult. Using vectors smaller than 100 nm and ligand-equipped vectors that recognize BOB receptors are two ways to overcome this limitation. Therefore, even though the intravenous route provides the delivery of larger volumes of the formulations and also repeated administrations, the therapeutic efficacy reached by this strategy is usually limited by the obstacles that limit access to the eye. This is the case even if the intravenous route permits the delivery of larger quantities of the formulations. intravitreal, subconjunctival and subretinal injections can bypass some of these barriers and are now considered to be the most common and effective ways of gene delivery to retinal ganglion cells and inner retinal layers [50]. To begin with, ocular tissue barriers such as the cornea, conjunctiva, sclera, and choroid all include epithelial tight junctions, proteoglycan matrices, and fibril collagen networks that prevent vector/DNA complexes from reaching the retina. Finally, the vitreous, an aqueous biogel consisting of collagen, hyaluronan, and proteoglycans, prevents retinal cell transfection. Methods such as using vectors of proper size, particular ligands, and mucoadhesive polymers are all examples of strategies that can be utilized in order to overcome the challenges posed by these obstacles [50].

Gene delivery to the brain

CNS anatomy and physiology make gene delivery difficult. The blood-brain barrier (BBB) protects the CNS against macromolecular drugs and over 98% of small molecule drugs [49]. The blood-cerebrospinal fluid barrier (BCSFB), constituted of choroid plexus epithelial cells, protects the spinal cord as part of the CNS [51]. Essential nutrients, such as glucose and amino acids, are transported into the CNS via BBB and BSCFB receptors. Neurons are distinct cell type within the CNS, they are difficult to transfect due to their post-mitotic nature, complicated structure, and

neural networking. Most attempts to cross the BBB following systemic administration of non-viral vector/DNA complexes employ receptor mediated absorption of transferrin (Tf), lactoferrin, and insulin, since their receptors are expressed on numerous cell types, including neurons and BBB capillary endothelial cells [51]. By adding a ligand to the non-viral delivery method, the vector/DNA combination can be transported to the CNS. Another method, known as the "Molecular Trojan Horse," employs peptidomimetic monoclonal antibodies that are designed to target specific receptors on the BBB and induce receptor-mediated transcytosis of the non-viral delivery system into the CNS. [52] This method uses peptidomimetic monoclonal antibodies. Other methods for systemic CNS distribution of traditional pharmaceuticals include transitory mechanical disruption of the BBB and RNAi-mediated silencing of tight junction proteins [51]. The most clinically acceptable method for CNS gene therapies is systemic administration. But because there are so many extracellular hurdles that vectors have to get through, recent studies have tried various administration strategies. Several pre-clinical investigations have tried brain injections or infusions. Even though local administration to the brain avoids extracellular barriers to the CNS, brain surgery to infuse a gene therapy vector limits its therapeutic application.

To summarize, gene therapy is becoming a viable option for treating genetic disorders. The advent of nanomedicine offers new opportunities for the development and use of non-viral vectors, like as niosomes, to treat both retinal and brain diseases. To this purpose, the incorporation of novel compounds into formulations and the selection of the most appropriate method for niosome elaboration, as well as an extensive biophysical characterization, *in vitro* and *in vivo* testing, may enable new possibilities and chances to enhance the treatment of various diseases through the use of a gene therapy strategy.

2. Methodology

2.1. Preparation of formulations and complexes

For the elaboration of niosomes, there are various well-described methods. The oil in water (o/w) emulsion technique is one of the most commonly used methods, and we used it to prepare the formulations in this doctoral thesis. In general, the cationic lipids and "helper" components are dissolved in a small volume of organic phase, followed by the addition of the aqueous phase containing the non-ionic surfactant. After a brief time of sonication, an emulsion is produced. This

will result in the resuspension of niosome vesicles in the aqueous phase. The following chemical reagents were used in this doctoral thesis: The cationic lipid employed was DOTMA, which was dissolved in the organic phase. Polysorbate 20 was chosen as a non-ionic surfactant for these formulations. As "helper" components, we used nanodiamonds and sphingolipids in our formulations. In the first experimental work, we introduced animal-derived sphingolipids as a "helper" component into niosome formulations to evaluate their biophysical properties as a gene delivery system. We compared two non-viral vector formulations based on cationic niosomes composed of the same cationic lipid and non-ionic surfactant, but with or without sphingolipids as a "helper" component, resulting in niosphingosomes or niosomes, respectively. We evaluate both formulations to determine the effect of the addition of the "helper" component on the gene delivery system. In the second experiment, nanodiamonds were incorporated as a "helper" component into niosome formulations in order to assess their biophysical capabilities as a gene delivery system. We examined two non-viral vector formulations based on cationic niosomes with or without nanodiamonds as a "helper" component, resulting in nanodiasomes or niosomes, respectively. To determine the effect of the addition of the "helper" component on the gene delivery mechanism, both formulations were evaluated. These resulting formulations were also used in the third experimental work to study their stability. The effect of the incorporation of nanodiamonds into niosome formulations was evaluated over time at different periods of time (0, 15 and 30 days) and storage temperatures (4°C and 25°C). Composition of each formulation in this thesis is shown in

Table 1.

Components Formulations	cationic lipid DOTMA	Non-ionic surfactant Polysorbate 20	"helper" component	
			Sphingolipids	Nanodiamonds
Niosomes	✓	✓		
Niosphingosomes	✓	✓	✓	
Nanodiasomes	✓	✓		✓

Table 1: Overview of the formulations components employed in these experimental studies.

The pCMS-EGFP plasmid (pCMS-EGFP, 5541 bp, average MW 3657060 g mol⁻¹) enhanced green fluorescent protein called pEGFP is used as a reporter in all experimental works of this doctoral thesis. The pCMS-EGFP plasmid was propagated with *Escherichia coli* DH5- α

and purified with the Maxi-prep kit, and the resulting pDNA was measured at an absorbance of 260 nm. The plasmid was added to niosomes, niosphingosomes or nanodiasomes at various cationic lipid/DNA mass ratios (w/w) to generate complexes. A 30 minute room temperature incubation period before use enable the cationic lipid and genetic material amine groups to better electrostatic interactions, which resulted in the formation of complexes. The mass ratio of cationic lipid to DNA varies depending on the volume of the niosome formulations and DNA stock solution used. The ratios used in the first experimental work for the complexes obtained upon the addition of plasmid DNA were 3/1, 7.5/1 and 15/1 cationic lipid/DNA and they were 2/1, 5/1, 10/1, and 15/1 cationic lipid/DNA mass ratios in the second experimental work. Plasmid pCMS-EGFP labeled with fluorescence isothiocyanate (FITC) has been used for tracking studies (FITC-pEGFP).

2.2. Physicochemical characterization of formulations and complexes

2.2.1. Size, dispersity, superficial charge and morphology

After formulations elaboration and prior to conducting any biological experiments, the most relevant physicochemical properties involved in the nucleic acid delivery of formulations are evaluated as a screening method to determine the optimal composition and concentration of the chemical components. The Zetasizer Nano ZS was used to evaluate particle size, dispersions, and surface charge, which employs Dynamic Light Scattering (DLS) to measure particle size and dispersions and Laser Doppler Velocimetry (LDC) for zeta potential. In the third experimental work, both formulations were subjected to physicochemical characterization for stability study. As a result, at 0, 15, and 30 days after storage at 4°C and 25°C. For each formulation, zeta potential, particle size, and dispersion were analyzed. While various microscopic techniques can be used to examine the morphology and distribution of niosome colloidal dispersions. Transmission electron microscopy (TEM) is used to study formulations morphology. In the second and third experimental works, additional Cryo-tomography-based microscopy investigations were conducted to investigate the distribution of nanodiamonds within nanodiasomes.

2.2.2. Gel retardation assay

Agarose gel electrophoresis experiment was used to evaluate the ability of complexes to condense, protect, and release the genetic material. Samples were put directly into a 0.8% agarose gel to evaluate the formulations DNA binding ability. After 30 minutes of incubation at 37 °C, 4 µL of DNase I enzyme and 6 µL of 10% sodium dodecyl sulfate (SDS) were added and incubated for another 10 minutes at room temperature to evaluate the DNA protection capacity of formulations. The same amount of SDS was added to the samples and incubated for 10 minutes at RT to evaluate the DNA release from the complexes. As a control, 200 ng of naked DNA was utilized. The agarose gel was immersed in a Tris-acetate EDTA solution and subjected to electrophoresis for 30 min at 120 V after the addition of 4 µL of loading buffer per sample. GelRed reagent was used to colorize the DNA bands, which were then visualized with a ChemiDoc MP Imaging System and analyzed with Image Lab Software.

2.2.3. Endosomal escape of the complexes from the late endosome

Endosomal release of the pDNA is one of the most crucial challenges to overcome in order to avoid lysosomal destruction. Comparatively to the endosomal compartment. In the second experimental work, Phosphatidylserine (PS) micelles were used to simulate the late endosomal compartment. PS was dissolved in 1.6 mM chloroform and the solvent was evaporated using magnetic agitation. PS micelles were isolated from the reconstituted dried material by ultrasonic dispersion in PBS. The PS micelles were incubated with or without the nanodiaplexes and nioplexes for one hour at a mass ratio of 1:50 pEGFP:PS. The amount of genetic material released from the complexes was measured using electrophoresis on samples loaded in a 0.8% agarose gel with 200 ng of DNA. As described in the Gel Retardation Assay section, the electrophoresis procedure, band staining, and analysis were all completed.

2.3. *In vitro* assays

2.3.1. Cell culture and *in vitro* transfection assays

In the first experimental work, a human retinal pigment epithelial cell line (ARPE-19), was selected for *in vitro* assays to evaluate gene transfection efficiency. ARPE-19 cells were seeded into 24-well plates at an initial density of 18×10^4 cells per well in order to reach 70–80 %

confluence at the time of the transfection assay in order to evaluate the transfection efficiency. Niosphingoplexes and nioplexes were formed at cationic lipid/DNA mass ratios 3/1, 5/1 and 10/1 in Opti-MEM™ transfection medium. In the second and third experimental works, a Human embryonic kidney 293 (HEK-293) cells were grown and maintained. To conduct transfection experiments, HEK-293 cells were seeded at a density of 20×10^4 cells per well in 24-well plates and incubated overnight to reach 70% confluence. In the second experimental work, nanodioplexes and nioplexes were formed at cationic lipid/DNA mass ratios 5/1, 10/1 and 15/1 in OptiMEM® transfection medium. While, freshly prepared complexes and stored for 15 and 30 days at 4°C and 25°C, at the cationic lipid/DNA mass ratio 5/1 were formed in the third experimental work. In all transfection experiments, after removing the growth media, the cells were exposed to the transfection complexes for 4 hours in the incubator. Following the removal of complexes, fresh medium was applied. Then cells were expanded for 48 hours in regular growth medium instead of OptiMEM®. This was followed by fluorescence microscopy qualitative analysis. The EGFP signal was captured in cells transfected with complexes at this time. Flow cytometry analysis was performed using a FACSCalibur flow cytometer to quantify the percentage of EGFP plasmid expression for the transfection assay. For this purpose, cells were washed with PBS and detached from the 24 wells with trypsin/EDTA at the end of the 48- hour incubation period. Positive and negative transfection controls were performed using OptiMEM® medium without complexes and Lipofectamine™ 2000-transfection reagent, respectively. Each condition was evaluated in triplicate.

Such cells were placed in tubes of a flow cytometer to measure the EGFP signal in living cells. Before performing flow cytometry, cell viability was determined by staining cells with propidium iodide. The fluorescent emission of both dead and transfected cells was evaluated at 650 nm (FL3) and 525 nm (FL1), respectively. In the FL1 channel, the mean fluorescence intensity (MFI) signal was analyzed from live, positive cells. The collection gate was constructed with nontransfected cells. Using cells transfected with Lipofectamine 2000, flow cytometer settings and channel compensation were performed. The data on cell viability and transfection were normalized using the respective values of negative and positive control cells. The experiments were conducted in triplicate, and a minimum of 10,000 events were collected for each sample.

2.3.2. Cellular uptake

Cellular uptake of complexes was determined by incubating cells with fluorescein isothiocyanate (FITC-pEGFP) for both 2 h and 4 h in the first experimental work and for 2 h in the second. In the third experimental work, the cellular uptake was analysed 4 h after exposure to nanodiaplexes and nioplexes at 5/1 lipid/DNA ratio (w/w) at day 0 and after 30 days of storage at 4°C. Niosomes and nanodiasomes were condensed with FITC- labelled pEGFP plasmid. For qualitative assays, cells were seeded on coverslips and subsequently fixed with 4% formaldehyde. After fixation, cells were washed with PBS and stained for 40 minutes with (5 µL) of phalloidin in PBS containing 1% BSA. After being washed with PBS, the cells were mounted with Fluoroshield with DAPI. After mounting the cells, they were examined using confocal laser scanning microscopy (Zeiss Axioobserver). Image analysis was performed using ImageJ software. Flow cytometry, as previously described, was used for quantitative analysis. Normalized cellular uptake data to positive control cells treated with Lipofectamine 2000 and expressed as the percentage of FITC-pEGFP positive cells.

2.3.3. Intracellular trafficking

Cellular internalization of complexes was examined by treating cells with FITC-labeled pEGFP (FITC-pEGFP) for 3 hours over coverslips. Then, specific markers of the endocytic pathways were co-incubated for 1 hour. In the first experimental work, transferrin Alexa Fluor 568 (2.5 µL) (5 mg mL⁻¹) was incubated to label clathrin mediated endocytosis (CME), cholera toxin B Alexa Fluor 594 (2.5 µL) (10 mg mL⁻¹) to label caveolae mediated endocytosis (CvME) and dextran Alexa Fluor 568 (30 µL) (1 mg mL⁻¹) was used to label macropinocytosis. While in the second experimental work we used transferrin-AlexaFluor594 (50 g/mL) to stain the clathrin-mediated endocytosis (CME), cholera toxin B-AlexaFluor594 (10 g/mL) to stain caveolae mediated endocytosis (CvME) and dextran-AlexaFluor594 (1 µg/µl) for macropinocytosis. LysoTracker Red-DND-99 (20 µM) was used for the lysosomal late endosomal compartment in all intracellular trafficking experiments in this thesis. Slides were examined under microscope after cell fixation and mounting to capture representative pictures to be analyzed by the ImageJ software. Colocalization of FITC-pEGFP and the endocytic pathway was assessed by crosscorrelation analysis of the green and red signals, respectively. In the second experimental work, specific endocytosis inhibitors were used to inhibit cellular uptake. HEK-293 cells were

exposed for 30 minutes to 200 μ M genistein, and for 60 min with 5 μ g/mL chlorpromazine hydrochloride, and 50 nM wortmannin as inhibitors for the CvME, CME, and macropinocytosis pathways, respectively, in a 24-well plate. The medium containing the inhibitors was then removed, a rapid wash was performed, and transfection was performed with both nioplexes and nanodiaplexes. As described previously, EGFP-positive cells were quantified using flow cytometry on processed cells. The data were normalized relative to the number of EGFP-positive cells following transfection with nanodiaplexes and nioplexes in the absence of endocytic pathway inhibitors. Experiments were conducted in triplicate collecting and analyzing over 5000 events per sample.

2.4. *In vivo* assays

2.4.1. Animal model

Rat embryonic E17-E18 (Sprague Dawley) brain cortex and retina were used to obtain primary CNS cells. Adult female C57BL/6 mice were employed for subretinal, intravitreal, and brain administration as experimental animals. All procedures involving the use of animals in scientific research were conducted in conformance with the RD 53/2013 Spanish and 2010/63/EU European Union regulations. The Miguel Hernandez University Standing Committee for Animal Use in the Laboratory (code UMH.IB) approved and supervised the procedures.

2.4.2. Transfection assays of complexes in rat primary retinal and neuronal cell cultures

E17-E18 rat embryos (Sprague Dawley) were used for the extraction of primary central nervous system (CNS) cells, from the cerebral cortex and retinal tissue. Cells were extracted and cultivated onto pre-coated glass coverslips in 24 well plates. Cortical and retinal cells were transfected with niosphingoplexes, freshly nanodiaplexes and nanodiaplexes stored for 30 days. Lipofectamine™ 2000 (ThermoFisher Scientific) was utilized as a positive control. Transfection tests were conducted three times for each condition. Transfection efficiency was assessed qualitatively by immunocytochemistry. Cell fixation was carried out with 4% paraformaldehyde for 25 minutes and permeabilized using 0.5% Triton X-100 during 5 min. After blocking with a solution of 10 % BSA (v/v) in PBS for 1 hour at RT, cells were treated with primary antibody chicken anti-EGFP overnight at 4°C. Secondary antibody 9 Alexa Fluor 555 goat anti-chicken IgG and Hoechst 33342 were applied for 1 hour at 4°C. Coverslips were analyzed with a Zeiss

AxioObserver Z1 (Carl Zeiss) microscope equipped with an ApoTome system and Leica TCS SPE spectral confocal microscope.

2.4.3. Subretinal, intravitreal and brain administration

In vivo transfections using niosphingoplexes, freshly prepared nanodiaplexes, and nanodiaplexes stored for 30 days were performed in C57BL/6J mice. Intravitreal or subretinal injections were administered under a microscope (Zeiss pico; Carl Zeiss Meditec GmbH, Jena, Germany) using a Hamilton microsyringe with a blunt 34-gauge needle. The untreated right eyes were used as negative controls. Additionally, niosphingoplexes were injected into the brain of ICR (CD-1) mice utilizing a microsyringe 33-gauge needle. The same level of mouse brain was injected with only the formulations, with no plasmid. It took five minutes for the needle to be slowly removed after the injection. The contralateral brain hemisphere of mice with no injection was also employed as a negative control. EGFP expression in mouse retina was evaluated qualitatively 1 week after the injection of complexes in wholemount and sagittal sections of the retina. Frozen sections and wholemount retinas were stained with Hoechst 33342 to reveal the nuclei. Brain samples were processed a week after surgery and EGFP expression in mice brains was evaluated qualitatively. Then, the 20 μ m brain slices were processed for immunohistochemistry. Nonspecific staining was blocked by incubating sections in 10% BSA with 0.5% Triton X-100 for 1 h, followed by overnight incubation with chicken anti-GFP (Invitrogen, 1:100). Then, sections were washed and incubated with Alexa Fluor 488-conjugated goat anti-chicken IgG (Invitrogen, 1:100) for one hour. Nuclei were stained with Hoechst 33342.

2.5. Statistical analysis

The Shapiro-Wilks and Levene tests validated the normality and homogeneity of variances. A Student's t test or a Mann-Whitney U test were used to compare two groups of unpaired data. In normality conditions, a 1-way ANOVA followed by the Student-Newman-Keuls test or an ANOVA followed by a post-hoc HSD Tukey test was used for multiple comparisons; in nonparametric conditions, a Kruskal-Wallis test followed by a Mann-Whitney U test was used. Data were expressed as mean \pm standard deviation (SD). A p value < 0.05 was considered statistically significant. The statistical packages IBM SPSS Statistics 22.0 and SPSS 15.0 were used to conduct the analyses.

3. Hypothesis and objectives

Non-viral vectors have recently become increasingly essential in gene therapy therapies. The high genetic carrier packing capacity, low immunogenicity, and affordable manufacture of non-viral vectors make them an attractive substitute for viral vectors, which exhibit superior transfection efficiency but serious biosafety concerns. In order to overcome their underlying issues, the scientific community has made significant advancements in the field of non-viral vectors. Numerous non-viral nanosized gene delivery vectors, such as cationic lipids, polymers, and magnetic nanoparticles, have been developed to date. Since the retinal and central nervous system are among the most difficult organs for both viral and non-viral gene delivery systems, these molecules can be nanoengineered to cross a variety of extracellular and intracellular barriers and transport therapeutic genes into specific organs or cell types. In particular, niosomes have developed as effective gene delivery nanoparticles. Niosomes, are synthetic, non-ionic surfactant vesicles with a closed bilayer structure that are biocompatible. Their physicochemical and biophysical properties are dependent on the formulation components and the technique of manufacture. Niosomes need to be properly characterized in order to determine how the formulation composition affects transfection effectiveness and cytotoxicity. Niosomes represents an encouraging nonviral nanoplatform strategy for the treatment of both retinal and brain diseases by gene therapy. For this purpose the nucleus of target cells must be reached, transfection efficacy and low immunogenicity must be demonstrated in order to overcome the barriers connected with the administration route as well as the extracellular and intracellular environments. The three main components of niosome formulations are cationic lipids, helper lipids, and non-ionic surfactants. The physicochemical characteristics of niosomes, such as size, surface charge, and morphology, are influenced by the general chemical properties of these components. These characteristics, in turn, determine the ability of niosomes to enter cells, follow a specific endocytic pathway, deliver the DNA cargo to the nucleus, and, consequently, the efficiency of their transfection. The development of niosomes has been facilitated by the discovery and addition of novel "helper" components in formulations. Although the roles of cationic lipids and the non-ionic surfactant component in the transfection process and efficiency mediated by niosomes have been extensively researched, there is still a big margin for transfection efficiency improvement. In order to obtain sustained and high levels of transgene expression, required for their biomedical application, and to optimize the design of niosome formulations, the influence of the helper components must thus

also be extensively understood. In view of these considerations, the main objective of the present work is to evaluate the relevant biophysic processes connected to the physicochemical properties and gene transfection mechanism, when helper components are added into a cationic niosome formulation for non-viral gene delivery to the central nervous system and different cells in mouse retina. Pharmaceutical science has devoted significant efforts to the discovery and development of safe and effective vectors for gene therapy applications. Few studies conduct an exhaustive assessment of the storage stability of gene carriers, which is a crucial quality for both large-scale production and clinical application. A helper lipid-niosome formulation combination may be required to improve the stability of gene delivery applications. As a result, the final formulation must be properly examined to determine the storage stability throughout time at a variety of storage temperature levels. With this knowledge, my PhD thesis aims to design and characterize non-viral vectors based on cationic niosomes after the incorporation of helper components, for gene therapy treatment of the retina and the central nervous system. Furthermore, to study long-term stability of the combined nanocarriers for non-viral gene delivery to the retina and the brain. The following are the four primary goals that must be met to achieve this purpose:

- To discuss the composition, preparation methods, physicochemical features, and the biological evaluation of niosomes and the related nioplexes that result from the addition of the genetic material onto the cationic surface of the niosomes. Moreover, to focus on the in situ application of such niosomes, which will involve delivering the genetic material into immune-privileged regions such as the brain cortex and the retina. (Appendix 1).
- To evaluate relevant biophysic processes connected to the physicochemical properties and gene transfection mechanism, when sphingolipids are added into a cationic niosome formulation for non-viral gene delivery to the central nervous system and different cells in mouse retina. (Appendix 2).
- To evaluate the biophysical performance of nanodiamonds as niosome helper components, named nanodiasomes, in order to develop a nonviral gene delivery system suitable for targeted therapy in CNS illnesses. (Appendix 3).
- To evaluate the influence of combined nanodiamonds within niosome non-viral vectors on long-term biological performance. Studies of the physicochemical characteristics, cellular

internalization, cell viability, and transfection efficiency of the resultant formulations are necessary overtime *in vitro* and *in vivo* in the rat retina. (Appendix 4).

4. Results and discussion

In the first experimental study, we introduced animal-derived sphingolipids as a "helper" component into niosome formulations to evaluate their biophysical properties as a gene delivery system. Amphiphilic biomolecules, sphingolipids have a polar terminal group (OH) and a hydrocarbon chain. Amphiphilic molecules can spontaneously organize themselves into colloidal vesicles when dispersed in water [53], which can enhance the ability of such system to deliver drugs. Due to their surface-active wetting ability, which can coat the crystals on the surface of hydrophobic substances to make them hydrophilic, sphingolipids offer desirable physicochemical qualities that help stabilize the emulsions. Sphingolipid metabolites are also bioactive signaling molecules involved in the control of cell metabolic processes, such as cell growth, differentiation, senescence, and apoptosis [54]. As a result of the comparative study of both niosphingosome and niosome formulations, as well as the corresponding complexes obtained upon the addition of plasmid DNA at cationic lipid/DNA mass ratios 3/1, 7.5/1 and 15/1 (Figure 3). The mean diameter size of niosphingosomes was 123.5 ± 12.5 . Interestingly, this value decreased up to 27 % after the addition of plasmid DNA for all the cationic lipid/DNA mass ratios studied. In the case of niosomes, the mean diameter size before the addition of plasmid DNA was higher, 158.9 ± 4.4 , nm and this value increased to 40 % at cationic lipid/DNA mass ratio 7.5/1, with no relevant changes at ratios 3/1 and 15/1. All formulations had positive charge values, which is necessary to prevent the formation of aggregates due to electrostatic interactions. In addition, all formulations and complexes exhibited particle sizes in the nanoscale range, making them appropriate for gene delivery. The addition of sphingolipids as a "helper" component to the formulation of cationic niosomes reduced particle size. Curiously, when the formulations were complexed with the EGFP plasmid, the variations in particle size were not only maintained but also reduced. In addition, niosphingoplexes had a smaller particle size than niosphingosomes at all examined cationic lipid/DNA mass ratios, likely due to the additional electrostatic interactions between the cationic niosphingosomes and the anionic plasmid DNA. In term of surface charge, all formulations showed positive values above zero, zeta potential of niosphingosomes and niosomes was 37.0 ± 7.8 mV and 25.0 ± 9.0 mV, respectively. In both cases, after the insertion of plasmid DNA at cationic

lipid/DNA mass ratio 3/1, these values decreased greatly and subsequently showed a moderate rising trend when increasing the cationic lipid/ DNA mass ratios to 7.5/1 and 15/1. The presence of sphingolipid amphiphilic biomolecules in the composition of niosomes raised the zeta potential across all cationic lipid/DNA mass ratios studied. The dispersity values of all samples were below 0.5 and no important changes were identified between both formulations, apart from niosphingoplexes at cationic lipid/DNA mass ratio 3/1, which displayed clearly lower PDI values (0.19 ± 0.01) than the rest of formulations, indicating that under this ratio, complexes are more homogeneous. Furthermore niosphingosomes exhibited a distinct spherical and homogenous morphology during transmission electron microscopy analysis, devoid of aggregates, most likely due to electrostatic repulsion between strongly positively charged particles.

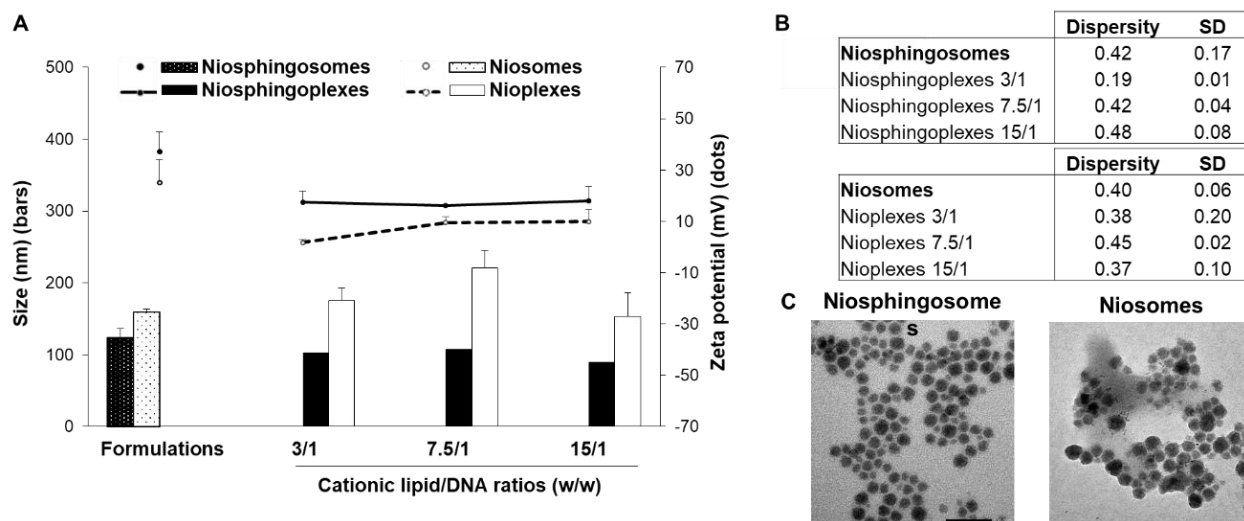


Figure 3: Physicochemical characterization of formulations and complexes prepared with helper component (niosphingosomes/niosphingoplexes) and without helper component (niosomes/nioplexes). (a) Size (bars) and zeta potential (dots). (b) Dispersity index and standard deviation values of formulations and complexes. Each value represents the mean \pm standard deviation of three measurements. (c) TEM images of niosphingosomes and niosomes. Scale bars: 100 nm.

Once the formulations were described in physicochemical terms, we conducted *in vitro* gene delivery investigations with niosphingoplexes and nioplexes at cationic lipid/DNA mass ratios of 3/1, 7.5/1, and 15/1 in ARPE-19 cell line, as these cells play a crucial role in retinal disorders [44]. Additionally, ARPE-19 cell is a well-known retinal cell type to assess gene

transfection efficacy. According to figure 4, the maximum transfection value ($P < 0.001$) was achieved for niosphingoplexes at a 3/1 cationic lipid/DNA mass ratio, with a normalized percentage of live cells expressing EGFP of $36.7 \pm 1.6\%$. When transfection percentages for nioplexes were around 3% at cationic lipid/DNA mass ratio 3/1, and increased to 22% and 15% at cationic lipid/DNA mass ratios 7.5/1 and 15/1, respectively. Curiously, although niosphingoplexes with different cationic lipid/DNA ratios exhibited comparable size and zeta potential values in previous physicochemical studies, they reported statistically significant differences in transfection efficiency and cell viability, indicating the difficulty of the transfection process. In parallel, MFI analysis was performed to evaluate not only the percentage of transfected living cells, but also the fluorescence signal intensity, which is closely connected to the amount of protein expressed after transfection. Such MFI measurements also demonstrated that ARPE-19 cells treated with niosphingoplexes at a 3/1 cationic lipid/DNA mass ratio achieved the maximum intensity value.

Overall, data obtained from transfection efficiency experiments indicate that the presence of sphingolipid biomolecules in the niosome composition at a 3/1 cationic lipid/DNA mass ratio not only increases the percentage of transfected cells, but also the amount of protein expressed in such transfected cells [16], which may have significant clinical impacts. Interestingly, the transfection experiments revealed that niosphingoplexes at all cationic lipid/DNA mass ratios had higher cell viability values (above 80% in ARPE-19 cells) than their niosome counterparts, indicating that the incorporation of sphingolipids into the niosome formulation has a biocompatibility effect. This biocompatibility of niosphingoplexes was clearly confirmed 48 hours after transfection by the healthy appearance of ARPE-19 cells under fluorescence microscopy. In contrast, the transfected positive control Lipofectamine™ 2000 demonstrated low cell viability values, less than 65% (data not given), demonstrating the toxicity associated with this commercial formulation, which limits its clinical applicability [55]. In terms of therapeutic applications, it is also essential to note that ARPE-19 cells subjected to niosphingoplexes at the lowest cationic lipid/DNA ratio of 3/1 showed the highest transfection efficiency and cell viability. Such a success would enable a larger gene loading capacity in the minimal injection quantities that are generally used to treat brain and retinal disorders via gene therapy.

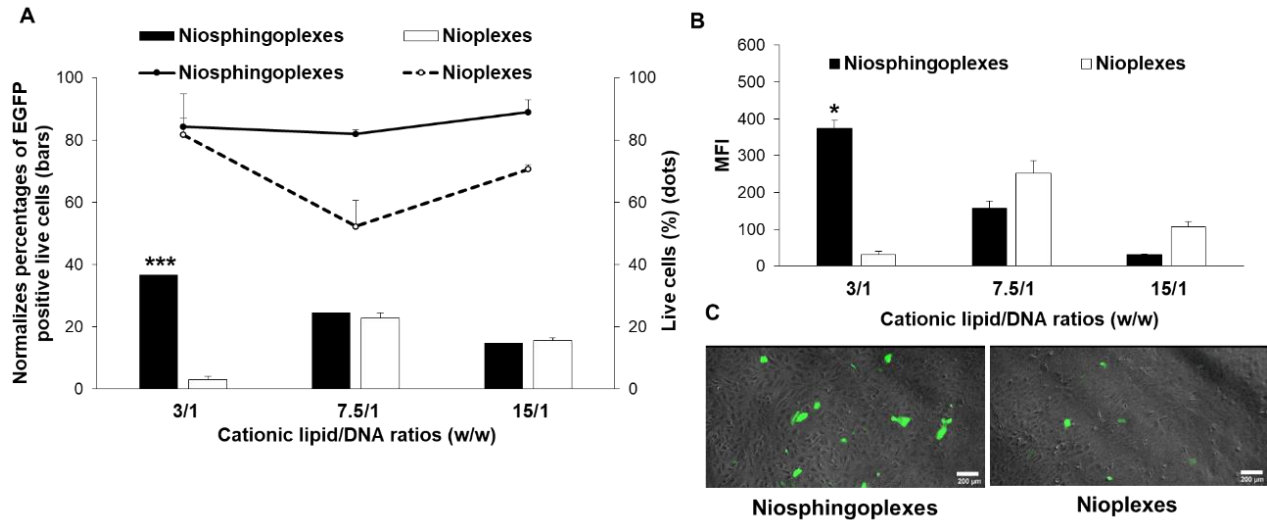


Figure 4: Transfection efficiency and cell viability in ARPE-19 cell line 48 h post-transfection with niosphingoplexes and nioplexes. (a) Normalized percentages of transfection efficiency (bars) and cell viability (dots). (b) MFI of niosphingoplexes and nioplexes. Each value represents the mean \pm standard deviation of three measurements. (c) Overlay phase contrast images showing EGFP signals in ARPE-19 cells transfected with niosphingoplexes and nioplexes at 3/1 cationic lipid/DNA ratio (w/w). Scale bar: 200 μ m. *** $P < 0.001$; * $P < 0.05$.

To further study the influence that the addition of sphingolipid biomolecules has on the transfection process, we also conducted a study on cellular uptake, as this parameter might have a significant impact on transfection efficiency. Furthermore, our experiments on cellular uptake found that there was no difference between the two formulations in terms of the proportion of cells that internalized the complexes and the amount that were internalized by cells. More than 98% of cells took up nioplexes and niosphingoplexes at the 3/1 cationic lipid/DNA mass ratio at 2 h and 4 h of treatment. We also evaluated the mean fluorescence intensity (MFI) of the cells that internalized the complexes for further uptake data. In any event, the internalization process was more effective when formulations were exposed to cells for 4h rather than 2h. Although no changes were seen between niosphingoplexes and niosome formulations (Figure 5), both complexes had significantly higher MFI values at 4 h than at 2 h following exposure to niosphingoplexes or nioplexes ($P < 0.001$) or ($P < 0.01$), respectively. These results show that the kinetics of the internalization process is important to the transfection efficiency.

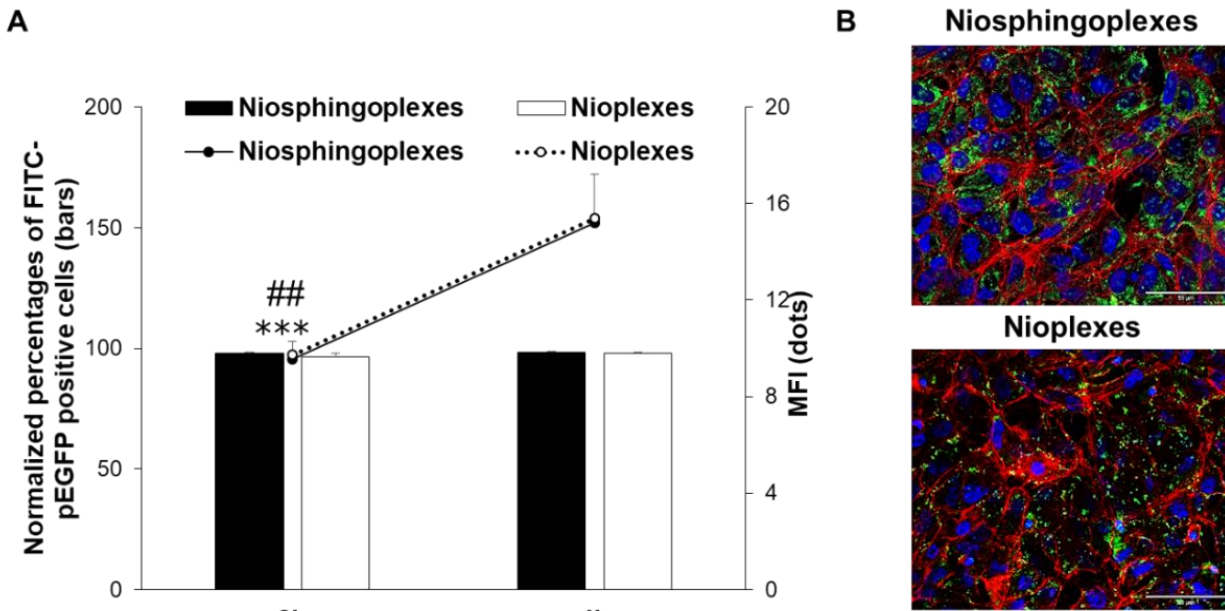


Figure 5: Cellular uptake in ARPE-19 cell line of both niosphingoplexes and nioplexes complexes at 3/1 cationic lipid/DNA ratio (w/w). (a) Percentages of FITC-pEGFP positive cells (bars) and mean fluorescence intensity (dots) at 2 h and 4 h of exposition. Each value represents the mean \pm standard deviation of three measurements. (b) Confocal microscopy images showing the cellular uptake of complexes in ARPE-19 cells at 4 h. Cell nuclei were colored in blue (DAPI); F-actin in red (Phalloidin). Scale bar: 50 μ m. *** $P < 0.001$ for niosphingoplexes; ## $P < 0.01$ for nioplexes.

We also examined additional biological factors, such as the intracellular trafficking process of both formulations. Intracellular trafficking experiments were conducted to determine the co-localization of formulations with the most frequently used endocytosis routes in ARPE-19 cells (Figure 6), including CvME, CME, and macropinocytosis [40, 41]. The CvME route demonstrated the greatest variation between the two formulations, according to our results. Niosphingoplexes had a lower CCF peak values of the CvME and CME pathways (0.25 and 0.31 CCF, respectively) than macropinocytosis ($p < 0.05$; 0.42 CCF peak value). Whereas niosomes were equally internalized by the three examined endocytosis pathways, CCF peak value was 0.35 for CME, 0.38 for macropinocytosis, and 0.41 for CvME. Consequently, our finding suggest that the presence of sphingolipids may switch the internalization process of niosphingoplexes from CvME to the macropinocytosis endocytic pathway. In this way, macropinocytosis has been associated with the internalization of cell-penetrating peptides and proteins into cells [56, 57]. In addition, co-localization investigations were performed in the late endosomal compartment. Niosphingoplexes

co-localized with lysosomes more frequently than nioplexes in this instance, there was a statistically significant difference in the peak CCF values between the niosphingoplexes and niosomes in this study ($P < 0.05$). It has been hypothesized that lysosomal activity is inhibited when complexes enter ARPE-19 cells via CvME and these complexes are localized surrounding the nucleus, preventing the release of DNA from the complexes [58]. Compared to niosphingoplexes, nioplexes entered the cell primarily via CvME, resulting in a lack of lysosomal activity. This hypothesis is consistent with our findings. Endosomal escape is a crucial factor that has a demonstrable effect on the transfection process of complexes designed for gene delivery. Due to their poor endosomal escape performance, various nucleic acid delivery methods failed to reach high levels of transfection efficiency while being successfully internalized into cells [59].

In order to analyze the release of the complexed plasmid DNA from the late endosomes and avoid lysosomal degradation, we next developed anionic micelles based on PS. In the agarose gel electrophoresis assay, as shown in figure 5d, a small amount of plasmid was released from niosphingoplexes (lane 2), whereas no plasmid was released from nioplexes (lane 3). These results imply that the incorporation of sphingolipids into the formulation of cationic niosomes could offer endosomal escape capabilities to the complexes, which could contribute to an improvement in transfection efficiency. The nuclear membrane is another biological barrier that inhibits the transfection process. In this way, and considering the essential signaling and regulatory roles that sphingolipids play in the nucleus [60], it is likely that such sphingolipids are encouraging gene delivery by a regulatory mechanism in the nucleus.

Recent research on nuclear sphingolipids has revealed that different types of sphingolipids support distinct nuclear roles through temporally and spatially distinct methods. For example, sphingomyelin is involved in the structure and regulation of chromatin architecture, DNA synthesis, and RNA stability, sphingosine is a ligand for the nuclear receptor steroidogenic factor 1 that regulates gene transcription, and sphingosine-1-phosphate regulates gene expression epigenetically via histone acetylation [61].

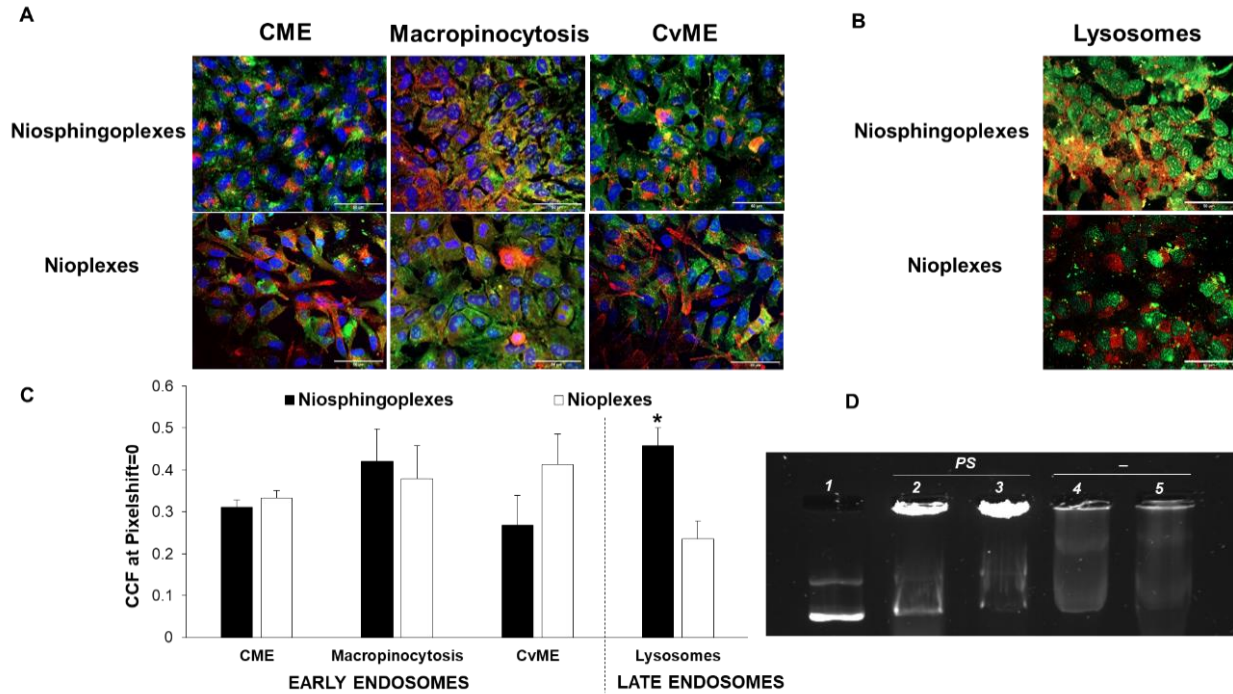


Figure 6: Intracellular trafficking pathway assay of complexes in ARPE-19 cells. (a) Confocal microscopy merged images showing ARPE-19 cells co-incubated with complexes containing the FITC-labeled pEGFP plasmid (green) and with one of the following endocytic vesicle markers (red): Transferrin Alexa Fluor 568 for CME, Dextran Alexa Fluor 568 for macropinocytosis, and Cholera toxin B Alexa Fluor 594 for CvME. Scale bar: 50 μ m. (b) Confocal microscopy merged images showing ARPE-19 cells co-incubated with complexes containing the FITC-labeled pEGFP plasmid (green) and with Lysotracker Red-DND-99 (red) to stain the late endosome. (c) Co-localization values of red and green signals assessed by cross-correlation function (CCF) analysis in complexes. Data represent the mean \pm standard deviation of three measurements; $*P < 0.05$ for niosphingoplexes vs nioplexes. (d) DNA release profiles in agarose gel electrophoresis assay. Lane 1 naked DNA, lane 2 niosphingoplexes co-incubated with PS, lane 3 nioplexes co-incubated with PS, lane 4 niosphingoplexes, lane 5 nioplexes. PS refers to phosphatidyl serine micelles.

Before conducting *in vivo* studies, we developed a proof of concept assay to determine if niosphingoplexes with a cationic lipid/DNA mass ratio of 3:1 (w/w) could efficiently deliver the EGFP plasmid to both rat embryonal retinal and cerebral cortex main cells. Results demonstrated EGFP expression in both retinal and cortical primary cells 72 h after transfection (Figure 7).

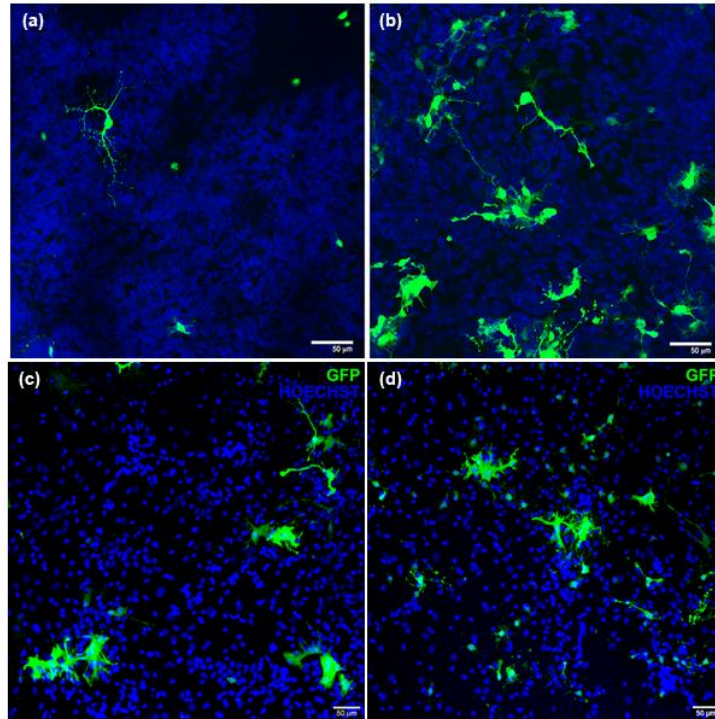


Figure 7: EGFP signal (green) in primary culture of rat retinal cells transfected with (a) niosphingoplexes at 3/1 cationic lipid/DNA ratio (w/w) and (b) the positive control Lipofectamine™ 2000. GFP signal (green) in embryonic rat cerebral cortex primary cells transfected with (c) niosphingoplexes at 3/1 cationic lipid/DNA ratio (w/w) and (d) the positive control Lipofectamine™ 2000. Scale bar: 50 μm. Hoechst 33342 stained blue.

In relation to the findings, niosphingoplexes were evaluated in *in vivo* tests to determine their ability to transfer genetic material to the retina and brain of mice following intravitreal and subretinal injection. Due to their important physiological functions, both the brain and the eye are immune-privileged regions that are separated from the rest of the organism by additional extracellular barriers such as the BBB and the BRB [62, 63]. An perfect outcome would involve the delivery of genetic material by a safe and effective non-viral vector to immune-privileged sites via non-invasive administration routes (Figure 8), such as the topical instillation in the cornea that avoids the BRB to reach the retina and the nose-to-brain administration to gain direct access to the brain by passing the BBB. Gene therapy may soon be used to treat serious disorders of the brain and retina. Although, at the current time, this potential is far from being implemented in standard medical practice. Consequently, we assessed the local administration of niosphingoplexes in the

retina and brain. In the case of the eye, intravitreal and subretinal injections are the most commonly used delivery routes to reach the retina. Several retinal layers and cells had EGFP expression following intravitreal and subretinal injections, as demonstrated by our results. Specifically, EGFP expression was mainly seen in the outer segments of photoreceptors, the outer plexiform layer, and the inner plexiform layer, where some end-foot Müller glia cells displayed green fluorescence signal. Gene delivery to the outer layers of the retina is of highest interest from a therapeutic aspect, as more than 200 gene alterations at this level have been associated with significant retinal diseases such as Stargardt disease, retinitis pigmentosa, and Lebers congenital amaurosis [64]. On the other hand, transfection of the ganglion cell layer in the retina has relevance for controlling glaucoma disease. We also observed EGFP expression in the cytoplasmic extensions of cortical cells near to the injection site in the case of brain administration at the cortex level. This region of the brain is typically affected by severe diseases of the central nervous system, such as epilepsy, Alzheimer's, and Parkinsons, resulting in significant disturbance and neurological abnormalities. Therefore, our preliminary proof-of-concept *in vivo* assay for delivering therapeutic genetic material into the retina and brain of animal models that mimic human disorders of these critical and immune-privileged tissues reveals promising results.

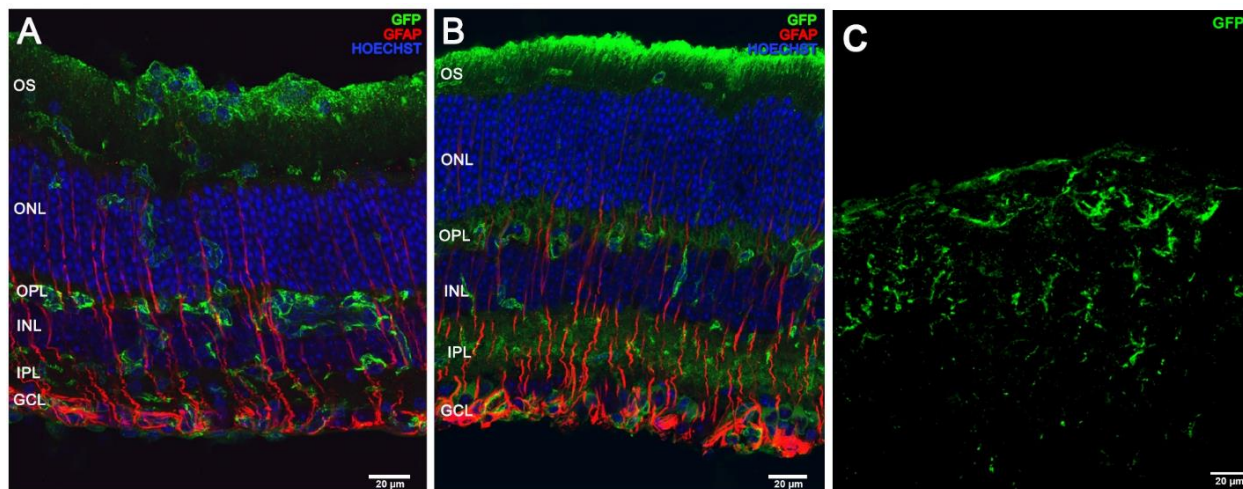


Figure 8: *In vivo* immunohistochemistry gene expression of EGFP (green) in frozen sections one week after subretinal (a), intravitreal (b) and cerebral cortex (c) injections of niosphingoplexes at 3/1 cationic lipid/DNA ratio (w/w). Scale bar: 20 μm. OS, outer segments; ONL outer nuclear layer; OPL outer plexiform layer; INL inner nuclear layer; IPL inner plexiform layer; GCL ganglion cell layer.

In the second experimental part of this doctoral thesis, the presence of carbon-based nanomaterials with promising properties reveals an attractive option to improve nonviral transfection efficiency, bringing us closer to overcome the existing hurdles to medicinal applications. In the area of carbon nanostructures, NDs have received attention due to their unique geometrical properties, specific surface chemistry with a high Young's modulus, large-scale industrial capacity, and nontoxic and biocompatible capabilities [65-67].

NDs are spherical structures with an average diameter of 5 nm, low dispersity index, and large surface area. Due to their nanoscale size and van der Waals forces, NDs have a tendency to self-agglomerate, which reduces their stability in numerous media. In reality, NDs alone in water suspension were found to have a mean size of 89 nm (Figure 9). Accordingly, NDs must be successfully prepared or attached to other components, mostly polymers, for gene transport, although some drug delivery studies have also bound NDs to liposome phospholipids [68, 69]. In this sense, NDs have been utilized in gene therapy due to their specific affinity to particular polymers, which grants them the capacity to bind and transport genetic material. Taking into account the natural ability of niosomes to contain large amounts of genetic material and the high biocompatibility of both NDs and niosomes, we propose a novel gene therapy strategy that combines their desirable features to create a suitable system with high transfection efficiency and biocompatibility.

Specifically, we integrated NDs into cationic niosomes, the developed nanoparticles named nanodiasomes, which are composed of DOTMA as cationic lipids and polysorbate 20 as a non-ionic surfactant. In the first step, a total of three nanodiasome formulations, NDT10, NDT11, and NDT12, were developed and assessed in terms of physicochemical features, as well as transfection ability and toxicity (Figure 9) (Figure 10). This screening of formulations led to the finding that the nanodiasome with the best biophysical performance for gene delivery purposes was the NDT12, which corresponds to the 1/2 ND/DOTMA mass ratio formulation. Further experiments used the same formulation devoid of NDs to study the effect of NDs incorporated as a helper component into niosomes. Curiously, as the concentration of DOTMA in the formulation increased, the nanodiasome size decreased, resulting in a slight increase in zeta potential. This decrease in nanoparticle size could be explained by electrostatic interactions between the positively charged cationic lipid and the negatively charged NDs. Thus, the more cationic lipid,

the greater the electrostatic interactions with NDs, thereby reducing the nanoparticle's final size. Although an increase in cationic lipids can cause cell death due to the positive charge that confers on the vector, the DOTMA concentrations ranging from 1.1 to 3.7 mM exhibited excellent biocompatibility in all cases. At 2/1 and 5/1 lipid/DNA ratios, cell viability values were approximately 95%, but at 10/1 and 15/1 ratios, getting higher cytotoxicity, reducing cell viability to 85%. With NDT12 at 5/1 lipid/DNA ratio, we were able to achieve the best balance between biocompatibility and transfection effectiveness. As a result, further studies were carried out using this nanodiasome formulation.

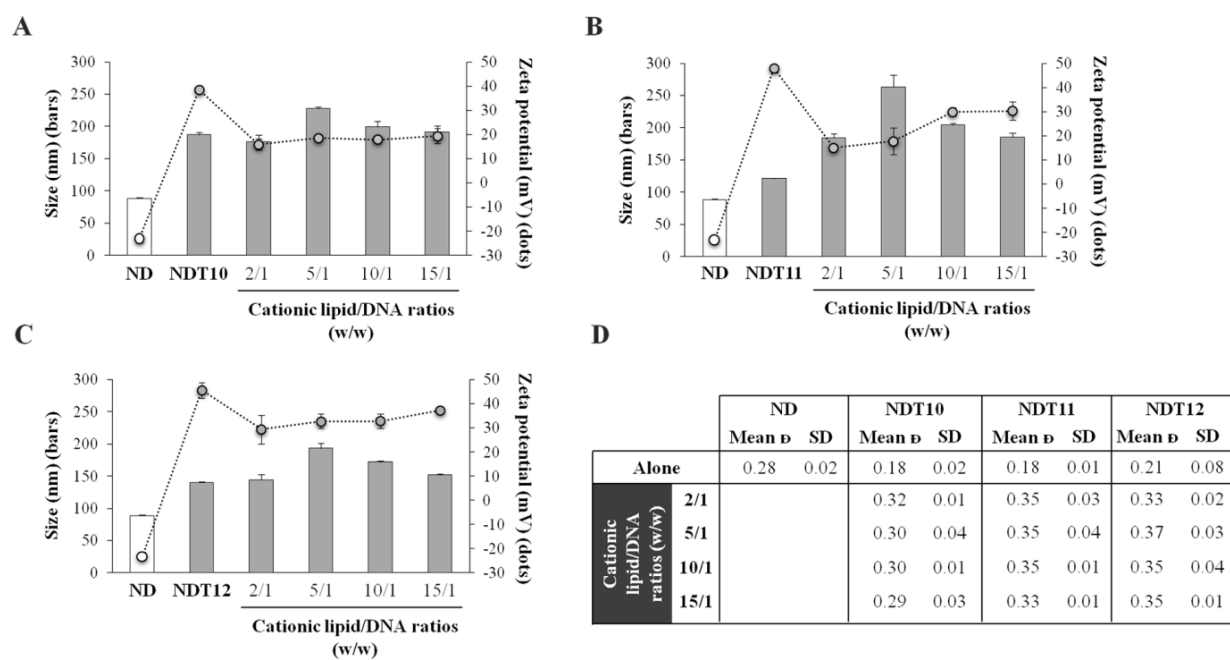


Figure 9: Physicochemical characterization of nanodiasome formulations, elaborated with ND as helper component at different ND/DOTMA mass ratios (1/0.5, named NDT10; 1/1, named NDT11 and 1/2, named NDT12), and nanodiaplexes at different DOTMA/DNA mass ratios (2/1, 5/1, 10/1 and 15/1). A-C. Size (bars) and zeta potential (dots) for (A) NDT10 and corresponding nanodiaplexes (B) NDT11 and corresponding nanodiaplexes, and (C) NDT12 and corresponding nanodiaplexes. D. Dispersion and SD values of nanodiamonds, nanodiasomes and nanodiaplexes. Each value represents the mean \pm standard deviation of three measurements. ND, means nanodiamonds; Ø, means dispersion.

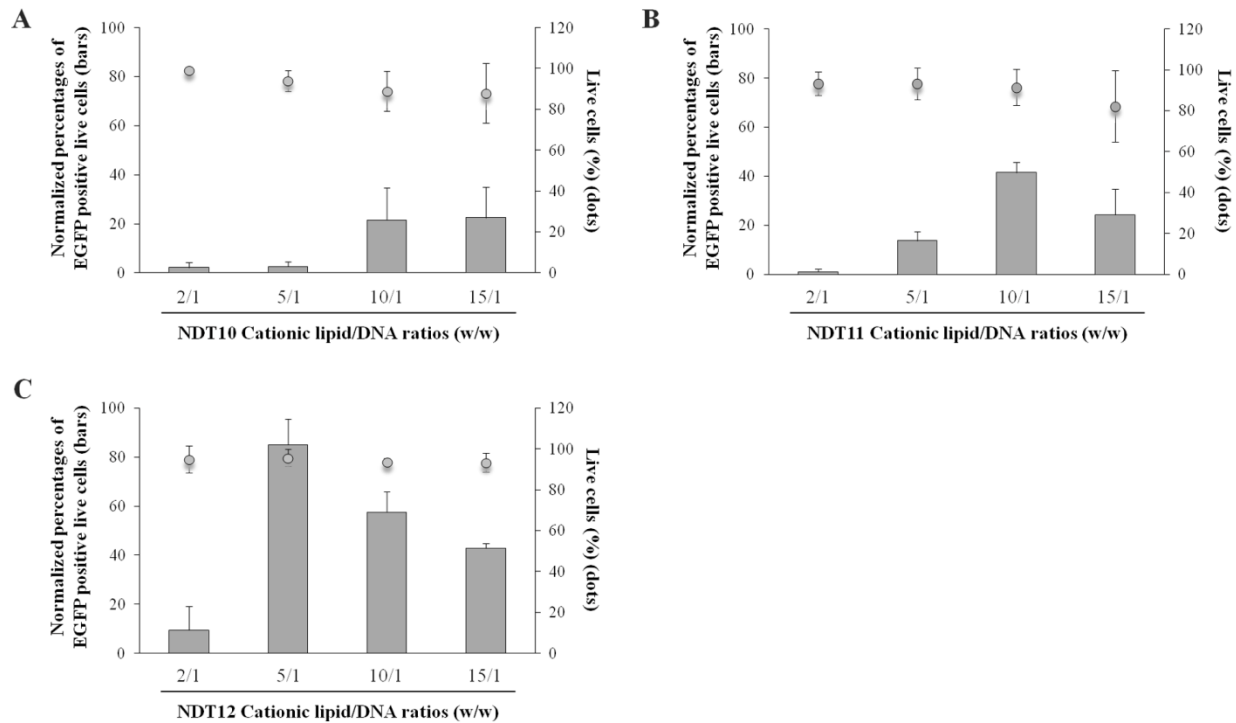


Figure 10: Normalized percentages of EGFP positive live cells (bars) and cell viability (dots) in HEK-293 cell line 48 hours post-transfection with nanodiasomes. A. NDT10 nanodiasomes B. NDT11 nanodiasomes. C. NDT12 nanodiasomes. Each value represents the mean \pm standard deviation of $n \geq 4$.

To investigate the impact of NDs incorporated as a helper component into niosomes, additional physicochemical, transfection, biocompatibility, and intracellular trafficking tests were conducted with NDT12 nanodiasomes compared to the same formulation devoid of NDs. In terms of physicochemical properties (Figure 11), nanodiasomes and nanodiasomes, had a particle size that was about 30% larger than niosomes and nioplexes due to the NDs content. As the lipid/DNA ratio was increased in both complexes, the mean particle size values increased slightly by nearly 40% when pEGFP was added to formulations, while keeping mean diameters below 200 nm in all cases. Nanodiasomes had zeta potentials over +30 mV, with a value of 35.2 ± 0.3 , while niosomes had a value of 20.2 ± 2.5 . Zeta potential for nanodiasomes and nioplexes at the 5/1 lipid/DNA ratio decreased moderately after plasmid condensation and increased slightly when the lipid/DNA ratios were raised, particularly for nanodiasomes. As hypothesized, when the formulations were complexed with plasmid genetic material, the sizes increased while the zeta potential reduced due to the neutralizing of positive and negative charges. Some mean dispersity values were slightly

elevated, such as those for niosomes, nioplexes at the 5/1 ratio and nanodiasomes at the 5/1 ratio. This could be caused on by a few aggregates in the sample. Nanodiasomes and nanodiaplexes had dispersity values below 0.4, while niosomes and nioplexes had values over 0.4. Overall, mean dispersity values were lower for nanodiasomes and nanodiaplexes, indicating greater homogeneity of this formulation.

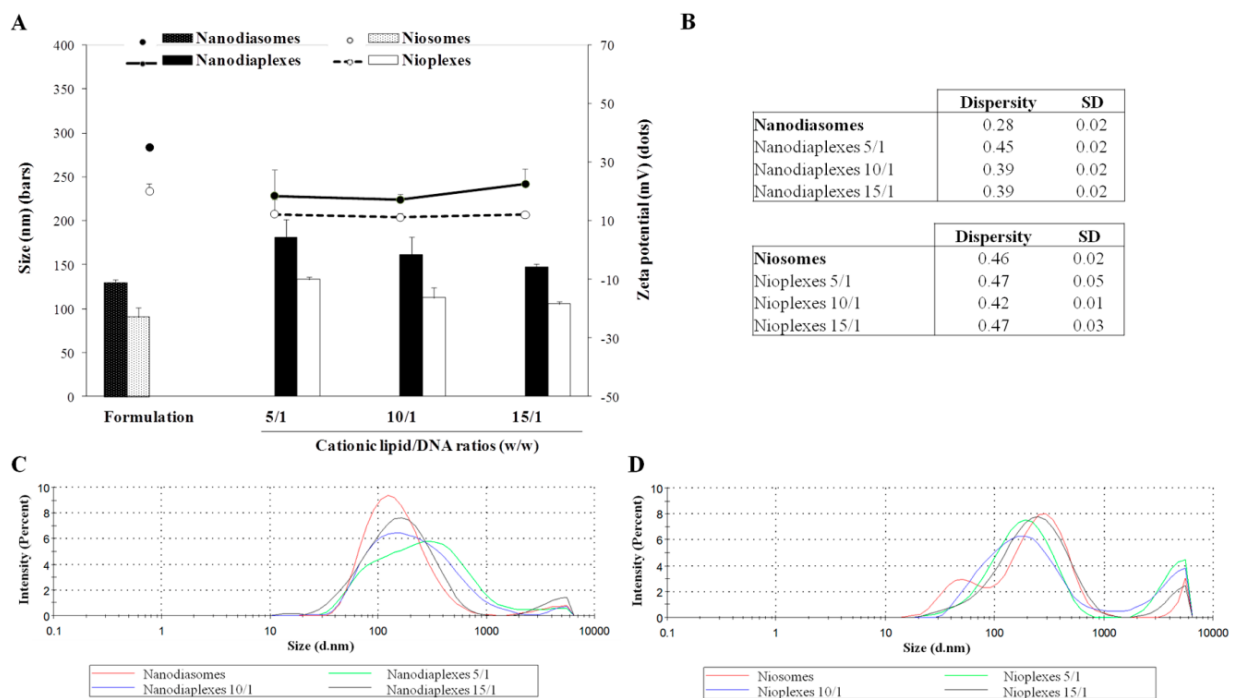


Figure 11: Characterization of formulations and complexes prepared with NDs (nanodiasomes/nanodiaplexes) and without NDs (niosome/ nioplexes). (A) Size (bars) and zeta potential (dots). (B) Dispersity values of formulations and complexes. Each value represents the mean \pm SD of three measurements. (C) Average size-distribution intensities of nanodiasomes (red line) and nanodiaplexes at different cationic lipid/DNA mass ratios (green, blue and black line for 5/1, 10/1, and 15/1 ratios, respectively). (D) Average size-distribution intensities of niosomes (red line) and nioplexes at different lipid/DNA ratios (green, blue, and black line for 5/1, 10/1, and 15/1 ratios, respectively).

In addition, TEM images of nanodiasomes without aggregates revealed a distinct spherical morphology (Figure 12), where ND particles are incorporated into the lipid layer of this non-viral vector.

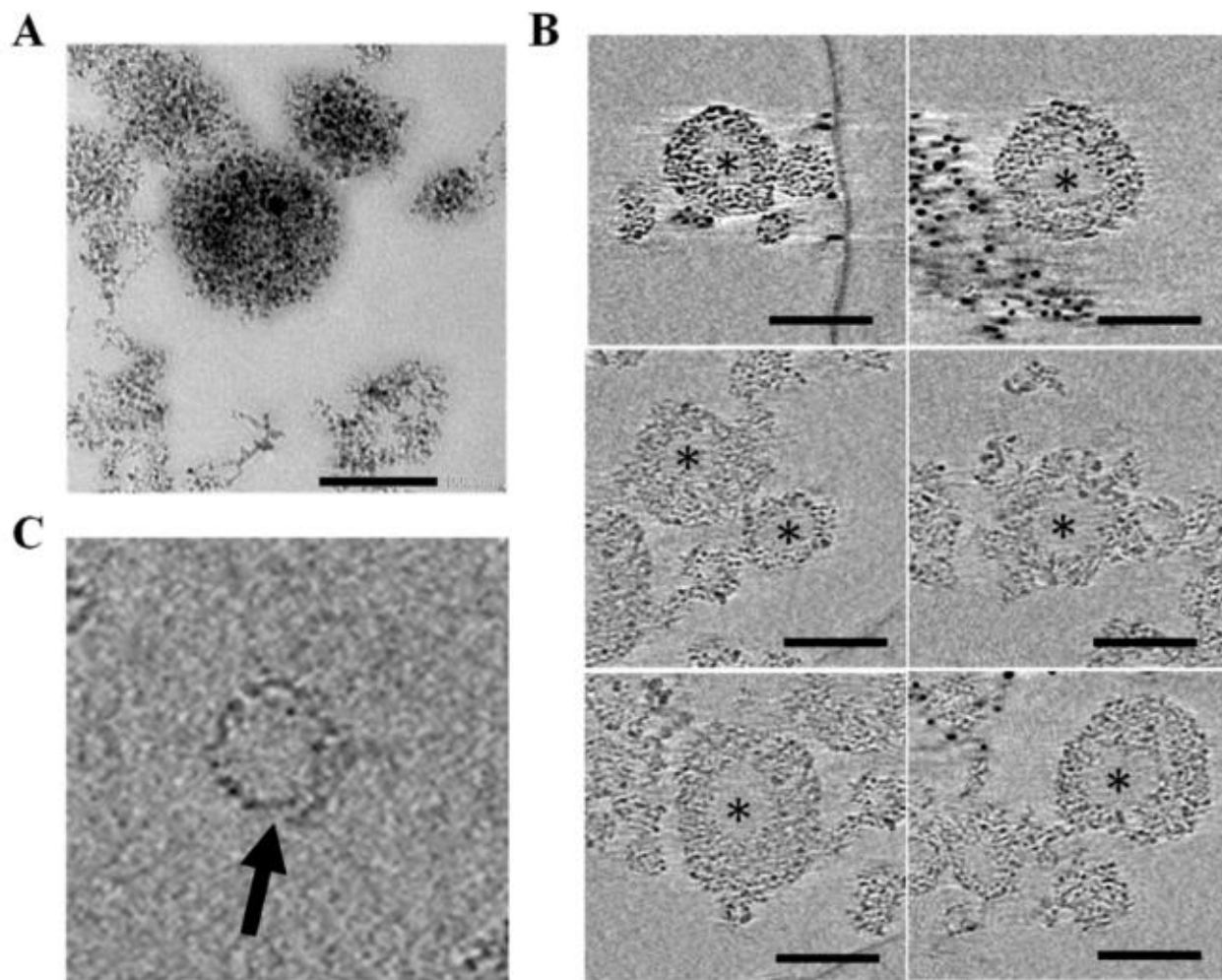


Figure 12: Microscopy images of nanodiasomes. (A) TEM image of nanodiasomes. Scale bar: 100 nm. (B) Cryo-TEM images of nanodiasomes; asterisks indicate the aqueous phase. Scale bar: 100 nm. (C) Lipid layer of nanodiasomes (black arrow) with NDs integrated into the lipid structure.

A gel retardation assay was used to compare the ability of nanodiasomes to condense, protect, and release DNA material with niosomes devoid of NDs (Figure 13). Nioplexes showed a higher capacity nanodiaplexes to bind the DNA, at 10/1 and 15/1 ratios. Both nioplexes and nanodiaplexes were unable to condense all the DNA on their surfaces at the 5/1 ratio. DNA was observed to be released after nanodiaplexes and nioplexes treatment with SDS at 5/1, 10/1, and 15/1 ratios (lanes 5, 8, and 11), and it was also protected against DNase I enzymatic digestion at all ratios (lanes 6, 9, and 12) for both nanodiaplexes and nioplexes.

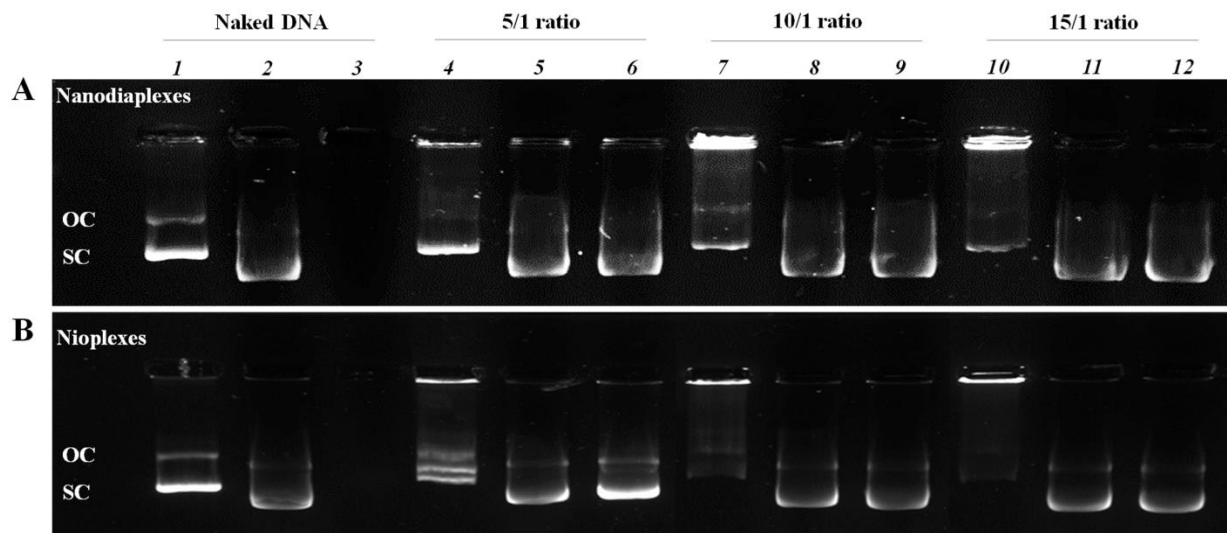


Figure 13: Agarose gel electrophoresis assay. (A) Nanodiaplexes. (B) Nioplexes. Lanes 1–3 correspond to free DNA; lanes 4–6, 5/1 ratio; lanes 7–9, 10/1 ratio; lanes 10–12, 15/1 ratio. Nanodiaplexes and nioplexes were treated with SDS (lanes 2, 5, 8, and 11) and DNase I + SDS (lanes 3, 6, 9, and 12). OC: open circular form; SC: supercoiled form. Following physicochemical characterisation, *in vitro* transfection investigations were conducted on the HEK-293 cell line, which is recognized as a good transfection model. The transfection efficacy of nanodiaplexes was much higher than that of nioplexes at all lipid/DNA ratios, a 75 % increase at the 5/1 ratio with a value of $89.1 \pm 7.7\%$ ($p < 0.001$), when compared to niosomes devoid of NDs ($22.7 \pm 2.4\%$). Such a pEGFP expression of nanodiaplexes over nioplexes has been observed at 10/1 (62.7 ± 2.7 vs $23.9 \pm 2.5\%$; $p < 0.001$) and 15/1 (43.2 ± 1.1 vs $16.8 \pm 4.7\%$; $p < 0.001$) ratios (Figure 14).

Importantly, this improvement of transfection efficiency was followed by an increase in cell viability values to almost 90%, however this parameter dropped to under 80% after transfection with nioplexes. EGFP signal MFI assay showed significant differences at all lipid/DNA ratios ($p < 0.001$), confirming the superior ability of nanodiaplexes over nioplexes for gene delivery purposes. In this regard, the 1.25 mg/mL concentration of NDs used in the current study is higher than the concentrations described in other investigations, which range from 0.01 to 1 mg/mL, in order to maintain adequate biocompatibility. As a result, these findings demonstrate the advantages of combining NDs with cationic niosomes to generate a biocompatible, stable and high loading capacity vector.

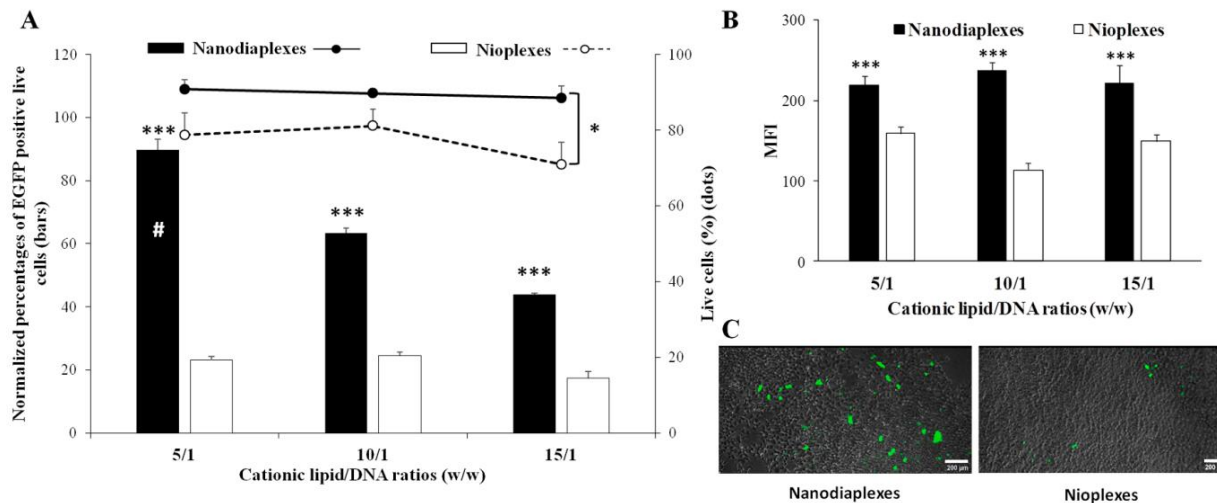


Figure 14: Transfection assay in the HEK-293 cell line 48 h post-transfection with nanodialogues and nioplexes. (A) Normalized percentages of EGFP-positive live cells (bars) and cell viability (dots). (B) MFI values. (C) Images showing the EGFP signal and cell integrity in HEK-293 cells transfected with nanodialogues and nioplexes at the 5/1 lipid/DNA ratio. Scale bar: 200 μm . Each value represents the mean \pm SD of three measurements. *** $p < 0.001$ and * $p < 0.05$ for nanodialogues vs nioplexes at the same lipid/DNA ratio; # $p < 0.001$ compared with all conditions.

Cellular uptake is one of the most important factors to consider when evaluating the transfer of material into cells. FITC-pEGFP positive signal in HEK-293 cells exposed to nanodialogues at a 5/1 lipid/DNA ratio was significantly higher than that of nioplexes (95.1 ± 3.9 vs $72.2 \pm 2.4\%$; $p < 0.05$) 4 hours after exposure to these complexes. The 25% increase in cellular uptake of nanodialogues relative to nioplexes could be considered as one of the possible reasons that increased their transfection efficiency (Figure 15), in agreement with previous findings in which NDs increased the cellular uptake of zwitterionic liposomes for drug delivery [69]. Important physicochemical properties of non-viral vectors, such as size, zeta potential, shape, and rigidity, appear to influence the internalization process and intracellular pathway followed by the nanoparticle and genetic material. In fact, rigid structures, small size, and positive zeta potential values are may be the most desirable characteristics for enhancing cellular uptake. In this respect, and knowing that nanodialogues are larger and slightly more positively charged than nioplexes, the physical and chemical features of NDs could contribute to the rigidity of the vector, thereby facilitating the internalization of nanodialogues by cells.

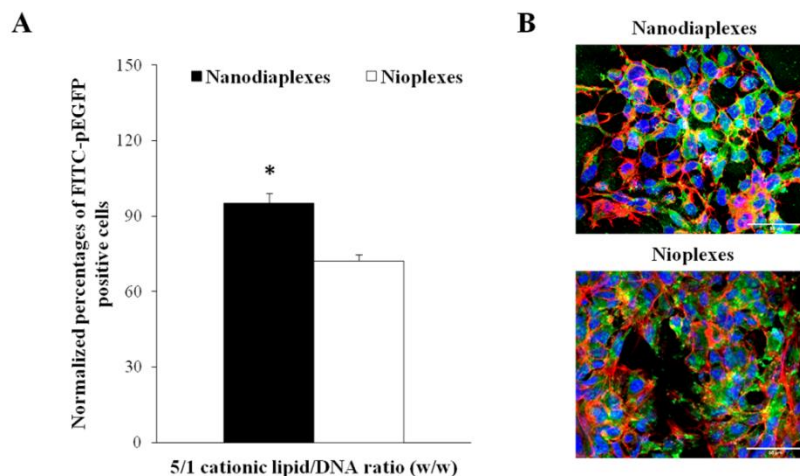


Figure 15: Cellular uptake of complexes at the 5/1 lipid/DNA ratio, analyzed 4 h after transfection in the HEK-293 cell line. (A) Normalized percentage of FITC-pEGFP positive cells. Each value represents the mean \pm SD of three measurements; * $p < 0.05$ for nanodiaplexes vs nioplexes. (B) Confocal microscopy images showing the cellular uptake of nanodiaplexes and nioplexes. Cell nuclei were colored in blue (DAPI), F-actin in red (Phalloidin), and nanodiaplexes and nioplexes in green (FITC). Scale bar: 50 μ m.

In addition, the internalization pathway followed by the vector and its DNA can play a significant role in determining its intracellular end. The majority of nanoparticles, including lipid-based vectors, are internalized mostly by pinocytosis, principally through receptor mediated endocytosis. We did not notice a prominent endocytic pathway when employing nanodiaplexes or nioplexes in this study, although our data revealed that nanodiaplexes were more likely to be trafficked via CME than nioplexes (Figure 16). In the case of particular endocytic pathway suppression experiments, our data revealed that when nanodiaplexes were administered to HEK-293 cells, endocytosis mediated by caveolae was the most potent endocytic pathway to transfect cells, because when this pathway was suppressed by genistein, the percentage of cells expressing EGFP plasmid reduced to approximately 30%. Accordingly, the addition of chemical components that trigger the CvME pathway could improve the transfection effectiveness of niosome formulations [70]. However, the suppression of CME and macropinocytosis reduced transfection efficiency levels to approximately 90%. In the instance of transfection efficiency mediated by nioplexes, the percentage of transfected cells reduced to approximately 70-80% with the suppression of CvME, CME and macropinocytosis, indicating that alternative endocytic route may

play a more significant role in the nioplex transfection process. Additional studies on trafficking going to the late endosomal compartment were conducted. It was observed that nanodiaplexes were shown to co-localize with lysosomes more than nioplexes (Figure 16). Indicating that NDs may promote the CME pathway, the internalized vesicle would lose its clathrin coat, resulting in the formation of an early endosome, a late endosome, and a lysosome.

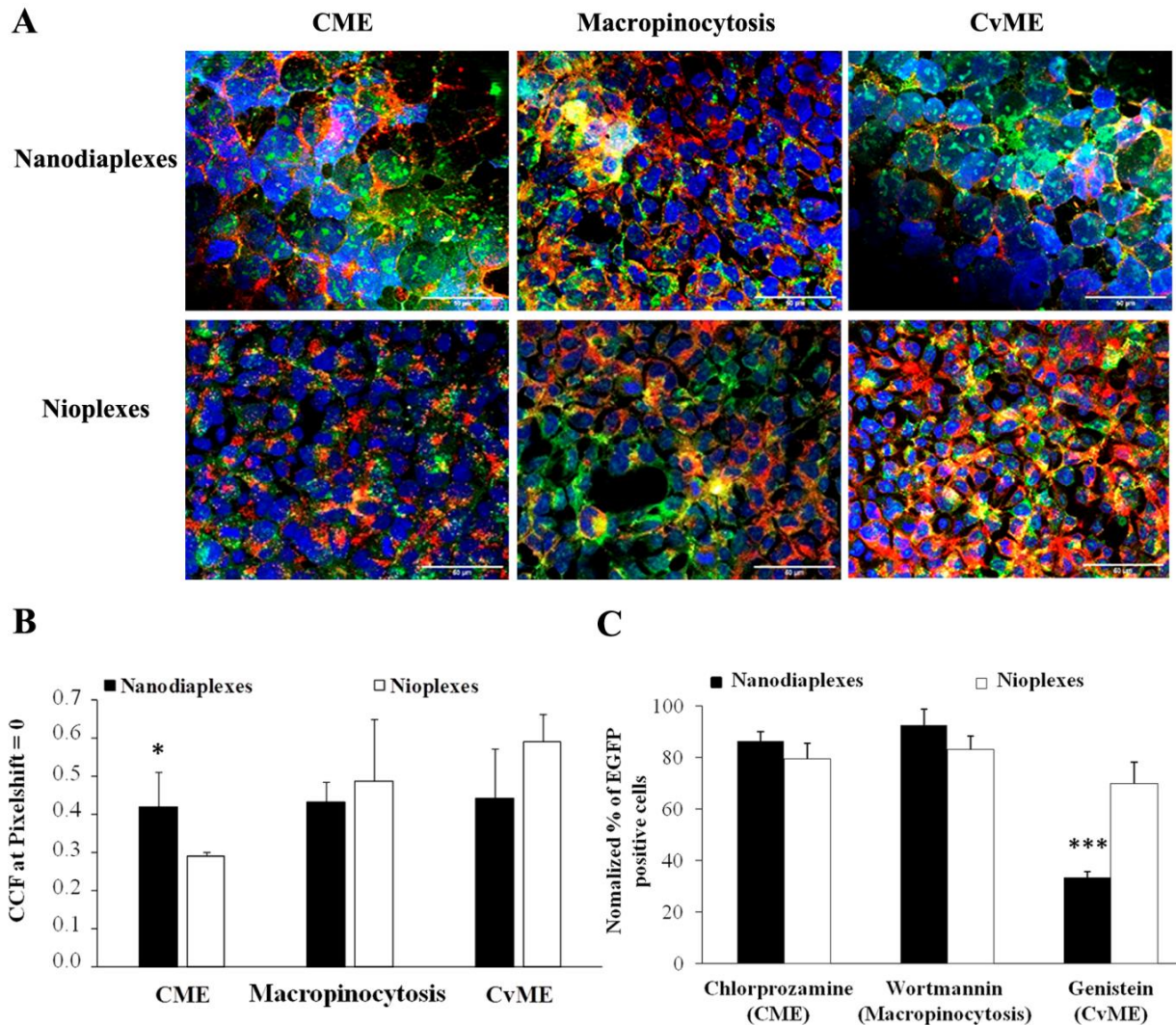


Figure 16: Intracellular disposition assay of nanodiaplexes and nioplexes in HEK-293 cells. (A) Qualitative analysis of colocalization by confocal microscopy. Scale bar: 50 μ m. (B) Quantitative determination of colocalization by cross-correlation analysis. Data are represented as mean \pm SD of three measurements; * $p > 0.05$ for nanodiaplexes vs nioplexes. (C) Transfection performance after the addition of specific endocytic inhibitors. The values were normalized to the transfection without an inhibitor. *** $p < 0.001$.

These results are in agreement with a prior but more fundamental intracellular trafficking analysis employing fluorescent NDs, which demonstrated their uptake in early endosomes and their localization in lysosomes. Curiously, the authors described the lysosomal compartment as a requirement for the exocytosis of these fluorescent NDs via lysosomal degradation pathway [71]. Notably, the artificial anionic PS micelles prepared in this study to simulate this late endosomal compartment (Figure 17) demonstrated that nanodiasomes had superior endosomal escape properties than niosomes, the resulting values were 32.26 % for nanodiaplexes and 22.63% for nioplexes.

These findings indicate that the addition of NDs in the formulation enhances the endosomal escape ability in HEK-293 cells by 1.43-fold (about 30 %) compared to the absence of NDs. The most likely escape mechanism for nanodiaplexes from endosomes involves the direct fusion of nanoparticles with the endosome membrane, as evidenced by their co-localization with lysosomes, and the formation of pores in the endosome surface due to the induction of stress and internal tension in the membrane, as indicated by the large amount of DNA released from this type of compartment [72]. Our observations imply that the increased transfection effectiveness of nanodiaplexes over nioplexes may be primarily attributable to the increased cellular uptake, the rigidity that NDs give to nanodiaplexes and the lysosomal escape capabilities encouraged by NDs.

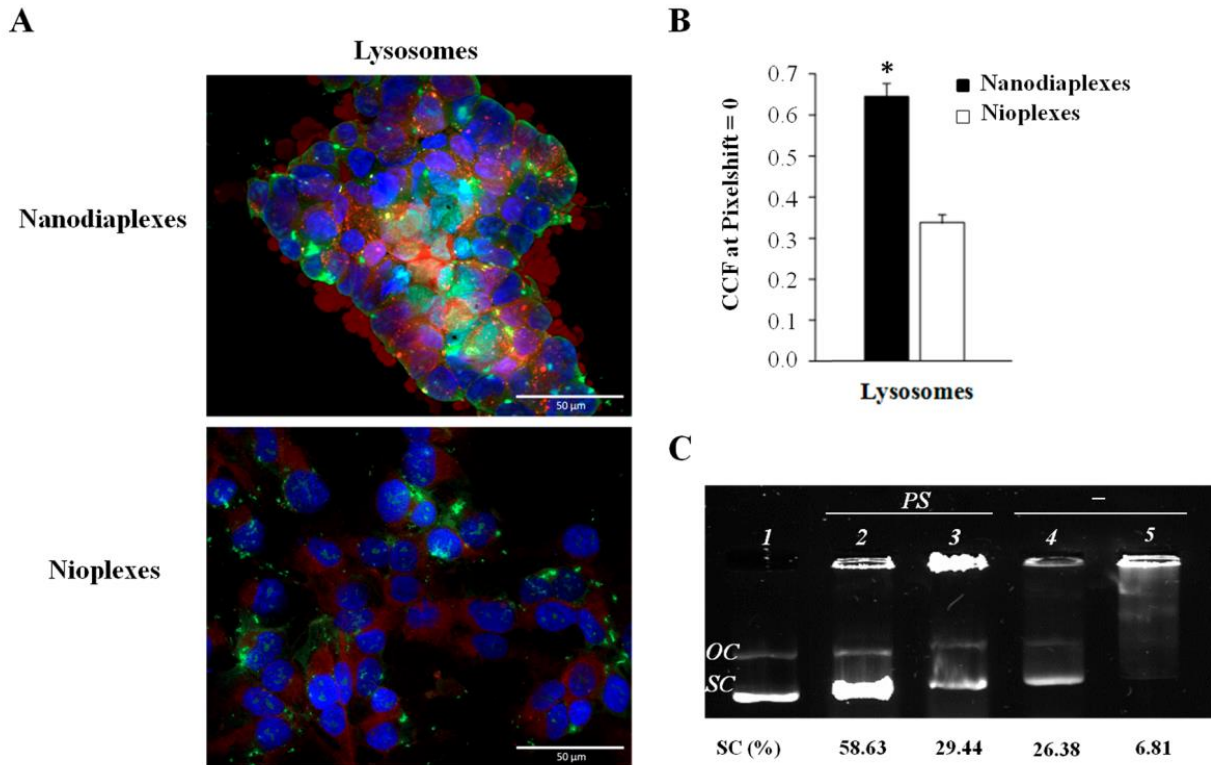


Figure 17: Biological performance of nanodiaplexes and nioplexes in lysosomes of HEK-2993 cells. (A) Qualitative analysis of colocalization by confocal microscopy. (B) Quantitative determination of colocalization by cross-correlation analysis. Data are represented as mean \pm SD of three measurements; * $p > 0.05$ for nanodiaplexes vs nioplexes. (C) DNA release profiles evaluated by gel electrophoresis. Lane 1, naked DNA; lane 2, nanodiaplexes incubated with PS; lane 3, nioplexes incubated with PS; lane 4, nanodiaplexes; lane 5, nioplexes. PS refers to phosphatidylserine micelles; OC: open circular form; SC: supercoiled form.

Additional gene delivery studies were conducted in primary CNS cells derived from cerebral and retinal sources employing nanodiaplexes with a 5/1 lipid/DNA ratio in order to advance to a more realistic *in vivo* model microenvironment. Immunocytochemistry revealed the GFP signal in both primary cell cultures (Figure 18), demonstrating the ability of nanodiaplexes to transfer genetic materials to CNS cells.

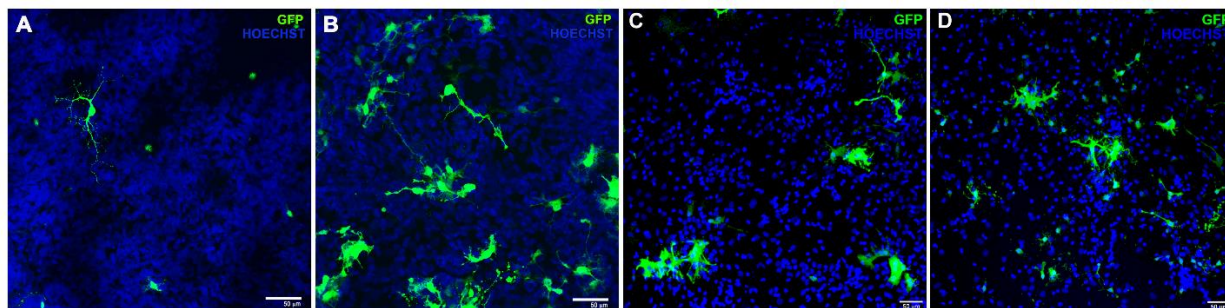


Figure 18: GFP expression in embryonic rat CNS primary cells. Neuronal and retinal primary cells transfected with nanodiamonds (A, C) at the 5/1 lipid/DNA ratio and the positive control Lipofectamine 2000 in primary neuronal (B) and retinal cells (D). Cell nuclei were stained with Hoechst 33342 (blue). Scale bar: 50 μm .

NDs incorporated into niosomes emerge as a promising and safe non-viral method with potential biological advantages for gene therapy, particularly for CNS diseases. These findings are still a proof of concept, and more research in animal models is needed to confirm the reported capability of nanodiamonds for gene transfer. NDs may be successfully fabricated with a wide variety of chemical compounds, have a high surface area-to-volume ratio, and their production process is easy to scale [73, 74]. Due to the limited stability of NDs in suspension, their combination with niosome formulations may be required to offer the improved stability required for gene delivery applications. Consequently, in the third experimental part of this doctoral thesis, we evaluated the stability of nanodiamonds and niosomes over time and at different storage temperatures. Physicochemical studies and transfection efficiency experiments *in vitro* and *in vivo* were conducted in the present study, the mean particle size of freshly prepared nanodiamond formulations at day 0 (Figure 19) was 128.7 ± 4.2 nm, which remained stable over time and only increased significantly ($P < 0.05$) after 30 days of storage at 25°C . Concerning the niosome formulation, the mean particle size at day 0 was 90.5 ± 10.3 nm and showed significant variations ($P < 0.05$) on days 15 and 30 of storage at 25°C and 4°C . The zeta potentials of nanodiamond showed greater variations than niosomes. We found that fresh-prepared nanodiamonds had an average zeta potential of 35.2 ± 0.3 mV at day 0, which increased significantly after 30 days of storage at both 4°C and 25°C . While the mean zeta potential of niosome formulations was 20.2 ± 2.5 mV on day 0, which increased significantly after 15 days of storage at 25°C ($P < 0.05$) and decreased after 30 days of storage at 4°C ($P < 0.05$) and 25°C ($P < 0.01$), respectively. Nanodiamond dispersity values were low and remained stable with few variations under all

investigated conditions, whereas niosome formulations exhibited higher dispersity values and more variations, especially after 15 days of storage at 25°C. The reduced dispersity values reported with nanodiasomes indicated a formulation with a more uniform particle size distribution than the niosomes. Both formulations exhibited statistically relevant variations in their physicochemical properties, particularly after 30 days of storage at 25°C, showing that formulations are better conserved if stored at 4°C compared to higher temperatures. Physicochemically, nanodiasomes are somewhat more stable than niosomes throughout time. NDs integration in the lipid structure of niosomes is able to provide more stability and rigidity to the formulation. NDs were shown to be incorporated in the lipid layer of Nanodiasomes seen under cryo-TEM.

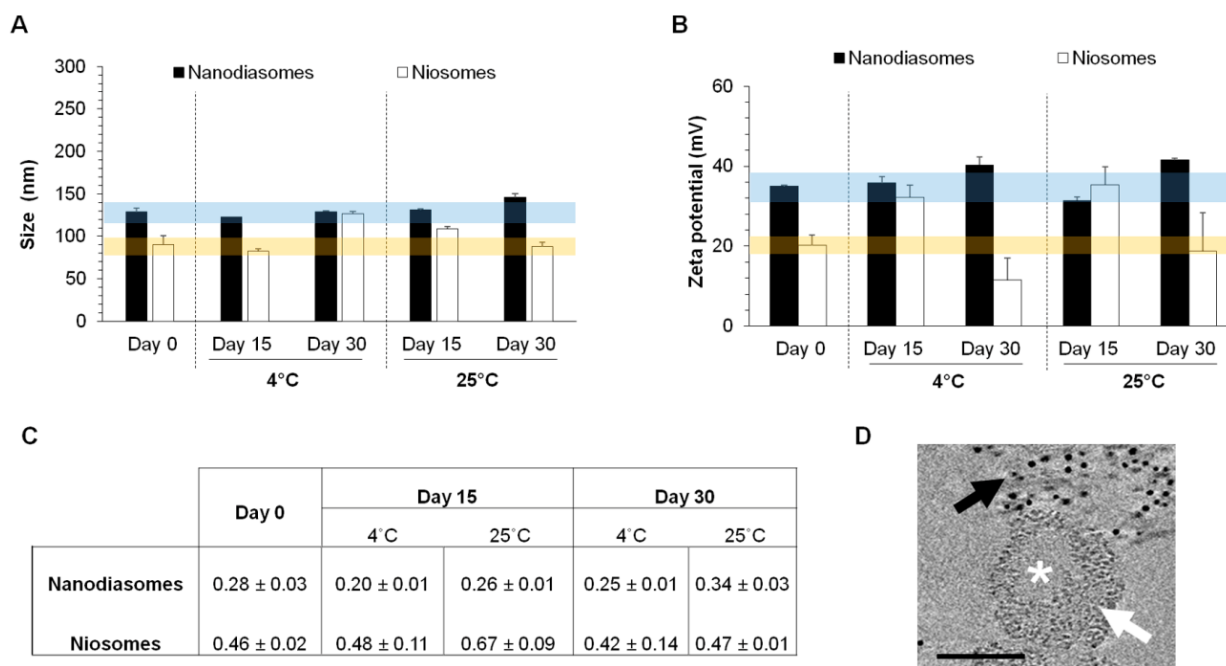


Figure 19: Physicochemical characterization and stability of formulations at different days and storage temperature. A. Mean particle size. B. Zeta potential. C. Dispersity. Each value shows the mean \pm SD of 3 readings. Blue and orange stripes represent $\pm 10\%$ deviation respect to nanodiasomes and niosomes parameters at day 0, respectively. D. Cryo-TEM image of a nanodiasome; asterisk indicates the aqueous phase; white arrow indicates the lipid layer of the nanodiasome with nanodiamonds integrated in the lipid structure; black arrow indicates higher densities of the tomogram (more electron-dense material), which correspond to gold nanoparticles added to the sample for tilt series alignment. Scale bar: 100 nm.

Following their determination of physicochemical parameters, HEK-293 transfection assays were conducted *in vitro*. We found that cells transfected with nanodiaplexes had greater cell viability than those transfected with nioplexes, indicating that formulations based on nanodiasomes are better tolerated by these cells. The mean percentage of live cells exposed to freshly prepared nanodiaplexes was $90.79 \pm 2.5\%$, while this value was significantly lower ($P < 0.001$) for nioplexes which presented a mean percentage of live cells of $78.8 \pm 5.8\%$ (Figure 3A, lines). These values remained relatively stable over time and at different storage temperatures, with little oscillations but no statistically relevant differences compared to the values of day 0 in both formulations. These results are in agreement with the great biocompatibility and low toxicity previously reported for NDs.

Additionally, the gene delivery efficiency of nanodiaplexes was about 4-fold greater than nioplexes the percentage of EGFP expressing live cells exposed to freshly prepared nanodiaplexes and nioplexes were $89.8 \pm 3.4\%$ and $23.3 \pm 1.1\%$, respectively (Figure 20). Higher transfection percentages in cells treated with nanodiaplexes than with nioplexes ($P < 0.001$), with significantly higher MFI values of nanodiaplexes over nioplexes ($P < 0.001$) was maintained over time and storage conditions. In this regard, it is important to note that the number of DNA copies per cell decreased gradually for nioplexes from day 15, but nanodiaplexes never had any alteration in this parameter until day 30. Taken all together, this could suggest that the integration of NDs with niosomes promotes the stability of the formulation, providing more regular and successful transfection results over time.

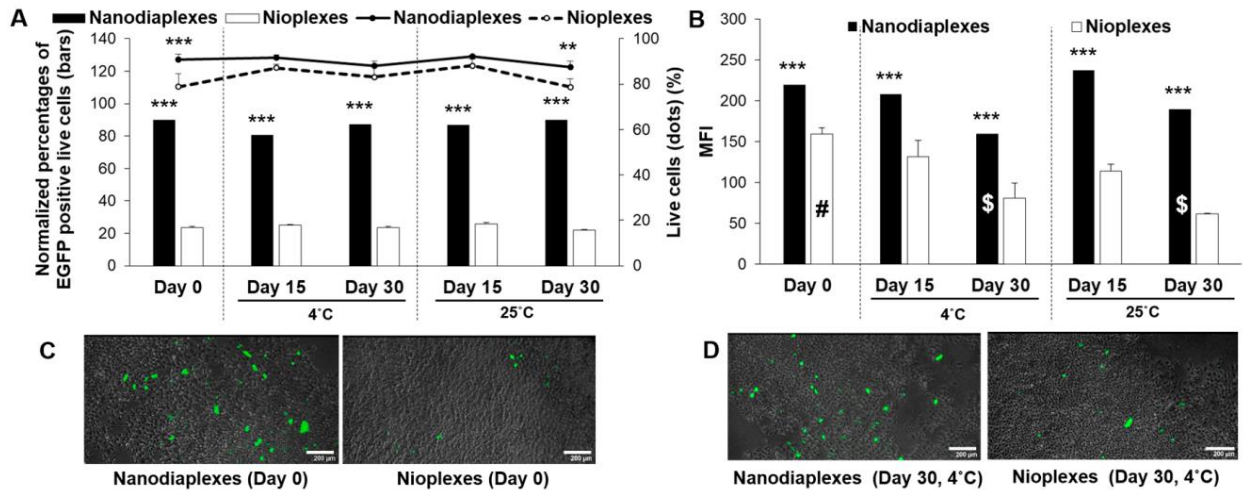


Figure 20: Gene delivery efficiency and toxicity of formulations in HEK-293 cells 48 hours after transfection with nanodiaplexes and nioplexes at 5/1 cationic lipid/DNA ratio (w/w) over time at 4°C and 25°C. A. Normalized percentages of EGFP positive live cells (bars) and cell viability (dots). B. Mean fluorescence intensity values. Each value represents the mean \pm SD of 3 measurements. C-D. Merged images showing EGFP signal in HEK-293 cells transfected with both complexes at 5/1 lipid/DNA ratio (w/w) at day 0 (C) and after 30 days of storage at 4°C (D). Scale bars: 200 μ m. *** $P < 0.001$; ** $P < 0.01$ for nanodiaplexes vs nioplexes, no negative significant differences in term of live cells (%) for nioplexes between day 0 and the rest of days and temperatures; # $P < 0.05$ for nioplexes between day 0 and the rest of days and temperatures; \$ $P < 0.05$ for nanodiaplexes at day 30 compared with the rest of days and temperatures.

To fully explain the variations seen between both formulations, we evaluated their cellular uptake after 0 and 30 days after being stored at 4°C (Figure 21). We found a significant variations ($P < 0.05$) in the percentage of cellular uptake between the two formulations, achieving about 100 % uptake with nanodiaplexes and around 70% uptake with nioplexes under both storage conditions, which could support the hypothesis that NDs increase the rigidity of the niosome formulation, improving cellular entry [75]. This improved cell uptake may partially explain the differences in transfection efficiency between the two formulations, but additional factors must also be considered. Endocytosis of non-viral vectors is traditionally mediated by the endosomal pathway, which usually ends in the formation of endosomal vesicles with an acidic environment and digestive enzymes. In these vesicles, DNA is susceptible to degradation before reaching the nucleus. Therefore, DNA endosomal escape becomes a crucial step for effective gene delivery. In

this regard, it has been reported that NDs are able to escape endosome restriction by rupturing the vesicle membrane shortly after cellular uptake, which would also explain the superior gene delivery efficiency of nanodiaplexes compared to nioplexes.

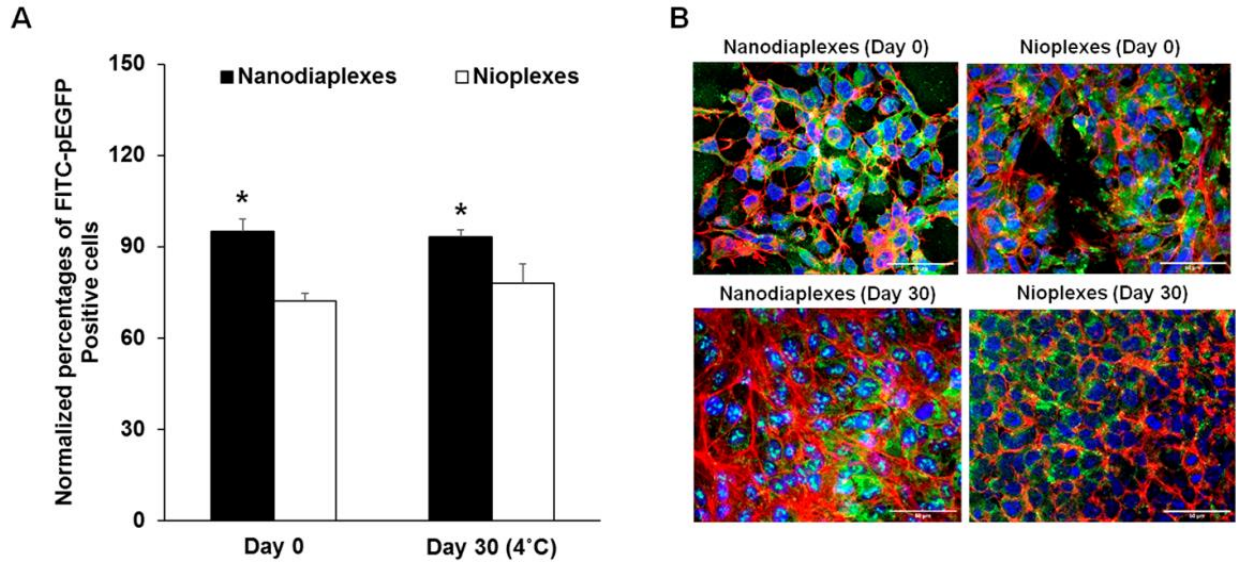


Figure 21: Cellular uptake in HEK-293 cells 4 h after exposure to nanodiaplexes and nioplexes at 5/1 lipid/DNA ratio (w/w) at day 0 and after 30 days of storage at 4°C. A. Normalized percentages of FITC-pEGFP positive live cells after the exposure to these complexes. Each value represents the mean \pm SD of 3 measurements. B. Confocal microscopy images. Cell nuclei were colored in blue (DAPI); F-actin in red (Phalloidin); nanodiaplexes and nioplexes in green (FITC). Scale bars: 50 μ m. * $P < 0.05$ for nanodiaplexes vs nioplexes.

Furthermore, additional transfection experiments on CNS cells (Figure 22), both retinal and neuronal primary cells, revealed successful transfection post transfection with freshly prepared and nanodiaplexes that had been maintained for 30 days.

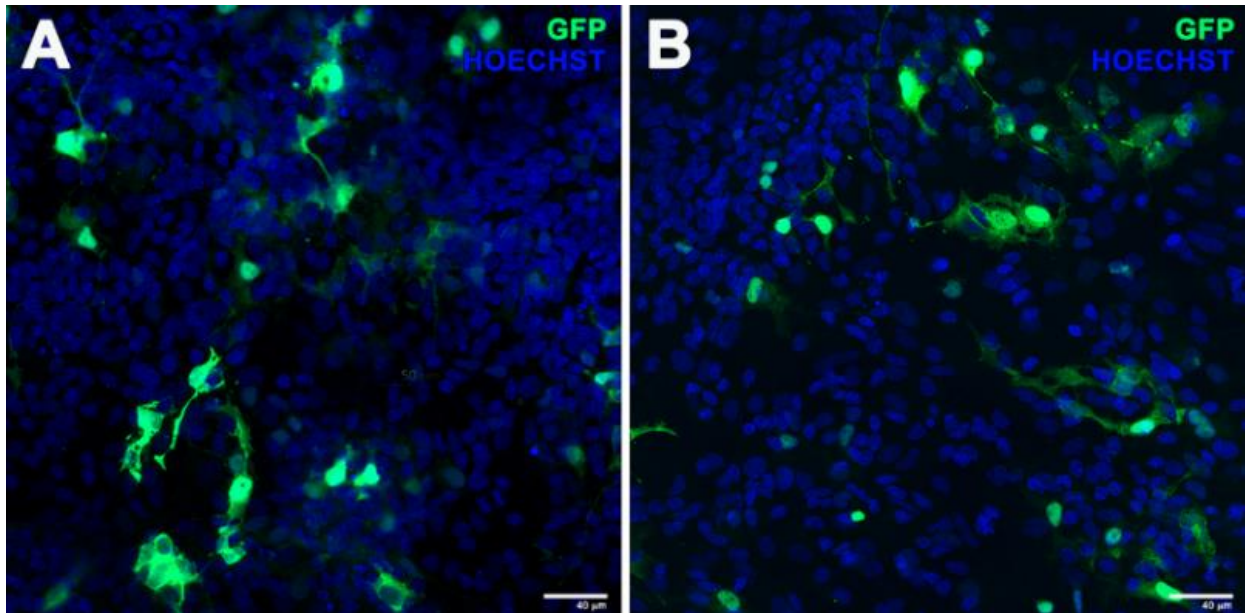


Figure 22: EGFP signal in primary culture of rat retinal cells transfected with freshly prepared (A) and 30 days stored at 4 °C (B) nanodiasomes at 5/1 lipid/DNA ratio (w/w). Scale bar: 40 μm. Blue: Hoechst 33,342 (cell nuclei); Green: EGFP. Scale bars: 40 μm.

Based on the results obtained, we conducted an *in vivo* assay in order to determine the gene delivery efficiency of fresh and 30 days stored nanodiaplexes in rat retina (Figure 23). Injections were administered via intravitreal and subretinal routes, which are commonly utilized in the clinic for the treatment of hereditary retinal diseases [76]. In most cases, following intravitreal injection, the retina's ganglion cell layer demonstrates high transgene expression levels, which could be useful for the treatment of glaucoma [77, 78], a widely common genetic retinal disorder that causes blindness. On the other hand, the more invasive subretinal route is useful for transfecting the outer layer of the retina [77, 78], which would be interesting for addressing retinal diseases like Leber's congenital amaurosis, Stargard's disease, and retinitis pigmentosa [79], that related to mutations at the photoreceptor and retinal pigment epithelium level.

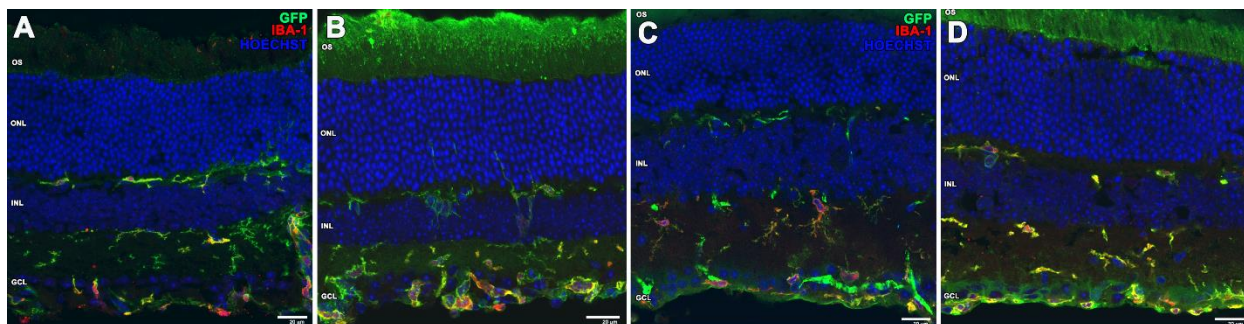


Figure 23: *In vivo* assays showing EGFP signal in rat retina after intravitreal (IV) (A-C) and subretinal (SR) (B-D) administration of freshly prepared (A-B) and 30 days stored (C-D) nanodiaplexes vectoring EGFP plasmid at 5/1 lipid/DNA ratio (w/w). Blue: Hoechst 33,342 (cell nuclei); Green: EGFP; Red: Iba-1. OS: outer segments; ONL: outer nuclear layer; INL; inner nuclear layer; GCL: ganglion cell layer. Scale bar: 20 μm .

In this work, EGFP signal was mostly detected in microglial cells. This expression was also found in both the inner and outer retinal layers after intravitreal and subretinal injections of nanodiaplexes, indicating that this formulation is capable of passing efficiently along the different retinal layers to achieve high transgene expression at different levels, which would be therapeutically useful. In addition, the results demonstrated a high level of EGFP expression *in vivo* following administrations of a formulation that had been stored at 4°C for 30 days, indicating that storage of the formulation at 4°C for 30 days has no effect on its transfection efficiency.

5. Bibliography

- [1] Gonçalves, Giulliana Augusta Rangel, and Raquel de Melo Alves Paiva. "Gene therapy: advances, challenges and perspectives." *Einstein* (Sao Paulo, Brazil) vol. 15,3 (2017): 369-375.
- [2] Muthuraman A, Mehdi S, Rishitha N. Chapter 4 - current trends in site and target specific delivery of nanomedicine for gene therapy. In: Grumezescu AM, ed. *Nanoparticles in pharmacotherapy*. William Andrew Publishing; 2019:73-112.
- [3] Sinclair A, Islam S, Jones S. Gene therapy: An overview of approved and pipeline technologies. In: *CADTH issues in emerging health technologies*. Ottawa (ON): Canadian Agency for Drugs and Technologies in Health; 2016.
- [4] Friedmann T. A brief history of gene therapy. *Nat Genet*. 1992;2(2):93-98. Accessed Jun 17, 2022.
- [5] Schneider BL, Gaugler MN, Aebischer P. Chapter 20 - viral vectors: A potent approach to generate genetic models of parkinson's disease. In: Nass R, Przedborski S, eds. *Parkinson's disease*. San Diego: Academic Press; 2008:269-284.
- [5] Gaj T, Gersbach CA, Barbas CF. ZFN, TALEN, and CRISPR/cas-based methods for genome engineering. *Trends in biotechnology* (Regular ed.). 2013;31(7):397-405.
- [6] Friedmann T. A brief history of gene therapy. *Nat Genet*. 1992;2(2):93-98. Accessed Jun 17, 2022. doi: 10.1038/ng1092-93.
- [7] Ramamoorth M, Narvekar A. Non viral vectors in gene therapy- an overview. *J Clin Diagn Res*. 2015;9(1):GE01-GE6.
- [8] Walther W, Stein U. Viral vectors for gene transfer: a review of their use in the treatment of human diseases. *Drugs*. 2000 Aug;60(2):249-71.
- [9] Nayerossadat N, Maedeh T, Ali PA. Viral and nonviral delivery systems for gene delivery. *Adv Biomed Res*. 2012;1:27.
- [10] Weber T. Anti-AAV Antibodies in AAV Gene Therapy: Current Challenges and Possible Solutions. *Front Immunol*. 2021 Mar 17;12:658399.
- [11] Glover, D., Lipps, H. & Jans, D. Towards safe, non-viral therapeutic gene expression in humans. *Nat Rev Genet* 6, 299–310 (2005).
- [12] Pezzoli D, Chiesa R, De Nardo L, Candiani G. We still have a long way to go to effectively deliver genes! *J Appl Biomater Funct Mater*. 2012 Sep 27;10(2):82-91.
- [13] Cantore A, Fraldi A, Meneghini V and Gritti A (2022) In vivo Gene Therapy to the Liver and Nervous System: Promises and Challenges. *Front. Med*. 8:774618.
- [14] Mears, Emily Rose et al. "A Review: The Current In Vivo Models for the Discovery and Utility of New Anti-leishmanial Drugs Targeting Cutaneous Leishmaniasis." *PLoS neglected tropical diseases* vol. 9,9 e0003889. 3 Sep. 2015

- [15] Baranyi L, Slepishkin V, Dropulic B. Chapter 1 - ex vivo gene therapy: Utilization of genetic vectors for the generation of genetically modified cell products for therapy. In: Lattime EC, Gerson SL, eds. Gene therapy of cancer (third edition). San Diego: Academic Press; 2014:3-18.
- [16] Sinclair A, Islam S, Jones S. Gene therapy: An overview of approved and pipeline technologies. In: CADTH issues in emerging health technologies. Ottawa (ON): Canadian Agency for Drugs and Technologies in Health; 2016
- [17] Li, H., Yang, Y., Hong, W. et al. Applications of genome editing technology in the targeted therapy of human diseases: mechanisms, advances and prospects. *Sig Transduct Target Ther* 5, 1 (2020).
- [18] Vítor AC, Huertas P, Legube G and de Almeida SF (2020) Studying DNA Double-Strand Break Repair: An Ever-Growing Toolbox. *Front. Mol. Biosci.* 7:24.
- [19] Sainz-Ramos, Myriam et al. "How Far Are Non-Viral Vectors to Come of Age and Reach Clinical Translation in Gene Therapy?." *International journal of molecular sciences* vol. 22,14 7545. 14 Jul. 2021, doi:10.3390/ijms22147545
- [20] Gottfried, Lynn, Dean, David. "Extracellular and Intracellular Barriers to Non-Viral Gene Transfer". *Novel Gene Therapy Approaches*, edited by Ming Wei, David Good, IntechOpen, 2013. 10.5772/54699.
- [21] Li, L.; Hu, S.; Chen, X. Non-Viral Delivery Systems for CRISPR/Cas9-Based Genome Editing: Challenges and Opportunities. *Biomaterials* 2018, 171, 207–218.
- [22] Escoffre, J.M.; Teissie, J.; Rols, M.P. Gene Transfer: How can the Biological Barriers be Overcome? *J. Membr.Biol.* 2010, 236, 61–74
- [23] Pérez-Martínez, F.C., Guerra, J., Posadas, I. et al. Barriers to Non-Viral Vector-Mediated Gene Delivery in the Nervous System. *Pharm Res* 28, 1843–1858 (2011).
- [24] Himawan E, Ekström P, Buzgo M, et al. Drug delivery to retinal photoreceptors. *Drug Discovery Today.* 2019;24(8):1637-1643.
- [25] Manzanares, Darío, and Valentín Ceña. "Endocytosis: The Nanoparticle and Submicron Nanocompounds Gateway into the Cell." *Pharmaceutics* vol. 12,4 371. 17 Apr. 2020,
- [26] Popova N.V., Deyev I.E., Petrenko A.G. Clathrin-mediated endocytosis and adaptor proteins. *Acta Nat.* 2013;5:62–73.
- [27] Pelkmans L., Burli T., Zerial M., Helenius A. Caveolin-stabilized membrane domains as multifunctional transport and sorting devices in endocytic membrane traffic. *Cell.* 2004;118:767–780.
- [28] Wang, Chensu et al. "Investigation of endosome and lysosome biology by ultra pH-sensitive nanoprobe." *Advanced drug delivery reviews* vol. 113 (2017): 87-96.

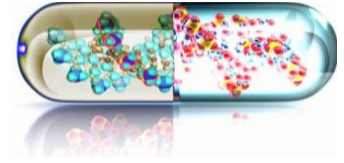
- [29] Dauty, E.; Verkman, A.S. Actin Cytoskeleton as the Principal Determinant of Size-Dependent DNA Mobility in Cytoplasm: A New Barrier for Non-Viral Gene Delivery. *J. Biol. Chem.* 2005, 280, 7823–7828.
- [30] Lukacs, G.L.; Haggie, P.; Seksek, O.; Lechardeur, D.; Freedman, N.; Verkman, A.S. Size-Dependent DNA Mobility in Cytoplasm and Nucleus. *J. Biol. Chem.* 2000, 275, 1625–1629.
- [31] Barua, Sutapa, and Samir Mitragotri. “Challenges associated with Penetration of Nanoparticles across Cell and Tissue Barriers: A Review of Current Status and Future Prospects.” *Nano today* vol. 9,2 (2014): 223-243. doi:10.1016/j.nantod.2014.04.008
- [32]. Macara IG. *Microbiol. Mol. Biol. Rev.* 2001;65:570.
- [33] Chee-Kai C, David AJ. *Immunol. Cell Biol.* 2002;80:119.
- [34] Akita, H.; Tanimoto, M.; Masuda, T.; Kogure, K.; Hama, S.; Ninomiya, K.; Futaki, S.; Harashima, H. Evaluation of the Nuclear Delivery and Intra-Nuclear Transcription of Plasmid DNA Condensed with Micro (Mu) and NLS-Micro by Cytoplasmic and Nuclear Microinjection: A Comparative Study with Poly-L-Lysine. *J. Gene Med.* 2006, 8, 198–206.
- [35] Al Qtaish N, Gallego I, Villate-Beitia I, Sainz-Ramos M, López-Méndez TB, Grijalvo S, Eritja R, Soto-Sánchez C, Martínez-Navarrete G, Fernández E, Puras G, Pedraz JL. Niosome-Based Approach for In Situ Gene Delivery to Retina and Brain Cortex as Immune-Privileged Tissues. *Pharmaceutics*. 2020 Feb 25;12(3):198.
- [36] Al-Dosari MS, Gao X. Nonviral gene delivery: principle, limitations, and recent progress. *AAPS J.* 2009 Dec;11(4):671-81. doi: 10.1208/s12248-009-9143-y. Epub 2009 Oct 16. PMID: 19834816; PMCID: PMC2782077.
- [37] Cevher, Erdal, Sezer, Ali, Çağlar, Emre. "Gene Delivery Systems: Recent Progress in Viral and Non-Viral Therapy". *Recent Advances in Novel Drug Carrier Systems*, edited by Ali Sezer, IntechOpen, 2012. 10.5772/53392.
- [38] Ge, Xuemei et al. “Advances of Non-Ionic Surfactant Vesicles (Niosomes) and Their Application in Drug Delivery.” *Pharmaceutics* vol. 11,2 55. 29 Jan. 2019.
- [39] Chidambaram SB, Ray B, Bhat A, et al. Chapter 5 - mitochondria-targeted drug delivery in neurodegenerative diseases. In: Shegokar R, ed. *Delivery of drugs*. Elsevier; 2020:97-117.
- [40] Sainz-Ramos M, Villate-Beitia I, Gallego I, A L Qtaish N, Lopez-Mendez TB, Eritja R, Grijalvo S, Puras G, Pedraz JL. Non-viral mediated gene therapy in human cystic fibrosis airway epithelial cells recovers chloride channel functionality. *Int J Pharm.* 2020 Oct 15;588:119757
- [41] Attia N., Mashal M., Grijalvo S., Eritja R., Puras G., Pedraz J.L. Cationic niosome-based hBMP7 gene transfection of neuronal precursor NT2 cells to reduce the migration of glioma cells in vit
- [42] Puras G, Mashal M, Zárata J, et al. A novel cationic niosome formulation for gene delivery to the retina. *J Controlled Release.* 2014;174:27-36.

- [43] Zhi D, Bai Y, Yang J, et al. A review on cationic lipids with different linkers for gene delivery. *Adv Colloid Interface Sci.* 2018;253:117-140.
- [44] Ojeda E, Puras G, Agirre M, et al. The role of helper lipids in the intracellular disposition and transfection efficiency of niosome formulations for gene delivery to retinal pigment epithelial cells. *Int J Pharm.* 2016;503(1):115-126.
- [45] A. P. Dabkowska, D. J. Barlow, R. A. Campbell, A. V. Hughes, P. J. Quinn, and M. J. Lawrence *Biomacromolecules* 2012 13 (8), 2391-2401
- [46]. Attia N, Mashal M, Puras G, Pedraz JL. Mesenchymal Stem Cells as a Gene Delivery Tool: Promise, Problems, and Prospects. *Pharmaceutics.* 2021;13(6):843. Published 2021 Jun 7.
- [47] Agirre, M.; Ojeda, E.; Zarate, J.; Puras, G.; Grijalvo, S.; Eritja, R.; Garcia del Cano, G.; Barrondo, S.; Gonzalez-Burguera, I.; Lopez de Jesus, M.; et al. New Insights into Gene Delivery to Human Neuronal Precursor NT2 Cells: A Comparative Study between Lipoplexes, Nioplexes, and Polyplexes. *Mol. Pharm.* 2015, 12, 4056–4066.
- [48] Grijalvo, S.; Puras, G.; Zarate, J.; Sainz-Ramos, M.; Qtaish, N.A.L.; Lopez, T.; Mashal, M.; Attia, N.; Diaz, D.; Pons, R.; et al. Cationic Niosomes as Non-Viral Vehicles for Nucleic Acids: Challenges and Opportunities in Gene Delivery. *Pharmaceutics* 2019, 11, 50.
- [49] Moraru AD, Costin D, Iorga RE, Munteanu M, Moraru RL and Branisteanu DC: Current trends in gene therapy for retinal diseases (Review). *Exp Ther Med* 23: 26, 2022
- [50] Rejman J, Oberle V, Zuhorn IS, Hoekstra D. Size-dependent internalization of particles via the pathways of clathrin- and caveolae-mediated endocytosis. *Biochem J.* 2004;377(Pt 1):159-169.
- [51] Grimaldi N, Andrade F, Segovia N, et al. Lipid-based nanovesicles for nanomedicine. *Chem Soc Rev.* 2016;45(23):6520-6545.
- [52]. BT H, AE A, LP, OS, MJ C, BL W. Intranasal administration of plasmid DNA nanoparticles yields successful transfection and expression of a reporter protein in rat brain. *Gene Ther.* 2014;21(5):514.
- [53] J. Li, X. Wang, T. Zhang, C. Wang, Z. Huang, X. Luo, Y. Deng, A Review on Phospholipids and their Main Applications in Drug Delivery Systems, *Asian J. Pharmaceutical Sci.* 10 (2) (2015) 81–98.
- [54] N. Bartke, Y.A. Hannun, Bioactive sphingolipids: metabolism and function, *J. Lipid. Res.* 50 (2009) S91–S96.
- [55] I. Villate-Beitia, I. Gallego, G. Martínez-Navarrete, J. Zarate, T. Lopez-Méndez, C. Soto-Sanchez, E. Santos-Vizcaíno, G. Puras, E. Fernandez, J.L. Pedraz, Polysorbate 20 non-ionic surfactant enhances retinal gene delivery efficiency of cationic niosomes after intravitreal and subretinal administration, *Int. J. Pharm.* 550 (1-2) (2018) 388–397.
- [56] A.T. Jones, searching for an endocytic identity and role in the uptake of cell penetrating peptides, *J. Cell. Mol. Med.* 11 (4) (2007) 670–684.

- [57] J.P. Lim, P.A. Gleeson, Macropinocytosis: an endocytic pathway for internalising large gulps, *Immunol. Cell. Biol.* 89 (8) (2011) 836–843.
- [58] D. Delgado, A. del Pozo-Rodríguez, M.A. Solinís, A. Rodríguez-Gascon, Understanding the mechanism of protamine in solid lipid nanoparticle-based lipofection: the importance of the entry pathway, *Eur. J. Pharm. Biopharm.* 79 (3) (2011) 495–502.
- [59] Liang, W. and Jenny K W Lam. “Endosomal Escape Pathways for Non-Viral Nucleic Acid Delivery Systems.”, 2012.
- [60] R.W. Ledeen, G. Wu, Nuclear sphingolipids: metabolism and signaling, *J. Lipid Res.* 49 (6) (2008 Jun) 1176–1186.
- [61] N.C. Lucki, M.B. Sewer, Nuclear Sphingolipid Metabolism, *Annu. Rev. Physiol.* 74 (1) (2012) 131–151.
- [62] A.M. O’Mahony, B.M. Godinho, J.F. Cryan, C.M. O’Driscoll, Non-Viral Nanosystems for Gene and Small Interfering RNA Delivery to the Central Nervous System: Formulating the Solution, *J. Pharm. Sci.* 102 (2013) 3469–3484.
- [63] Y. Zhang, F. Schlachetzki, J.Y. Li, R.J. Boado, W.M. Pardridge, Organ-specific gene expression in the rhesus monkey eye following intravenous non-viral gene transfer, *Mol. Vis.* 3 (9) (2003 Oct) 465–472.
- [64] M. Mashal, N. Attia, G. Puras, G. Martinez-Navarrete, E. Fernandez, J.L. Pedraz, Retinal Gene Delivery Enhancement by Lycopene Incorporation into Cationic Niosomes Based on DOTMA and Polysorbate 60, *J. Control. Release* 254 (2017) 55–64.
- [65] Ho, D.; Wang, C. H.; Chow, E. K. Nanodiamonds: The Intersection of Nanotechnology, Drug Development, and Personalized Medicine. *Sci. Adv.* 2015, 1, No. e1500439.
- [66] Chauhan, S.; Jain, N.; Nagaich, U. Nanodiamonds with Powerful Ability for Drug Delivery and Biomedical Applications: Recent Updates on In Vivo Study and Patents. *J. Pharm. Anal.* 2020, 10, 1–12.
- [67] Zhu, Y.; Li, J.; Li, W.; Zhang, Y.; Yang, X.; Chen, N.; Sun, Y.; Zhao, Y.; Fan, C.; Huang, Q. The Biocompatibility of Nanodiamonds and Their Application in Drug Delivery Systems. *Theranostics* 2012, 2, 302–312.
- [68] Zhang, Z.; Niu, B.; Chen, J.; He, X.; Bao, X.; Zhu, J.; Yu, H.; Li, Y. The Use of Lipid-Coated Nanodiamond to Improve Bioavailability and Efficacy of Sorafenib in Resisting Metastasis of Gastric Cancer. *Biomaterials* 2014, 35, 4565–4572.
- [69] Wang, F.; Liu, J. Nanodiamond Decorated Liposomes as Highly Biocompatible Delivery Vehicles and a Comparison with Carbon Nanotubes and Graphene oxide. *Nanoscale* 2013, 5, 12375– 12382.
- [70] Delgado, D.; del Pozo-Rodríguez, A.; Solinís, M. A.; RodríguezGascon, A. Understanding the Mechanism of Protamine in Solid Lipid Nanoparticle-Based Lipofection: the Importance of the Entry Pathway. *Eur. J. Pharm. Biopharm.* 2011, 79, 495–502.

- [71] Prabhakar, N.; Khan, M. H.; Peurla, M.; Chang, H. C.; Hanninen, P. E.; Rosenholm, J. M. Intracellular Trafficking of Fluorescent Nanodiamonds and Regulation of Their Cellular Toxicity. *ACS Omega* 2017, 2, 2689–2693.
- [72] Varkouhi, A. K.; Scholte, M.; Storm, G.; Haisma, H. J. Endosomal Escape Pathways for Delivery of Biologicals. *J. Controlled Release* 2011, 151, 220–228. (57) Kimura, S.; Harashim
- [73] Liu KK, Cheng CL, Chang CC, Chao JI. Biocompatible and detectable carboxylated nanodiamond on human cell. *Nanotechnology* 2007;18(32):325102.
- [74] Krüger A, Liang Y, Jarrea G, Stegka J. Surface functionalisation of detonation diamond suitable for biological applications. *Journal of Materials Chemistry* 2006;16:2322-2328.
- [75] Manzanares D, Cena V. Endocytosis: The Nanoparticle and Submicron Nanocompounds Gateway into the Cell. *Pharmaceutics* 2020;12:10.3390/pharmaceutics12040371.
- [76] Conley SM, Naash MI. Nanoparticles for retinal gene therapy. *Prog Retin Eye Res* 2010;29:376-397.
- [77] Almasieh M, Wilson AM, Morquette B, Cueva Vargas JL, Di Polo A. The molecular basis of retinal ganglion cell death in glaucoma. *Prog Retin Eye Res* 2012;31:152-181.
- [78] Kachi S, Oshima Y, Esumi N, Kachi M, Rogers B, Zack DJ, et al. Nonviral ocular gene transfer. *Gene Ther* 2005;12:843-851.
- [79] Lipinski DM, Thake M, MacLaren RE. Clinical applications of retinal gene therapy. *Prog Retin Eye Res* 2013;32:22-47.

Chapter 2

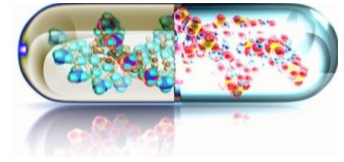


CONCLUSIONS

The following are the key conclusions of this PhD thesis based on the findings of the research studies:

1. Sphingolipids were integrated into a cationic niosome formulation for non-viral gene delivery to the central nervous system. Niosphingosomes and related complexes were smaller in particle size and higher surface charge than niosomes. ARPE-19 cells treated with niosphingoplexes demonstrated increased cell viability and transfection efficiency. It demonstrated less endocytosis through caveolae, enhanced co-localization with the lysosomal compartment, and endosomal escape properties in the case of niosphingoplexes. Additionally, niosphingoplexes transfected not only primary central nervous system cells but also various retinal and brain cortex cells from mice, depending on the route of administration.
2. The impact of inclusion of NDs in the niosome formulations was evaluated in terms of physicochemical characteristics, cellular uptake, intracellular disposition, biocompatibility, and transfection efficiency. Complexes, nanodiasomes, and niosomes achieved the physicochemical requirements for applications in gene therapy. In terms of biology, the inclusion of NDs into niosomes increased cellular uptake, biocompatibility, and transfection efficiency. When compared to nioplexes, nanodiaplexes had higher levels of endocytosis via clathrins, higher lysosomal colocalization, and endosomal escape properties. However, endocytosis mediated by caveolae was the most effective pathway in the case of nanodiaplexes. Nanodiaplexes successfully transfected retinal and neuronal cells, according to studies in CNS primary cells.
3. The influence of NDs on physicochemical characteristics, cellular internalization, cell viability, and transfection efficiency was studied in a rat retina throughout time. All of these parameters were evaluated over a 30 days period at various storage temperatures. The main results suggest that adding nanodiamonds to niosome formulations enhanced transfection efficiency, and this effect was maintained throughout time. Additionally, both formulations were more stable at low storage temperatures and nanodiasomes maintained their physicochemical properties more consistently than niosomes. Finally, nanodiasomes were successful in achieving high transgene expression levels in the rat retina following subretinal and intravitreal administration, both when injecting freshly prepared nanodiasome formulations as well as those that had been stored for 30 days at 4°C.

Chapter 3



APPENDICES

Published articles

Appendix 1

Niosome-Based Approach for In Situ Gene Delivery to Retina and Brain Cortex as Immune-Privileged Tissues

Pharmaceutics 2020, 12, 198;

doi:10.3390/pharmaceutics12030198

IF: 6.321 (2020)

Niosome-Based Approach for In Situ Gene Delivery to Retina and Brain Cortex as Immune-Privileged Tissues

Nuseibah AL Qtaish ^{1,2}, Idoia Gallego ^{1,2}, Iliia Villate-Beitia ^{1,2}, Myriam Sainz-Ramos ^{1,2}, Tania Belén López-Méndez ^{1,2}, Santiago Grijalvo ^{3,4}, Ramón Eritja ^{3,4}, Cristina Soto-Sánchez ^{5,6}, Gema Martínez-Navarrete ^{5,6}, Eduardo Fernández ^{5,6}, Gustavo Puras^{1,2,*} and José Luis Pedraz^{1,2,*}

¹ NanoBioCel group, University of the Basque Country (UPV/EHU), City Postcode, Spain; nusaiba.qtaish@gmail.com (N.A.Q.); idoialgallego@hotmail.com (I.G.); aneilia.villate@ehu.eus (I.V.-B.); myri.2694@gmail.com (M.S.-R.); tblopez01@gmail.com (T.B.L.-M.)

² Networking Research Centre of Bioengineering, Biomaterials and Nanomedicine (CIBER-BBN), Vitoria-Gasteiz Postcode, Spain

³ Networking Research Centre of Bioengineering, Biomaterials and Nanomedicine (CIBER-BBN), Barcelona Postcode, Spain; srgma@cid.csic.es (S.G.); recgma@cid.csic.es (R.E.)

⁴ Institute for Advanced Chemistry of Catalonia, (IQAC-CSIC), City Postcode, Spain

⁵ Neuroprosthesis and Neuroengineering Research Group, Miguel Hernández University, Elche Postcode, Spain; csoto@goumh.umh.es (C.S.-S.); gemamartineznavarrete@gmail.com (G.M.-N.); e.fernandez@umh.es (E.F.)

⁶ Networking Research Centre for Bioengineering, Biomaterials and Nanomedicine (CIBER-BBN), Elche Postcode, Spain

* Correspondence: joseluis.pedraz@ehu.eus (J.L.P.) and gustavo.puras@ehu.eus (G.P.)
Tel: +34945013091 (J.L.P.); +34945014536 (G.P.)

Abstract:

Non-viral vectors have emerged as a promising alternative to viral gene delivery systems due to their safer profile. Among non-viral vectors, recently, niosomes have shown favorable properties for gene delivery, including low toxicity, high stability, and easy production. The three main components of niosome formulations include a cationic lipid that is responsible for the

electrostatic interactions with the negatively charged genetic material, a non-ionic surfactant that enhances the long-term stability of the niosome, and a helper component that can be added to improve its physicochemical properties and biological performance. This review is aimed at providing recent information about niosome-based non-viral vectors for gene delivery purposes. Specially, we will discuss the composition, preparation methods, physicochemical properties, and biological evaluation of niosomes and corresponding nioplexes that result from the addition of the genetic material onto their cationic surface. Next, we will focus on the in situ application of such niosomes to deliver the genetic material into immune-privileged tissues such as the brain cortex and the retina. Finally, as future perspectives, non-invasive administration routes and different targeting strategies will be discussed.

Keywords: gene delivery; non-viral vectors; niosomes; brain; retina

1. Introduction

It has been a long journey, with promising expectations and serious setbacks since gene therapy was referred as a potential strategy to face monogenetic disorders 45 years ago, until nowadays, where this advanced therapy is considered a realistic, although still uncommon, medical option for the treatment of both inherited and acquired human diseases [1]. The knowledge gained on the molecular basis of genetic diseases along with recent advances in different research areas, such as biotechnology or nanomedicine, have contributed to increasing the number of clinical trials based on gene therapy up to around 2000 (<http://www.abedia.com/wiley/>). Such interest has accelerated the research investment of many companies involved in the development of gene therapy-based drugs, and consequently, it is expected that the therapeutic armamentarium will soon increase [2].

The main concept of gene therapy is quite simple and basically relies on the incorporation of enough exogenous genetic material into a specific target cell in a safe way to modulate protein expression related to the development of diseases that cannot be faced with conventional treatments [3]. More specifically, therapeutic genetic material can be supplied to cells with genetically modified viruses (virotherapy) due to their natural ability to infect cells [4]. This approach is particularly interesting to selectively infect and kill cancer cells, although the use of biological agents such as infecting viruses for medical applications raises relevant safety

concerns [5]. Another alternative to enhance the expression of a specific protein whose low levels accelerate the development of certain diseases is through the administration of bacterial plasmid DNA (pDNA) [6]. This strategy is normally applied for the treatment of genetic diseases that follow an autosomic recessive inheritance pattern. However, the main drawbacks of plasmid administration include the immune response generated against the bacterial elements [7] and, in some cases, the big size of the plasmid that decreases transfection efficiency process [8]. To minimize such disadvantages, unmethylated cytosine-phosphate-guanine (CpG) dinucleotides from bacterial origin and other not relevant sequences related to the origin of replication and the resistance to antibiotics have been removed from conventional plasmids resulting in minicircle DNAs (mcDNAs), which reduce immunogenic response and enhance transfection efficiency, allowing a sustained expression of the therapeutic gene (transgene) [9]. Other different approach include the administration of exogenous genetic material in the form of small interfering RNA (siRNA), or aptamers to inhibit protein expression by different mechanisms at a post-transcriptional level, or the synthesis of antisense oligonucleotides (ASOs) that can regulate the expression of both precursor RNA (pre-RNA) or mature RNA in the nucleus or cytosol, respectively [10–13]. These therapeutic oligonucleotides are very sensitive to enzymatic degradation, and therefore, the biomacromolecules must be stabilized with chemical modifications on their structure [11, 14].

Normally, and in clear contrast to conventional drug-based therapies, marketed gene therapy products are designed to get long-lasting therapeutic benefits and focus their interest on rare and specific disorders that affect a reduced number of patients. In this sense, it is worth mentioning the case of the recently approved Milasen® drug, which has been specifically designed for a single patient suffering from Batten disease [13]. The unusual characteristics of gene therapy-based drugs also raise ethical and social concerns related to the cost of such innovative treatments [2]. Some *in vivo* gene therapy products currently approved for human use are summarized in Table 1.

Table 1. Gene therapy-based drugs on market for *in vivo* human use, including synthetic oligonucleotides.

Year (Agency)	Name	Indication	Genetic Material	Administration	Delivery System
2003 (FDA, China)	Gendicine	Head and neck squamous cell carcinoma	Bacterial plasmid	Intratumoral injection	Adenovirus
2004 (FDA, USA)	Macugen	Age-related macular degeneration	Synthetic aptamer	Intravitreal Injection	-
2005 (FDA, China)	Oncorine	Nasopharyngeal cancer	Viral DNA	Intratumoral injection	Adenovirus
2010 (FDA, USA)	Rexin-G	Metastatic pancreatic cancer	Viral RNA	Intravenous infusion	Retrovirus
2012 (Russian ministry of Healthcare)	Neovasculgen	Atherosclerotic peripheral arterial disease	Bacterial plasmid	Intramuscular injection	-
2013 (FDA, USA)	Kynamro (Mipomersen)	Homozygous familial hypercholesterolemia	Synthetic ASO	Subcutaneous injection	-
2016 (FDA, EMA)	Imylgic	Multiple solid tumors	Viral DNA	Intratumoral injection	Oncolytic Herpes simple Virus
2016 (FDA, EMA)	Exondys 51 (Eteplirsen)	Duchene muscular dystrophy	Synthetic ASO	Intravenous infusion	-
2016 (FDA, EMA)	Spinraza (Nusinersen)	Spinal muscular atrophy	Synthetic ASO	Intrathecal administration	-
2016 (FDA, EMA)	Defibrotide	Veno-occlusive disease of liver	Single-stranded oligodeoxyribo nucleotides	Intravenous infusion	-
2018 (FDA, EMA)	Patisiran (Onpatro)	Familial amyloid polyneuropathy	RNA interference	Intravenous perfusion	Lipid nanoparticle
2018 (FDA, EMA)	Luxturna	Leber congenital amaurosis type 2	RPE 65 plasmid	Subretinal injection	Adeno-associated Virus
2018 (FDA)	Tegsedi (Inotersen)	Transthyretin-mediated amyloidosis	Synthetic ASO	Subcutaneous injection	-
2019 (FDA)	Givlaari (Givosiran)	Acute hepatic porphiria	RNA interference	Subcutaneous injection	-
2019 (EMA)	Waylivra (Volanesorsen)	Familial chylomicronemia syndrome (FCS)	Synthetic ASO	Subcutaneous injection	-
2019 (FDA)	Vyondys 53 (Golodirsen)	Duchene muscular dystrophy	Synthetic ASO	Intravenous injection	-
2019 (FDA)	Zolgensma	Spinal muscular atrophy	Bacterial plasmid	Intravenous infusion	Adeno-associated Virus

Another emerging strategy to deliver transgenes into the organism is through the extraction of cells from the patient, which after *ex vivo* genetic manipulation are implanted again into the organism [15,16]. In fact, recently, many *ex vivo* gene therapy products such as Zalmoxis, Zyntelgo, Invossa, Yeskarta, Kymriah and Strimvelis have been commercialized [17]. Such approaches use both retro and lentivirus vectors to transduce allogenic and autologous cells for the treatment of hematopoietic malignancies, osteoarthritis, or severe combined immunodeficiency diseases. In addition to the previously described gene therapy approaches based on both gene supplementation and gene suppression strategies, recent advances on genome editing tools by CRISPR/Cas technology allow the correction of a specific mutation at a genomic level [18]. Due to the huge treatment possibilities of such revolutionary genome editing tools, the number of scientific publications in this area has considerably increased since 2014, and many clinical trials are underway, especially in cancer and pathological disorders of the blood and eye [19]. In any case, although highly promising, still some concerns mainly related to the delivery strategy, the possibility of permanent off target effects, or the efficiency to repair the mutation in a controlled manner need to be resolved before reaching the market [20]. In this sense, the new modified version of the CRISPR/Cas systems referred as “prime editing” holds great potential to promote the translation of this technology into clinical practice [21]. Although few gene therapy products are available for human use, there is no doubt that this market has significantly increased in the last few years. Consequently, it is reasonably estimated that some products that nowadays are under clinical trials evaluation will soon reach the clinical practice, which justify the optimism and financial investment of many biotechnology firms [1]. In any case, more research efforts need to be focused on the development of safe and efficient genetic material delivery systems to overcome the biological barriers that hamper the clinical application of gene therapy. This issue is particularly relevant for the treatment of diseases that affect to sensitive and immunologically isolated organs, such as brain and eye, where gene therapy-based drugs should be preferably administered by non-invasive administration routes.

2. Biological barriers

To be active at the place of action, gene delivery systems need to overcome both extracellular and intracellular barriers for *in vivo* applications, while for *ex vivo* purposes, only intracellular barriers can hamper their final performance [22]. Extracellular biological barriers to

overcome will depend mainly on the administration route, while intracellular barriers will differ according to the target cell.

2.1. Extracellular barriers

From a practical point of view, the intravenous administration of gene therapy-based drugs represents a promising approach to face diseases that affect the liver due to the natural tendency to be accumulated in such an organ [23]. In addition, because there is not an absorption process, the bioavailability of drugs is 100%. Considering that cancer disease represents around 65% of current gene therapy clinical trials (<http://www.abedia.com/wiley/>) this route of administration is also interesting to treat disseminated cancer cells that affect many organs. However, despite these relevant advantages, its effect is highly hampered by the possible drug-induced hepatotoxicity [24] and by the relevant biological extracellular barriers that the genetic material needs to overcome [25]. Consequently, biomacromolecules such as ASOs, plasmids, siRNAs, or ribonucleoproteins (RNPs) are normally administered with different kinds of gene delivery systems (viral or non-viral vectors) specifically designed to make the process more efficient [26]. Usually, such biomacromolecules, in the “naked” form (without any gene delivery system or chemical modification) can be easily degraded immediately after administration by proteases and nucleases present in the blood. In addition, biomacromolecules can also be phagocytosed by macrophages, and the bacterial origin of their components can induce both cellular and humoral immune responses, which not only jeopardize their final performance but can also have deleterious effects on the safety profile after their administration [27]. In circulation, innate immune responses can occur through the activation of different kind of toll-like receptors (TLRs) by impurities such as endotoxins or by bacterial components such as CpG motifs present on the genetic material. Furthermore, an adaptive immune response can also be activated in the case of pre-existing immunity [28]. In the case of genetic material delivered by non-viral vectors, some physicochemical parameters such as zeta potential, particle size distribution, polydispersity index, or hydrophobicity/hydrophilicity balance can also contribute to the compatibility with the immune system [29]. Another relevant issue that needs to be considered is the natural tendency to accumulate in the liver after intravenous administration, and the fact that such biomacromolecules, due to their small size, below 5.5 nm, can be cleared quickly from systemic circulation through kidneys by renal excretion [30]. In any case, although genetic material remains stable in

bloodstream without eliciting an immune response, the time required to reach therapeutic concentrations—the transfection process—can be even more challenging if isolated and immune-privileged organs such as brain and eye are the final target of the gene therapy treatment. In this case, additional extracellular barriers that protect the brain and eye from the rest of the organism such as the blood–brain barrier (BBB) and the blood–retinal barrier (BRB) need to be overcome [31,32]. Due to the critical obstacles that extracellular barriers represent, the design of effective and safe gene delivery systems for *in vivo* gene therapy represents a really stimulating task for the scientific community. A schematic representation of extracellular barriers is shown in Figure 1.

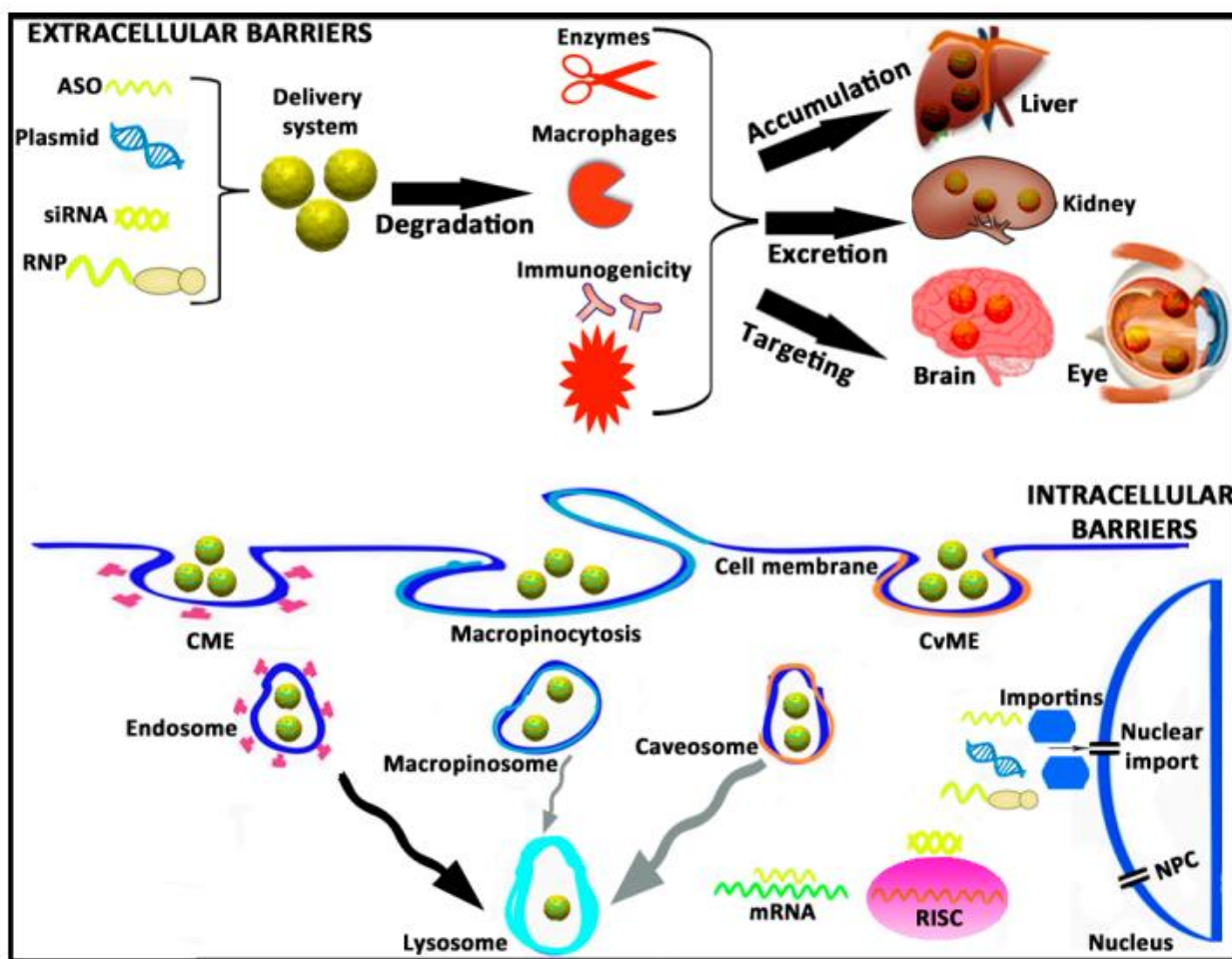


Figure 1. A brief schematic representation of both extracellular and intracellular barriers that genetic material needs to overcome during the transfection process. ASO, antisense oligonucleotide; siRNA, small interfering RNA; RNP, ribonucleoprotein; CME, clathrin-mediated endocytosis; CvME, caveolae-mediated endocytosis; RISC, RNA-induced silencing complex; mRNA, messenger RNA; NPC, nuclear pore complex.

2.2. Intracellular barriers

Once extracellular barriers have been overcome, biomacromolecules still need to reach sufficient amounts at cytoplasmic, or even nuclear levels, preferably only on the target cells, in order to be biologically active. Again, this intracellular trafficking is another arduous journey full of hurdles to beat for the genetic material [33]. First of all, negatively charged ASOs, plasmids, siRNAs, and RNPs are electrostatically repelled by the hydrophilic anionic proteins of the cell membrane, which jeopardizes their cellular uptake and posterior internalization process [34]. In the absence of antibodies or cell-specific ligands that promote a targeting effect, biomacromolecules can be internalized by different pathways, of which clathrin-mediated endocytosis (CME), macropinocytosis and caveolae-mediated endocytosis (CvME) are the most representative ones, forming the corresponding intracellular vesicles referred as endosomes, macropinosomes, and caveosomes, respectively [35]. Although there is not a unique consensus, and results in this research area are quite controversial, it is estimated that those endocytosis pathways are connected, in a great (CME) or less extension (CvME and macropinocytosis), to the lysosomes, where the acidic pH value degrades the genetic material. Consequently, the transfection process is strongly affected [36]. If biomacromolecules escape on time from the acidic environment of lysosomes, they still need to move quickly and properly through the cytosol to reach the RNA-induced silencing complex (RISC) in the case of siRNA, or the target mRNA in the case of ASOs that inactivate mature RNA. In the case of plasmids, RNPs, and some ASOs that act on pre-RNA, the impermeability of the nuclear membrane represents another hurdle to overcome, especially in quiescent and non-dividing cells [37, 38].

Nuclear pore complexes (NPC) present on the nuclear membrane of cells with a small 9 nm channel diameter that prevents the entry into the nucleus of chemical compounds with a molecular weight over 45 kDa [38]. Other alternative to cross the nuclear membrane is through active mechanisms mediated mainly by importins of the cytoplasm that promote nuclear translocation [39]. Once inside the nucleus, or even before during the cytoplasmic trafficking, biomacromolecules need to be dissociated from gene delivery systems to get access into the transcriptional machinery of the target cell and produce the final biological effect [40]. A brief schematic representation of intracellular hurdles is shown in figure 1.

3. Non-viral gene delivery systems

Classically, gene delivery systems designed to overcome biological barriers are classified as viral and non-viral vectors. Viruses, independently of their origin, have evolved over millions of years to gain access into host eukaryotic cells in order to shuttle their genetic cargo. Nowadays, recombinant viruses have been modified in the laboratory to reduce their pathogenic effect and to deliver the transgene of interest into target cells [41]. During the last few years, relevant improvements have been made mainly regarding their production methodology, safety profile, and genetic material packing capacity. However, their biological origin hampers the commercialization process by regulatory authorities, which clearly impacts on their final price [2, 42]. In contrast, the non-viral vectors counterparts are classically recognized for their safety profile, higher packing capacity, and low cost of production [43]. In any case, non-viral vectors for plasmid-based gene therapy have not yet reached clinical practice, although research on this topic has quickly increased during the last few years, which has been especially motivated by the impact that CRISPR/Cas technology has had on scientific community and the need to deliver such genetic material in a safe and efficient way to target cells. In this sense, at a preclinical level, non-viral vectors for CRISPR/Cas delivery predominate over the use of viral vectors (70% versus 30%, respectively) [44]. Among non-viral gene delivery systems, we can differentiate the development of physical and chemical methods.

3.1. Physical methods

Basically, physical methods are vector-free systems based on a controlled and reversible deformation of cytoplasmic membrane during short periods of time that allow the entry of genetic material on target cells [22]. Although highly effective, these methods are normally restricted to *ex vivo* gene therapy, which is mainly due to the challenge that represents the fine control of physical parameters that produce the formation of transient pores into the cellular membrane *in vivo* conditions. Such technological limitations can result not only in a loss of action but also in an increase of the cellular toxicity [45]. Transient pores on cellular and even nuclear membranes can be induced by the application of external electrical pulses, whose amplitude and duration are controlled, and depend on the particular characteristics of the target cell [22]. Pores can also be created if a cell's membrane is mechanically deformed when cells are forced to pass through microfluidic-based channels which the diameter is smaller than that of the cell [46]. Other physical

methods that also can be used to deliver genetic material into target cells efficiently include the direct microinjection of genetic material into cells by a micropipette, the induction of cellular uptake by stimulation of the micropinocytosis pathway with a hyperosmolar buffer containing sodium chloride and propanbetaine, or the hydrodynamic injection. This last technique consists of the quick injection of genetic material into the tail of rodents in volumes close to 10% of the total body weight [47].

3.2. Chemical methods

Although inorganic compounds such as magnetite, silica, or calcium phosphate, to name just a few ones, have shown great potential to shuttle genetic material, most chemical vectors are based on organic compounds such as cationic lipids or cationic polymers [48]. Amphiphilic cationic lipids for gene delivery applications normally share four domains in their chemical structure [49]: a hydrophilic polar head group, a hydrophobic apolar group, a linker, and a backbone. The positively charged hydrophilic polar head group interacts electrostatically with the negatively charged genetic material, obtaining the corresponding lipoplexes [50]. The composition of the hydrophobic apolar group can affect the relevant physicochemical and biological parameters that influence the transfection process such as the stability of the formulation, the DNA protection from nucleases, or the endosomal escape. The chemical composition of the linker domain influences both the flexibility and degradation of cationic lipids. Finally, the backbone group is the domain that separates the hydrophilic polar group from the hydrophobic apolar group, of which asymmetric glycerol-based backbone domains are the most commonly used for gene delivery purposes. A schematic representation of the general chemical structure of cationic lipids for gene therapy applications can be observed in figure 2. Small changes in the chemical structure of any of the four domains can affect both the physicochemical and biological parameters that regulate the transfection process [51]. Normally, to enhance the transfection efficiency of cationic lipids, they are incorporated into vesicles made up of phospholipids resulting in corresponding liposomes [52], or solid lipid nanoparticles (SLNs) if the core of the nanoparticle is a solid lipid stabilized with surfactants [53]. Lipid nanoparticles have been used in the formulation of Patisiran® to deliver siRNA genetic material in the liver after intravenous administration to suppress the production of transthyretin in hereditary transthyretin-mediated amyloidosis (hATTR) patients [54].

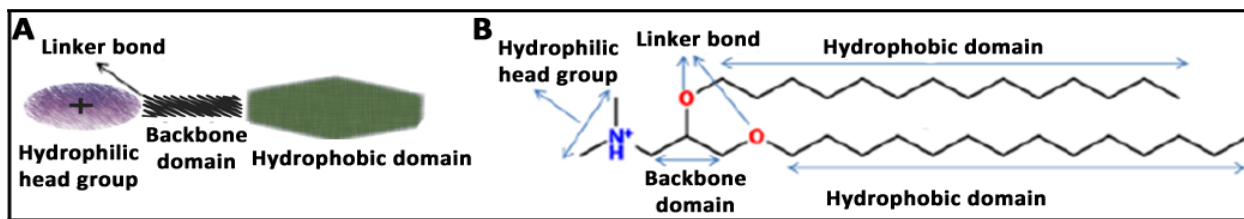


Figure 2. (A) General chemical structure of cationic lipids for gene therapy applications with four domains. (B) Chemical structure of cationic lipid 2,3-di(tetradecyloxy)propan-1-amine. The hydrophilic head domain consists on a protonated amine group, the backbone is a glycerol-based structure, the linker is an ether, and the hydrophobic domain consists of a double hydrocarbonated alkyl chain of 14 carbon atoms.

Apart from cationic lipids, cationic polymers with different physicochemical properties are also often used as gene delivery systems, obtaining the corresponding polyplexes after genetic material is adsorbed on their surface or entrapped into the polymeric matrix. Most of those cationic polymers include chitosans [55], polyethylenimine [56], or poly (L-lysine) [57]. Moreover, hybrid compounds, made by a combination of both polycationic and polyanionic polymers, and with different organic and inorganic materials such as polymers, magnetite, or lipids can be used also to deliver genetic material for different purposes [58–62].

In addition to classic chemical compounds, due to recent advances on nanotechnology and the interest in the development of non-viral vectors, other materials have recently emerged as promising gene delivery systems [48]. For instance, nanodiamonds (NDs) present fitting properties for gene delivery applications due to their high surface area-to-volume ratio, biocompatibility, scalability, and precise particle distribution [63]. Additionally, NDs can be easily functionalized to obtain hybrid compounds by electrostatic interactions with hydrophilic cationic polymers such as polyethylenimine [64, 65], lysine [66], or polyallylamine hydrochloride [67]. Another strategy is to include cationic groups, i.e., silane-NH₂ or polyamidoamine (PAMAM) [68], on the chemical structure of NDs by the formation of covalent bonds. Apart from NDs, graphene oxide (GO), a precursor of graphene, is another material that has been recently investigated for gene delivery applications. GO is a biocompatible material that is easy to synthesize, reproducible, and cheap. In addition, GO has high dispersibility in water, and it can be easily functionalized with different kinds of polymers such as polyethylene glycol (PEG) [69], polyethylenimine (PEI) [70], or chitosan [71].

4. Niosome nanoparticles for gene delivery

Niosomes are non-ionic-based surfactant unilamellar or multilamellar vesicles with a bilayer structure that have been used for around 40 years as drug delivery systems for different applications with low toxicity and desired targeting properties [72]. As in the case of liposomes, hydrophilic heads are orientated toward an aqueous solution, whereas hydrophobic groups are orientate toward an organic solution, so both hydrophobic and hydrophilic drugs can be delivered by niosomes [73]. The main difference between both nanocarriers is that in the case of niosomes, the phospholipids of liposome vesicles have been substituted by non-ionic surfactants [74]. Compared to liposome counterparts, niosomes are recognized for their higher chemical and storage stability, due to the presence of non-ionic surfactants in their structure [75]. In addition, niosomes can be easily prepared at a low cost, and they are less toxic than liposomes due to the presence of non-ionic surfactants [76, 77]. All these characteristics justify the research on niosomes as an interesting platform for gene delivery applications.

4.1. Components on niosome formulations

In addition to the non-ionic surfactant, which enhances the stability and is the main component of niosomes, other chemical compounds can be incorporated into the niosome vesicles such as cationic lipids that interact electrostatically with the negatively charged genetic material to obtain corresponding nioplexes at different cationic lipid/genetic material ratios and “helper” components that improve their biological performance [78]. Any slight modification of both the relationship and the chemical structure of these components can affect, in a significant way, the relevant physicochemical parameters of the formulation that regulate the transfection process such as the size, polydispersity index, and morphology [79].

Non-ionic surfactants can be classified into four different categories: alkyl ethers, alkyl esters, alkyl amides, and esters of fatty acids [73]. Some non-ionic surfactants that have been used in niosomes designed for gene delivery applications include polyoxyethylene alkyl ether (Brij© [73]), polysorbates (Tween© [80]), sorbitan fatty acid esters (Span© [81]), or poloxamers [82]. The most relevant parameters of non-ionic surfactants to consider are the hydrophilic/lipophilic balance (HLB), which can be used as a “saving guide” parameter to select the appropriate surfactant [83], the critical packing parameter (CPP), which plays an important role in the

vesicular-forming ability of niosomes [84], or the gel liquid transition temperature (TC), which has a relevant impact on the drug entrapped efficiency [85]. Among the cationic lipids, some of the most employed in the elaboration of niosomes for gene delivery purposes include 2,3-di(tetradecyloxy)propan-1-amine hydrochloride salt [86], 3β -[N-(dimethylaminoethane)-carbamoyl]-cholesterol hydrochloride salt (DC-Chol, [87]), N-[1-(2,3-Dioleoyloxy)propyl]-N,N,N-trimethylammonium methylsulfate salt (DOTAP, [88]), 1,2-di-O-octadecenyl-3-trimethylammonium propane chloride salt [83], or 1-(2-dimethylaminoethyl)-3-[2,3-di(tetradecoxy) propyl] urea [51], to name just a few. Any slight change of any of the four chemical domains of cationic lipids influences the transfection efficacy mediated by niosomes [49]. Regarding “helper” lipids, they are normally neutral components i.e., cholesterol, that when used in appropriate amounts enhance both the rigidity and the colloidal stability of formulations, promoting the gel liquid transition temperature of niosomes and the interactions with the apolar group of non-ionic surfactants [89]. In addition, they can affect biological parameters such as the cellular uptake and posterior intracellular trafficking of niosomes [90]. Squalene and squalane, which are natural lipids belonging to the terpenoid family, as well as biochemical precursors of the synthesis of cholesterol and other steroids, have also been incorporated in niosome formulations [90, 91]. Another commonly used “additional” component on niosome vesicles is PEG. When niosomes “decorated” with hydrophilic PEG chains are administered into the bloodstream, the aqueous layer on the vesicular surface avoids endocytosis by the reticuloendothelial system (RES), and it therefore increases the half-live period of such niosomes in blood [92].

4.2. Niosome preparation methods

Niosomes can be easily elaborated by the solvent-evaporation method. Basically, both the cationic and “helper” lipids are dissolved in a small volume of organic phase, where the aqueous phase containing the non-ionic surfactant is added. After a brief sonication period, an emulsion is obtained. Such emulsion can be left under manetic agitation to evaporate the organic solvent, which will produce the resuspension of the niosome vesicles into the aqueous phase [93]. A brief schematic representation of the niosome components and their elaboration by the solvent evaporation process can be observed in figure 3.

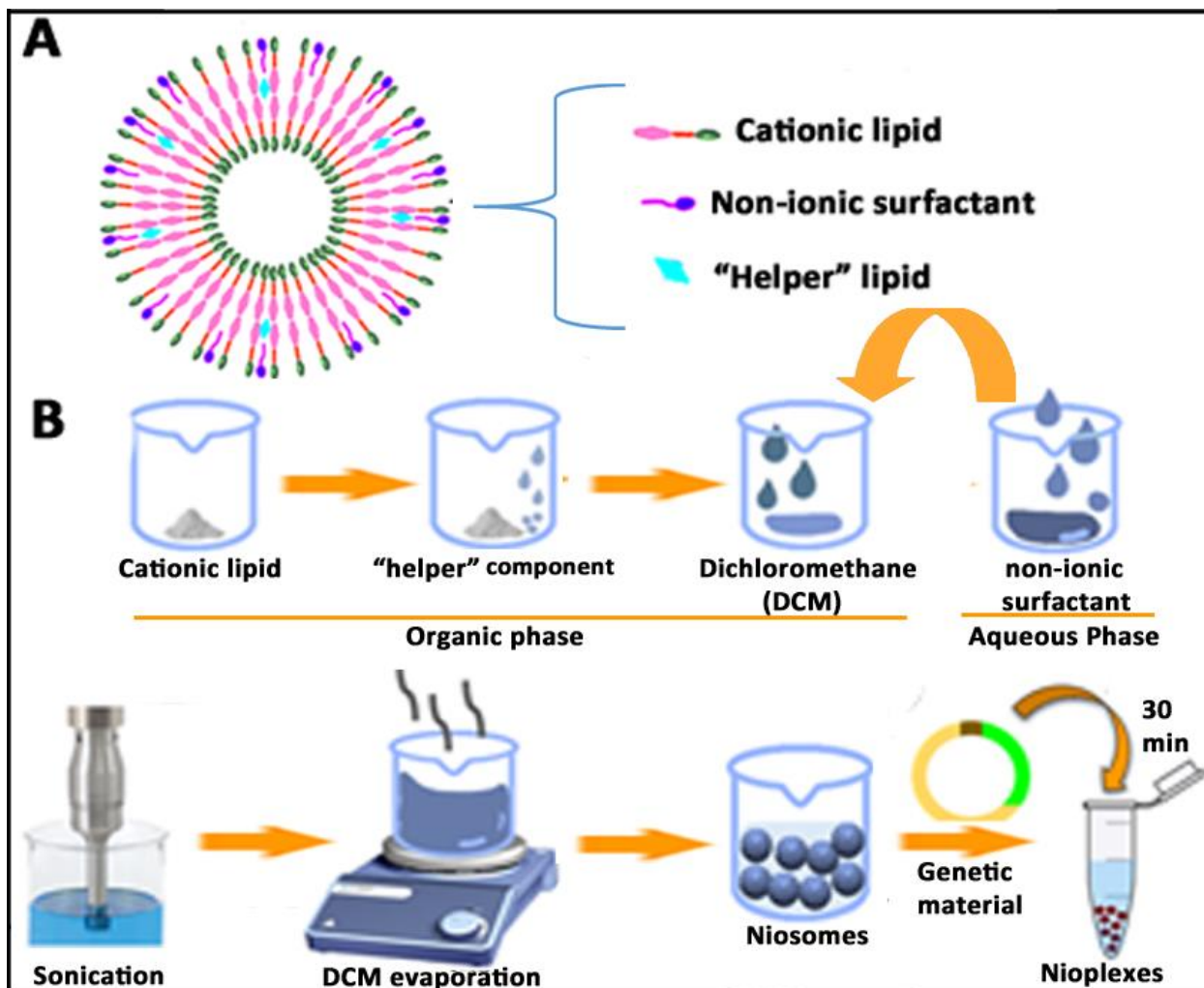


Figure 3. (A) Bilayer structure of niosomes and disposition of components. (B) Schematic representation of the solvent evaporation method for the elaboration of niosomes and corresponding nioplexes.

The film-hydration method is basically a modification of the previously described solvent evaporation method, in which the organic solvent is evaporated in a round-bottomed flask using a rotatory vacuum evaporator. As a result, a dry film of lipids will be formed, which is thereafter hydrated with the aqueous phase above the transition temperature of the surfactant [94]. Another interesting and single-step alternative to elaborate niosomes without the use of organic solvents is the bubble method. In this case, large unilamellar niosomes vesicles can be obtained when both the surfactant and lipids are heated over 70 °C in a buffer solution. Then, the dispersion is mixed with a high shear homogenizer followed by the bubbling of nitrogen gas at 70 °C [73]. In addition to the bubble method, other alternative to obtain niosomes without the use of organic solvent is

the lipid injection method. In this case, lipids and surfactants are melted and thereafter injected into an aqueous phase under heat and continuous agitation to get a final suspension of niosomes [95]. In order to obtain small unilamellar niosome vesicles, the microfluidization method can be used. In this case, niosomes are obtained when two fluidized streams pumped at specific speed interact with each other in small and specifically designed microchannels for fast mixing [95]. Interestingly, this technique allows the possibility of working in parallel with large volumes, which enhances the scalability of the production process [96]. The precise and detailed elaboration of niosomes by other different techniques such as trans-membrane pH gradient uptake, supercritical reverse phase evaporation, or the freeze and thaw process can be looked up in two excellent articles that have been recently published [73, 85].

Once niosomes have been prepared using any of the previously above-mentioned techniques, the corresponding nioplexes can be obtained after the addition of a solution of the pertinent genetic material to the colloidal suspension of niosomes (Figure 3). Due to the electrostatic interactions between the positively charged amine groups of the cationic lipids incorporated into the niosome vesicles and the negatively charged phosphate groups of the genetic material, nioplexes can be easily obtained at different cationic lipid/genetic material ratios [76]. In the case the obtained niosomes are not going to be used soon, they can be stored at 4 °C during several weeks, without affecting the main physicochemical parameters that influence the gene delivery process [9].

4.3. Physicochemical characterization of niosome nanoparticles

Normally, after niosome elaboration and before performing any biological experiments, some of the most relevant physicochemical properties involved in the nucleic acid delivery of niosomes are evaluated as a screening methodology to select the most suitable composition and concentration of the chemical components [78]. Dynamic light scattering (DLS) can evaluate the hydrodynamic diameter and the polydispersity index (PDI) of both niosomes and corresponding nioplexes in a Zetasizer instrument, while the morphology and distribution of niosome colloidal dispersions can be examined by different microscopic techniques [76]. The DLS technique is based on the random Brownian movement of small particles and the light scattered when a laser irradiates the colloidal suspension, which is highly dependent on the ion concentration [78]. The hydrodynamic diameter is usually obtained by cumulative analysis, which requires a narrow

and monodisperse sample distribution, typically with PDI values below 0.5 for comparative purposes [97]. When genetic material binds to the surface of cationic niosomes at different cationic lipid/genetic material ratios, normally, the nioplexes size fluctuates slightly due to the condensation effect produced by the electrostatic interaction, which would decrease the size and the space demanded by the genetic material, which would increase in vesicular size [91]. Such slight alteration of the final size can affect the endocytosis pathway and consequently the posterior intracellular trafficking of niosomes [34, 90, 98]. In addition to size, the PDI value also changes upon the incorporation of genetic material on the surface of cationic niosomes. In this case, polydispersion typically increases due to the heterogeneous distribution of such genetic material [49].

Normally, niosomes exhibit spherical morphology that can be evaluated under transmission electron microscopy (TEM) and cryo-TEM [76]. These techniques can require the addition of staining agents, and they can also be used to evaluate the size and distribution of niosomes, although they may not correlate with DLS due the difference regarding the manipulation of the samples [91]. If the samples to analyze are in solid form, scanning electron microscopy (SEM) can also provide information about the morphology of niosomes. For a more precise analysis, for instance, to determine the characteristics of bilayers, scanning tunneling microscopy (STM) or small angle X-ray scattering (SAXS) techniques can be used [99, 100]. The degree of the buffering capacity of cationic niosomes represents the potential of such non-viral vectors to escape from the degradation in the acidic compartment of lysosomes due to the incorporation of H⁺ into the lipid structure. Such buffering capacity can be measured by an acid–base titration assay [101]. Briefly, colloidal suspensions of niosome formulations are titrated with a solution of NaOH to reach a basic pH value. Next, niosomes are titrated again, but in this case with an HCl acid solution, to evaluate the capacity to absorb H⁺ when different volumes of the acid solution are added.

Another relevant parameter that can be determined to predict the stability of niosomes is the zeta potential (ζ). This value is related to the superficial charge of the formulation and can be obtained from a Zetasizer instrument by a laser Doppler velocimetry (LDV) technique [86]. Typically, it is accepted that ζ values of nanoparticles over 20 mV (either negative or positive) prevent aggregation by electrostatic repulsion [102]. When nioplexes are elaborated, positively

charged cationic groups of niosomes are partially neutralized by the negatively charged phosphate groups of genetic material, resulting in a decrease of superficial charge which will depend on the cationic lipid/genetic material ratio [83]. Normally, nioplexes are elaborated at positive cationic lipid/genetic material ratios to enhance the cellular uptake of such nioplexes by interaction with the negatively charged cell membranes. Additionally, the interaction between the cationic lipids of niosomes and the genetic material can also be evaluated at a molecular level by isothermal titration calorimetry through the measurement of the heat released when such binding occurs [103]. Agarose gel electrophoresis assays can be used to evaluate the capacity of niosomes to condense, release, and protect the genetic material from enzymatic digestion [86]. In this sense, it is well established that a delicate balance between condensation and release capacity needs to be obtained at an appropriate cationic lipid/genetic material ratio to guarantee the condensation and protection efficiency, as well as the release of such genetic material to reach the nucleus of the target cell [91].

The stability of non-viral vectors is another issue that needs to be considered, due to its relevant effect not only on physicochemical parameters, but also on biological properties [85]. To evaluate the stability, some of the previously commented parameters such as particle size, PDI, or ζ value are monitored in different temperature and humidity conditions over time [104–106]. An interesting approach to enhance the physical stability of niosomes is to obtain a stable dry powder formulation by lyophilization that can later be resuspended in the appropriate solvent before use. In this case, the selection and the concentration of the cryoprotector, along with the parameters of the lyophilization process need to be evaluated to guarantee the stability of the dry powder [107, 108]. The analysis of some of the previously described physicochemical parameters on a niosome formulation can be observed in figure 4.

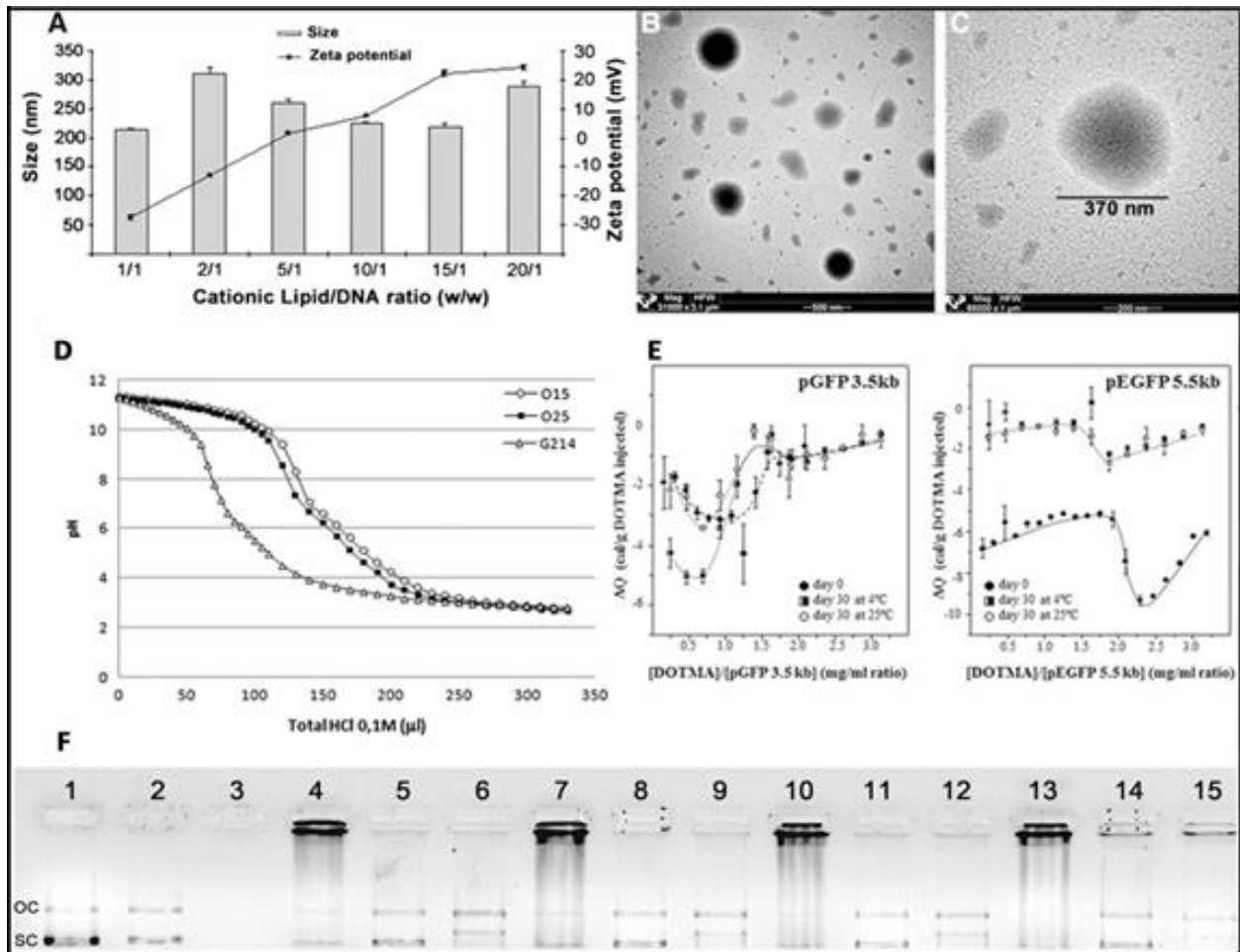


Figure 4. Physicochemical characterization of niosome formulations in terms of size, superficial charge (A), and morphology (B, C), adapted with permission from Puras et al. [91]. Buffering capacity assay (D) and isothermal titration calorimetry (E), adapted with permission from Agirre et al. [101]. Copyright 2019, Elsevier B.V and Gallego et al. [9]. Copyright 2014, Elsevier B.V. DNA binding capacity, release and protection from enzymatic digestion (F), adapted with permission from Puras et al. [91]. Copyright 2014, Elsevier B.V. OC, Open circular, SC supercoiled.

4.4. *In vitro* biological evaluation of niosomes for gene delivery

Once the most relevant physicochemical parameters that affect the transfection process have been analyzed, and before performing any *in vivo* assay, several *in vitro* studies are normally performed to evaluate the toxicity and the efficiency of different formulations as a screening methodology of different candidate formulations. The cationic lipids in the structure of the

niosome vesicles destabilize the cell membrane, induce apoptosis, and therefore be toxic at high doses [109]. To minimize these effects, different strategies can be followed such as to increase the incorporation of the non-ionic surfactant, reduce the cationic lipid/genetic material ratio, or reduce the exposition time of nioplexes [49]. Since cell toxicity is mainly caused by the chemical structure of the cationic lipid and also has a clear cell-dependent effect, each application needs to be individually addressed [110]. Cell viability can be qualitatively evaluated by microscopy or can be quantified by flow cytometry with the use of appropriate fluorescent dyes such as propidium iodide or 7-Amino-actinomycin D (7-AAD), which penetrate into damaged cells [97]. Alternatively, colorimetric assays, such as CCK-8 (Cell Counting Kit-8) or MTT (3-[4,5-dimethylthiazole-2-yl]-2,5-diphenyltetrazolium bromide; succinate dehydrogenase activity), can be used to evaluate cell viability by absorbance [49]. Normally, dead cells are excluded from the transfection efficiency results. A common strategy to evaluate the initial transfection efficiency of niosomes is the use of reporter plasmids based on the luciferase or fluorescence [111, 112] (Figure 5). It is worth mentioning that to get an optimal therapeutic effect, both the percentage of cells that incorporate the transgene, along with the amount of protein expression by transfected cells need to be considered. Although this approach can provide an overview of the gene delivery efficiency of niosomes, further readjustments on cationic lipid/genetic material ratio need to be performed when moving to therapeutic plasmids, since both the composition and size of the plasmid directly influence the transfection efficiency process [113].

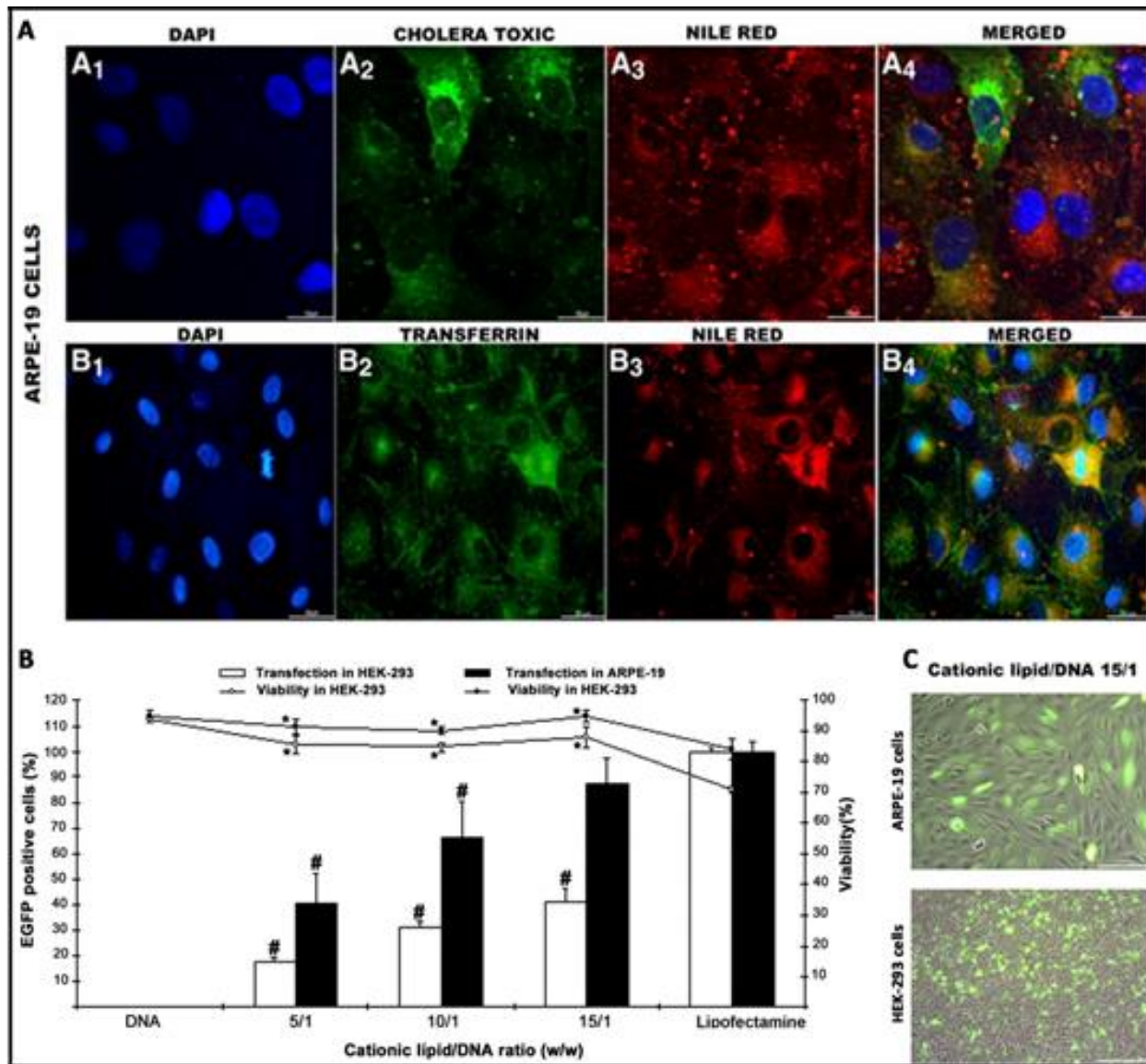


Figure 5. Biological evaluation of niosomes in terms of intracellular trafficking (A), transfection efficiency (B), and morphology (C), adapted with permission from Puras et al. [91]. Copyright 2014, Elsevier B.V.

The knowledge of the endocytosis pathway and the posterior intracellular trafficking to reach the nucleus of target cells can be useful to design more efficient and safer niosome vesicles for gene delivery applications [51]. For that purpose, specific fluorescent endocytic markers such as dextrans, cholera toxin B, or transferrin can be used to stain the most representative endocytosis pathways (macropinocytosis, caveolae, and clathrin-mediated endocytosis, respectively). The colocalization of such dyes with fluorescent labelled niosomes, or preferably, fluorescent plasmids

attached on the surface of niosomes can be qualitatively evaluated by confocal microscopy [91], or quantified by different overlay coefficients, such as Mander's or Pearson's colocalization coefficients [9, 114] (Figure 5). Additionally, intracellular trafficking studies can be completed with lysosome markers such as lysotracker [90] or with different uptake inhibitors such as genistein, wortmannin, or chlorpromazine, to inhibit selectively caveolae, macropinocytosis, or clathrin-mediated endocytosis, respectively [115].

All of the previously mentioned *in vitro* studies can be performed as a proof of concept in Human Embryonic Kidney (HEK-293) culture cells, which is one of the most employed models for transfection studies [116]. However, because transfection efficiency is a highly cell-dependent process, other cell lines that are more representative such as ARPE-19 or NT2 cells can be used for retinal and brain gene delivery purposes [91, 93]. Additionally, and as a more realistic scenario that resembles *in vivo* conditions, primarily the culture cells of both retina and brain can be used [51]. When primarily culture cells are used, the transfection efficiency decreases considerably when compared to values obtained in immortalized cells lines. Therefore, primarily cultures are normally used to evaluate the kind of cells that have been transfected by immunohistochemistry rather than the transfection efficiency in quantitative terms [9, 51]. In the case of immune-privileged organs such as the brain and eye, in addition to culture cells, different and sophisticated *in vitro* models based on microfluidic chips of both the BBB and BRB can be used to better mimic the *in vivo* conditions and predict their behavior performance [117, 118].

5. Eye as main goal

The old concept of immune privilege appeared in 1948, when this term was applied to sites in the body where foreign tissue grafts can survive for extended periods of time, whereas similar grafts placed at a regular site in the body are acutely rejected [119]. This concept needs to be differentiated from the privileged immunity concept, which refers to the capacity of specific organs to select the most suitable and effective immune response to guarantee their proper functions in health and pathology [120]. In this review, we will refer to eye as an immune-privileged central nervous system (CNS) organ, in the sense that such organs are less likely to react against the inflammatory processes caused by foreign agents, because they are protected from the rest of the organism by the BBB [121].

5.1. General concepts

The eye has been classically considered as an amenable organ to be targeted by in situ gene therapy [122]. Due to its reduced size and compartmentalized anatomy, small amounts of vector are required to get a satisfactory effect, and such vectors can be placed in close proximity to the target cells, rather than being systemically administered, which minimizes the potential adverse reactions [123]. Furthermore, due to the isolation from the rest of the organism, the risk of adverse effects is considerably reduced [124]. In addition, the visual function and retinal structure can be evaluated through non-invasive methods [125], and because most of the inherited retinal diseases are symmetric, the untreated eye can be used as control, reducing the number of experimental animals in the laboratory at a preclinical level [126].

The recently approved by FDA (Food and Drug Administration) and EMA (European Medicines Agency) Luxturna® drug represents the most successful example of retinal gene therapy. Luxturna® is indicated for the treatment of Leber congenital amaurosis type 2 (LCA2) disease due to bi-allelic mutations in the RPE65 gene expressed in RPE cells. With this gene therapy strategy, a functional copy of the required gene is delivered into the subretinal space by adenoassociated virus (AAV) vectors [127]. Although the results obtained by Luxturna® offer an encouraging future for gene therapy applied in ophthalmology, the translation of such success to other retinal conditions will not be an easy task. AAV vectors target mainly the RPE layer, where the RPE65 gene codifies the required enzyme of the visual cycle. However, most of the genetic mutations of the retina affect the cells of the neuroretina, especially photoreceptors (PR), where AAV are not so efficient [128]. In addition, it has been reported that AAV virus can enter into the visual pathways of brain after subretinal injection, which rises major concerns due to the potential to trigger unexpected outcome effects [129]. In addition, AAV packing capacity is limited to approximately 4.7 kb, which jeopardizes its use to deliver genes with larger coding sequences i.e., ABCA4, MYO7A, or CEP290 for the treatment of relevant pathologies of the retina such as Stargardt disease, Usher syndrome type 1B, or LCA type 10, respectively [122]. Another relevant concern is the high cost of AAV-based Luxturna® treatment, which is around \$850,000 per-patient in the U.S., which makes it difficult for affected patients to access to such innovative treatments. Therefore, it looks logical to explore other safer and cheaper alternatives to deliver

genetic material into the retina. In this sense, non-viral vectors based on cationic niosomes have recently shown promising results at a preclinical level.

5.2. Niosomes for gene delivery to the retina

The first evidence of niosome vesicles as efficient gene delivery systems into the retina was reported in 2014, when niosomes based on the 2,3-di(tetradecyloxy)propan-1-amine cationic lipid, combined with the squalene “helper” lipid and polysorbate 80 non-ionic surfactant were able to deliver in a safe and efficient way the reported EGFP (Enhanced Green Fluorescent Protein) plasmid to the rat retina after both intravitreal and subretinal administrations [91]. Previously, it was reported that the aforementioned cationic lipid was able to silence gene expression upon covalent conjugation with RNA molecules [130], and that corresponding lipoplexes transfected efficiently RPE and some PR cells after subretinal injection [50]. These data reflect the suitability of such cationic lipids to be used for gene delivery purposes and its inclusion in a novel niosome formulation where non-ionic surfactant polysorbate 80 was incorporated to enhance the stability of vesicles. In addition, squalene, a natural lipid belonging to the terpenoid family, was also incorporated as a “helper” lipid due to the promising transfection results obtained previously with this compound in other cationic lipid emulsions [131,132]. Nioplexes around 200 nm and +25 mV were obtained upon addition of the reported pCMS-EGFP plasmid at a 15/1 cationic lipid/DNA ratio. Such nioplexes entered mainly by the clathrin-mediated endocytosis pathway in cultured RPE cells, and immunohistochemistry studies reflected that nioplexes were able to deliver the reported plasmid into different layers of the retina, depending on the administration route. Interestingly, protein expression was still observed 28 days after both subretinal and intravitreal injections.

The following year, in 2015, a ternary non-viral vector based on protamine/DNA/niosome expressed locally the EGFP protein in PR close to the in situ subretinal administration, and a more uniform distribution of the protein expression was observed in the inner layers of the retina, especially in ganglion cells, after intravitreal injection. As in the previous study, protein expression persisted for at least one month after both administrations [86]. Protamine is an FDA-approved small peptide obtained from the sperm of herring and salmon that efficiently condenses DNA due to its positive charge. Arginine sequences on protamine promote the nuclear import of genetic material, which is especially relevant in slow-dividing retinal cells [133].

However, the high hydrosolubility of protamine hinders the interaction with lipophilic membrane cells [134]. Consequently, to enhance such interaction, protamine was incorporated in lipid formulations such as SLNs [135] or liposomes [136] but not in niosomes for retinal gene delivery. The incorporation of protamine in ternary vectors (protamine/DNA/niosomes, at 1:1:5 ratios, respectively) reduced the size to 150 nm and enhanced DNA condensation capacity. Interestingly, it also reduced the amount of cationic lipid required to transfect the rat retina, and therefore, increased cell viability.

Since small modifications on the chemical structure of the components in the cationic niosomes can affect the gene delivery capacity, in 2016, the transfection efficiency of three different cationic lipids was evaluated in rat retina [51]. Such cationic lipids shared the same hydrophobic tail and the same glycerol-based building block, differing only among them on the polar head formed by an amino group, a glycine triglycine, and a dimethylaminoethyl group. Both squalene and polysorbate 80 were used as “helper” lipids and non-ionic surfactants, respectively. After an extensive physicochemical characterization and *in vitro* evaluation in different cell lines, the results showed that nioplexes based on the cationic lipid that had the dimethylaminoethyl structure on the polar head group were the most efficient for retinal gene delivery. After the intravitreal injection of nioplexes at a 30/1 cationic lipid/DNA ratio, EGFP expression was uniformly distributed, overall, in the ganglion cell layer. The PEG chains on the polysorbate 80 non-ionic surfactant could prevent the aggregations of cationic niosomes with negatively charged components, glycosaminoglycans, and fibrillar structures present in the vitreous, enhancing therefore the diffusion through the vitreous humor and the transfection efficiency [137]. Interestingly, after intravitreal injection, protein expression was also detected in some outer cells of the retina. The transfection of PR and RPE cells by intravitreal injection instead of subretinal injection represent a great challenge to face genetic pathologies that affect the outer segments of the retina, avoiding the harm of sensitive neuronal tissue that is classically associated to Subretinal injection [138].

As in the case of squalene, lycopene is another natural terpenoid compound found at high concentration levels in the eye, which is classically known by its biological properties as an antioxidant agent, cytoprotector, and immunomodulator, among many others [139]. Therefore, in 2017, lycopene-based niosome formulations were elaborated by the solvent evaporation

technique and evaluated for retinal gene delivery capacity prior to physicochemical and biological characterization [140]. The resulting nioplexes at an 18/1 mass ratio showed nanometric size with low polydispersion, spherical shape, positive superficial charge, and the capacity to stabilize DNA against enzymatic degradation. The cellular uptake of such nioplexes was mediated mainly by the macropynocytosis and caveolae pathways. After intravitreal injection, the outer segments of the retina were also efficiently transfected in a safe way.

As the main component of a niosome vesicle is the non-ionic surfactant, it looks logical to study the influence of different non-ionic surfactants in the design of niosomes for retinal gene delivery applications. In fact, in 2018, three niosome formulations that only differed in the polysorbate non-ionic tensioactive were elaborated by the solvent evaporation technique. The three niosome vesicles shared the same commercially available cationic lipid 1,2-di-O-octadecenyl-3-trimethylammonium propane (DOTMA), the same “helper” lipid squalene, and had polysorbate 20, polysorbate 80 or polysorbate 85 as non-ionic tensioactives [83]. Polysorbate 20 has the highest HLB value (16.7) and upon the incorporation of reported pCMSEGFP plasmid on the surface of corresponding niosomes to obtain nioplexes at a 2/1 ratio of cationic lipid/DNA, RPE cultured cells were successfully transfected without signs of toxicity. Intracellular trafficking studies showed that the hydrophilic nature of the polysorbate 20 non-ionic surfactant promoted caveolae-mediated endocytosis and evaded colocalization with the lysosome compartment, which to some extent could explain the difference observed in transfection efficiency among the three niosome formulations. In the primary culture cells of retina, such formulations were well tolerated, in contrast to the commercially available Lipofectamine 2000TM, and they expressed the fluorescent protein mainly in glial cells. After in situ subretinal injection, protein expression was observed mostly in RPE cells and also in the inner layers of the retina, whereas intravitreal injection transfected overall the ganglion cell layer.

However, the success of gene therapy does not only rely on the composition of the gene delivery system. In fact, vectors are only one part of the complex formulation. The other half is conditioned by the characteristics of the genetic material. In this sense, in 2019, the same cationic niosome formulation and three different GFP-encoding genetic materials consisting of minicircle (2.3 kb), its parental plasmid (3.5 kb), and a larger plasmid (5.5 kb) were combined to form nioplexes. Obtained results showed that the lack of unmethylated CpG regions in the mcDNA

rendered nioplexes with better physicochemical properties, stability, cell tolerance, and transfection efficiency in different layers of the rat retina after both intravitreal and subretinal injections, which reinforce the importance of the genetic material size and composition in the design of gene therapy vectors.

Taking into account that cationic niosomes represent a tunable platform for retinal gene delivery applications, in 2019, chloroquine was incorporated as a “helper” component into cationic niosomes based on the 2,3-di(tetradecyloxy)propan-1-amine (hydrochloride salt) cationic lipid, and a mixture of both poloxamer 188 and polysorbate 80 as non-ionic surfactants [115]. Chloroquine is a 4-aminoquinoline drug with promising properties for retinal gene therapy, since it can cross the BRB, interacts with negatively charged DNA molecules, and also promotes endosomal escape [141]. However, its clinical application is limited due to the high toxicity exhibited [142]. Therefore, chloroquine was incorporated within a niosome formulation to keep its gene delivery properties at low doses, reducing its toxic effect. At a 10/1 cationic lipid/DNA ratio, the resulting chloroquine concentration was only 25 μg , and it did not induce any significant cytotoxicity. In contrast, protein expression through different layers of the retina was increased as can be observed in figure 6.

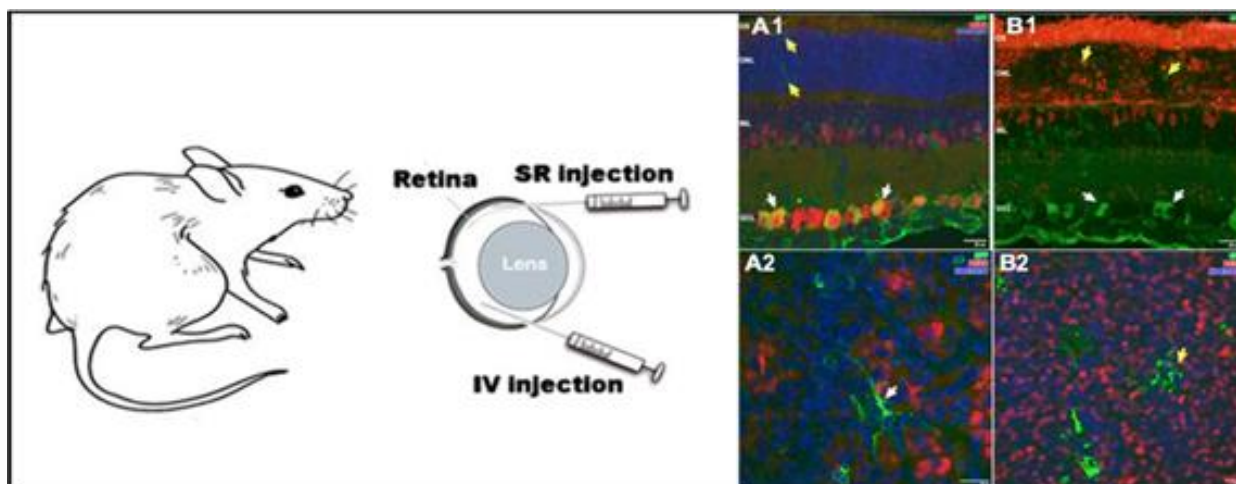


Figure 6. *In vivo* applications of niosomes in retina. Niosomes transfected different layers in the rat retina, depending on the administration route. Retinal cross sections micrographs obtained by confocal microscopy (A1, B1), confocal fluorescence micrographs of whole mount (A2, B2). Adapted with permission from Mashal et al. [114]. Copyright 2019, Elsevier B.V.

6. Brain as main goal

As in the case of vision, brain functions are essential for survival. Therefore, sophisticated mechanisms have been developed over many years of evolution to protect and isolate such sensitive organs with limited regeneration capacity from potentially damaging effects [31]. In the case of the brain, the tightly joined endothelial cells of BBB are impermeable for almost 100% of macromolecular and over 98% of small molecular drugs [143]. The transport of essential nutrients such as amino acids and glucose is mediated by specific receptors present in the BBB [31]. Although recent advances on gene therapy offer reasonable hope to face some devastating pathologies that affect relevant CNS organs such as the brain and eye, the isolation of those organs from the rest of the organism by the BBB and BEB prevents delivery systems from crossing such hurdles [43, 144]. Consequently, effective gene therapy approaches to treat both inherited and acquired diseases of brain rely on the in situ administration of genetic material by invasive routes [43]. Such cumbersome gene delivery strategy can jeopardize the acceptance of treatments and increase aftercare cost due to the treatment of related side effects [145].

6.1. General concepts

Gene therapy has shown great progress in clinical trials over the last decade to face both inherited and acquired devastating brain diseases that do not have a reasonably effective treatment with conventional drugs (<https://alliancerm.org/publication/q2-2019-data-report>). In the case of inborn metabolism mutations of one gene that affect the brain, such as mucopolysaccharidoses or Canavan disease, the approach normally consists of the delivery of a functional copy of the gene to restore the normal phenotype [146–148]. However, in the case of brain-acquired diseases, where more than one gene can be affected, such as brain cancer, Alzheimer's, or Parkinson's diseases, the genetic approach is more challenging, since the molecular basis of those disorders are still not understood [148–150]. BBB hampers the entry of gene expression vectors into the brain; consequently, gene treatments must be given after an invasive craniotomy, which in many cases jeopardizes the acceptance of patients enrolled in clinical trials due to the cumbersome approach and related side effects that increase the after-care cost as a consequence of additional hospital visits [151]. Moreover, because of the low diffusion of genetic material after in situ brain administration by craniotomy, few cells can be targeted by vectors, which prevent the access of the genetic material to the rest of the brain cells [152].

Apart from the route of administration, another confounding factor in brain gene therapy is the challenge that represents the delivery of genetic material into neurons. Brain neurons show strict organization to form complex neuronal networks, limited regenerative capacity, and low division rate, which hampers the entry of exogenous DNA into the nucleus [153]. Additionally, the molecular bases of many neurological disorders that affect the brain are still not understood. Previously commented limiting factors, along with the need to use appropriate vehicles that are able to deliver efficiently the genetic material, justify the hard path of brain gene therapy to reach clinical practice. In fact, although many phase I clinical trials have been reported; only a few have reached phase II [154]. However, with the new emerging technologies applied to gene therapy, the cure of brain diseases might look like a reasonable option in the near future [155]. One of the most promising approaches is to explore the use of non-viral vectors as gene delivery systems due to their safer profile, easy production capacity, and lower cost when compared to their viral vector counterparts [154].

6.2. Niosomes for gene delivery to the brain

Among non-viral vectors, niosomes based on cationic lipid 1-(2-dimethylaminoethyl)-3-[2,3-di (tetradecoxy) propyl] urea, combined with squalene as a “helper” lipid and polysorbate 80 non-ionic surfactant, were recently able to transfect the rat cerebral cortex after in situ administration [51]. Such cationic niosomes were elaborated by the solvent evaporation technique and exhibited a diameter of 200 nm with a low PDI value (0.21) and positive superficial charge over 30 mV. Physicochemical parameters were maintained after 100 days when formulations were stored at 4 °C. Upon the addition of reporter pCMSEGF plasmid in their surface by electrostatic interactions at a 30/1 cationic lipid/DNA ratio, the resulting nioplexes were able to transfect efficiently both neurons and non-neuron cells in primary cultures obtained from the cortex of rat embryos, as revealed by immunohistochemistry studies as can be observed in figure 7.

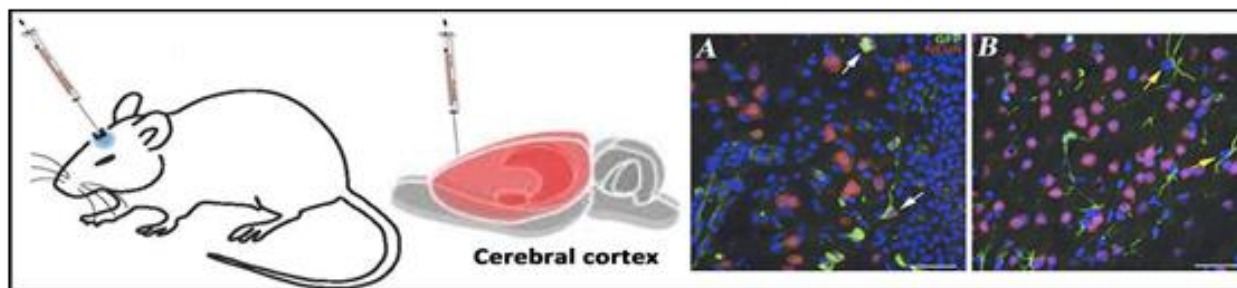


Figure 7. *In vivo* applications of niosomes in brain. (A) White arrows in the right side indicated identified neurons (red) that express EGFP (green). (B) Non-neuron cells (NeuN⁻) with glia morphology that express EGFP (green) were indicated by yellow arrows. Adapted with permission from Ojeda et al. [51]. Copyright 2017, Elsevier B.V.

In 2018, another niosome formulation elaborated with a commercially available DOTMA cationic lipid, lycopene as a “helper” lipid and polysorbate 60 as a non-ionic surfactant, exhibited high levels of protein expression in both primary cortical cultures of rat embryos and in *in vivo* conditions after intracranial injection in the cortex [114]. Such niosomes were characterized in terms of size, superficial charge, polydispersity, or capacity to protect genetic material against enzymatic digestion in an agarose gel electrophoresis assay. After physicochemical characterization, *in vitro* studies were performed in human neuronal precursors NT2 cells. NT2 cells are considered as an attractive model to evaluate CNS gene delivery efficiency, which is mainly due to their potential capacity to be easily differentiated into both glial and neuronal cells, upon exposition to retinoic acid [93, 156]. Additionally, genetically modified NT2 cells can be transplanted into CNS and migrate to specific regions of brain, acting as an interesting cell-based gene delivery platform to repair brain damages [157]. After 24 h post-transfection, nioplexes formulated at a 14/1 cationic lipid/DNA ratio exhibited approximately half the transfection capacity of the commercially available Lipofectamine® 2000 but higher cell viability. Intracellular trafficking studies performed with both specific dye markers and blockers of most representative endocytosis pathways revealed higher cellular internalization by both caveolae and clathrin-mediated endocytosis than by macropinocytosis. In addition, buffering capacity studies revealed endosomal properties that could explain, at least in part, the high transfection efficiency observed in NT2 cells. Next, and before brain administration into the rat cerebral cortex, the primary cortical cultures of rat embryos were exposed to nioplexes in order to better mimic the *in vivo* conditions. In this scenario, NeuN⁻ cells with glial morphology expressed

the protein, which was probably due to their phagocytic and mitotic activity [158]. The lack of protein expression into neurons was confirmed after the *in situ* intracranial injection of nioplexes. Again, only NeuN- cells (neuroglia and cells in blood vessel wall) expressed the protein. In any case, although this niosome formulation failed to transfect brain neurons after intracranial injection, high levels of protein expression in glial cells suggest its possible application into CNS in glia-related neurological disorders such as epilepsy, Alzheimer's, or Parkinson's diseases, to name some of the most representatives ones [159].

Considering the previously reported properties of poloxamer 188 regarding biocompatibility and capacity to protect neurons against brain injury [160], its incorporation into niosomes based on the hydrochloride salt of 2,3-di(tetradecyloxy)propan-1-amine cationic lipid and polysorbate 80 surfactant was evaluated [82]. Therefore, two niosome formulations that differed only regarding the presence or absence of the non-ionic surfactant poloxamer 188 were elaborated by the reverse-phase evaporation technique and characterized to deliver the genetic material into the rat brain cortex. When poloxamer 188 was incorporated into the niosomes, the sizes of niosomes increased, which was probably due to the high HLB value of poloxamer 188 and to the interaction with the cationic lipid [161]. However, no significant change in zeta potential was reported, being over +40 mV. Agarose gel electrophoresis assays revealed that out of all the cationic lipid/DNA ratios studied, nioplexes based on niosome formulated with both non-ionic surfactants polysorbate 80 and poloxamer 188 at equal mass ratios protected the genetic material from enzymatic degradation. However, in the case of niosomes formulated only with polysorbate 80 as a non-ionic surfactant, at low cationic lipid/DNA ratios, the genetic material was degraded, which was probably due to the negative zeta potential value of those nioplexes that were able to condense but not protect the DNA. *In vitro* experiments on NT2 cells revealed that the addition of poloxamer 188 to niosomes enhanced the cell viability and the cellular uptake mediated by caveolae and macropinocytosis, which could explain the higher transfection values observed. In primary cortical cultures of rat embryos, gene expression was mainly observed in neurons with no signs of toxicity. However, when moving to *in situ* intracranial administration, nioplexes transfected glial cells but not the neurons of the cortex. Such *in vitro* and *in vivo* discrepancy could be explained by the different gene delivery mechanism in both biological scenarios.

Interestingly, the following year, in 2019, the same niosome formulation based on the 2,3-di(tetradecyloxy)propan-1-amine cationic lipid and a mixture at equal weight ratios of both polysorbate 80 and poloxamer 188 non-ionic surfactant was able to deliver the pUNO1-hBMP7 plasmid into NT2 (NTera2/D1 teratocarcinoma-derived) cells [162]. The human bone morphogenetic protein 7 (hBMP7) belongs to the transforming growth factor β superfamily, and its role is relevant for the development of bone, kidney, and nervous tissues [163]. At a 6/1 cationic lipid/DNA ratio, a significant release of hBMP7 (5.7 ng/mL) was detected in the supernatants of transfected cells, with no signs of toxicity. Next, the tumor-suppressive effect of hBMP7-expressing NT2 cells was investigated on the glioma cell line C6 in a transwell indirect co-culture system to avoid the drawbacks of direct co-culture system. *In vitro* co-culture results showed that the BMP7-overexpressing NT2 cells hampered the migration of C6 glioma cells, which highlights the potential of NT2 cell-based delivery of hBMP7 for impeding the metastasis of glioma cells [162].

7. Future perspectives

After more than three decades of hard work, with normal ups and downs, nowadays, gene therapy represents a real and revolutionary clinical option, not only to treat but also to cure the molecular basis of some serious disease. In any case, and despite the promising future that awaits gene therapy, some controversial issues still need to be improved. At the moment, all of the gene therapy treatments approved for human use by different regulatory authorities are based on viral vectors, which rises controversy regarding their safety profile, limited gene-packing capacity, large-scale production, and high costs [164]. Consequently, during the last years, research on non-viral vectors has gained “momentum” as a safer alternative to their viral vectors counterparts, and the number of clinical trials has considerably increased since 2010 (www.clinicaltrials.gov).

In the case of eye and brain, which according to the old immune-privileged concept are organs isolated and protected from the systemic immune response of the organism [119], the use of less immunogenic non-viral vectors [165] is even more relevant to avoid damage in such sensitive organs [43]. In addition, in order to develop a more friendly approach, at a preclinical level, many nanotechnology-based formulations of different materials, shapes, and compositions can be tailored with specific ligands to overcome both BRB and BBB and deliver

their cargo by non-invasive routes of administration such as topical instillation on ocular [166–169] and nose surfaces [170, 171] (Figure 8). Considering the versatility of the cationic niosome platform for gene delivery applications, some of the biomaterials commonly used to overcome the BRB and BBB, such as transferrin, Annexin V, insulin, or gemini surfactants, could be incorporated in novel niosome vesicles, bearing in mind the recent results reported after the in situ administration of such non-viral vectors in both retina and brain cortex tissues.

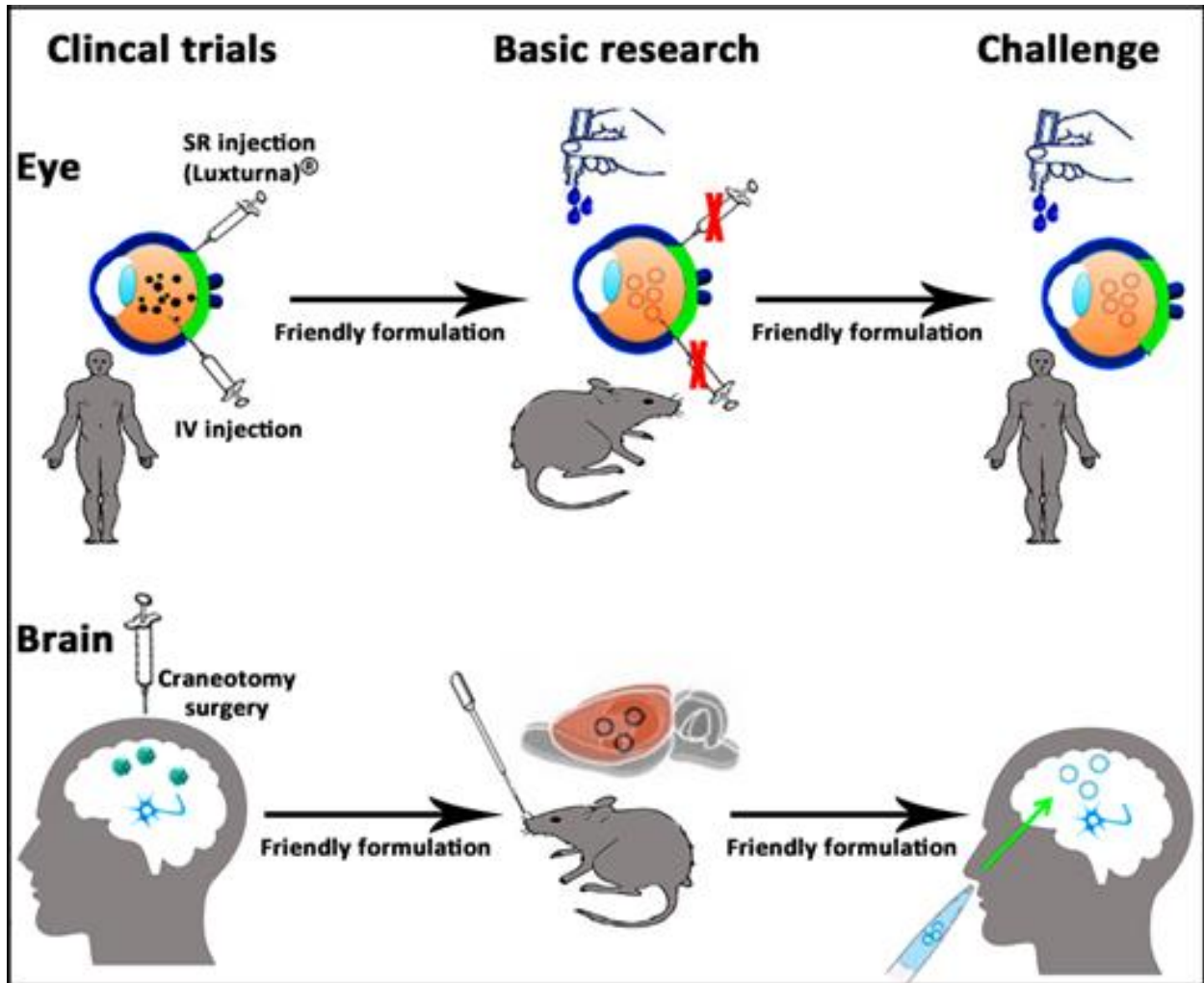


Figure 8. Schematic representation of a gene therapy approach based on non-viral vectors and non-invasive administration route to face brain and eye diseases.

Although it is possible to reach the brain cortex and retina in small animals at a preclinical level by non-invasive routes of administration, in order to reach the regular clinical practice, enough gene expression should be reached selectively in the specific target cells of those tissues

in larger species, avoiding the distribution of the delivered gene in other tissues. At present, non-invasive approaches to reach both the brain cortex and retina require multiple administration doses at high concentrations, which enhance systemic absorption, and therefore, the appearance of unwanted effects in other tissues. In this sense, the use of cell-type specific promoters, inducible promoters, or the rapamycin regulation system offer a reasonable option to confine gene expression only in specific cell types, which avoids off-target effects in other cells [153]. Hence, the future direction to design non-viral vectors based on novel cationic niosomes to face inherited and acquired diseases of eye and brain by non-invasive routes of administration requires not only the use of appropriate biomaterials and targeting ligands coupled to the niosome platform but also the selection of the appropriate genetic material with its intrinsic characteristics. In any case, it is clear that such ambitious goals need to be addressed by a multidisciplinary approach. In this sense, the design of novel smart imaging and sensing catheter devices for surgical interventions based on next-generation technologies at the point of intervention would also minimize both the damage and cost occasioned by the in situ administration of gene therapy-based drugs in the brain and retina.

Funding: This work was supported by the Basque Country Government (Department of Education, University and Research, pre-doctoral grant PRE_2016_2_0302 and Consolidated Groups IT907-16). Additional funding was provided by the University of Basque Country UPV/EHU (predoctoral grant PIF17/19), the CIBER of Bioengineering, Biomaterials and Nanomedicine (CIBER-BBN), and initiative of the Carlos III Health Institute (ISCIII).

Acknowledgments: The authors wish to thank the intellectual and technical assistance from the ICTS “NANBIOSIS,” more specifically by the Drug Formulation Unit (U10) of the CIBER in Bioengineering, Biomaterials and Nanomedicine (CIBER-BBN) at the University of Basque Country (UPV/EHU).

Conflicts of Interest: The authors declare no conflict of interest. The funders had no role in the design of the study; in the collection, analyses, or interpretation of data; in the writing of the manuscript, or in the decision to publish the results.

References

1. Dunbar, C.E.; High, K.A.; Joung, J.K.; Kohn, D.B.; Ozawa, K.; Sadelain, M. Gene Therapy Comes of Age. *Science* 2018, 359, eaan4672. [CrossRef] [PubMed]
2. Orkin, S.H.; Reilly, P. MEDICINE. Paying for Future Success in Gene Therapy. *Science* 2016, 352, 1059–1061. [PubMed]
3. Mullard, A. Gene Therapy Boom Continues. *Nat. Rev. Drug Discov.* 2019, 18, 737. [PubMed]
4. Lee, C.L.; Veeramani, S.; Molouki, A.; Lim, S.H.E.; Thomas, W.; Chia, S.L.; Yusoff, K. Virotherapy: Current Trends and Future Prospects for Treatment of Colon and Rectal Malignancies. *Cancer Investig.* 2019, 37, 393–414.
5. Terrivel, M.; Gromicho, C.; Matos, A.M. Oncolytic Viruses: What to Expect from its use in Cancer Treatment. *Microbiol. Immunol.* 2019. [CrossRef]
6. del Pozo-Rodriguez, A.; Delgado, D.; Solinis, M.A.; Pedraz, J.L.; Gascon, A.R. Solid lipid nanoparticles as potential tools for gene therapy: in vivo protein expression after intravenous administration. *Int. J. Pharm.* 2010, 385, 1–2.
7. McLachlan, G.; Stevenson, B.J.; Davidson, D.J.; Porteous, D.J. Bacterial DNA is Implicated in the Inflammatory Response to Delivery of DNA/DOTAP to Mouse Lungs. *Gene Ther.* 2000, 7, 384–392.
8. Gill, D.R.; Pringle, I.A.; Hyde, S.C. Progress and Prospects: The Design and Production of Plasmid Vectors. *Gene Ther.* 2009, 16, 165–171.
9. Gallego, I.; Villate-Beitia, I.; Martinez-Navarrete, G.; Menendez, M.; Lopez-Mendez, T.; Soto-Sanchez, C.; Zarate, J.; Puras, G.; Fernandez, E.; Pedraz, J.L. Non-Viral Vectors Based on Cationic Niosomes and Minicircle DNA Technology Enhance Gene Delivery Efficiency for Biomedical Applications in Retinal Disorders. *Nanomedicine* 2019, 17, 308–318.
10. Talbot, K.; Wood, M.J.A. Wrangling RNA: Antisense Oligonucleotides for Neurological Disorders. *Sci. Transl. Med.* 2019, 11. [CrossRef]
11. Dias, N.; Stein, C.A. Antisense Oligonucleotides: Basic Concepts and Mechanisms. *Mol. Cancer Ther.* 2002, 1, 347–355.
12. Coutinho, M.F.; Matos, L.; Santos, J.I.; Alves, S. RNA Therapeutics: How Far have we Gone? *Adv. Exp. Med. Biol.* 2019, 1157, 133–177. [PubMed]
13. Kim, J.; Hu, C.; Moufawad El Achkar, C.; Black, L.E.; Douville, J.; Larson, A.; Pendergast, M.K.; Goldkind, S.F.; Lee, E.A.; Kuniholm, A.; et al. Patient-Customized Oligonucleotide Therapy for a Rare Genetic Disease. *N. Engl. J. Med.* 2019, 381, 1644–1652. [PubMed]
14. Terrazas, M.; Kool, E.T. RNA Major Groove Modifications Improve siRNA Stability and Biological Activity. *Nucleic Acids Res.* 2009, 37, 346–353. [PubMed]
15. Gowing, G.; Svendsen, S.; Svendsen, C.N. Ex Vivo Gene Therapy for the Treatment of Neurological Disorders. *Prog. Brain Res.* 2017, 230, 99–132.

16. Gregory-Evans, K.; Bashar, A.M.; Tan, M. Ex Vivo Gene Therapy and Vision. *Curr. Gene Ther.* 2012, 12, 103–115.
17. Shahryari, A.; Saghaeian Jazi, M.; Mohammadi, S.; Razavi Nikoo, H.; Nazari, Z.; Hosseini, E.S.; Burtscher, I.; Mowla, S.J.; Lickert, H. Development and Clinical Translation of Approved Gene Therapy Products for Genetic Disorders. *Front. Genet.* 2019, 10, 868.
18. Xu, X.; Wan, T.; Xin, H.; Li, D.; Pan, H.; Wu, J.; Ping, Y. Delivery of CRISPR/Cas9 for Therapeutic Genome Editing. *J. Gene Med.* 2019, 21, e3107.
19. Schacker, M.; Seimetz, D. From Fiction to Science: Clinical Potentials and Regulatory Considerations of Gene Editing. *Clin. Transl. Med.* 2019, 8, 27.
20. Burgess, D.J. CRISPR Screens Come into Sight. *Nat. Rev. Genet.* 2020, 21, 1.
21. Anzalone, A.V.; Randolph, P.B.; Davis, J.R.; Sousa, A.A.; Koblan, L.W.; Levy, J.M.; Chen, P.J.; Wilson, C.;
Newby, G.A.; Raguram, A.; et al. Search-and-Replace Genome Editing without Double-Strand Breaks Or Donor DNA. *Nature* 2019, 576, 149–157. [PubMed]
22. Sung, Y.K.; Kim, S.W. Recent Advances in the Development of Gene Delivery Systems. *Biomater. Res.* 2019, 23, 8. [PubMed]
23. Yin, H.; Xue, W.; Chen, S.; Bogorad, R.L.; Benedetti, E.; Grompe, M.; Koteliansky, V.; Sharp, P.A.; Jacks, T.; Anderson, D.G. Genome Editing with Cas9 in Adult Mice Corrects a Disease Mutation and Phenotype. *Nat. Biotechnol.* 2014, 32, 551–553.
24. Baskaran, U.L.; Sabina, E.P. Clinical and Experimental Research in Antituberculosis Drug-Induced Hepatotoxicity: A Review. *J. Integr. Med.* 2017, 15, 27–36. [PubMed]
25. Li, S.D.; Huang, L. Gene Therapy Progress and Prospects: Non-Viral Gene Therapy by Systemic Delivery. *Gene Ther.* 2006, 13, 1313–1319.
26. Gardlik, R.; Palffy, R.; Hodossy, J.; Lukacs, J.; Turna, J.; Celec, P. Vectors and Delivery Systems in Gene Therapy. *Med. Sci. Monit.* 2005, 11, RA110–RA121.
27. Escoffre, J.M.; Teissie, J.; Rols, M.P. Gene Transfer: How can the Biological Barriers be Overcome? *J. Membr. Biol.* 2010, 236, 61–74.
28. Eoh, J.; Gu, L. Biomaterials as Vectors for the Delivery of CRISPR-Cas9. *Biomater. Sci.* 2019, 7, 1240–1261.
29. Li, L.; Hu, S.; Chen, X. Non-Viral Delivery Systems for CRISPR/Cas9-Based Genome Editing: Challenges and Opportunities. *Biomaterials* 2018, 171, 207–218.
30. Wang, M.; Glass, Z.A.; Xu, Q. Non-Viral Delivery of Genome-Editing Nucleases for Gene Therapy. *Gene Ther.* 2017, 24, 144–150.

31. O'Mahony, A.M.; Godinho, B.M.; Cryan, J.F.; O'Driscoll, C.M. Non-Viral Nanosystems for Gene and Small Interfering RNA Delivery to the Central Nervous System: Formulating the Solution. *J. Pharm. Sci.* 2013, 102, 3469–3484. [PubMed]
32. Zhang, Y.; Schlachetzki, F.; Li, J.Y.; Boado, R.J.; Pardridge, W.M. Organ-Specific Gene Expression in the Rhesus Monkey Eye Following Intravenous Non-Viral Gene Transfer. *Mol. Vis.* 2003, 9, 465–472. [PubMed]
33. Vaughan, E.E.; DeGiulio, J.V.; Dean, D.A. Intracellular Trafficking of Plasmids for Gene Therapy: Mechanisms of Cytoplasmic Movement and Nuclear Import. *Curr. Gene Ther.* 2006, 6, 671–681.
34. Perez Ruiz de Garibay, A. Endocytosis in Gene Therapy with Non-Viral Vectors. *Wien. Med. Wochenschr.* 2016, 166, 227–235. [PubMed]
35. Ilina, P.; Hyvonen, Z.; Saura, M.; Sandvig, K.; Yliperttula, M.; Ruponen, M. Genetic Blockage of Endocytic Pathways Reveals Differences in the Intracellular Processing of Non-Viral Gene Delivery Systems. *J. Control Release* 2012, 163, 385–395.
36. Luzio, J.P.; Gray, S.R.; Bright, N.A. Endosome-Lysosome Fusion. *Biochem. Soc. Trans.* 2010, 38, 1413–1416.
37. Dauty, E.; Verkman, A.S. Actin Cytoskeleton as the Principal Determinant of Size Dependent DNA Mobility in Cytoplasm: A New Barrier for Non-Viral Gene Delivery. *J. Biol. Chem.* 2005, 280, 7823–7828.
38. Lukacs, G.L.; Haggie, P.; Seksek, O.; Lechardeur, D.; Freedman, N.; Verkman, A.S. Size-Dependent DNA Mobility in Cytoplasm and Nucleus. *J. Biol. Chem.* 2000, 275, 1625–1629.
39. Masuda, T.; Akita, H.; Harashima, H. Evaluation of Nuclear Transfer and Transcription of Plasmid DNA Condensed with Protamine by Microinjection: The use of a Nuclear Transfer Score. *FEBS Lett.* 2005, 579, 2143–2148.
40. Akita, H.; Tanimoto, M.; Masuda, T.; Kogure, K.; Hama, S.; Ninomiya, K.; Futaki, S.; Harashima, H. Evaluation of the Nuclear Delivery and Intra-Nuclear Transcription of Plasmid DNA Condensed with Micro (Mu) and NLS-Micro by Cytoplasmic and Nuclear Microinjection: A Comparative Study with Poly-L-Lysine. *J. Gene Med.* 2006, 8, 198–206. [PubMed]
41. Pezzoli, D.; Chiesa, R.; De Nardo, L.; Candiani, G. We Still have a Long Way to Go to Effectively Deliver Genes! *J. Appl. Biomater. Funct. Mater.* 2012, 10, 82–91. [PubMed]
42. Kay, M.A. State-of-the-Art Gene-Based Therapies: The Road Ahead. *Nat. Rev. Genet.* 2011, 12, 316–328.
43. Foldvari, M.; Chen, D.W.; Nafissi, N.; Calderon, D.; Narsineni, L.; Rafiee, A. Non-Viral Gene Therapy: Gains and Challenges of Non-Invasive Administration Methods. *J. Control Release* 2016, 240, 165–190.

44. Shim, G.; Kim, D.; Park, G.T.; Jin, H.; Suh, S.K.; Oh, Y.K. Therapeutic Gene Editing: Delivery and Regulatory Perspectives. *Acta Pharmacol. Sin.* 2017, 38, 738–753. [PubMed]
45. Cwetsch, A.W.; Pinto, B.; Savardi, A.; Cancedda, L. In Vivo Methods for Acute Modulation of Gene Expression in the Central Nervous System. *Prog. Neurobiol.* 2018, 168, 69–85. [PubMed]
46. Sharei, A.; Cho, N.; Mao, S.; Jackson, E.; Poceviciute, R.; Adamo, A.; Zoldan, J.; Langer, R.; Jensen, K.F. Cell Squeezing as a Robust, Microfluidic Intracellular Delivery Platform. *J. Vis. Exp.* 2013, 81, e50980.
47. Liu, C.; Zhang, L.; Liu, H.; Cheng, K. Delivery Strategies of the CRISPR-Cas9 Gene-Editing System for Therapeutic Applications. *J. Control Release* 2017, 266, 17–26. [PubMed]
48. Keles, E.; Song, Y.; Du, D.; Dong, W.J.; Lin, Y. Recent Progress in Nanomaterials for Gene Delivery Applications. *Biomater. Sci.* 2016, 4, 1291–1309.
49. Ojeda, E.; Puras, G.; Agirre, M.; Zarate, J.; Grijalvo, S.; Pons, R.; Eritja, R.; Martinez-Navarrete, G.; Soto-Sanchez, C.; Fernandez, E.; et al. Niosomes Based on Synthetic Cationic Lipids for Gene Delivery: The Influence of Polar Head-Groups on the Transfection Efficiency in HEK-293, ARPE-19 and MSC-D1 Cells. *Org. Biomol. Chem.* 2015, 13, 1068–1081.
50. Ochoa, G.P.; Sesma, J.Z.; Diez, M.A.; Diaz-Tahoces, A.; Aviles-Trigueros, M.; Grijalvo, S.; Eritja, R.; Fernandez, E.; Pedraz, J.L. A Novel Formulation Based on 2,3-Di(Tetradecyloxy)Propan-1-Amine Cationic Lipid Combined with Polysorbate 80 for Efficient Gene Delivery to the Retina. *Pharm. Res.* 2014, 31, 1665–1675.
51. Ojeda, E.; Puras, G.; Agirre, M.; Zarate, J.; Grijalvo, S.; Eritja, R.; Martinez-Navarrete, G.; Soto-Sanchez, C.; Diaz-Tahoces, A.; Aviles-Trigueros, M.; et al. The Influence of the Polar Head-Group of Synthetic Cationic Lipids on the Transfection Efficiency Mediated by Niosomes in Rat Retina and Brain. *Biomaterials* 2016, 77, 267–279. [PubMed]
52. de Lima, M.C.; da Cruz, M.T.; Cardoso, A.L.; Simoes, S.; de Almeida, L.P. Liposomal and Viral Vectors for Gene Therapy of the Central Nervous System. *Curr. Drug Targets CNS Neurol. Disord.* 2005, 4, 453–465. [PubMed]
53. del Pozo-Rodriguez, A.; Delgado, D.; Solinis, M.A.; Gascon, A.R.; Pedraz, J.L. Solid Lipid Nanoparticles for Retinal Gene Therapy: Transfection and Intracellular Trafficking in RPE Cells. *Int. J. Pharm.* 2008, 360, 177–183. [PubMed]
54. Milani, P.; Mussinelli, R.; Perlini, S.; Palladini, G.; Obici, L. An Evaluation of Patisiran: A Viable Treatment Option for Transthyretin-Related Hereditary Amyloidosis. *Expert Opin. Pharmacother.* 2019, 20, 2223–2228.
55. Agirre, M.; Zarate, J.; Ojeda, E.; Puras, G.; Rojas, L.A.; Alemany, R.; Pedraz, J.L. Delivery of an Adenovirus Vector Plasmid by Ultrapure Oligochitosan Based Polyplexes. *Int. J. Pharm.* 2015, 479, 312–319.
56. Lungwitz, U.; Breunig, M.; Blunk, T.; Gopferich, A. Polyethylenimine-Based Non-Viral Gene Delivery Systems. *Eur. J. Pharm. Biopharm.* 2005, 60, 247–266.

57. Mandal, H.; Katiyar, S.S.; Swami, R.; Kushwah, V.; Katare, P.B.; Kumar Meka, A.; Banerjee, S.K.; Popat, A.; Jain, S. Epsilon-Poly-L-Lysine/Plasmid DNA Nanoplexes for Efficient Gene Delivery in Vivo. *Int. J. Pharm.* 2018, 542, 142–152.
58. Zhang, T.; Ma, J.; Li, C.; Lin, K.; Lou, F.; Jiang, H.; Gao, Y.; Yang, Y.; Ming, C.; Ruan, B. Coreshell Lipid Polymer Nanoparticles for Combined Chemo and Gene Therapy of Childhood Head and Neck Cancers. *Oncol. Rep.* 2017, 37, 1653–1661.
59. Megias, R.; Arco, M.; Ciriza, J.; Saenz Del Burgo, L.; Puras, G.; Lopez-Viota, M.; Delgado, A.V.; Dobson, J.P.; Arias, J.L.; Pedraz, J.L. Design and Characterization of a Magnetite/PEI Multifunctional Nanohybrid as Non-Viral Vector and Cell Isolation System. *Int. J. Pharm.* 2017, 518, 270–280.
60. de la Fuente, M.; Seijo, B.; Alonso, M.J. Novel Hyaluronic Acid-Chitosan Nanoparticles for Ocular Gene Therapy. *Investig. Ophthalmol. Vis. Sci.* 2008, 49, 2016–2024.
61. Pilipenko, I.; Korzhikov-Vlakh, V.; Sharoyko, V.; Zhang, N.; Schafer-Korting, M.; Ruhl, E.; Zoschke, C.; Tennikova, T. pH-Sensitive Chitosan-Heparin Nanoparticles for Effective Delivery of Genetic Drugs into Epithelial Cells. *Pharmaceutics* 2019, 11, 317. [CrossRef]
62. Osipova, O.; Sharoyko, V.; Zashikhina, N.; Zakharova, N.; Tennikova, T.; Urtti, A.; Korzhikova-Vlakh, E. Amphiphilic Polypeptides for VEGF siRNA Delivery into Retinal Epithelial Cells. *Pharmaceutics* 2020, 12, 39. [CrossRef]
63. Terada, D.; Genjo, T.; Segawa, T.F.; Igarashi, R.; Shirakawa, M. Nanodiamonds for Bioapplications-Specific Targeting Strategies. *Biochim. Biophys. Acta Gen. Subj.* 2020, 1864. [CrossRef]
64. Zhang, X.Q.; Chen, M.; Lam, R.; Xu, X.; Osawa, E.; Ho, D. Polymer-Functionalized Nanodiamond Platforms as Vehicles for Gene Delivery. *ACS Nano* 2009, 3, 2609–2616.
65. Kim, H.; Man, H.B.; Saha, B.; Kopacz, A.M.; Lee, O.S.; Schatz, G.C.; Ho, D.; Liu, W.K. Multiscale Simulation as a Framework for the Enhanced Design of Nanodiamond-Polyethylenimine-Based Gene Delivery. *J. Phys. Chem. Lett.* 2012, 3, 3791–3797.
66. Alwani, S.; Kaur, R.; Michel, D.; Chitanda, J.M.; Verrall, R.E.; Karunakaran, C.; Badea, I. Lysine-Functionalized Nanodiamonds as Gene Carriers: Development of Stable Colloidal Dispersion for in Vitro Cellular Uptake Studies and siRNA Delivery Application. *Int. J. Nanomed.* 2016, 11, 687–702.
67. Edgington, R.; Spillane, K.M.; Papageorgiou, G.; Wray, W.; Ishiwata, H.; Labarca, M.; Leal-Ortiz, S.; Reid, G.; Webb, M.; Foord, J.; et al. Functionalisation of Detonation Nanodiamond for Monodispersed, Soluble DNA-Nanodiamond Conjugates using Mixed Silane Bead-Assisted Sonication Disintegration. *Sci. Rep.* 2018, 8, 1–11.
68. Lim, D.G.; Rajasekaran, N.; Lee, D.; Kim, N.A.; Jung, H.S.; Hong, S.; Shin, Y.K.; Kang, E.; Jeong, S.H. Polyamidoamine-Decorated Nanodiamonds as a Hybrid Gene Delivery Vector and siRNA Structural Characterization at the Charged Interfaces. *ACS Appl. Mater. Interfaces* 2017, 9, 31543–31556.

69. Wu, L.; Xie, J.; Li, T.; Mai, Z.; Wang, L.; Wang, X.; Chen, T. Gene Delivery Ability of Polyethylenimine and Polyethylene Glycol Dual-Functionalized Nanographene Oxide in 11 Different Cell Lines. *R. Soc. Open Sci.* 2017, 4, 170822.
70. Kim, H.; Namgung, R.; Singha, K.; Oh, I.K.; Kim, W.J. Graphene Oxide-Polyethylenimine Nanoconstruct as a Gene Delivery Vector and Bioimaging Tool. *Bioconjug. Chem.* 2011, 22, 2558–2567.
71. Bao, H.; Pan, Y.; Ping, Y.; Sahoo, N.G.; Wu, T.; Li, L.; Li, J.; Gan, L.H. Chitosan-Functionalized Graphene Oxide as a Nanocarrier for Drug and Gene Delivery. *Small* 2011, 7, 1569–1578. [PubMed]
72. Rajera, R.; Nagpal, K.; Singh, S.K.; Mishra, D.N. Niosomes: A Controlled and Novel Drug Delivery System. *Biol. Pharm. Bull.* 2011, 34, 945–953. [PubMed]
73. Moghassemi, S.; Hadjizadeh, A. Nano-Niosomes as Nanoscale Drug Delivery Systems: An Illustrated Review. *J. Control Release* 2014, 185, 22–36. [PubMed]
74. Ge, X.; Wei, M.; He, S.; Yuan, W.E. Advances of Non-Ionic Surfactant Vesicles (Niosomes) and their Application in Drug Delivery. *Pharmaceutics* 2019, 11, 55. [CrossRef]
75. Khatoon, M.; Shah, K.U.; Din, F.U.; Shah, S.U.; Rehman, A.U.; Dilawar, N.; Khan, A.N. Proniosomes Derived Niosomes: Recent Advancements in Drug Delivery and Targeting. *Drug Deliv.* 2017, 24, 56–69.
76. Grijalvo, S.; Puras, G.; Zarate, J.; Sainz-Ramos, M.; Qtaish, N.A.L.; Lopez, T.; Mashal, M.; Attia, N.; Diaz, D.; Pons, R.; et al. Cationic Niosomes as Non-Viral Vehicles for Nucleic Acids: Challenges and Opportunities in Gene Delivery. *Pharmaceutics* 2019, 11, 50. [CrossRef]
77. Muzzalupo, R.; Mazzotta, E. Do Niosomes have a Place in the Field of Drug Delivery? *Exp. Opin. Drug Deliv.* 2019, 16, 1145–1147.
78. Ojeda, E.; Agirre, M.; Villate-Beitia, I.; Mashal, M.; Puras, G.; Zarate, J.; Pedraz, J.L. Elaboration and Physicochemical Characterization of Niosome-Based Nioplexes for Gene Delivery Purposes. *Methods Mol. Biol.* 2016, 1445, 63–75.
79. Grijalvo, S.; Alagia, A.; Puras, G.; Zarate, J.; Pedraz, J.L.; Eritja, R. Cationic Vesicles Based on Non-Ionic Surfactant and Synthetic Aminolipids Mediate Delivery of Antisense Oligonucleotides into Mammalian Cells. *Colloids Surf. B Biointerfaces* 2014, 119, 30–37.
80. Primavera, R.; Palumbo, P.; Celia, C.; Cilurzo, F.; Cinque, B.; Carata, E.; Carafa, M.; Paolino, D.; Cifone, M.G.; Di Marzio, L. Corrigendum to “an Insight of in Vitro Transport of PEGylated Non-Ionic Surfactant Vesicles (NSVs) Across the Intestinal Polarized Enterocyte Monolayer”. *Eur. J. Pharm. Biopharm.* 2018, 128, 259.
81. Barani, M.; Mirzaei, M.; Torkzadeh-Mahani, M.; Nematollahi, M.H. Lawsone-Loaded Niosome and its Antitumor Activity in MCF-7 Breast Cancer Cell Line: A Nano-Herbal Treatment for Cancer. *Daru* 2018, 26, 11–17. [PubMed]

82. Attia, N.; Mashal, M.; Soto-Sanchez, C.; Martinez-Navarrete, G.; Fernandez, E.; Grijalvo, S.; Eritja, R.; Puras, G.; Pedraz, J.L. Gene Transfer to Rat Cerebral Cortex Mediated by Polysorbate 80 and Poloxamer 188 Nonionic Surfactant Vesicles. *Drug Des. Devel. Ther.* 2018, 12, 3937–3949. [PubMed]
83. Villate-Beitia, I.; Gallego, I.; Martinez-Navarrete, G.; Zarate, J.; Lopez-Mendez, T.; Soto-Sanchez, C.; Santos-Vizcaino, E.; Puras, G.; Fernandez, E.; Pedraz, J.L. Polysorbate 20 Non-Ionic Surfactant Enhances Retinal Gene Delivery Efficiency of Cationic Niosomes After Intravitreal and Subretinal Administration. *Int. J. Pharm.* 2018, 550, 388–397. [PubMed]
84. Pardakhty, A.; Varshosaz, J.; Rouholamini, A. In Vitro Study of Polyoxyethylene Alkyl Ether Niosomes for Delivery of Insulin. *Int. J. Pharm.* 2007, 328, 130–141. [PubMed]
85. Chen, S.; Hanning, S.; Falconer, J.; Locke, M.; Wen, J. Recent Advances in Non-Ionic Surfactant Vesicles (Niosomes): Fabrication, Characterization, Pharmaceutical and Cosmetic Applications. *Eur. J. Pharm. Biopharm.* 2019, 144, 18–39. [PubMed]
86. Puras, G.; Martinez-Navarrete, G.; Mashal, M.; Zarate, J.; Agirre, M.; Ojeda, E.; Grijalvo, S.; Eritja, R.; Diaz-Tahoces, A.; Aviles-Trigueros, M.; et al. Protamine/DNA/Niosome Ternary Nonviral Vectors for Gene Delivery to the Retina: The Role of Protamine. *Mol. Pharm.* 2015, 12, 3658–3671.
87. Ruyschaert, J.M.; el Ouahabi, A.; Willeaume, V.; Huez, G.; Fuks, R.; Vandenbranden, M.; Di Stefano, P. A Novel Cationic Amphiphile for Transfection of Mammalian Cells. *Biochem. Biophys. Res. Commun.* 1994, 203, 1622–1628.
88. Regelin, A.E.; Fankhaenel, S.; Gurtesch, L.; Prinz, C.; von Kiedrowski, G.; Massing, U. Biophysical and Lipofection Studies of DOTAP Analogs. *Biochim. Biophys. Acta* 2000, 1464, 151–164.
89. Barani, M.; Nematollahi, M.H.; Zaboli, M.; Mirzaei, M.; Torkzadeh-Mahani, M.; Pardakhty, A.; Karam, G.A. In Silico and in Vitro Study of Magnetic Niosomes for Gene Delivery: The Effect of Ergosterol and Cholesterol. *Mater. Sci. Eng. C. Mater. Biol. Appl.* 2019, 94, 234–246.
90. Ojeda, E.; Puras, G.; Agirre, M.; Zarate, J.; Grijalvo, S.; Eritja, R.; DiGiacomo, L.; Caracciolo, G.; Pedraz, J.L. The Role of Helper Lipids in the Intracellular Disposition and Transfection Efficiency of Niosome Formulations for Gene Delivery to Retinal Pigment Epithelial Cells. *Int. J. Pharm.* 2016, 503, 115–126.
91. Puras, G.; Mashal, M.; Zarate, J.; Agirre, M.; Ojeda, E.; Grijalvo, S.; Eritja, R.; Diaz-Tahoces, A.; Martinez Navarrete, G.; Aviles-Trigueros, M.; et al. A Novel Cationic Niosome Formulation for Gene Delivery to the Retina. *J. Control Release* 2014, 174, 27–36. [PubMed]
92. Hong, M.; Zhu, S.; Jiang, Y.; Tang, G.; Pei, Y. Efficient Tumor Targeting of Hydroxycamptothecin Loaded PEGylated Niosomes Modified with Transferrin. *J. Control Release* 2009, 133, 96–102. [PubMed]
93. Agirre, M.; Ojeda, E.; Zarate, J.; Puras, G.; Grijalvo, S.; Eritja, R.; Garcia del Cano, G.; Barrondo, S.; Gonzalez-Burguera, I.; Lopez de Jesus, M.; et al. New Insights into Gene

Delivery to Human Neuronal Precursor NT2 Cells: A Comparative Study between Lipoplexes, Nioplexes, and Polyplexes. *Mol. Pharm.* 2015, 12, 4056–4066. [PubMed]

94. Balakrishnan, P.; Shanmugam, S.; Lee, W.S.; Lee, W.M.; Kim, J.O.; Oh, D.H.; Kim, D.D.; Kim, J.S.; Yoo, B.K.; Choi, H.G.; et al. Formulation and in Vitro Assessment of Minoxidil Niosomes for Enhanced Skin Delivery. *Int. J. Pharm.* 2009, 377, 1–8.

95. Marianecchi, C.; Di Marzio, L.; Rinaldi, F.; Celia, C.; Paolino, D.; Alhaique, F.; Esposito, S.; Carafa, M. Niosomes from 80s to Present: The State of the Art. *Adv. Colloid Interface Sci.* 2014, 205, 187–206.

96. Shah, V.M.; Nguyen, D.X.; Patel, P.; Cote, B.; Al-Fatease, A.; Pham, Y.; Huynh, M.G.; Woo, Y.; Alani, A.W. Liposomes Produced by Microfluidics and Extrusion: A Comparison for Scale-Up Purposes. *Nanomedicine* 2019, 18, 146–156.

97. Puras, G.; Zarate, J.; Diaz-Tahoces, A.; Aviles-Trigueros, M.; Fernandez, E.; Pedraz, J.L. Oligochitosan Polyplexes as Carriers for Retinal Gene Delivery. *Eur. J. Pharm. Sci.* 2013, 48, 323–331.

98. Islam, M.A.; Firdous, J.; Choi, Y.J.; Yun, C.H.; Cho, C.S. Regulation of Endocytosis by Non-Viral Vectors for Efficient Gene Activity. *J. Biomed. Nanotechnol.* 2014, 10, 67–80.

99. Manosroi, A.; Jantrawut, P.; Manosroi, J. Anti-Inflammatory Activity of Gel Containing Novel Elastic Niosomes Entrapped with Diclofenac Diethylammonium. *Int. J. Pharm.* 2008, 360, 156–163.

100. Tristram-Nagle, S.; Nagle, J.F. Lipid Bilayers: Thermodynamics, Structure, Fluctuations, and Interactions. *Chem. Phys. Lipids* 2004, 127, 3–14.

101. Agirre, M.; Zarate, J.; Puras, G.; Ojeda, E.; Pedraz, J.L. Improving Transfection Efficiency of Ultrapure Oligochitosan/DNA Polyplexes by Medium Acidification. *Drug Deliv.* 2015, 22, 100–110. [PubMed]

102. Patil, S.; Sandberg, A.; Heckert, E.; Self, W.; Seal, S. Protein Adsorption and Cellular Uptake of Cerium Oxide Nanoparticles as a Function of Zeta Potential. *Biomaterials* 2007, 28, 4600–4607. [PubMed]

103. Falconer, R.J. Applications of Isothermal Titration Calorimetry—The Research and Technical Developments from 2011 to 2015. *J. Mol. Recognit.* 2016, 29, 504–515. [PubMed]

104. Manconi, M.; Sinico, C.; Valenti, D.; Lai, F.; Fadda, A.M. Niosomes as Carriers for Tretinoin. III. A Study into the in Vitro Cutaneous Delivery of Vesicle-Incorporated Tretinoin. *Int. J. Pharm.* 2006, 311, 11–19.

105. Kassem, A.A.; Abd El-Alim, S.H.; Asfour, M.H. Enhancement of 8-Methoxypsoralen Topical Delivery via Nanosized Niosomal Vesicles: Formulation Development, in Vitro and in Vivo Evaluation of Skin Deposition. *Int. J. Pharm.* 2017, 517, 256–268.

106. Abd-Elbary, A.; El-laithy, H.M.; Tadros, M.I. Sucrose Stearate-Based Proniosome-Derived Niosomes for the Nebulisable Delivery of Cromolyn Sodium. *Int. J. Pharm.* 2008, 357, 189–198.

107. Ertekin, Z.C.; Bayindir, Z.S.; Yuksel, N. Stability Studies on Piroxicam Encapsulated Niosomes. *Curr. Drug Deliv.* 2015, 12, 192–199.
108. Arafa, M.G.; Ghalwash, D.; El-Kersh, D.M.; Elmazar, M.M. Propolis-Based Niosomes as Oromuco-Adhesive Films: A Randomized Clinical Trial of a Therapeutic Drug Delivery Platform for the Treatment of Oral Recurrent Aphthous Ulcers. *Sci. Rep.* 2018, 8, 18056. [CrossRef]
109. Lv, H.; Zhang, S.; Wang, B.; Cui, S.; Yan, J. Toxicity of Cationic Lipids and Cationic Polymers in Gene Delivery. *J. Control Release* 2006, 114, 100–109.
110. Yingyongnarongkul, B.E.; Radchatawedchakoon, W.; Krajarng, A.; Watanapokasin, R.; Suksamrarn, A. High Transfection Efficiency and Low Toxicity Cationic Lipids with Aminoglycerol-Diamine Conjugate. *Bioorg. Med. Chem.* 2009, 17, 176–188.
111. Opanasopit, P.; Leksantikul, L.; Niyomtham, N.; Rojanarata, T.; Ngawhirunpat, T.; Yingyongnarongkul, B.E. Cationic Niosomes an Effective Gene Carrier Composed of Novel Spermine-Derivative Cationic Lipids: Effect of Central Core Structures. *Pharm. Dev. Technol.* 2017, 22, 350–359. [PubMed]
112. Villate-Beitia, I.; Truong, N.F.; Gallego, I.; Zarate, J.; Puras, G.; Pedraz, J.L.; Segura, T. Hyaluronic Acid Hydrogel Scaffolds Loaded with Cationic Niosomes for Efficient Non-Viral Gene Delivery. *RSC Adv.* 2018, 8, 31934–31942. [PubMed]
113. Mashal, M.; Attia, N.; Soto-Sanchez, C.; Martinez-Navarrete, G.; Fernandez, E.; Puras, G.; Pedraz, J.L. Non-Viral Vectors Based on Cationic Niosomes as Efficient Gene Delivery Vehicles to Central Nervous System Cells into the Brain. *Int. J. Pharm.* 2018, 552, 48–55.
114. Mashal, M.; Attia, N.; Martinez-Navarrete, G.; Soto-Sanchez, C.; Fernandez, E.; Grijalvo, S.; Eritja, R.; Puras, G.; Pedraz, J.L. Gene Delivery to the Rat Retina by Non-Viral Vectors Based on Chloroquine-Containing Cationic Niosomes. *J. Control Release* 2019, 304, 181–190. [PubMed]
115. Puras, G.; Zarate, J.; Aceves, M.; Murua, A.; Diaz, A.R.; Aviles-Triguero, M.; Fernandez, E.; Pedraz, J.L. Low Molecular Weight Oligochitosans for Non-Viral Retinal Gene Therapy. *Eur. J. Pharm. Biopharm.* 2013, 83, 131–140.
116. Musafargani, S.; Mishra, S.; Gulyas, M.; Mahalakshmi, P.; Archunan, G.; Padmanabhan, P.; Gulyas, B. Blood Brain Barrier: A Tissue Engineered Microfluidic Chip. *J. Neurosci. Methods* 2019, 331, 108525.
117. Yeste, J.; Garcia-Ramirez, M.; Illa, X.; Guimera, A.; Hernandez, C.; Simo, R.; Villa, R. A Compartmentalized Microfluidic Chip with Crisscross Microgrooves and Electrophysiological Electrodes for Modeling the Blood-Retinal Barrier. *Lab. Chip* 2017, 18, 95–105.
118. MEDAWAR, P.B. Immunity to Homologous Grafted Skin; the Fate of Skin Homografts Transplanted to the Brain, to Subcutaneous Tissue, and to the Anterior Chamber of the Eye. *Br. J. Exp. Pathol.* 1948, 29, 58–69.
119. Benhar, I.; London, A.; Schwartz, M. The Privileged Immunity of Immune Privileged Organs: The Case of the Eye. *Front. Immunol.* 2012, 3, 296.

120. Streilein, J.W. Ocular Immune Privilege: Therapeutic Opportunities from an Experiment of Nature. *Nat. Rev. Immunol.* 2003, 3, 879–889.
121. Trapani, I.; Auricchio, A. Has Retinal Gene Therapy Come of Age? From Bench to Bedside and Back to Bench. *Hum. Mol. Genet.* 2019, 28, R108–R118.
122. Liu, M.M.; Tuo, J.; Chan, C.C. Gene Therapy for Ocular Diseases. *Br. J. Ophthalmol.* 2011, 95, 604–612. [PubMed]
123. Anand, V.; Duffy, B.; Yang, Z.; Dejneka, N.S.; Maguire, A.M.; Bennett, J. A Deviant Immune Response to Viral Proteins and Transgene Product is Generated on Subretinal Administration of Adenovirus and Adeno-Associated Virus. *Mol. Ther.* 2002, 5, 125–132. [PubMed]
124. Pichi, F.; Morara, M.; Veronese, C.; Nucci, P.; Ciardella, A.P. Multimodal Imaging in Hereditary Retinal Diseases. *J. Ophthalmol.* 2013, 2013, 634351. [PubMed]
125. Bakondi, B.; Lv, W.; Lu, B.; Jones, M.K.; Tsai, Y.; Kim, K.J.; Levy, R.; Akhtar, A.A.; Breunig, J.J.; Svendsen, C.N.; et al. In Vivo CRISPR/Cas9 Gene Editing Corrects Retinal Dystrophy in the S334ter-3 Rat Model of Autosomal Dominant Retinitis Pigmentosa. *Mol. Ther.* 2016, 24, 556–563.
126. Russell, S.; Bennett, J.; Wellman, J.A.; Chung, D.C.; Yu, Z.F.; Tillman, A.; Wittes, J.; Pappas, J.; Elci, O.; McCague, S.; et al. Efficacy and Safety of Voretigene Neparvovec (AAV2-hRPE65v2) in Patients with RPE65-Mediated Inherited Retinal Dystrophy: A Randomised, Controlled, Open-Label, Phase 3 Trial. *Lancet* 2017, 390, 849–860.
127. Trapani, I.; Puppo, A.; Auricchio, A. Vector Platforms for Gene Therapy of Inherited Retinopathies. *Prog. Retin. Eye Res.* 2014, 43, 108–128.
128. Han, Z.; Conley, S.M.; Makkia, R.; Guo, J.; Cooper, M.J.; Naash, M.I. Comparative Analysis of DNA Nanoparticles and AAVs for Ocular Gene Delivery. *PLoS ONE* 2012, 7, e52189.
129. Grijalvo, S.; Ocampo, S.M.; Perales, J.C.; Eritja, R. Synthesis of Lipid-Oligonucleotide Conjugates for RNA Interference Studies. *Chem. Biodivers.* 2011, 8, 287–299.
130. Reddy, L.H.; Couvreur, P. Squalene: A Natural Triterpene for use in Disease Management and Therapy. *Adv. Drug Deliv. Rev.* 2009, 61, 1412–1426.
131. Kim, Y.J.; Kim, T.W.; Chung, H.; Kwon, I.C.; Sung, H.C.; Jeong, S.Y. The Effects of Serum on the Stability and the Transfection Activity of the Cationic Lipid Emulsion with various Oils. *Int. J. Pharm.* 2003, 252, 241–252. [PubMed]
132. Duvshani-Eshet, M.; Keren, H.; Oz, S.; Radzishhevsky, I.S.; Mor, A.; Machluf, M. Effect of Peptides Bearing Nuclear Localization Signals on Therapeutic Ultrasound Mediated Gene Delivery. *J. Gene Med.* 2008, 10, 1150–1159. [PubMed]

133. Liu, J.; Guo, S.; Li, Z.; Liu, L.; Gu, J. Synthesis and Characterization of Stearyl Protamine and Investigation of their Complexes with DNA for Gene Delivery. *Colloids Surf. B Biointerfaces* 2009, 73, 36–41. [PubMed]
134. Torrecilla, J.; del Pozo-Rodriguez, A.; Apaolaza, P.S.; Solinis, M.A.; Rodriguez-Gascon, A. Solid Lipid Nanoparticles as Non-Viral Vector for the Treatment of Chronic Hepatitis C by RNA Interference. *Int. J. Pharm.* 2015, 479, 181–188. [PubMed]
135. Li, S.; Rizzo, M.A.; Bhattacharya, S.; Huang, L. Characterization of Cationic Lipid-Protamine-DNA (LPD) Complexes for Intravenous Gene Delivery. *Gene Ther.* 1998, 5, 930–937.
136. Peeters, L.; Sanders, N.N.; Braeckmans, K.; Boussery, K.; Van de Voorde, J.; De Smedt, S.C.; Demeester, J. Vitreous: A Barrier to Nonviral Ocular Gene Therapy. *Investig. Ophthalmol. Vis. Sci.* 2005, 46, 3553–3561.
137. Koirala, A.; Conley, S.M.; Naash, M.I. A Review of Therapeutic Prospects of Non-Viral Gene Therapy in the Retinal Pigment Epithelium. *Biomaterials* 2013, 34, 7158–7167.
138. Bernstein, P.S.; Khachik, F.; Carvalho, L.S.; Muir, G.J.; Zhao, D.Y.; Katz, N.B. Identification and Quantitation of Carotenoids and their Metabolites in the Tissues of the Human Eye. *Exp. Eye Res.* 2001, 72, 215–223.
139. Mashal, M.; Attia, N.; Puras, G.; Martinez-Navarrete, G.; Fernandez, E.; Pedraz, J.L. Retinal Gene Delivery Enhancement by Lycopene Incorporation into Cationic Niosomes Based on DOTMA and Polysorbate 60. *J. Control Release* 2017, 254, 55–64.
140. Erbacher, P.; Roche, A.C.; Monsigny, M.; Midoux, P. Putative Role of Chloroquine in Gene Transfer into a Human Hepatoma Cell Line by DNA/Lactosylated Polylysine Complexes. *Exp. Cell Res.* 1996, 225, 186–194.
141. Zhang, X.; Sawyer, G.J.; Dong, X.; Qiu, Y.; Collins, L.; Fabre, J.W. The in Vivo use of Chloroquine to Promote Non-Viral Gene Delivery to the Liver Via the Portal Vein and Bile Duct. *J. Gene Med.* 2003, 5, 209–218.
142. Kashyap, K.; Shukla, R. Drug Delivery and Targeting to the Brain through Nasal Route: Mechanisms, Applications and Challenges. *Curr. Drug Deliv.* 2019, 16, 887–901.
143. Maguire, C.A.; Ramirez, S.H.; Merkel, S.F.; Sena-Esteves, M.; Breakefield, X.O. Gene Therapy for the Nervous System: Challenges and New Strategies. *Neurotherapeutics* 2014, 11, 817–839. [PubMed]
144. Mathias, N.R.; Hussain, M.A. Non-Invasive Systemic Drug Delivery: Developability Considerations for Alternate Routes of Administration. *J. Pharm. Sci.* 2010, 99, 1–20.
145. Yamaguchi, A.; Katsuyama, K.; Suzuki, K.; Kosaka, K.; Aoki, I.; Yamanaka, S. Plasmid-Based Gene Transfer Ameliorates Visceral Storage in a Mouse Model of Sandhoff Disease. *J. Mol. Med.* 2003, 81, 185–193. [PubMed]

146. Leone, P.; Janson, C.G.; McPhee, S.J.; During, M.J. Global CNS Gene Transfer for a Childhood Neurogenetic Enzyme Deficiency: Canavan Disease. *Curr. Opin. Mol. Ther.* 1999, 1, 487–492. [PubMed]
147. Mischel, P.S.; Cloughesy, T.F. Targeted Molecular Therapy of GBM. *Brain Pathol.* 2003, 13, 52–61. [PubMed]
148. Raza, C.; Anjum, R.; Shakeel, N.U.A. Parkinson's Disease: Mechanisms, Translational Models and Management Strategies. *Life Sci.* 2019, 226, 77–90. [PubMed]
149. Wang, S.; Huang, R. Non-Viral Nucleic Acid Delivery to the Central Nervous System and Brain Tumors. *J. Gene Med.* 2019, 21, e3091.
150. Chen, Y.H.; Clafin, K.; Geoghegan, J.C.; Davidson, B.L. Sialic Acid Deposition Impairs the Utility of AAV9, but Not Peptide-Modified AAVs for Brain Gene Therapy in a Mouse Model of Lysosomal Storage Disease. *Mol. Ther.* 2012, 20, 1393–1399.
151. Krewson, C.E.; Klarman, M.L.; Saltzman, W.M. Distribution of Nerve Growth Factor Following Direct Delivery to Brain Interstitium. *Brain Res.* 1995, 680, 196–206.
152. Ingusci, S.; Verlengia, G.; Soukupova, M.; Zucchini, S.; Simonato, M. Gene Therapy Tools for Brain Diseases. *Front. Pharmacol.* 2019, 10, 724.
153. Jayant, R.D.; Sosa, D.; Kaushik, A.; Atluri, V.; Vashist, A.; Tomitaka, A.; Nair, M. Current Status of Non-Viral Gene Therapy for CNS Disorders. *Expert Opin. Drug Deliv.* 2016, 13, 1433–1445.
154. Bjorklund, T. Repairing the Brain: Gene Therapy. *J. Parkinsons Dis.* 2018, 8, S123–S130. [PubMed]
155. Cacciotti, I.; Ceci, C.; Bianco, A.; Pistrutto, G. Neuro-Differentiated Ntera2 Cancer Stem Cells Encapsulated in Alginate Beads: First Evidence of Biological Functionality. *Mater. Sci. Eng. C. Mater. Biol. Appl.* 2017, 81, 32–38. [PubMed]
156. Tinsley, R.; Eriksson, P. Use of Gene Therapy in Central Nervous System Repair. *Acta Neurol. Scand.* 2004, 109, 1–8. [PubMed]
157. Schafer, D.P.; Stevens, B. Phagocytic Glial Cells: Sculpting Synaptic Circuits in the Developing Nervous System. *Curr. Opin. Neurobiol.* 2013, 23, 1034–1040.
158. Barres, B.A. The Mystery and Magic of Glia: A Perspective on their Roles in Health and Disease. *Neuron* 2008, 60, 430–440.
159. Gu, J.H.; Ge, J.B.; Li, M.; Xu, H.D.; Wu, F.; Qin, Z.H. Poloxamer 188 Protects Neurons Against Ischemia/Reperfusion Injury through Preserving Integrity of Cell Membranes and Blood Brain Barrier. *PLoS ONE* 2013, 8, e61641.
160. Bnyan, R.; Khan, I.; Ehtezazi, T.; Saleem, I.; Gordon, S.; O'Neill, F.; Roberts, M. Surfactant Effects on Lipid-Based Vesicles Properties. *J. Pharm. Sci.* 2018, 107, 1237–1246.

161. Attia, N.; Mashal, M.; Grijalvo, S.; Eritja, R.; Puras, G.; Pedraz, J. Cationic niosome-based hBMP7 gene transfection of neuronal precursor NT2 cells to reduce the migration of glioma cells in vitro. *J. Drug Deliv. Sci. Technol.* 2019, 53, 1–7.
162. Attia, N.; Mashal, M.; Grijalvo, S.; Eritja, R.; Zarate, J.; Puras, G.; Pedraz, J.L. Stem Cell-Based Gene Delivery Mediated by Cationic Niosomes for Bone Regeneration. *Nanomedicine* 2018, 14, 521–531. [PubMed]
163. Razi Soofiyani, S.; Baradaran, B.; Lotfipour, F.; Kazemi, T.; Mohammadnejad, L. Gene Therapy, Early Promises, Subsequent Problems, and Recent Breakthroughs. *Adv. Pharm. Bull.* 2013, 3, 249–255. [PubMed]
164. Ganger, S.; Schindowski, K. Tailoring Formulations for Intranasal Nose-to-Brain Delivery: A Review on Architecture, Physico-Chemical Characteristics and Mucociliary Clearance of the Nasal Olfactory Mucosa. *Pharmaceutics* 2018, 10, 116. [CrossRef]
165. Alqawlaq, S.; Sivak, J.M.; Huzil, J.T.; Ivanova, M.V.; Flanagan, J.G.; Beazely, M.A.; Foldvari, M. Preclinical Development and Ocular Biodistribution of Gemini-DNA Nanoparticles After Intravitreal and Topical Administration: Towards Non-Invasive Glaucoma Gene Therapy. *Nanomedicine* 2014, 10, 1637–1647.
166. Ying, L.; Tahara, K.; Takeuchi, H. Drug Delivery to the Ocular Posterior Segment using Lipid Emulsion Via Eye Drop Administration: Effect of Emulsion Formulations and Surface Modification. *Int. J. Pharm.* 2013, 453, 329–335. [PubMed]
167. Lajunen, T.; Hisazumi, K.; Kanazawa, T.; Okada, H.; Seta, Y.; Yliperttula, M.; Urtti, A.; Takashima, Y. Topical Drug Delivery to Retinal Pigment Epithelium with Microfluidizer Produced Small Liposomes. *Eur. J. Pharm. Sci.* 2014, 62, 23–32.
168. Gu, Y.; Xu, C.; Wang, Y.; Zhou, X.; Fang, L.; Cao, F. Multifunctional Nanocomposites Based on Liposomes and Layered Double Hydroxides Conjugated with Glycylsarcosine for Efficient Topical Drug Delivery to the Posterior Segment of the Eye. *Mol. Pharm.* 2019, 16, 2845–2857.
169. Bonferoni, M.C.; Rossi, S.; Sandri, G.; Ferrari, F.; Gavini, E.; Rassa, G.; Giunchedi, P. Nanoemulsions for “Nose-to-Brain” Drug Delivery. *Pharmaceutics* 2019, 11, 84. [CrossRef]
170. Alexander, A.; Saraf, S. Nose-to-Brain Drug Delivery Approach: A Key to Easily Accessing the Brain for the Treatment of Alzheimer’s Disease. *Neural Regen. Res.* 2018, 13, 2102–2104.
171. Piazzini, V.; Landucci, E.; D’Ambrosio, M.; Tiozzo Fasiolo, L.; Cinci, L.; Colombo, G.; Pellegrini-Giampietro, D.E.; Bilia, A.R.; Luceri, C.; Bergonzi, M.C. Chitosan Coated Human Serum Albumin Nanoparticles: A Promising Strategy for Nose-to-Brain Drug Delivery. *Int. J. Biol. Macromol.* 2019, 129, 267–280. [PubMed]

Appendix 2

Sphingolipid extracts enhance gene delivery of cationic lipid vesicles into retina and brain

European Journal of Pharmaceutics and Biopharmaceutics 169 (2021) 103–112

<https://doi.org/10.1016/j.ejpb.2021.09.011>

IF: 5.589 (2021)

Sphingolipid extracts enhances gene delivery of cationic lipid vesicles into retina and brain.

Nuseibah AL Qtaish^{a,b†}, Idoia Gallego^{a,b,c†}, Ilia Villate- Beitia^{a,b,c}, Myriam Sainz-Ramos^{a,b,c}, Gema Martínez-Navarrete^{b,d}, Cristina Soto-Sánchez^{b,d}, Eduardo Fernández^{b,d}, Patricia Gálvez Martín^e, Tania B. Lopez-Mendez^{a,b,c}, Gustavo Puras^{a,b,c}, José Luis Pedraz^{a,b,c*}.*

^a *NanoBioCel Research Group, Laboratory of Pharmacy and Pharmaceutical Technology. Faculty of Pharmacy, University of the Basque Country (UPV/EHU), Paseo de la Universidad 7, 01006 Vitoria-Gasteiz, Spain.*

^b *Networking Research Centre of Bioengineering, Biomaterials and Nanomedicine (CIBER-BBN), Institute of Health Carlos III, Av Monforte de Lemos 3-5, 28029 Madrid, Spain*

^c *Bioaraba, NanoBioCel Research Group, Calle José Achotegui s/n, 01009 Vitoria-Gasteiz, Spain.*

^d *Neuroprosthesis and Neuroengineering Research Group, Institute of Bioengineering, Miguel Hernández University, Avenida de la Universidad, 03202 Elche, Spain.*

^e *R&D Human Health, Bioibérica S.A.U., Plaza Francesc Macià, 08029 Barcelona, Spain.*

[†] N. AL Qtaish and Dr. I. Gallego contributed equally to this work

***Correspondence:** Address all correspondence to: (José Luis Pedraz. Phone: + (34)-945013091. Fax number: + (34)-945013040, Gustavo Puras. Phone: + (34)-945014536. Fax number: + (34)-945013040).

Laboratory of Pharmacy and Pharmaceutical Technology. Faculty of Pharmacy, University of the Basque Country, Paseo de la Universidad 7, 01006, Vitoria-Gasteiz, Spain.

Email addresses of authors: nusaiba.qtaish@gmail.com (Nuseibah A.L. Qtaish), idoia.gallego@ehu.eus (Idoia Gallego), anelia.villate@ehu.eus (Ilia Villate-Beitia), miriam.sainz@ehu.eus (Myriam Sainz-Ramos), gema.martinez@umh.es (Gema Martínez-Navarrete), csoto@goumh.umh.es (Cristina Soto-Sánchez), e.fernandez@umh.es (Eduardo Fernández), pgalvez@bioiberica.com (Patricia Gálvez Martín), tania.lopez@ehu.eus (Tania B. Lopez-Mendez), gustavo.puras@ehu.eus (Gustavo Puras) and joseluis.pedraz@ehu.eus (José Luis Pedraz).

Abstract

Relevant biophysics processes related to the gene transfection mechanism were evaluated when sphingolipids were incorporated into a cationic niosome formulation for the aim of gene delivery to the rat retina and brain. Two non-viral vector formulations named niosphingosomes and niosomes devoid of sphingolipid extracts, as control, were developed by the oil-in water emulsion technique. Both formulations and the corresponding complexes, obtained upon the addition of the reporter EGFP plasmid, were characterized in terms of particle size, superficial charge, dispersity and morphology. Additionally, biological studies were performed to evaluate cellular uptake and intracellular trafficking pathways in ARPE-19 cells before conducting *in vivo* administrations. Compared to niosomes, niosphingosomes, and the corresponding complexes decreased particle size and increased superficial charge. Although there were not significant differences in the cellular uptake, cell viability and transfection efficiency increased when ARPE-19 cells were exposed to niosphingoplexes. Endocytosis via caveolae decreased in the case of niosphingoplexes, which showed higher co-localization with lysosomal compartment, and endosomal escape properties. Moreover, niosphingoplexes transfected different cells in mice retina, contingent on the administration route, and brain cortex. These preliminary results suggest that niosphingosomes represent a promising non-viral vector formulation purposed for the treatment of both retinal and brain diseases by gene therapy approach.

Keywords

Gene therapy, niosomes, niosphingosomes, sphingolipids, brain, retina.

1. INTRODUCTION

Gene therapy is an arising medical option for treating inherited and acquired diseases, that has captured the interest and investment of many pharmaceutical companies during the last few years [1]. Its main concept lays on the delivery of foreign genetic material into a target cell in order to correct a specific pathology [2]. However, the regular practice of this advanced technology needs to surpass the biological extracellular obstacles that the exogenous genetic materials in order to reach the target cells, which depends on both the organ/cell type to be treated and the route of administration [3]. This fact is mostly relevant in the case of immune-privileged organs, which are isolated from the rest of the organism by the blood-brain-barrier (BBB) and blood-retinal-barrier (BRB), such as brain and retina, respectively [4,5]. Moreover, to be biological effective, it is

necessary to deliver enough genetic material inside target cells. In this sense, the endocytosis mechanism and following intracellular trafficking clearly affects the final disposition of the genetic material at the place of action [6]. Therefore, in order to overcome both extracellular and intracellular barriers, safe and effective gene delivery systems need to be developed [7].

Research on the design, development and application of non-viral vectors has considerably increased during the last years to enhance gene delivery efficiency [8]. Among the different kinds of non-viral vectors, those related to cationic lipids are the most studied ones [9]. In fact, Pfizer/BioNTech and Moderna companies, with the approval of regulatory agencies, have recently applied this lipid based-technology to formulate mRNA vaccines, to face the devastating Covid-19 disease. Any slight variation on the composition of these lipid structures can impact on both the physicochemical properties and gene delivery capacity [10]. In order to increase biophysical activity, such cationic lipids are normally incorporated into colloidal vesicles made up of phospholipids, leading to the formation of corresponding liposomes [11]. If cationic lipids are combined with non-ionic surfactant components to enhance chemical stability, a colloidal dispersion of niosomes is obtained [12]. Such niosomes have been recognized during last years to deliver efficiently and safely the genetic material for different applications [13]. In addition to cationic lipid and the non-ionic surfactant, other chemical agents referred as “helper” compounds can also be incorporated into the niosome vesicles to enhance their biological performance [14]. Some compounds that have been successfully incorporated into niosomes as “helper” components include cholesterol [15], squalene [16], lycopene [17] or chloroquine [18], to name just a few.

Sphingolipids are biomaterials referred a class of natural complex lipids mainly found in membranes of central nervous system tissue, which play a relevant biological role in cell signaling processes [19]. Such sphingolipids derive from sphingosine, an alkalonamime of 18 carbons. Sphingolipids are obtained when a long saturated or unsaturated fatty acid chain is bound to the amino reactive group and another radical consisting of phosphocoline or sugar, binds to the final carboxyl group of the sphingosine, resulting in the formation of ceramides [20]. Sphingolipid extracts can be obtained from animals, plants and can also be produced from genetically modified microorganisms. However, in mammals, endogenous sphingolipids contain high levels of sphingosine, which is not present in extracts from plants or in sphingolipids obtained from microorganisms. Therefore, sphingolipid extracts obtained from animal origin show a more

suitable lipid profile to obtain ceramides [21]. It has been suggested that glycosphingolipids might be involved in transmembrane transport and binding of bacteria and bacterial toxins to intestinal epithelial cells. The composition of glycolipids in the rat small intestinal mucosa demonstrated alterations during normal differentiation and development, pointing to possible roles for glycosphingolipids in these processes as well [22].

Sphingolipids have been successfully incorporated as structural components into different nanocarrier systems for drug delivery purposes [23-25]. However, currently, there is not any report related to the use of such sphingolipids on the transfection process mediated by cationic niosomes. Therefore, to address such issue, we performed a comparative study of two non-viral vector formulations based on cationic niosomes consisting of the same cationic lipid and non-ionic tensioactive, but with or without sphingolipids as "helper" compound, obtaining niosphingosomes or niosomes, respectively. Both formulations were developed by the oil-in water (o/w) emulsion technique, and the corresponding complexes obtained after the addition of the EGFP reporter plasmid at different cationic lipid/DNA ratios (w/w) were physicochemically characterized, before performing transfection experiments in ARPE-19 cells to evaluate cell viability, reporter gene expression, cellular uptake and intracellular trafficking. Preliminary *in vivo* experiments were carried out to evaluate gene expression of the most promising complexes in rat brain, after cerebral cortex injection, and in rat retina, after both intravitreal and subretinal administration.

2. MATERIALS AND METHODS

2.1 Preparation of formulations

The cationic formulations were developed by the o/w emulsion technique. The 1,2-di-O-octadecenyl-3-trimethylammonium propane chloride salt (DOTMA, Sigma-Aldrich) cationic lipid, in combination with 2-2-3,4-bis(2-hydroxyethoxy) oxolan-2-yl-2-2-hydroxyethoxy ethoxy ethyl dodecanoate (Tween 20, Bio-Rad) non-ionic surfactant, were mixed or not with sphingolipids from animal origin found in the intestinal mucosa of mammal with high levels of sphingomyelin (Bioiberica laboratory, *Sus scrofa*, pig), as helper components, obtaining niosphingosomes and niosomes, respectively (Figure 1). Briefly, the cationic lipid (3.4 mg) were gently grounded with sphingolipids (100 µg), then, dichloromethane (DCM) (500 µL) (Panreac, Barcelona, Spain) were added to this lipid mixture and emulsified with the non-ionic surfactant aqueous solution of polysorbate 20 (2.5 mL) (0.5%, w/w). Components were sonicated (Branson

Sonifier 250, Danbury) for 30 s at 50 W. Next, the DCM organic solvent was evaporated and eliminated from the emulsion by using magnetic stirrer for 2 h at room temperature inside a extraction hood. Upon DCM evaporation, a colloidal dispersion carrying the formulations was obtained with a final cationic lipid concentration of 1.5 mg mL⁻¹.

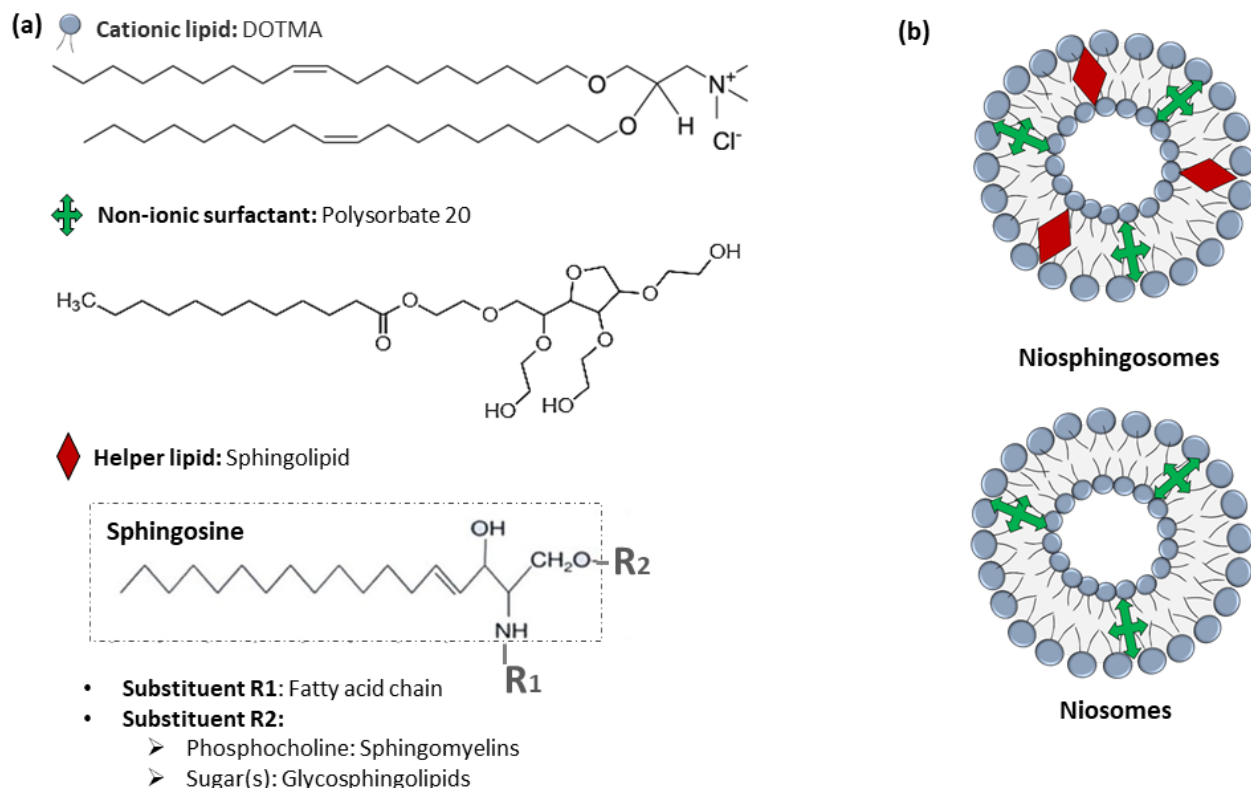


Figure 1. Scheme of composition of niosphingosomes and niosomes. (a) General chemical structure of cationic lipid, non-ionic surfactant and helper component. (b) General scheme showing the disposition of the components in the formulations of both niosphingosomes and niosomes.

2.2 Plasmid propagation and complexes elaboration.

The pCMS-EGFP plasmid (Plasmid Factory, Bielefeld, Germany) was propagated with *Escherichia coli* DH5- α and purified as previously described [15]. The stock solution of plasmid pCMS-EGFP (0.5 mg mL⁻¹) was estimated to be around 0.137 μ M (pCMS-EGFP, 5541 bp, average MW 3657060 g mol⁻¹). Complexes between these formulations and plasmid DNA were formed by adding an adequate volume of the plasmid to niosomes and niosphingosomes at different cationic lipid/DNA mass ratios (w/w). The mixture was incubated for 30 min at room temperature before

use to promote the electrostatic interactions between the amine groups of the cationic lipid and the phosphate groups of the genetic material to obtain the resulting complexes.

2.3 Physicochemical characterization of formulations

The hydrodynamic diameter of nanoparticles was recorded to report the particle size by dynamic light scattering and laser doppler velocimetry was used to determine zeta potential, using Zetasizer Nano ZS (Malvern Instrument, UK) as previously described [15]. All measurements were performed in triplicate. Transmission electron microscopy (TEM) was used to define the morphology of formulations as previously described [12].

2.4 Qualitative analysis of transfection efficiency and cellular uptake

To evaluate transfection efficiency qualitatively, ARPE-19 cells were seeded into 24 well plates at an initial density of 18×10^4 cells per well, to reach 70–80% of confluence at the time of transfection assay. Next, cells were exposed to formulations containing EGFP (1.25 μg) plasmid during 4 h in OptiMEM[®] transfection medium (Gibco[®], Life Technologies, S.A., Madrid, Spain). Afterwards, OptiMEM[®] was replaced by DMEM/F-12 regular growth medium (Gibco[®], Life Technologies, S.A., Madrid, Spain) containing 10% bovine serum, and cells were permitted to grow for 48 h until their observation under fluorescence microscopy. Images showing EGFP signal in ARPE-19 cells transfected with niosphingoplexes and nioplexes were captured at this time. To evaluate cellular uptake, cells were processed, fixed and analyzed as previously described [26].

2.5 Quantitative analysis of EGFP expression, cell viability and cellular uptake

FACSCalibur flow cytometer (Becton Dickinson Bioscience, San Jose, USA) was used to perform flow cytometry analysis in order to quantify the percentage of EGFP and FITC-labeled EGFP plasmid (Dare Bioscience) expression for transfection and cellular uptake assays, respectively. For this purpose, at the end of incubation time, 48 h for transfection assay and both 2 h and 4 h for cellular uptake assay, cells were washed with PBS (Gibco[™], San Diego, California, USA) and detached from the 24 well plates with trypsin/EDTA (200 μL) (Gibco[™] San Diego, California, USA). The cells were prepared and analyzed as previously described [15].

2.6 Endocytic trafficking

Cells were seeded in 24 well plates with coverslips at an initial density of 18×10^4 cells per well. DMEM/F-12 (300 μ L) containing 10% bovine serum was added to each well and incubated at 37 °C with 5% CO₂ atmosphere to reach 70–80% of confluence at the time of internalization assay. Next, cells were exposed to formulations containing EGFP plasmid (1.25 μ g per well) during 3 h in OptiMEM[®] transfection medium and endocytic fluorescent markers for 1 hour at 37 °C and 5% CO₂ atmosphere. Briefly Transferrin Alexa Fluor 568 (2.5 μ L) (5 mg mL⁻¹) was incubated for 60 min to label clathrin mediated endocytosis (CME). Dextran Alexa Fluor 568 (30 μ L) (1 mg mL⁻¹) a fluid-phase uptake marker, was incubated for 60 min to label macropinocytosis. Cholera toxin B Alexa Fluor 594 (2.5 μ L) (10 mg mL⁻¹) was incubated for 60 min to label caveolae mediated endocytosis (CvME), and LysoTracker[®] (50 μ L) (20 μ M) was incubated for 60 min to label lysosomes. All markers were purchased from Life Technologies (Eugene, OR, USA). Next, the medium containing the complexes and endocytic markers was removed, and cells were washed twice with PBS. Afterwards, the cells were fixed, mounted and observed under fluorescence microscopy as described above. ImageJ software was used to quantify the co-localization of the green and red signal by a cross-correlation analysis as previously described [27].

2.7 Endosomal escape

Phosphatidylserine (PS) (Sigma-Aldrich, Spain) anionic micelles were elaborated as an analogue of the late endosomal compartment, as previously described [28]. Briefly, PS was dissolved in chloroform (1.6 mM), which was evaporated and eliminated from the emulsion by using magnetic stirrer. Next, PBS was added to hydrate the PS sample and sonicated for 30 s at 50 W to obtain a dispersed solution. PS micelles and the complexes were incubated at a w/w ratio of 1:50 (pCMS-EGFP: PS) for 1 hour. Finally, the amount of the released DNA from each complex was determined by agarose gel electrophoresis after staining with GelRed.

2.8 Animal model

Adult male Sprague–Dawley rats were used for the extraction of primary central nervous system cells, from the brain cortex and retinal tissue and adult C57BL/6 mice were used as experimental animals for subretinal, intravitreal and brain administration. All experimental procedures were carried out in accordance with the RD 53/2013 Spanish and 2010/63/EU

European Union regulations for the use of animals in scientific research. Procedures were approved and supervised by the Miguel Hernandez University Standing Committee for Animal Use in the Laboratory with code UMH.IB.EFJ.03.19/02.18.

2.9 Transfection efficiency assays of niosphingoplexes in rat primary retinal and neuronal cell cultures

Embryonic rat retinal primary cells were extracted from E17.5 rat embryos from $n = 4$ Sprague Dawley rats. Extraction of primary neuronal cells was conducted from the cortical tissue of E17-E18 rat embryos from $n = 2$. Then, the chemical dissociation of the tissue, seeding of the cells, maintenance and transfection procedures were carried out as previously described [26, 29] employing niosphingoplexes. Lipofectamine™ 2000 (Invitrogen, California, USA) at 2/1 ratio was employed as a positive control. Each condition was performed in triplicate.

2.10 Subretinal, intravitreal and brain administration

Adult C57BL/6 mice (6–7 weeks old and 20-25 g body weight) were used as experimental animal model. Niosphingoplexes were injected in the eyes intravitreally ($n = 3$) or subretinally ($n = 3$) under an operating microscope (Zeiss OPMI® pico; Carl Zeiss Meditec GmbH, Jena, Germany) with the aid of a Hamilton microsyringe (Hamilton Co., Reno, NV), as previously described [18]. Brain administration of niosphingoplexes at cortex level were also performed in C57BL/6 mice ($n = 3$) following the procedure previously reported [29].

2.11 Evaluation of EGFP expression in mouse retina and brain

EGFP expression in mouse retina was evaluated qualitatively 1 week after the injection of niosphingoplexes in wholemount and sagittal sections of the retina, as previously described [30]. Nuclei were stained with Hoechst 33342 (Thermo Fisher Scientific) in frozen sections and wholemount retinas. EGFP expression in mice brains was evaluated qualitatively 1 week after surgery once brain samples were processed as previously described [31]. Then, the 20 μm brain slices were processed for immunohistochemistry. For blocking non-specific staining, sections were incubated in 10% BSA with 0.5% Triton in PBS for 1 hour and then incubated overnight with chicken anti-GFP (Invitrogen, 1:100) diluted in PBS containing 0.5% Triton X-100. Then sections were washed and incubated in Alexa Fluor 488-conjugated goat anti-chicken IgG (Invitrogen, 1:100) for one hour. Nuclei were stained with Hoechst 33342.

2.12 Statistical analysis

To analyze the differences between more than two groups, a 1-way ANOVA followed by Student–Newman–Keuls test was performed once normality had been proven; otherwise, the non-parametric Kruskal–Wallis test followed by a Mann–Whitney *U* test was used. Data were expressed as mean \pm SD. A *P* value \leq 0.05 was considered statistically significant. Analyses were performed with the IBM SPSS Statistics 22.0 statistical package.

3. RESULTS

3.1 Physicochemical characterization of formulations

The physicochemical properties of the niosphingosome and niosome formulations, as well as the corresponding complexes obtained upon the addition of plasmid DNA at cationic lipid/DNA mass ratios (w/w) 3/1, 7.5/1 and 15/1, are represented in figure 2. The mean diameter size of niosphingosomes was 123.5 ± 12.5 nm and this value decreased slightly up to 27% after the addition of plasmid DNA at all the cationic lipid/DNA mass ratios studied (Figure 2a, black bars). In the case of niosomes, the mean diameter size before the addition of plasmid DNA was higher, 158.9 ± 4.4 , nm and this value slightly increased to 40% at cationic lipid/DNA mass ratio 7.5/1, with no relevant changes at ratios 3/1 and 15/1 (Figure 2a, white bars).

Regarding zeta potential, all formulations showed positive values above zero, being zeta potential values of formulations containing sphingolipids higher than their counterparts. Before the addition of plasmid DNA, zeta potential of niosphingosomes and niosomes was 37.0 ± 7.8 mV and 25.0 ± 9.0 mV, respectively. In both cases, after the addition of plasmid DNA at cationic lipid/DNA mass ratio 3/1, these values declined considerably and then showed a moderate upward trend when incrementing the cationic lipid/DNA mass ratios to 7.5/1 and 15/1 (Figure 2a, lines). The dispersity values of all samples were below 0.5 (Figure 2b) and no relevant differences were found between both formulations, except for niosphingoplexes at cationic lipid/DNA mass ratio 3/1, which presented clearly lower PDI values (0.19 ± 0.01) than the rest of formulations. Under TEM microscopy, both sphingoniosome and niosome formulations showed a clear spherical and regular shape (Figure 2c).

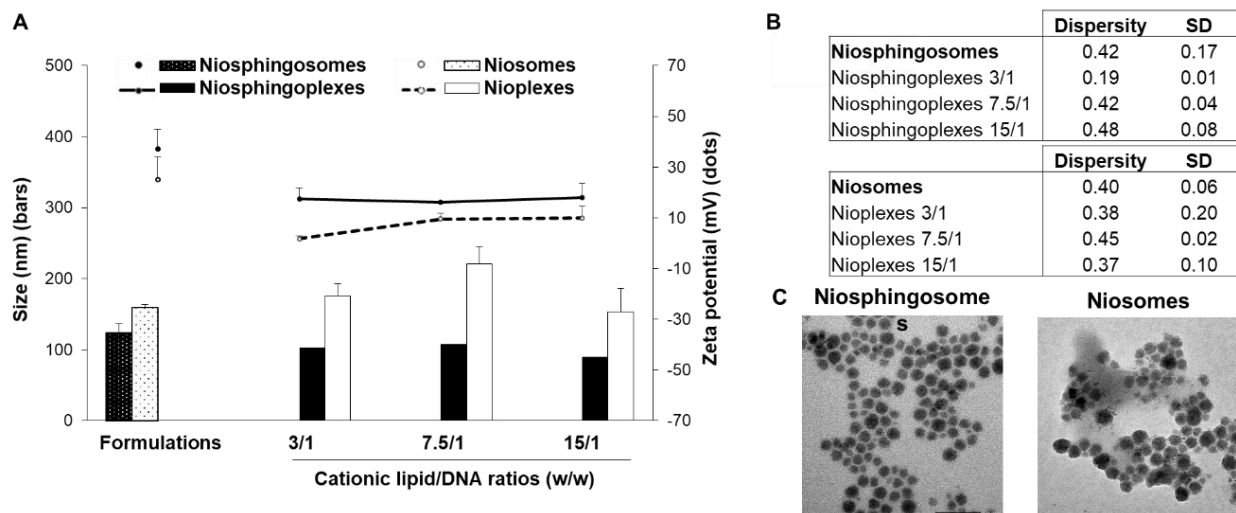


Figure 2. Physicochemical characterization of formulations and complexes prepared with helper component (niosphingosomes/niosphingoplexes) and without helper component (niosomes/nioplexes). (a) Size (bars) and zeta potential (dots). (b) Dispersity index and standard deviation values of formulations and complexes. Each value represents the mean \pm standard deviation of three measurements. (c) TEM images of niosphingosomes and niosomes. Scale bars: 100 nm.

3.2 Cell viability and transfection efficiency in ARPE-19 cells

Cell viability and transfection assays were performed with niosphingoplexes and nioplexes at cationic lipid/DNA mass ratios 3/1, 7.5/1 and 15/1 in ARPE-19 cells (Figure 3) LipofectamineTM 2000 was employed as a positive control at a cationic lipid/DNA mass ratio 2/1, obtaining $39.56 \pm 1.7\%$ of live EGFP expressing cells. All data were normalized in relation to this value. As shown in figure 3a, niosphingoplexes at cationic lipid/DNA mass ratio 3/1 obtained the highest transfection value ($P < 0.001$), with a normalized percentage of live EGFP expressing cells of $36.7 \pm 1.6\%$ (Figure 3a, black bars). Regarding nioplexes, transfection percentages at cationic lipid/DNA mass ratio 3/1 were clearly lower than those values obtained with niosphingoplexes, around 3%, and increased to 22% and to 15% when using cationic lipid/DNA mass ratios 7.5/1 and 15/1, respectively (Figure 3a, white bars). A similar pattern was observed when transfection was analyzed by mean fluorescence intensity (MFI) (Figure 3b), corroborating the highest transfection efficiency of niosphingoplexes at 3/1 cationic lipid/DNA mass ratio ($P < 0.05$). Percentages of living cells were also higher when cells were exposed to niosphingoplexes, obtaining values above 80% at all conditions. In the case of nioplexes, percentage of living cells

reached the lowest value (56%) at 7.5/1 cationic lipid/DNA mass ratios (Figure 3a, lines). These data were further confirmed by fluorescence microscopy, where figure 3c shows representative images of EGFP signal in ARPE-19 cells transfected with niosphingoplexes and with nioplexes at cationic lipid/DNA mass ratio 3/1.

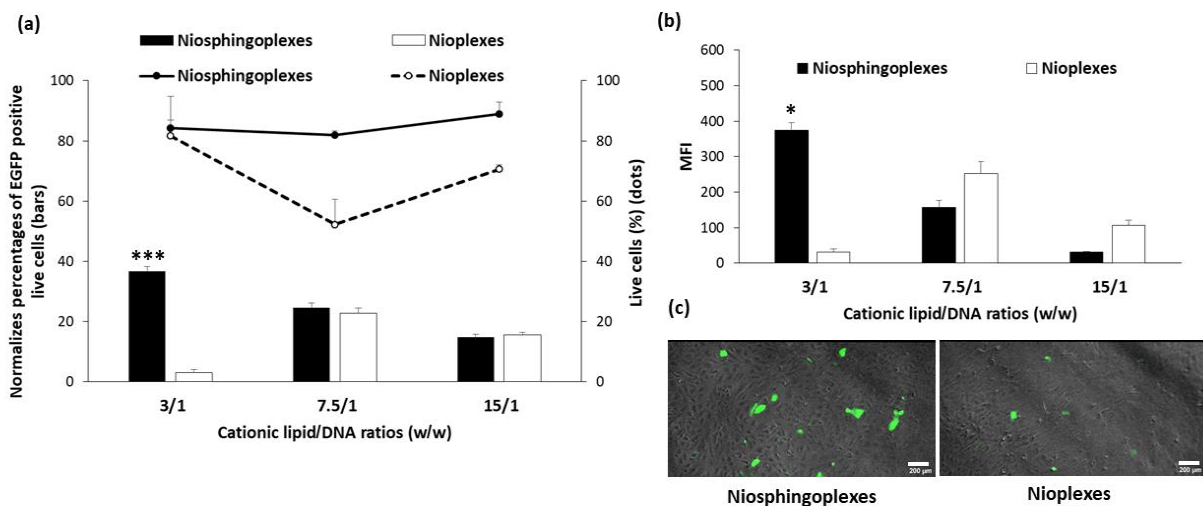


Figure 3. Transfection efficiency and cell viability in ARPE-19 cell line 48 h post-transfection with niosphingoplexes and nioplexes. (a) Normalized percentages of transfection efficiency (bars) and cell viability (dots). (b) MFI of niosphingoplexes and nioplexes. Each value represents the mean \pm standard deviation of three measurements. (c) Overlay phase contrast images showing EGFP signals in ARPE-19 cells transfected with niosphingoplexes and nioplexes at 3/1 cationic lipid/DNA ratio (w/w). Scale bar: 200 μ m. *** $P < 0.001$; * $P < 0.05$.

3.3 Cellular uptake and intracellular trafficking pathways of complexes in ARPE-19 cells

Cell uptake percentages results (Figure 4a, bars) showed that both nioplexes and niosphingoplexes at cationic lipid/DNA mass ratio 3/1 were almost totally internalized by all the cells (more than 98 %) at 2h and 4h of exposition. LipofectamineTM 2000 was employed as a positive control at a cationic lipid/DNA mass ratio 2/1, obtaining values around 95 %. For additional uptake data, we also analyzed the mean fluorescence intensity (MFI) of the cells that internalized the complexes (Figure 4a, dots and lines). In this case, again, niosphingoplexes and nioplexes showed similar values. However, MFI values were clearly higher for both complexes at 4h than at 2h after the exposition to niosphingoplexes ($P < 0.001$) or nioplexes ($P < 0.01$). All data were normalized in relation to those values.

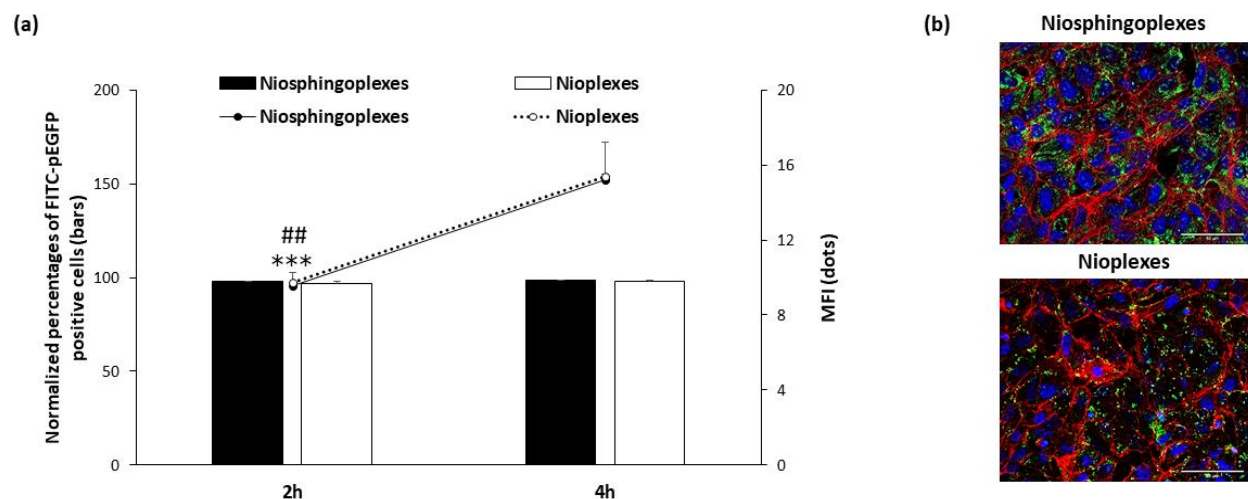


Figure 4. Cellular uptake in ARPE-19 cell line of both niosphingoplexes and nioplexes complexes at 3/1 cationic lipid/DNA ratio (w/w). (a) Percentages of FITC-pEGFP positive cells (bars) and mean fluorescence intensity (dots) at 2 h and 4 h of exposition. Each value represents the mean \pm standard deviation of three measurements. (b) Confocal microscopy images showing the cellular uptake of complexes in ARPE-19 cells at 4 h. Cell nuclei were colored in blue (DAPI); F-actin in red (Phalloidin). Scale bar: 50 μ m. *** $P < 0.001$ for niosphingoplexes; ## $P < 0.01$ for nioplexes.

Intracellular distribution studies of these formulations in ARPE-19 cells were qualitatively analyzed by representative confocal fluorescence microscopy images, showing co-localization between intracellular trafficking pathways and the complexes (Figure 5a). The quantitative analysis elicited that niosphingoplexes had a less participation of the CvME pathway with a 0.25 peak value of cross-correlation function (CCF) compared to both CME (0.31 CCF peak value) and macropinocytosis ($p < 0.05$; 0.42 CCF peak value), as can be observed in figure 5c, (black bars). However, in the case of niosome formulations, the three pathways studied exhibited a more uniform participation in endocytosis process. CCF peak value was 0.35 for CME, 0.38 for macropinocytosis, and 0.41 for Cv ME (Figure 5c, white bars). Additionally, the co-localization of the complexes with lysosomes was also evaluated. In this case, niosphingoplexes exhibited a higher and statistically significant co-localization value (0.45 ± 0.03 CCF peak value) compared to niosomes (0.23 ± 0.05 CCF peak value). A representative fluorescence image obtained by confocal microscopy of co-localization between complexes and lysosomes is shown in figure 5b. Interestingly, the co-incubation of the complexes with the PS micelles that resemble the late endosome compartment in an agarose gel assay showed that DNA incorporated in

niosphingosomes was more efficiently released from the micelles (Figure 5d, lane 2) than DNA bound to niosomes (Figure 5d, lane 3).

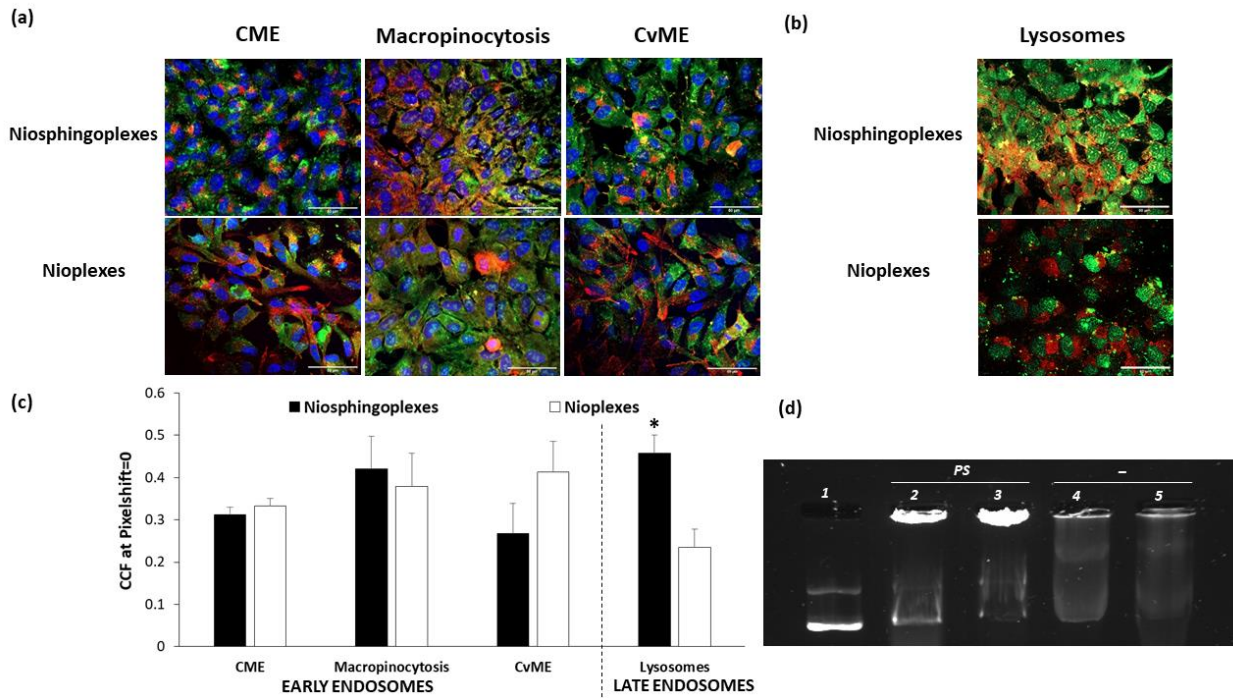


Figure 5. Intracellular trafficking pathway assay of complexes in ARPE-19 cells. (a) Confocal microscopy merged images showing ARPE-19 cells co-incubated with complexes containing the FITC-labeled pEGFP plasmid (green) and with one of the following endocytic vesicle markers (red): Transferrin Alexa Fluor 568 for CME, Dextran Alexa Fluor 568 for macropinocytosis, and Cholera toxin B Alexa Fluor 594 for CvME. Scale bar: 50 μ m. (b) Confocal microscopy merged images showing ARPE-19 cells co-incubated with complexes containing the FITC-labeled pEGFP plasmid (green) and with LysoTracker Red-DND-99 (red) to stain the late endosome. (c) Co-localization values of red and green signals assessed by cross-correlation function (CCF) analysis in complexes. Data represent the mean \pm standard deviation of three measurements; * $P < 0.05$ for niosphingosomes vs nioplexes. (d) DNA release profiles in agarose gel electrophoresis assay. Lane 1 naked DNA, lane 2 niosphingosomes co-incubated with PS, lane 3 nioplexes co-incubated with PS, lane 4 niosphingosomes, lane 5 nioplexes. PS refers to phosphatidyl serine micelles.

3.4 *In vivo* transfection efficiency of niosphingosomes in mice retina and brain

In vivo preliminary studies were carried out to evaluate the capacity of niosphingosomes to deliver the EGFP into the mice retinas after both subretinal (Figure 6a) and intravitreal (Figure 6

b) injections. Data revealed that EGFP expression was present in several retinal layers including outer segments of photoreceptors, outer plexiform layer, inner plexiform layer and ganglion cell layer where some end-foot of the Müller glia cells (red colour) colocalized with EGFP after subretinal and intravitreal administration of niosphingoplexes. Additionally, EGFP expression was also present in the cytoplasmic extensions of cortical cells of the mice brains in the superficial region of the cerebral cortex injected area (Figure 6c).

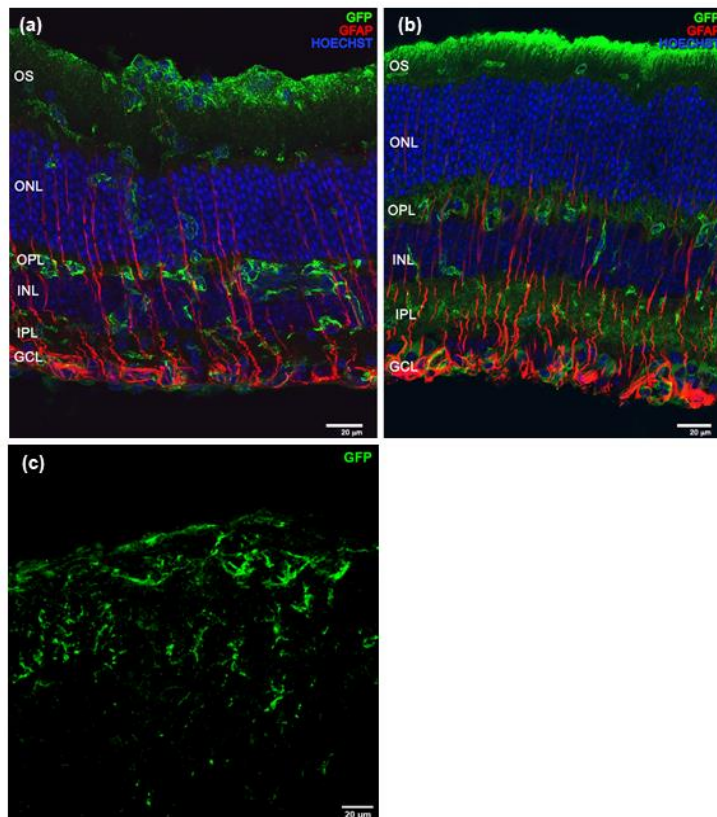


Figure 6. *In vivo* immunohistochemistry gene expression of EGFP (green) in frozen sections one week after subretinal (a), intravitreal (b) and cerebral cortex (c) injections of niosphingoplexes at 3/1 cationic lipid/DNA ratio (w/w). Scale bar: 20μm. OS, outer segments; ONL outer nuclear layer; OPL outer plexiform layer; INL inner nuclear layer; IPL inner plexiform layer; GCL ganglion cell layer.

2. DISCUSSION

Sphingolipids are amphiphilic biomolecules, with a polar terminal group (OH) and a hydrocarbon chain. When amphiphilic molecules are dispersed in water, they can spontaneously

organize themselves into micelles or liposomes [32], which can enhance the drug delivery capacity of such systems. Besides, sphingolipids have desirable physicochemical properties that can stabilize the emulsions, since their surface-active wetting capacity can coat the surface of crystals to enhance the hydrophilicity of hydrophobic drugs [33]. *In addition to all of the above-mentioned properties*, sphingosine, and sphingosine-1-phosphate among other sphingolipids metabolites, call attention as bioactive signaling molecules engaged in the regulation of cell metabolism processes, such as cell growth, differentiation, senescence, and apoptosis [34], by modifying the properties of cell membranes [35]. Such sphingosine predominates into sphingolipids extract obtained from animal origin, which show a more suitable profile to obtain ceramides [21].

In this study, we incorporated sphingolipids from animal origin as “helper” component into niosome formulations, in order to evaluate the biophysical properties as gene delivery system. The physicochemical characterization results (Figure 2) showed that all formulations showed positive charge values, which is required to prevent the formation of aggregates due to electrostatic interactions [16]. Moreover, all formulations and complexes presented particle sizes in the nanoscale range, suitable for gene delivery purposes [36]. The incorporation of sphingolipids as "helper" component into the cationic niosome formulation decreased particle size. Interestingly, such differences in particle size were not only maintained but also decreased when the formulations were complexed with the EGFP plasmid. Additionally, compared to niosphingosomes, niosphingoplexes had smaller particle size at all cationic lipid/DNA mass ratios studied, probably by cause of the additional electrostatic interactions between the cationic niosphingosomes and the anionic plasmid DNA [15, 36]. In fact, regarding superficial charge, the presence of sphingolipid amphiphilic biomolecules in the composition of niosomes increased zeta potential, and this higher zeta potential was maintained also at all the cationic lipid/DNA mass ratios studied. Regarding dispersity index, niosphingoplexes at cationic lipid/DNA mass ratio 3/1 showed the lowest value of this parameter (0.19 ± 0.01), which point out that at this condition a better homogeneity of complexes is obtained. Additionally, niosphingosomes presented a clear spherical and homogeneous morphology under TEM examination, without aggregations, probably due to the electrostatic repulsion among highly positive charged particles.

Once the formulations were characterized in physicochemical terms we performed *in vitro* gene delivery studies with niosphingoplexes and nioplexes at cationic lipid/DNA mass ratios 3/1,

7.5/1 and 15/1 in ARPE-19 cell line, since these cells play an important role in retinal diseases [15]. Moreover, ARPE-19 cell is a well recognized retinal cell model to evaluate gene transfection efficiency. Interestingly, although niosphingoplexes with different cationic lipid/DNA ratios showed similar size and zeta potential values in previously conducted physicochemical studies, they reported statistical differences in terms of transfection efficiency and cell viability, which reveals the complexity of the transfection process. In particular, we observed that niosphingoplexes at cationic lipid/DNA mass ratio 3/1 reached the highest percentage of transfected cells ($P < 0.001$) compared to the rest of conditions. In parallel, MFI analysis was also analyzed to evaluate not only the percentage of live cells transfected, but also the intensity of the fluorescence signal, which is close related to the quantity of protein expressed after the transfection process. Such MFI studies also revealed that the highest intensity value was reached when ARPE-19 cells were treated with niosphingoplexes at 3/1 cationic lipid/DNA mass ratio. Altogether, data obtained from transfection efficiency experiments suggest that at 3/1 cationic lipid/DNA mass ratio, the presence of sphingolipid biomolecules in the niosome composition not only increases the percentage of transfected cells, but also the quantity of protein expressed in such transfected cells [15], which can have critical clinical relevance. Interestingly, data obtained from transfection experiments also revealed that niosphingoplexes at all cationic lipid/DNA mass ratios showed higher cell viability values (above 80% in ARPE-19 cells), than their niosome counterparts, which point out the biocompatibility effect that incorporation of sphingolipids has into the niosome formulation. This biocompatibility of niosphingoplexes as well was confirmed, qualitatively, by the healthful look of ARPE-19 cells under fluorescence microscope examination 48 h after transfection. On the contrary, transfection positive control Lipofectamine™ 2000 showed low cell viability values below 65% (data not shown) revealing the toxicity associated to such formulation which hampers its clinical application [27]. In terms of clinical applications, it is also important to highlight that the best transfection efficiency with high cell viability was obtained when ARPE-19 cells were exposed to niosphingoplexes at the lowest cationic lipid/DNA ratio of 3/1. Such achievement would allow higher gene loading capacity in small injection volumes that normally are required to face devastating pathologies of both brain in retina, by means of gene therapy approach.

To further evaluate the impact that the incorporation of sphingolipid biomolecules has on the transfection process we performed also a cellular uptake study, since this parameter can

drastically affect to the transfection efficiency [15]. However, our cellular uptake studies revealed that there were no difference in the cellular uptake of both formulations, in terms of both percentage of cells that internalized the complexes and quantity of particles that were internalized in cells. In any case, the internalization process was more efficient when cells were exposed to formulations during 4 h instead of 2 h. These data suggest the relevance that the kinetic of the internalization process has on the transfection efficiency, although in this case, there were not differences observed between niosphingoplexes and niosome formulations. Therefore, we also studied other biological parameters such as the intracellular trafficking process of both formulations to further explore the influence that the integration of sphingolipids in niosome composition has on the transfection process [37].

Intracellular trafficking studies were carried out to analyse the co-localization of the formulations with the most employed endocytosis pathways present in ARPE-19 cells such as CvME, CME and macropinocytosis [38, 39]. Our data revealed that the highest difference between both formulations was found in the CvME pathway. This endocytic pathway was minority in the case of niosphingoplexes formulation, which in fact preferred the macropinocytosis pathway, while niosomes were equally internalized by the three endocytosis pathways studied. Therefore, our data suggest that the presence of sphingolipids might turn the internalization mechanism of niosphingoplexes from CvME to macropinocytosis endocytic pathway. In this sense, it has been described that macropinocytosis is implicated in the internalization of cell penetrating peptides and proteins into cells [40, 41]. Moreover, co-localization studies in the late endosomal compartment were also conducted. In this case, niosphingoplexes co-localized with lysosomes in a higher rate than nioplexes (Figure 5c). It has been suggested that there is a suppression of lysosomal activity when complexes enter into ARPE-19 cells by CvME, and such complexes are located around the nucleus, which hampers the release of DNA from the complexes [39]. This suggestion supports our results, since compared to niosphingoplexes, nioplexes (that showed less transfection efficiency) entered into the cell mainly via CvME, with the consequent lack of lysosomal activity. Another critical parameter that clearly impact on transfection process of complexes designed for gene delivery is the endosomal scape. Some nucleic acid delivery systems failed to achieve good levels of transfection efficiencies, despite being efficiently internalized into the cells, due to their poor of endosomal escape performance [42].

Thus, we next elaborated anionic micelles based on PS, as, in the interest to evaluate the release of the complexed plasmid DNA from the late endosomes to avoid lysosomal degradation. As observed in figure 5d, a small amount of plasmid was released from niosphingoplexes (lane 2), and no release of plasmid was observed from the nioplexes (lane 3) in the agarose gel electrophoresis assay. Such data suggest that the incorporation of sphingolipids into the cationic niosome formulation could provide endosomal escape properties to the complexes, which in fact could contribute to increase transfection efficiency. Another biological barrier that hampers transfection process is the nuclear membrane. In this sense, and taking into account the crucial signaling and regulatory roles that sphingolipids have in the nucleus [43], it is likely that such sphingolipids could be promoting gene delivery by a regulatory mechanism in the cell nucleus. Recent findings concerning nuclear sphingolipids found that different kind of sphingolipids have particular nuclear functions by temporally and spatially specific mechanisms. For example, sphingomyelin is involved in the structure and regulation of chromatin architecture, DNA synthesis and RNA stability, while sphingosine acts as ligand for the nuclear receptor steroidogenic factor 1 regulating gene transcription; and sphingosine-1-phosphate regulates gene expression epigenetically by histone acetylation [44]. Before perming *in vivo* experiments, we made a probe of concept assay to evaluate if niosphingoplexes at cationic lipid/DNA mass ratio 3/1 (w/w) were able to deliver the EGFP plasmid in an efficient way to both rat embryonal retinal and cerebral cortex primary cells. Our results (Supplementary material) revealed EGFP expression in both retinal (Figure S1a) and cortical (Figure S1c) primary cells evaluated 72h after transfection.

Therefore, motivated by those results, niosphingoplexes were implemented in *in vivo* studies to assess their capacity to deliver the genetic material to mouse retina, after both intravitreal and subretinal injection, and to mouse brain, after administration of niosphingoplexes at the cortex level. Because of their relevant physiological function, both brain and eye are immune-privileged sites isolated from the rest of the organism by additional extracellular barriers such the BBB and the BRB [45, 46]. An ideal scenario would contemplate the delivery of genetic material by a safe and efficient non-viral vector to immune-privileged sites through non-invasive administration routes, such as the topical instillation in the cornea that circumvent the BRB to reach the retina, and the nose-to-brain administration to access directly into the brain bypassing the BBB [47]. However, at moment this possibility is far away to be applied into the regular medical practice to face by gene therapy devastating diseases that affect to brain and retina. Therefore, we evaluated

the local administration of niosphingoplexes in retina and brain. In the case of the eye, at the moment, most employed administration routes to reach the retina at a clinical level include the intravitreal and subretinal injection [18]. Our data revealed that after intravitreal and subretinal injections, EGFP expression was present in several layers and cells of the retina. More specifically, EGFP expression was observed mainly in the outer segments of photoreceptors, outer plexiform layer, and in the inner plexiform layer, where some end-foot of the Müller glia cells exhibited green fluorescence signal. Gene delivery to the outer layers of the retina is of utmost importance from a therapeutic standpoint, since there have been described more than 200 mutations in genes at this level, related to relevant pathologies of the retina such as Stargardt disease, retinitis pigmentosa, or Leber's congenital amaurosis, to name just the most relevant ones [17]. On the other hand, transfection of ganglion cell layer in the retina has relevance to face glaucoma disease where these cells are affected [48]. Interestingly, in the case of brain administration at the cortex level, we also found EGFP expression in the cytoplasmic extensions of cortical cells, close to the injection site. This area of the brain is usually affected in devastating diseases of the central nervous systems, such as epilepsy, Alzheimer's and Parkinson's diseases, leading to relevant perturbation and neurological disorders [49, 50]. Therefore, our preliminary proof of concept *in vivo* assay, shows promising results to deliver in the future therapeutic genetic material in to retina and brain of animal models that resembles human diseases of these relevant and immune-privileged sites.

5. CONCLUSION

Overall, this manuscript points out the biophysical properties of sphingolipid extracts from animal origin for gene delivery purposes when they are incorporated into cationic niosomes. Such biomaterial impacts not only on relevant physicochemical properties of cationic niosomes that influence on transfection efficiency, such as particle size or zeta potential, but also in biological properties, such as their intracellular disposition or endosomal escape properties. Moreover, our proof of concept *in vivo* results suggest that niosphingosomes represent a promising non-viral vector biomaterial for the treatment of both retinal and brain diseases by gene therapy approach.

6. FUNDING

This work was supported by the Basque Country Government (Department of Education, University and Research, Consolidated Groups IT907-16). Additional funding was provided by

the CIBER of Bioengineering, Biomaterials and Nanomedicine (CIBER-BBN), and initiative of the Carlos III Health Institute (ISCIII). I.V.B. and M.S.R. thank the University of the Basque Country (UPV/EHU) for the granted postdoctoral fellowship (ESPDOC19/47) and the granted pre-doctoral fellowship (PIF17/79), respectively.

7. AUTHOR'S CONTRIBUTIONS

J.L.P. and G.P.: Conceptualization. N.A.Q., C.S.S., G.M.N., M.S.R. T.B.L.M., P.G.M.: Methodology and investigation. . N.A.Q., I.G., I.V.B.: Formal analysis. N.A.Q., I.G.: Writing. N.A.Q., I.G., I.V.B, C.S.S., G.M.N.: Visualization. All authors: Review & editing. J.L.P. G.P. E.F.: Supervision and project administration. J.L.P.: Funding acquisition.

8. DECLARATIONS OF INTEREST: none

9. ACKNOWLEDGEMENTS

Authors wish to thank the intellectual and technical assistance from the ICTS “NANBIOSIS,” more specifically by the Drug Formulation Unit (U10) of the CIBER in Bioengineering, Biomaterials and Nanomedicine (CIBER-BBN) at the University of Basque Country (UPV/EHU). Technical and human support provided by SGIKER (UPV/EHU) is also gratefully acknowledged. I.V.B. and M.S.R. thank the University of the Basque Country (UPV/EHU) for the granted postdoctoral fellowship (ESPDOC19/47) and the granted pre-doctoral fellowship (PIF17/79), respectively.

10. REFERENCES

- [1] Dunbar, C.E.; High, K.A.; Joung, J.K.; Kohn, D.B.; Ozawa, K.; Sadelain, M. Gene Therapy Comes of Age. *Science* **2018**, *359*, 10.1126/science.aan4672.
- [2] Mullard, A. Gene Therapy Boom Continues. *Nat. Rev. Drug Discov.* **2019**, *18*, 737-019-00154-0.
- [3] Sung, Y.K.; Kim, S.W. Recent Advances in the Development of Gene Delivery Systems. *Biomater. Res.* **2019**, *23*, 8-019-0156-z. eCollection 2019.
- [4] Ingusci, S.; Verlengia, G.; Soukupova, M.; Zucchini, S.; Simonato, M. Gene Therapy Tools for Brain Diseases. *Front. Pharmacol.* **2019**, *10*, 724.
- [5] Streilein, J.W. Ocular Immune Privilege: Therapeutic Opportunities from an Experiment of Nature. *Nat. Rev. Immunol.* **2003**, *3*, 879-889.

- [6] Vaughan, E.E.; DeGiulio, J.V.; Dean, D.A. Intracellular Trafficking of Plasmids for Gene Therapy: Mechanisms of Cytoplasmic Movement and Nuclear Import. *Curr. Gene Ther.* **2006**, *6*, 671-681.
- [7] Nayerossadat, N.; Maedeh, T.; Ali, P.A. Viral and Nonviral Delivery Systems for Gene Delivery. *Adv. Biomed. Res.* **2012**, *1*, 27-9175.98152. Epub 2012 Jul 6.
- [8] Foldvari, M.; Chen, D.W.; Nafissi, N.; Calderon, D.; Narsineni, L.; Rafiee, A. Non-Viral Gene Therapy: Gains and Challenges of Non-Invasive Administration Methods. *J. Control. Release* **2016**, *240*, 165-190.
- [9] Zhi, D.; Bai, Y.; Yang, J.; Cui, S.; Zhao, Y.; Chen, H.; Zhang, S. A Review on Cationic Lipids with Different Linkers for Gene Delivery. *Adv. Colloid Interface Sci.* **2018**, *253*, 117-140.
- [10] Ojeda E, Puras G, Agirre M, Zárate J, Grijalvo S, Pons R, Eritja R, Martínez-Navarrete G, Soto-Sánchez C, Fernández E, Pedraz JL. Niosomes based on synthetic cationic lipids for gene delivery: the influence of polar head-groups on the transfection efficiency in HEK-293, ARPE-19 and MSC-D1 cells. *Org Biomol Chem.* **2015** Jan 28; *13*(4):1068-81.
- [11] Riley, M.K.; Vermerris, W. Recent Advances in Nanomaterials for Gene Delivery-A Review. *Nanomaterials (Basel)* **2017**, *7*, 10.3390/nano7050094.
- [12] Puras G, Mashal M, Zárate J, Agirre M, Ojeda E, Grijalvo S, Eritja R, Diaz-Tahoces A, Martínez Navarrete G, Avilés-Trigueros M, Fernández E, Pedraz JL. A novel cationic niosome formulation for gene delivery to the retina. *J Control Release.* **2014** Jan 28; *174*:27-36.
- [13] Grijalvo S, Puras G, Zárate J, Sainz-Ramos M, Qtaish NAL, López T, Mashal M, Attia N, Díaz D, Pons R, Fernández E, Pedraz JL, Eritja R. Cationic Niosomes as Non-Viral Vehicles for Nucleic Acids: Challenges and Opportunities in Gene Delivery. *Pharmaceutics.* **2019** Jan 22; *11*(2):50.
- [14] Bartelds, R.; Nematollahi, M.H.; Pols, T.; Stuart, M.C.A.; Pardakhty, A.; Asadikaram, G.; Poolman, B. Niosomes, an Alternative for Liposomal Delivery. *PLoS One* **2018**, *13*, e0194179.
- [15] Ojeda, E.; Puras, G.; Agirre, M.; Zarate, J.; Grijalvo, S.; Eritja, R.; DiGiacomo, L.; Caracciolo, G.; Pedraz, J.L. The Role of Helper Lipids in the Intracellular Disposition and Transfection Efficiency of Niosome Formulations for Gene Delivery to Retinal Pigment Epithelial Cells. *Int. J. Pharm.* **2016**, *503*, 115-126.
- [16] Ojeda E, Puras G, Agirre M, Zarate J, Grijalvo S, Eritja R, Martínez-Navarrete G, Soto-Sánchez C, Diaz-Tahoces A, Aviles-Trigueros M, Fernández E, Pedraz JL. The influence of the polar head-group of synthetic cationic lipids on the transfection efficiency mediated by niosomes in rat retina and brain. *Biomaterials.* **2016** Jan; *77*:267-79.
- [17] Mashal, M.; Attia, N.; Puras, G.; Martínez-Navarrete, G.; Fernandez, E.; Pedraz, J.L. Retinal Gene Delivery Enhancement by Lycopene Incorporation into Cationic Niosomes Based on DOTMA and Polysorbate 60. *J. Control. Release* **2017**, *254*, 55-64.
- [18] Mashal, M.; Attia, N.; Martínez-Navarrete, G.; Soto-Sánchez, C.; Fernandez, E.; Grijalvo, S.; Eritja, R.; Puras, G.; Pedraz, J.L. Gene Delivery to the Rat Retina by Non-Viral Vectors Based on Chloroquine-Containing Cationic Niosomes. *J. Control. Release* **2019**, *304*, 181-190.

- [19] Chun, J.; Hartung, H.P. Mechanism of Action of Oral Fingolimod (FTY720) in Multiple Sclerosis. *Clin. Neuropharmacol.* **2010**, *33*, 91-101.
- [20] Alrbyawi, H.; Poudel, I.; Dash, R.P.; Srinivas, N.R.; Tiwari, A.K.; Arnold, R.D.; Babu, R.J. Role of Ceramides in Drug Delivery. *AAPS PharmSciTech* **2019**, *20*, 287-019-1497-6.
- [21] Cerrato S, Ramió-Lluch L, Brazís P, Fondevila D, Segarra S, Puigdemont A. Effects of sphingolipid extracts on the morphological structure and lipid profile in an in vitro model of canine skin. *Vet J.* **2016** Jun;212:58-64.
- [22] Dahiya R, Brasitus TA. Distribution of glycosphingolipids and ceramide of rat small intestinal mucosa. *Lipids.* **1986** Feb;21(2):112-6.
- [23] Tessema, E.N.; Gebre-Mariam, T.; Paulos, G.; Wohlrab, J.; Neubert, R.H.H. Delivery of Oat-Derived Phytoceramides into the Stratum Corneum of the Skin using Nanocarriers: Formulation, Characterization and in Vitro and Ex-Vivo Penetration Studies. *Eur. J. Pharm. Biopharm.* **2018**, *127*, 260-269.
- [24] Yilmaz, E.; Borchert, H.H. Design of a Phytosphingosine-Containing, Positively-Charged Nanoemulsion as a Colloidal Carrier System for Dermal Application of Ceramides. *Eur. J. Pharm. Biopharm.* **2005**, *60*, 91-98.
- [25] Park, S.N.; Lee, M.H.; Kim, S.J.; Yu, E.R. Preparation of Quercetin and Rutin-Loaded Ceramide Liposomes and Drug-Releasing Effect in Liposome-in-Hydrogel Complex system. *Biochem Biophys Res Commun.* **2013** Jun 7;435(3):361-6.
- [26] Sainz-Ramos M, Villate-Beitia I, Gallego I, et al. Non-viral mediated gene therapy in human cystic fibrosis airway epithelial cells recovers chloride channel functionality. *Int J Pharm.* **2020**;588.
- [27] Villate-Beitia I, Gallego I, Martínez-Navarrete G, Zárata J, López-Méndez T, Soto-Sánchez C, Santos-Vizcaíno E, Puras G, Fernández E, Pedraz JL. Polysorbate 20 non-ionic surfactant enhances retinal gene delivery efficiency of cationic niosomes after intravitreal and subretinal administration. *Int J Pharm.* **2018** Oct 25;550(1-2):388-397.
- [28] Agirre M, Ojeda E, Zarate J, Puras G, Grijalvo S, Eritja R, García del Caño G, Barrondo S, González-Burguera I, López de Jesús M, Sallés J, Pedraz JL. New Insights into Gene Delivery to Human Neuronal Precursor NT2 Cells: A Comparative Study between Lipoplexes, Nioplexes, and Polyplexes. *Mol Pharm.* **2015** Nov 2;12(11):4056-66.
- [29] Gallego I, Villate-Beitia I, Soto-Sánchez C, Menéndez M, Grijalvo S, Eritja R, Martínez-Navarrete G, Humphreys L, López-Méndez T, Puras G, Fernández E, Pedraz JL. Brain Angiogenesis Induced by Nonviral Gene Therapy with Potential Therapeutic Benefits for Central Nervous System Diseases. *Mol Pharm.* **2020** Jun 1;17(6):1848-1858.
- [30] Gallego I, Villate-Beitia I, Martínez-Navarrete G, Menéndez M, López-Méndez T, Soto-Sánchez C, Zárata J, Puras G, Fernández E, Pedraz JL. Non-viral vectors based on cationic niosomes and minicircle DNA technology enhance gene delivery efficiency for biomedical applications in retinal disorders. *Nanomedicine.* **2019** Apr;17:308-318.
- [31] Soto-Sánchez C, Martínez-Navarrete G, Humphreys L, Puras G, Zarate J, Pedraz JL, Fernández E. Enduring high-efficiency in vivo transfection of neurons with non-viral

magnetoparticles in the rat visual cortex for optogenetic applications. *Nanomedicine*. **2015** May;11(4):835-43.

[32] Margineanu A. Chapter 14 - Biological Applications of Nanoparticles in Optical Microscopy. *Polymeric Nanomaterials in Nanotherapeutics* **2019**:469-495.

[33] Jing, Xuling Wang, Ting Zhang, Chunling Wang, Zhenjun Huang, Xiang Luo, and Yihui Deng. A Review on Phospholipids and their Main Applications in Drug Delivery Systems. *Asian Journal of Pharmaceutical Sciences*. **2015**; 10 (2): 81-98.

[34] Bartke N, Hannun YA. Bioactive sphingolipids: metabolism and function. *J Lipid Res*. **2009** Apr;50 Suppl(Suppl):S91-6.

[35] Goñi FM, Alonso A. Biophysics of sphingolipids I. Membrane properties of sphingosine, ceramides and other simple sphingolipids. *Biochimica et Biophysica Acta (BBA) - Biomembranes* **2006**;1758(12):1902-1921.

[36] Villate-Beitia I, Puras G, Soto-Sanchez C, Agirre M, Ojeda E, Zarate J, Fernandez E, Pedraz JL. Non-viral vectors based on magnetoplexes, lipoplexes and polyplexes for VEGF gene delivery into central nervous system cells. *Int.J.Pharm.* **2017**; 521:130-40.

[37] Wissing SA, Kayser O, Müller RH. Solid lipid nanoparticles for parenteral drug delivery. *Adv Drug Deliv Rev*. **2004** May 7;56(9):1257-72.

[38] Manzanares D, Ceña V. Endocytosis: The Nanoparticle and Submicron Nanocompounds Gateway into the Cell. *Pharmaceutics*. **2020** Apr 17;12(4):371.

[39] Delgado D, del Pozo-Rodríguez A, Solinís MÁ, Rodríguez-Gascón A. Understanding the mechanism of protamine in solid lipid nanoparticle-based lipofection: the importance of the entry pathway. *Eur J Pharm Biopharm.* **2011**;79(3):495-502.

[40] Jones AT. Macropinocytosis: searching for an endocytic identity and role in the uptake of cell penetrating peptides. *J Cell Mol Med*. **2007** Jul-Aug;11(4):670-84.

[41] Lim JP, Gleeson PA. Macropinocytosis: an endocytic pathway for internalising large gulps. *Immunol Cell Biol*. **2011** Nov;89(8):836-43.

[42] Liang, W. and Jenny K W Lam. “Endosomal Escape Pathways for Non-Viral Nucleic Acid Delivery Systems.” (2012).

[43] Ledeen RW, Wu G. Nuclear sphingolipids: metabolism and signaling. *J Lipid Res*. **2008** Jun;49(6):1176-86.

[44] Lucki NC, Sewer MB. Nuclear Sphingolipid Metabolism. *Annual Review of Physiology* **2012**;74(1):131-151.

[45] O’Mahony A.M., Godinho B.M., Cryan J.F., O’Driscoll C.M. Non-Viral Nanosystems for Gene and Small Interfering RNA Delivery to the Central Nervous System: Formulating the Solution. *J. Pharm. Sci.* **2013**;102:3469–3484

[46] Zhang Y, Schlachetzki F, Li JY, Boado RJ, Pardridge WM. Organ-specific gene expression in the rhesus monkey eye following intravenous non-viral gene transfer. *Mol Vis*. **2003** Oct 3;9:465-72.

[47] Al Qtaish N, Gallego I, Villate-Beitia I, Sainz-Ramos M, López-Méndez TB, Grijalvo S, Eritja R, Soto-Sánchez C, Martínez-Navarrete G, Fernández E, Puras G, Pedraz JL. Niosome-Based Approach for In Situ Gene Delivery to Retina and Brain Cortex as Immune-Privileged Tissues. *Pharmaceutics*. **2020** Feb 25;12(3):198.

[48] Puras G, Martínez-Navarrete G, Mashal M, Zárate J, Agirre M, Ojeda E, Grijalvo S, Eritja R, Diaz-Tahoces A, Avilés-Trigueros M, Fernández E, Pedraz JL. Protamine/DNA/Niosome Ternary Nonviral Vectors for Gene Delivery to the Retina: The Role of Protamine. *Mol Pharm*. **2015** Oct 5;12(10):3658-71.

[49] Barres BA. The mystery and magic of glia: a perspective on their roles in health and disease. *Neuron*. **2008** Nov 6;60(3):430-40.

[50] Milligan ED, Watkins LR. Pathological and protective roles of glia in chronic pain. *Nat Rev Neurosci*. **2009** Jan;10(1):23-36.

Supplementary Material

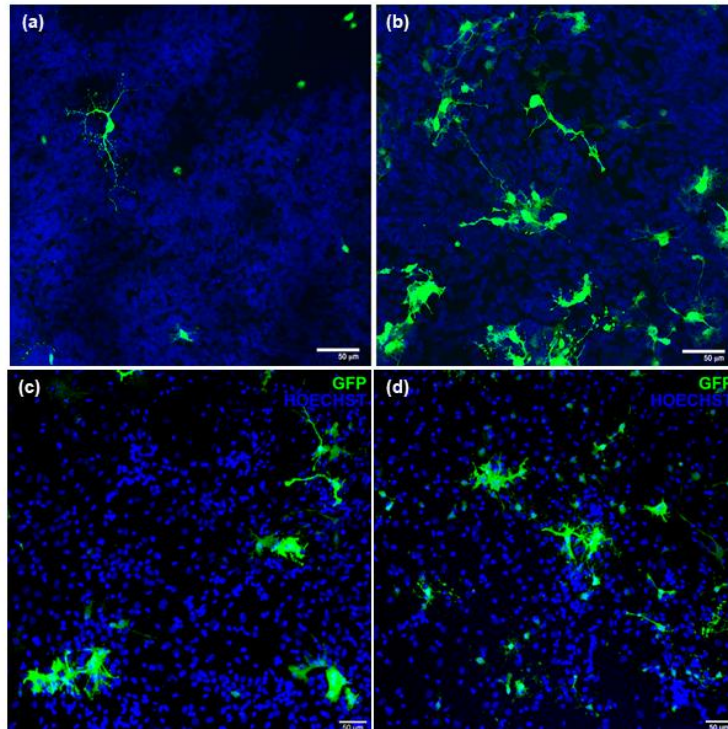


Figure S1: EGFP signal (green) in primary culture of rat retinal cells transfected with (a) niosphingoplexes at 3/1 cationic lipid/DNA ratio (w/w) and (b) the positive control Lipofectamine™ 2000. GFP signal (green) in embryonic rat cerebral cortex primary cells transfected with (c) niosphingoplexes at 3/1 cationic lipid/DNA ratio (w/w) and (d) the positive control Lipofectamine™ 2000. Scale bar: 50 μm. Hoechst 33342 stained blue.

Appendix 3

Nanodiamond Integration into Niosomes as an Emerging and Efficient Gene Therapy Nanoplatfom for Central Nervous System Diseases

ACS Appl. Mater. Interfaces 2022, 14, 13665–13677

<https://doi.org/10.1021/acsami.2c02182>

IF: 10.383 (2021)

Nanodiamonds Integration into Niosomes as an Emerging and Efficient Gene Therapy Nanoplatform for Central Nervous System Diseases

*Nuseibah AL Qtaish^{a,b,‡}, Idoia Gallego^{a,b,c,‡}, Alejandro J. Paredes^{d,e}, Ilia Villate-Beitia^{a,b,c},
Cristina Soto-Sánchez^{b,f}, Gema Martínez-Navarrete^{b,f}, Myriam Sainz-Ramos^{a,b,c}, Tania B. Lopez-
Mendez^{a,b,c}, Eduardo Fernández^{b,f}, Gustavo Puras^{a,b,c,*}, and José Luis Pedraz^{a,b,c,*}.*

^a NanoBioCel Research Group, Laboratory of Pharmacy and Pharmaceutical Technology. Faculty of Pharmacy, University of the Basque Country (UPV/EHU), Paseo de la Universidad 7, 01006 Vitoria-Gasteiz, Spain.

^b Networking Research Centre of Bioengineering, Biomaterials and Nanomedicine (CIBER-BBN), Institute of Health Carlos III, 28029 Madrid, Spain

^c Bioaraba, NanoBioCel Research Group, 01009 Vitoria-Gasteiz, Spain.

^d Research and Development Unit in Pharmaceutical Technology (UNITEFA), CONICET and Department of Pharmaceutical Sciences, Chemistry Sciences Faculty, National University of Córdoba. Haya de la Torre y Medina Allende, X5000XHUA, Córdoba, Argentina.

^e School of Pharmacy, Queen's University Belfast, Medical Biology Centre, 97 Lisburn Road, Belfast, BT9 7BL, Northern Ireland, UK.

^f Neuroprosthesis and Neuroengineering Research Group, Institute of Bioengineering, Miguel Hernández University, Avenida de la Universidad, 03202 Elche, Spain.

‡These authors contributed equally

*Corresponding authors

KEYWORDS: nanodiamonds, niosomes, cationic lipids, gene delivery, nanomedicine, CNS diseases

ABSTRACT: Nanodiamonds (NDs) are promising materials for gene delivery due to their unique physicochemical and biological features, along with their possibility of combination with other non-viral systems. Our aim was to evaluate the biophysic performance of NDs as helper component of niosomes, named as nanodiasomes, to address a potential non-viral gene delivery nanoplatform for therapeutic applications in central nervous system (CNS) diseases.

Nanodiasomes, niosomes and their corresponding complexes, obtained after genetic material addition at different ratios (w/w), were evaluated in terms of physicochemical properties, cellular uptake, intracellular disposition, biocompatibility and transfection efficiency in HEK-293 cells. Nanodiasomes, niosomes and complexes fulfilled the physicochemical features for gene therapy applications. Biologically, the incorporation of NDs into niosomes enhanced 75% transfection efficiency ($p < 0.001$) and biocompatibility ($p < 0.05$) to values over 90%, accompanied by a higher cellular uptake ($p < 0.05$). Intracellular trafficking analysis showed higher endocytosis via clathrins ($p < 0.05$) in nanodiaplexes compared with nioplexes, followed by higher lysosomal colocalization ($p < 0.05$), that coexisted with endosomal escape properties, whereas endocytosis mediated by caveolae was most efficient pathway in the case of nanodiaplexes. Moreover, studies in CNS primary cells revealed that nanodiaplexes successfully transfected neuronal and retinal cells. These proof of concept study points out that NDs integration into niosomes represents an encouraging non-viral nanoplatform strategy for the treatment of CNS diseases by gene therapy.

INTRODUCTION

Since more than fifty years, it has been hypothesized by scientific community that therapies based on the delivery of genetic material could be an appealing option to face human diseases. In theory, this strategy, so-called gene therapy, would offer the possibility of achieving durable and curative clinical benefit. At present, this approach is widely applied in clinical trials, with some of them recently achieving approved drug status in the United States and Europe.¹ Nevertheless, this approach is still far from being considered a mainstream therapeutic option, as used vectors have not demonstrated the desirable characteristics in terms of safety, efficacy or associated costs.

The most basic form of gene therapy is naked plasmid DNA, however, its poor cellular uptake, degradation by nucleases and low transfection efficiency make necessary the use of vectors able to protect and suitably deliver the nucleic acids.² At present, most DNA delivery strategies use viral or non-viral vectors. Although viral vectors such as lentiviruses,³ adenoviruses⁴ and recombinant adeno-associated viruses⁵ provide higher efficiency over a longer period, there are important limitations concerning safety issues, including toxicity, immunogenicity, mutagenesis and inflammatory potential, as well as high production costs.⁶ These limitations have boosted the need to develop safer and less cytotoxic nucleic acid carriers, as is the case of non-viral systems.⁷

Research on chemical non-viral vectors, has gained momentum as they are comparatively less invasive than viral ones, show less immune and inflammatory responses, are cheaper to produce, and have higher genetic material cargo capacity.⁸ However, their low transfection efficiency represents the most important handicap for clinical applications. Therefore, the scientific community continues to seek novel strategies able to overcome this obstacle.

Nanomaterials, such as carbon atom based molecules, have captured the attention in the field of nanotechnology intended for biomedical applications. In particular, nanodiamonds (NDs) constitute an attractive platform for drug and gene delivery because of their unique physicochemical features, biocompatibility, near-spherical shape, narrow particle size distribution, water dispersibility, high specific area and ease of surface functionalization.^{9, 10} Specifically, some authors have vectored plasmid DNA^{11, 12} or siRNA¹³⁻¹⁵ by NDs after functionalization with polyethylemine 800, polyglycerol, lysine or polyallylamine hydrochloride through the formation of electrostatic bonded complexes. In contrast, other works have achieved those deliveries by covalent derivatization of NDs with silane-NH₂ groups^{11, 16} and polyamidoamine (PANAM),¹⁷ or by joining NDs to EDA (joint arm) and H-Arg-GlyAsp-Val-OH (targeting agent).¹⁸ Nevertheless, some of the limitations of these carbon based nanostructures include their need of binding to other vectors for their stabilization and the low gene packing capacity achieved to date with the conventional linkers. Hence, there arises the need for developing other systems able to overcome the concerns related to NDs.

In this sense, lipidic vectors such as niosomes are high DNA packing gene delivery systems that offer the ability to condense, protect and suitably release DNA in a safe manner, making it a widely used prime candidate for non-viral gene therapy.¹⁹⁻²¹ Basically, niosomes for gene delivery are composed of a cationic lipid to promote electrostatic interactions with negative charged molecules,²² non-ionic surfactants to enhance the stability,²³ and exists the possibility to include a helper component that would improve the biological activity of the vector.^{24, 25} Although the main limitation of this kind of vectors is their lower transfection efficiency compared to viral ones, we hypothesize that the incorporation of emerging nanomaterials like NDs as a helper component in the structure of niosomes could potentially improve this ability and might lead to a powerful gene delivery tool for translational therapeutic applications, and particularly for CNS diseases, where

the blood-brain and blood-retinal barriers hamper even more the implementation of therapeutic strategies.²⁶

Therefore, and in the absence of any evidence related to the incorporation of NDs into niosomes, the aim of this study was to combine NDs with the components used for the preparation of niosomes to develop an optimized non-viral vector based nanoplatform for efficient and safe gene therapy with potential translation into biomedical application. To this end, we employed monodispersed ND particles, the cationic lipid 1,2-di-O-octadecenyl-3-trimethylammonium propane (DOTMA) and the non-ionic surfactant polysorbate Tween[®] 20, obtaining NDs integrated into niosomes, named nanodiasomes, and niosomes devoid of NDs. These vectors were combined with pEGFP plasmid to form the corresponding nanodiaplexes and nioplexes, respectively; all of them were physicochemically characterized concerning particle size, zeta potential, dispersity and morphology, and were assessed in terms of capacity to condense, protect and release the DNA from enzymatic digestion. The biological performance of NDs into niosomes was additionally analyzed by *in vitro* assays to determine the biocompatibility and transfection efficiency of this gene delivery systems in HEK-293 cell line, as well as the cellular uptake and intracellular disposition of nanodiaplexes versus nioplexes. Finally, experiments in rat central nervous system (CNS) primary cells, from neuronal and retinal origin, were performed to assess the gene delivery ability of this novel nanoplatform in a more closer to reality biological scenario aimed at treating CNS diseases by gene therapy.

EXPERIMENTAL SECTION

Elaboration of formulations

All the formulations were elaborated by the oil in water emulsion technique. NDs were purchased as ultra nanocrystalline diamonds with particle size smaller than 10 nm (Sigma-Aldrich Madrid, Spain, ID: 900180). A volume of 250 μ l of NDs (10 mg/ml in H₂O) were ultrasonicated for 30 minutes and mixed with 2 ml of 0.5% Tween[®] 20 (Sigma-Aldrich Madrid, Spain) and 1.75 ml of MilliQ[®] water, as the aqueous phase. On the other hand, 1.25, 2.5 or 5 mg of the cationic lipid DOTMA (Avanti Polar Lipids, Inc., Alabama, USA) were accurately weighted to obtain 1/0.5, 1/1 and 1/2 ND/DOTMA mass ratios, respectively. The DOTMA was diluted in 1 ml of dichloromethane (DCM) (Panreac, Barcelona) which constituted the organic phase. This phase

was added upon the aqueous phase and immediately sonicated for 30 seconds at 50 W (Branson Sonifier 250, Danbury). DCM was evaporated for 2 hours at room temperature under magnetic stirring obtaining formulations named as nanodiosomes NDT10, NDT11 and NDT12, for ND/DOTMA at 1/0.5, 1/1 and 1/2 mass ratios, respectively. The elaboration of niosomes, as control formulations with no ND, was carried out following the same abovementioned protocol using the same amounts of DOTMA in the organic phase. Figure 1 shows the components employed for their elaboration of both formulations, as well as a schematic representation of the distribution of these components in nanodiosomes (Figure 1A) and niosomes (Figure 1B).

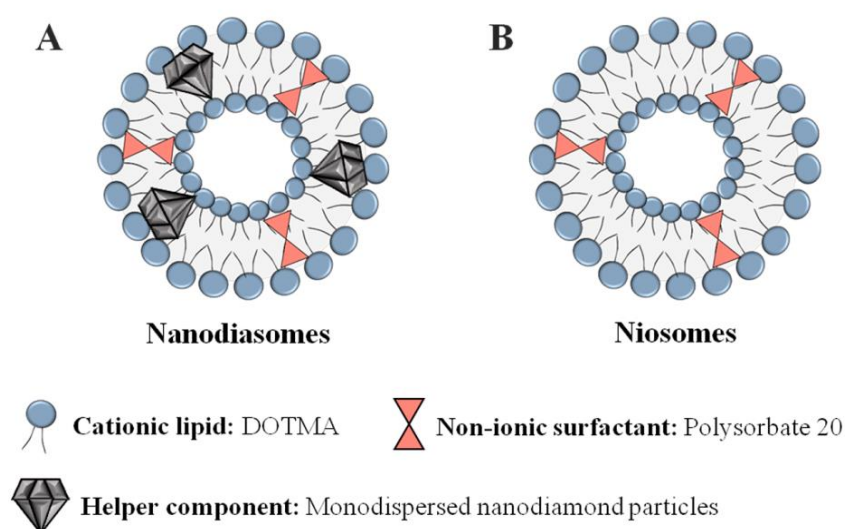


Figure 1: Overview of the components and their disposition in **(A)** nanodiosomes and **(B)** niosomes.

Preparation of complexes

Complexes, named as nanodiaplexes and nioplexes, were prepared by mixing nanodiosomes or niosomes with propagated pEGFP plasmid following previously reported methodology²⁵, to obtain complexes at 2/1, 5/1, 10/1 and 15/1 cationic lipid/DNA mass ratios.

Physicochemical characterization of formulations and complexes

Mean particle size and dispersity index (δ) of nanodiosomes, niosomes and their corresponding nanodiaplexes and nioplexes, were determined by cumulative analysis as previously described.²¹

Morphological characterization

To assess the shape and morphology of the formulations, transmission electron microscopy (TEM) was employed as previously described.²⁷ To analyze the disposition of nanodiamonds in the nanodiosomes, further microscopy studies were performed by means of cryo-tomography. For that, 1 mg/ml sample was diluted to 0.5 mg/ml with BSA-gold nanoparticles (10 nm) required for accurate tomographic tilt series alignment. (<https://aurion.nl/products/aurion-gold-tracers/>). After vortex shaking, 3 μ l of the sample were applied to Cu/Rh R2/2 Quantifoil grid and vitrified using ThermoFisher Scientific Vitrobot Mark IV at 22 °C 95% humidity.

Vitrified samples were entered in a Talos Arctica (ThermoFisher Scientific, Spain) operated at liquid Nitrogen Temperature (200 Kv). Dose symmetric tilt scheme²⁸ was used to acquire tilted series to a final total dose of 130 e-Å² using Tomography software from ThermoFisher Scientific. (Step 3°, \pm 65° at 28.000 X with a pixelsize of 1.44 nm/pix). Tilt series alignment was done using IMOD²⁹ and reconstruction with SIRT using TOMO3D.³⁰ Reconstructed volumes were analyzed with ImageJ^{31,32} and 3D rendering was performed with USFC Chimera.³³

Gel retardation assay

The capacity of both complexes at different cationic lipid/DNA mass ratios to condense, protect and release the genetic material was assessed by a 0.8% (w/w) agarose (Sigma-Aldrich, Spain) gel electrophoresis assay. To analyze the DNA binding capacity of formulations, samples were directly loaded into the gel. To evaluate the DNA protection capacity of formulations, 4 μ l of DNase I enzyme (Thermo Fisher Scientific, Spain) were added and incubated for 30 min at 37 °C, then, 6 μ l of 10% sodium dodecyl sulfate (SDS) (Sigma-Aldrich, USA) were added and incubated for 10 min at room temperature (RT). To examine the DNA release from the complexes, a same quantity of SDS was added to the samples and incubated for 10 min at RT. After the addition of 4 μ l of loading buffer per sample, the agarose gel was immersed in a Tris-acetate-EDTA buffer and subjected to electrophoresis for 30 min at 120 V. Naked DNA was used as a control, being 200 ng the amount of DNA used per well in all cases. DNA bands were stained with GelRed reagent and observed under a ChemiDocTM MP Imaging System, for further analysis by Image LabTM Software (BioRad, USA).

Cell culture and *in vitro* transfection assays

Human embryonic kidney cells 293 (HEK-293; ATCC, CRL1573) were cultured and maintained as previously described.²⁷ To carry out transfection experiments, HEK-293 cells were seeded in 24 well plates at a density of 20×10^4 cells per well in medium without antibiotics and incubated overnight to achieve 70% of confluence. Nanodiaplexes and nioplexes at different cationic lipid/DNA mass ratios were prepared by their incubation with pEGFP in OptiMEM transfection medium (Gibco, San Diego, CA, USA) for 30 min at RT. After removing the growth medium, cells were exposed to these complexes for transfection during 4 hours in an incubator. Hereinafter, complexes were removed and fresh medium was added. Positive and negative controls of transfection were performed using Lipofectamine 2000™ (Invitrogen, Carlsbad, CA, USA) and non-treated cells exposed only to OptiMEM during 4 h, respectively. Each condition was performed in triplicate.

Transfection efficiency was reported, both qualitatively and quantitatively, 48 h after the addition of complexes by fluorescence microscopy (EclipseTE2000-S, Nikon) and flow cytometry technique (FACSCalibur, Becton Dickinson Bioscience, San Jose, USA), respectively. In the latter case, after a rapid wash step, HEK-293 cells were exposed to 300 μ l of 0.05% trypsin/EDTA for detachment. Later, growth medium was added to block trypsin effect. Thereafter, cells were centrifuged to obtain the cell pellet eliminating the supernatant. Next, the pellet was resuspended with PBS, and diluted in FACSFlow liquid. Such cells were placed in flow cytometer tubes to quantify EGFP signal in living cells. Cell viability was evaluated by staining cells with propidium iodide (Sigma-Aldrich, USA) before performing flow cytometry. The fluorescent emission of both dead and transfected cells were evaluated at 650 nm (FL3) and 525 nm (FL1), respectively. Mean fluorescence intensity (MFI) signal was analyzed from live positive cells in FL1 channel. The collection gate was established employing non-transfected cells. Flow cytometer settings and channel compensation was performed using cells transfected with Lipofectamine 2000™. Cell viability and transfection data were normalized considering the values of negative and positive control cells, respectively. The experiments were carried out in triplicate, collecting a minimum of 10,000 events for each sample. FlowJo software (Becton Dickinson) was used to analyze the data.

Cellular uptake

The uptake of nanodiaplexes and nioplexes was analyzed by incubating cells with FITC labeled pEGFP (FITC-pEGFP) for 4 hours. FITC positive signal was analyzed both, qualitatively and quantitatively. For qualitative assays, cells were seeded on coverslips to fix them with 4% formaldehyde (Panreac, Spain) after the incubation. Once fixed, cells were washed with PBS and exposed to phalloidin (5 μ L) in PBS with 1% bovine serum albumin for 40 min to stain their cytoskeleton. After a PBS washing step, cells were mounted with Fluoroshield™ with DAPI (Sigma-Aldrich, USA). Afterwards, mounted cells were analyzed with confocal laser scanning microscopy (Zeiss Axioobserver). Images were examined with ImageJ software. Quantitative analysis was carried out by flow cytometry as described before. Cellular uptake data were normalized to positive control cells treated with Lipofectamine 2000™, and expressed as the percentage of FITC-pEGFP positive cells.

Intracellular trafficking

Cellular internalization of nanodiaplexes and nioplexes was analyzed by incubating cells with FITC labeled pEGFP (FITC-pEGFP) for 3 hours over coverslips as described before. Afterwards, specific endocytic pathway markers were co-incubated for 1 h: transferrin-AlexaFluor594 (50 μ g/ml) to stain clathrin mediated endocytosis (CME), cholera toxin B-AlexaFluor594 (10 μ g/ml) to stain caveolae mediated endocytosis (CvME), dextran-AlexaFluor594 (1 μ g/ μ l) for macropinocytosis, or lysotracker Red-DND-99 (20 μ M) for the lysosomal late endosomal compartment. After fixation of cells and mounting, slides were observed under microscopy in order to capture representative images for their analysis by the ImageJ software. Green and red signal co-localization, corresponding to the endocytic pathway and to FITC-pEGFP, respectively, was measured by cross-correlation analysis.^{34,35}

Additionally, specific endocytosis inhibitors were used to inhibit cellular uptake prior to the transfection assay. For this, in a 24-well plate, HEK-293 cells were exposed for 30 min with 200 μ M genistein, and for 60 min with 5 μ g/ml chlorpromazine hydrochloride and with 50 nM wortmannin (Thermo Fisher Scientific, Madrid, Spain), as inhibitors for CvME, CME and macropinocytosis pathways, respectively. Then, the medium containing the inhibitors was removed, a rapid wash was performed and transfection was carried out with both nioplexes and

nanodiaplexes vectoring pEGFP plasmid, as described before. Cells were processed and EGFP positive cells were quantitatively assessed by flow cytometry as detailed before. Data were normalized in relation to the value of EGFP positive cells after transfection with nanodiaplexes and nioplexes and with no inhibitors of the endocytic pathways. The experiments were carried out in triplicate collecting and analyzing more than 5,000 events for each sample.

Endosomal escape of the complexes from the late endosome

Anionic micelles based on PS (Sigma-Aldrich, Spain) were prepared to mimic the late endosomal compartment. Chloroform at 1.6 mM was used to dissolve PS and exposed to-magnetic agitation to evaporate the solvent. The dried sample was reconstituted in PBS and sonicated to obtain a dispersed solution containing PS micelles. Nanodiaplexes and nioplexes were incubated, or not, with the PS micelles for 1 hour at 1:50 pEGFP:PS mass ratio. Samples, containing 200 ng of DNA, were loaded in a 0.8% agarose gel and subjected to electrophoresis to observe the amount of genetic material released from the complexes. Electrophoresis process, bands staining and analysis were carried out as previously mentioned in the gel retardation assay section.

Animals, procedures and exposure to nanodiaplexes

Procedures carried out with animals for scientific research purposes were performed following the RD 53/2013 Spanish and 2010/63/EU European Union regulations, and according to the Miguel Hernandez University Standing Committee for Animal Use in the Laboratory. Primary CNS cells were extracted from the brain cortex and retinal tissue of E17-E18 rat embryos (Sprague Dawley) and processed as described elsewhere.^{36, 37} Lipofectamine™ 2000 (Invitrogen, California, USA) at 2/1 ratio was employed as a positive control. Each condition was performed in triplicate.

Evaluation of gene transfection in central nervous system primary cells

EGFP expression from primary neuronal and retinal transfected cells was examined 72 h after their exposure to nanodiaplexes to qualitatively assess the transfection efficiency by immunocytochemistry.³⁶ Briefly, cover slips were incubated overnight with chicken anti-EGFP (Invitrogen, 1:300). Cells were incubated for 1 hour with secondary antibody Alexa Fluor555 goat anti-chicken IgG (Invitrogen, 1:100) which was pseudocolored in green to visualize EGFP

expression. Nuclei were stained with Hoechst 33342 (Sigma-Aldrich, Spain). Confocal images were obtained using laser-confocal microscope (Leica TCS SPE Microsystems GmbH, Germany).

Statistical analysis

Normality and homogeneity of variances was confirmed by the Shapiro-Wilks and the Levene tests, respectively. Then, a 1-way ANOVA followed by Student–Newman–Keuls test was performed to analyze the differences between more than two groups. In non-parametric conditions, Kruskal–Wallis test followed by a Mann–Whitney *U* test was employed. Differences between two groups for unpaired data were analyzed using a Student’s *t* test or a Mann–Whitney *U* test, as appropriate. Data were expressed as mean \pm standard deviation (SD). A *P* value < 0.05 was considered statistically significant. SPSS 15.0 statistical software was used to analyze data.

RESULTS

Biophysical screening of nanodiasome formulations

Three nanodiasome formulations with different DOTMA composition, named as NDT10, NDT11 and NDT12, were elaborated (Supporting Information) and evaluated in terms of physicochemical properties (Figure S1, Supporting Information), as well as transfection ability and cytotoxicity (Figure S2, Supporting Information). This screening of formulations led to the conclusion that the nanodiasome with better biophysical performance for gene delivery purposes was the NDT12, which corresponds to the 1/2 ND/DOTMA mass ratio formulation. In consequence, this NDT12 nanodiasome formulation and its respective niosome control, devoid of NDs, were employed for further studies.

Physicochemical characterization of formulations and complexes

The particle size of formulations and their corresponding complexes was below 200 nm in all cases (Figure 2A, bars). In particular, nanodiasome and nanodiaplexes presented nearly a 30% higher particle size than niosomes and nioplexes. Upon the addition of pEGFP to formulations, the mean particle size values slightly increased around 40% at 5/1 ratio and gradually decreased when increasing the lipid/DNA ratio in both complexes. Zeta potential values for nanodiasomes were above +30 mV, precisely 35.2 ± 0.3 , while for niosomes were below this number, with a value of

20.2 ± 2.5 (Figure 2A, dots). After plasmid condensation, zeta potential of nanodiamonds and nioplexes at 5/1 lipid/DNA ratio decreased moderately, and increased slightly when augmenting the lipid/DNA ratios, especially in the case of nanodiamonds (Figure 2A, dots). Regarding dispersity (\mathcal{D}) (Figure 2B), values for nanodiamonds and nanodiamonds were in general below 0.4, while for niosomes and nioplexes were above 0.4. DLS size-distribution profiles of niosomes, nanodiamonds and their complexes can be observed in figure 2C, D.

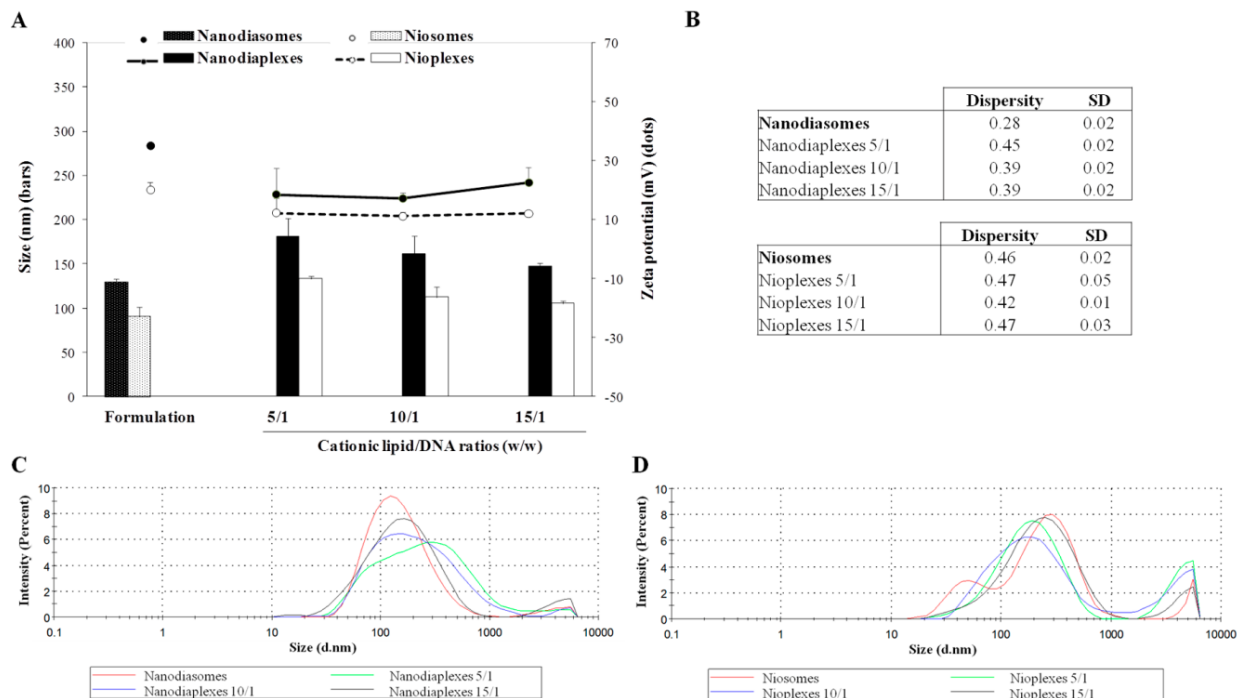


Figure 2: Characterization of formulations and complexes prepared with nanodiamonds (nanodiamonds/ nanodiamonds) and without nanodiamonds (niosome/nioplexes). **A.** Size (bars) and zeta potential (dots). **B.** Dispersity values of formulations and complexes. Each value represents the mean ± standard deviation of three measurements. **C.** Average size distribution intensities of nanodiamonds (red line) and nanodiamonds at different cationic lipid/DNA mass ratios (green, blue and black line for 5/1, 10/1 and 15/1 ratios, respectively). **D.** Average size distribution intensities of niosomes (red line) and nioplexes at different lipid/DNA ratios (green, blue and black line for 5/1, 10/1 and 15/1 ratios, respectively).

Morphological characterization

Nanodiasomes observed under TEM (Figure 3A) presented a clear spherical morphology. To go in depth into the disposition of ND particles in the niosome structure to form nanodiasomes, cryo-tomography studies were performed. As observed in figure 3B, NDs were integrated in the lipid layer of niosomes (Figure 3B, C), rather than on their surface or in their inner aqueous phase (Figure 3B, asterisks). Cryo-tomography reconstruction and the volumetric representation of the tomograms can be observed in the Supporting Information document (Video 1 and Video 2 Supporting Information, respectively).

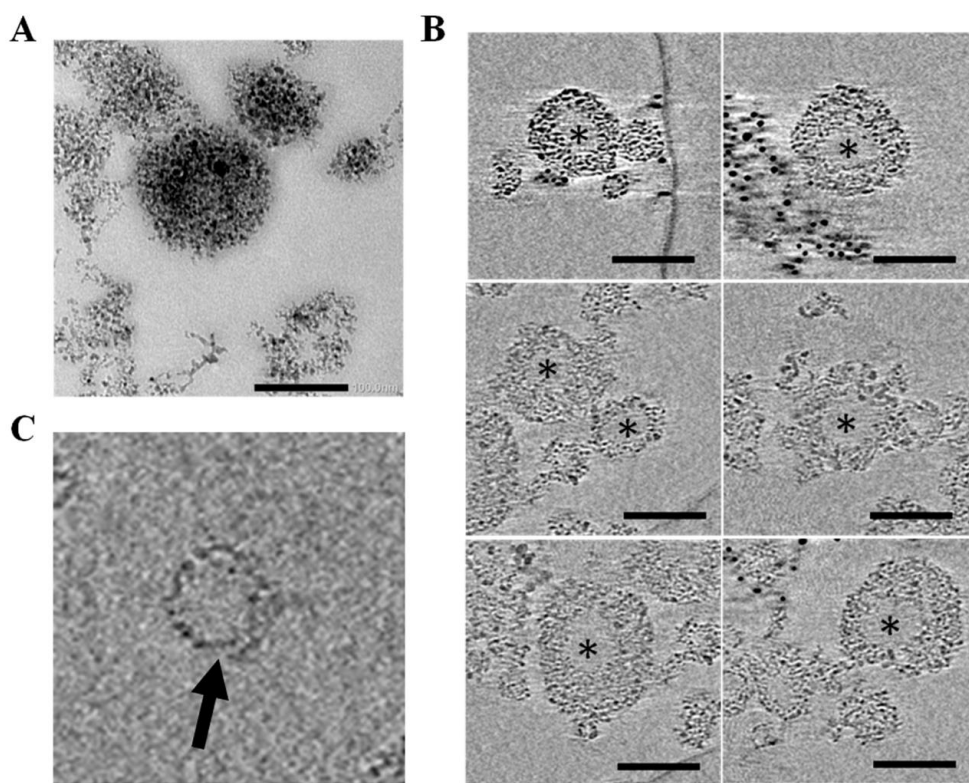


Figure 3. Microscopy images of nanodiasomes. **A.** TEM image of nanodiasomes. Scale bar: 100 nm. **B.** Cryo-TEM images of nanodiasomes; asterisks indicate the aqueous phase. Scale bar: 100 nm. **C.** Lipid layer of nanodiasomes (black arrow) with nanodiamonds integrated in the lipid structure.

To determine the capacity of nanodiasomes to condense, protect and release the DNA material in comparison with niosomes devoid of ND, a gel retardation assay was performed (Figure

4). Nioplexes (Figure 4B) showed a greater ability than nanodiaplexes (Figure 4A) to bind the DNA, at 10/1 and 15/ ratios, since no SC bands were visualized on lanes 7 and 10 respectively. At lower 5/1 ratio neither nioplexes nor nanodiaplexes were able to condense all DNA on their surfaces. As expected, no condensation was observed in the control naked DNA (lane 1), which in fact migrated completely in the gel. In this assay, SDS was added to the complexes in order to mimic a gene delivery microenvironment and promote the release of all the cargo to the media. It was observed that the DNA was released after the addition of SDS to nanodiaplexes and nioplexes at 5/1, 10/1 and 15/1 ratios (lanes 5, 8 and 11, respectively), additionally, it was also protected from DNase I enzymatic digestion at all ratios (lanes 6, 9 and 12) for both, nanodiaplexes (Figure 4A) and nioplexes (Figure 4B). The absence of band on lane 3 demonstrated that naked DNA suffered from DNase I enzymatic digestion.

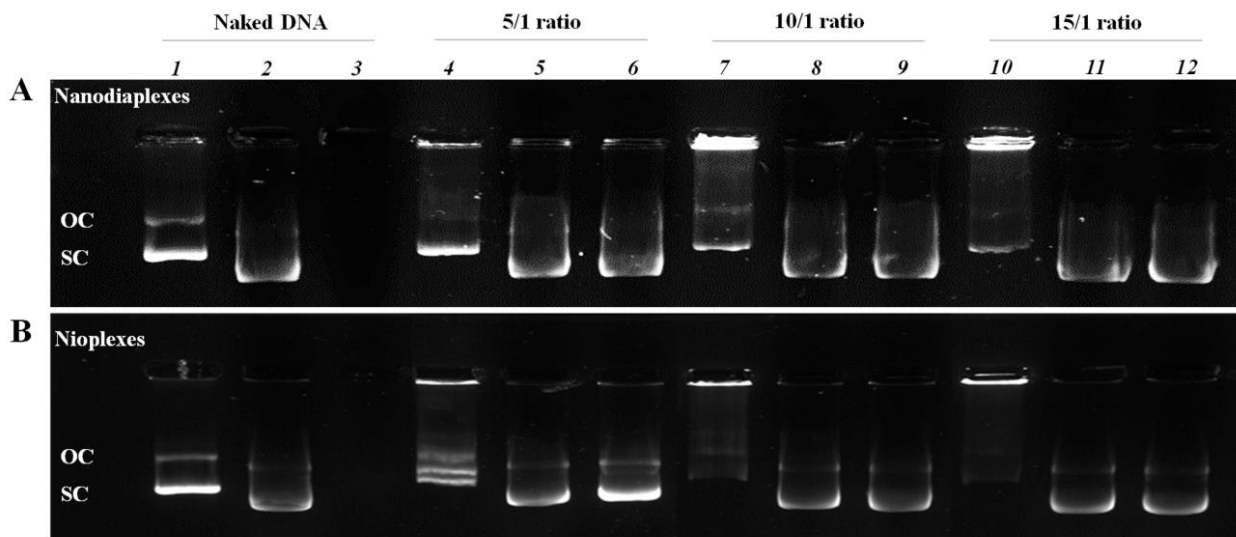


Figure 4: Agarose gel electrophoresis assay. **A.** Nanodiaplexes. **B.** Nioplexes. Lanes 1–3 correspond to free DNA; lanes 4–6, 5/1 ratio; lanes 7–9, 10/1 ratio; lanes 10–12, 15/1 ratio. Nanodiaplexes and nioplexes were treated with SDS (lanes 2, 5, 8 and 11) and DNase I + SDS (lanes 3, 6, 9 and 12). OC: open circular form, SC: supercoiled form.

Cytotoxicity and transfection efficiency *in vitro*

Transfection with nanodiaplexes showed high biocompatibility presenting cell viability values around 90% at all lipid/DNA ratios, while this parameter declined significantly ($p < 0.05$) below 80% when transfecting with nioplexes (Figure 5A, dots). Nanodiaplexes at 5/1 lipid/DNA

ratio was the condition with the highest percentage of EGFP-positive live cells, with a value of $89.1 \pm 7.7\%$ ($p < 0.001$). This transfection efficiency supposes a 75% of increment ($p < 0.001$) in comparison with its counterpart nioplexes devoid of ND ($22.7 \pm 2.4\%$). This greater pEGFP expression of nanodialogues over nioplexes was also observed at 10/1 ($62.7 \pm 2.7\%$ vs $23.9 \pm 2.5\%$; $p < 0.001$) and 15/1 ($43.2 \pm 1.1\%$ vs $16.8 \pm 4.7\%$; $p < 0.001$) ratios (Figure 5A, bars). Lipofectamine™ was employed as a positive control for transfection, which presented a 43% of EGFP expression in live cells (data not shown). All data was normalized in relation to this percentage value.

The superior ability of nanodialogues over nioplexes for gene delivery purposes was further corroborated by the mean fluorescence intensity assay of EGFP signal (Figure 5B), with significant differences at all lipid/DNA ratios ($p < 0.001$). Representative fluorescence microscopy images of EGFP signal in transfected HEK-293 cell line at 5/1 ratio can be observed in figure 5C.

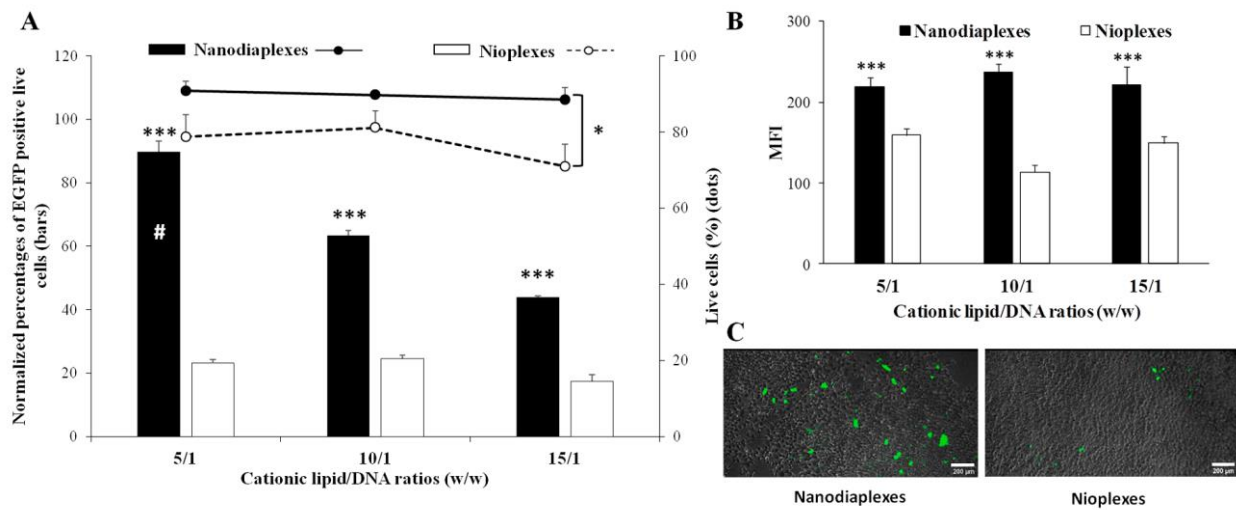


Figure 5: Transfection assay in HEK-293 cell line 48 hours post-transfection with nanodialogues and nioplexes. **A.** Normalized percentages of EGFP positive live cells (bars) and cell viability (dots). **B.** Mean fluorescence intensity values. **C.** Images showing EGFP signal and cell integrity in HEK-293 cells transfected with nanodialogues and nioplexes at 5/1 lipid/DNA ratio. Scale bar: 200 μm . Each value represents the mean \pm standard deviation of three measurements. *** $p < 0.001$ and * $p < 0.05$ for nanodialogues vs nioplexes at the same lipid/DNA ratio; # $p < 0.001$ compared with all conditions.

Cellular uptake

Cell internalization of nanodialogues at 5/1 lipid/DNA ratio in HEK-293 cell line 4 hours after their exposure to these complexes showed significant higher values of FITC-pEGFP positive signal than their counterpart nioplexes ($95.1 \pm 3.9\%$ vs $72.2 \pm 2.4\%$; $p < 0.05$) (Figure 6A). The positive control of transfection Lipofectamine™ 2000 showed 60% of FITC-pEGFP positive cells 4 hours after the exposure of cells to lipoplexes (data not shown) and all data was normalized in relation to this percentage value. Representative confocal microscopy images exhibiting cellular uptake of nanodialogues and nioplexes at 5/1 ratio are shown in figure 6B.

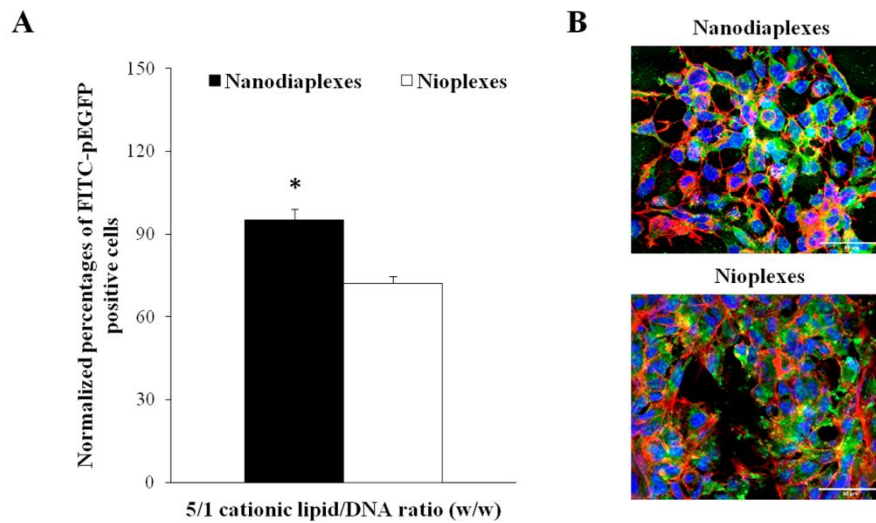


Figure 6: Cellular uptake of complexes at 5/1 lipid/DNA ratio, analyzed 4 hours after transfection in HEK-293 cell line. **A.** Normalized percentage of FITC-pEGFP positive cells. Each value represents the mean \pm standard deviation of three measurements; * $p < 0.05$ for nanodialogues vs nioplexes. **B.** Confocal microscopy images showing the cellular uptake of nanodialogues and nioplexes. Cell nuclei were colored in blue (DAPI), F-actin in red (Phalloidin), and nanodialogues and nioplexes in green (FITC). Scale bar: 50 μm .

Intracellular trafficking and endosomal escape

Representative images showing the co-localization of the complexes (green signal) with the intracellular pathway as early endosomes (red signal), either CME, macropinocytosis or

CvME, can be observed in figure 7A. Co-localization of red and green fluorescence signals led to yellow/orange dots.

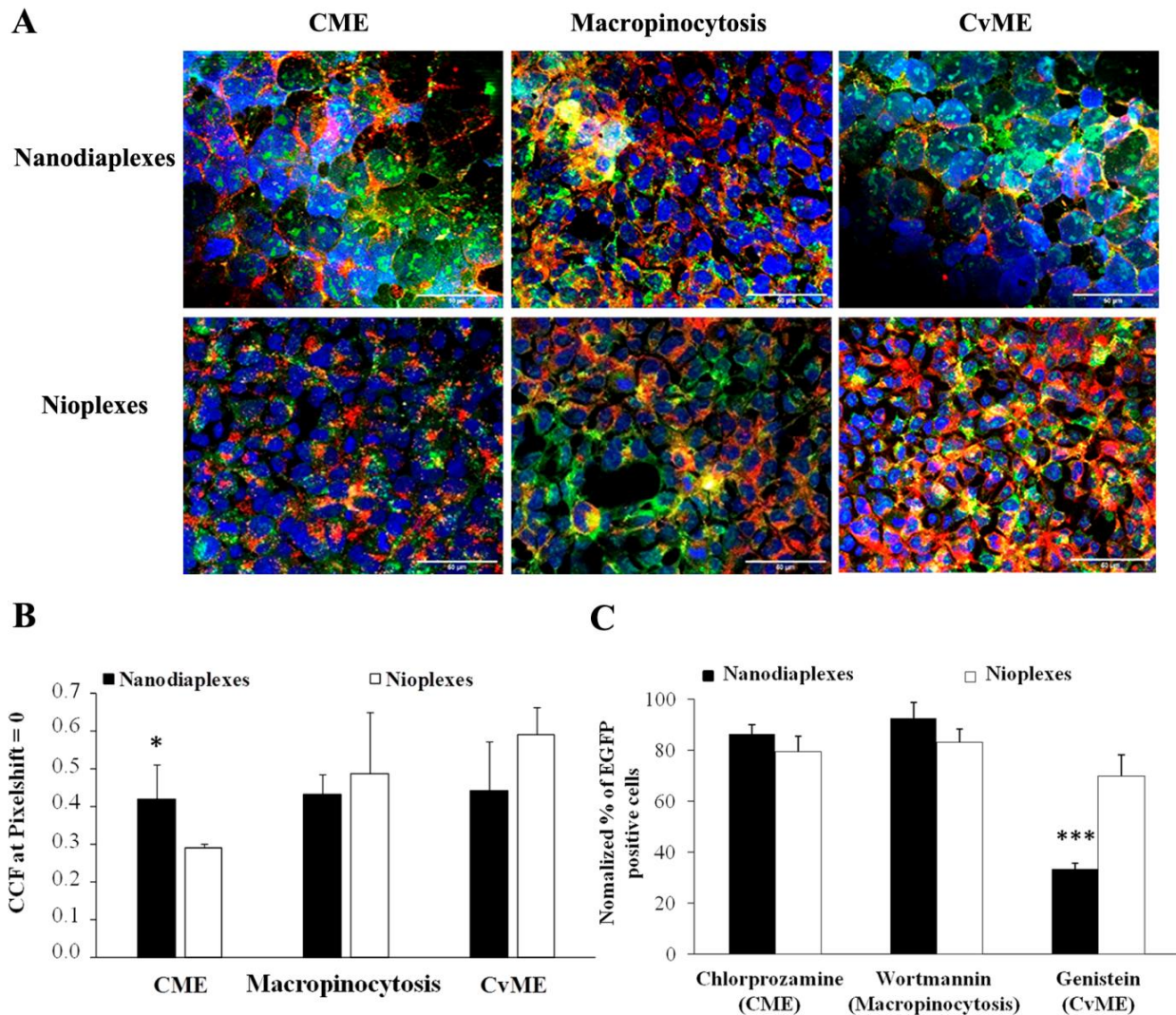


Figure 7: Intracellular disposition assay of nanodiaplexes and nioplexes in HEK-293 cells. **A.** Qualitative analysis of co-localization by confocal microscopy. Scale bar: 50 μm . **B.** Quantitative determination of co-localization by cross-correlation analysis. Data are represented as mean \pm standard deviation of three measurements; * $p < 0.05$ for nanodiaplexes vs nioplexes. **C.** Transfection performance after the addition of specific endocytic inhibitors. The values were normalized to the transfection without inhibitor. *** $p < 0.001$.

The quantification of the co-localization signal for each formulation, indicated that there was not an endocytic pathway that rose above the others (Figure 7B). However, it pointed out that the

highest difference between nanodiaplexes and nioplexes was observed in CME pathway ($p < 0.05$), where nanodiaplexes co-localized more than nioplexes in this pathway. Interestingly, regarding the involvement of each pathway in transfection efficiency, the selective inhibition of CvME (genistein) significantly decreased transfection efficiency mediated by nanodiaplexes ($p < 0.001$), while in the case of nioplexes, transfection efficiency was slightly affected, overall when clathrin and micropinocytosis were inhibited with chlorpromazine hydrochloride and wortmannin inhibitors, respectively (Figure 7C).

Following the trafficking of complexes along the cell to the late endosomes, further assays regarding to the co-localization of the complexes (green signal) with lysosomes as the late endosomal compartment (red signal) were performed (Figure 8A). Data showed that nanodiaplexes co-localized more in lysosomes compared to nioplexes ($p < 0.05$) (Figure 8B). As observed in figure 8C, in the case of nioplexes and in absence of PS vesicles (lane 5), practically all DNA was retained, since percentage of SC bands (the most bioactive form)^{38, 39}, only represented 6.81% of all DNA signal. However, in the case of nanodiaplexes (lane 4), the percentage of SC signal increased to 26.38% of all DNA signal, which means that nioplexes showed a greater ability to bind DNA than nanodiaplexes. These results are in agreement with those obtained in figure 4. However, when both complexes were co-incubated with PS vesicles to evaluate endosomal escape properties, we observed a stronger SC signal in the case of nanodiaplexes (lane 2, 58.63% of all DNA signal) compared to nioplexes (lane 3, 29.44%). Consequently, the presence of NDs into the niosome formulation increased 1.4-fold times the endosomal escape properties, as can be deduced by subtracting the % of SC DNA signals of control lane 4 (26.38%) and lane 5 (6.81%), that correspond to nanodiaplexes and nioplexes respectively, to the % of SC DNA signal on lane 2 (58.63%) and lane 3 (29.44%).

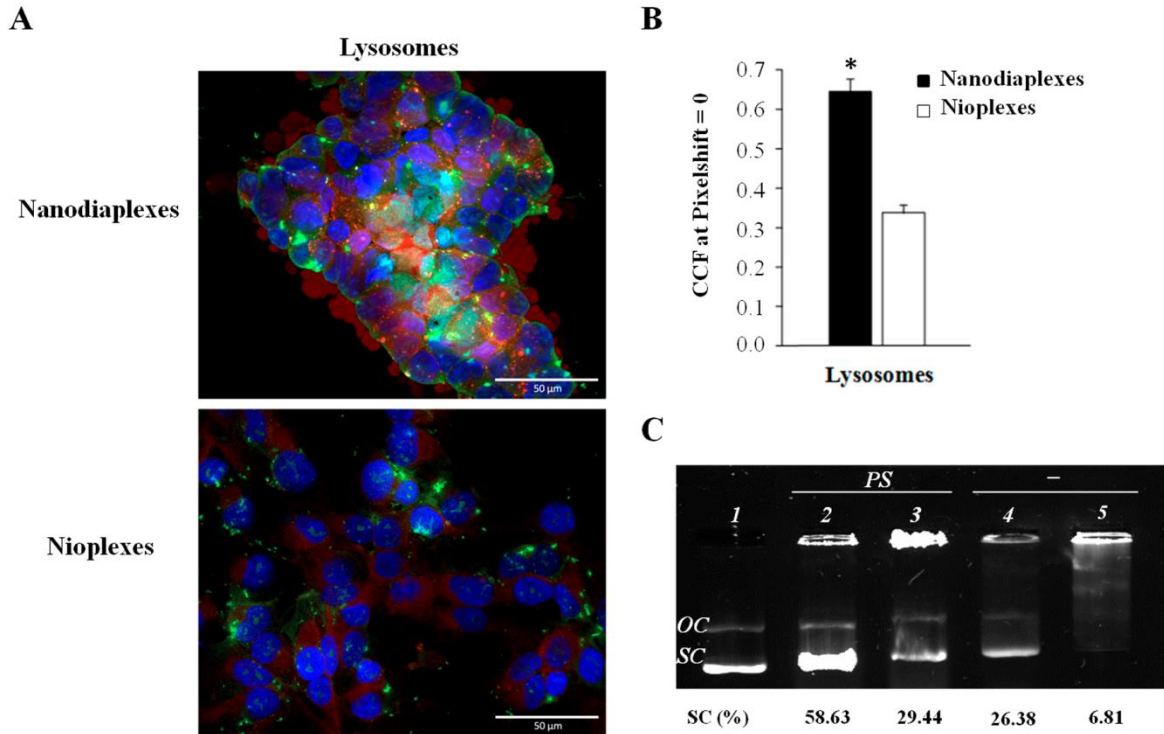


Figure 8: Biological performance of nanodialogues and nioplexes in lysosomes of HEK-293 cells. **A.** Qualitative analysis of co-localization by confocal microscopy. **B.** Quantitative determination of co-localization by cross-correlation analysis. Data are represented as mean \pm standard deviation of three measurements; $*p < 0.05$ for nanodialogues vs nioplexes. **C.** DNA release profiles evaluated by gel electrophoresis. Lane 1, naked DNA; lane 2, nanodialogues incubated with PS; lane 3, nioplexes incubated with PS; lane 4, nanodialogues; lane 5, nioplexes. PS refers to phosphatidylserine micelles; OC: open circular form, SC: supercoiled form.

Gene delivery capacity of nanodialogues to primary central nervous system cells

The assessment of the transfection process in primary CNS cells from cerebral (Figure 9A) and retinal (Figure 9C) cultures exposed to nanodialogues at 5/1 ratio, showed GFP signal in both cases, compared with Lipofectamine™ 2000 positive control in cerebral and retinal primary cells, respectively (Figure 9B and 9D). These results corroborate the gene delivery capacity of this vector into CNS cells.

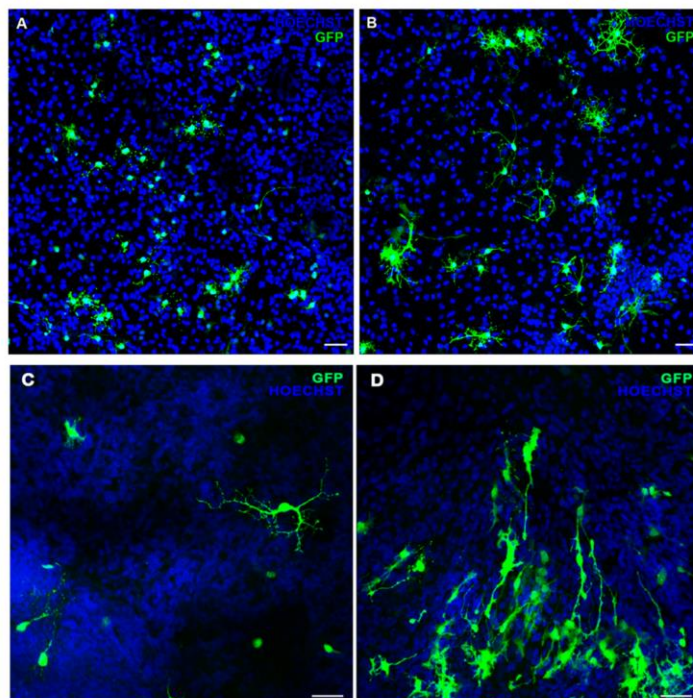


Figure 9: GFP expression in embryonic rat central nervous system primary cells. Neuronal and retinal primary cells transfected with nanodiamonds (A, C) at 5/1 lipid/DNA ratio and the positive control Lipofectamine™ 2000 in primary neuronal (B) and retinal cells (D). Cell nuclei were stained with Hoechst 33342 (blue). Scale bar: 50 μm.

DISCUSSION

The existence of carbon based nanomaterials with promising features for gene therapy purposes emerges as an attractive strategy to improve non-viral transfection efficiency, moving ever closer to overcome the present translational barrier to biomedical applications. In this field of carbon nano-structures, such as nanotubes, graphene and graphene oxide, NDs have gained momentum due to their particular geometrical characteristics, particular surface chemistry with high Young's modulus and large scale production capability, as well as non-toxic and biocompatible properties.⁴⁰⁻⁴² NDs are spherical shape structures with an average diameter of ~5 nm accompanied by a low dispersity index and relatively large surface area. One of the main issues of ND is the tendency to self-agglomeration caused by their nanometer size and Van der Waals forces, which also confers them a poor stability in a variety of media. In fact, a mean size of 89 nm was found for NDs alone in water suspension (Figure S1). Therefore, NDs must be

functionalized or bound to other components, normally polymers⁴³ for gene delivery purposes, although some drug delivery works have also bound NDs to liposome phospholipids.^{44, 45} In this regard, NDs have been used in gene therapy by their single binding to specific polymers which confer them the ability to bind and deliver the genetic material.¹¹⁻¹⁵

Other state-of-the-art non-viral approach are niosomes which are cationic lipid based vesicles with non-ionic surfactants widely used in gene therapy and that are gaining interest over liposomes due to their lower cost, higher biocompatibility and stability.^{20, 46} Taking into account the natural ability of niosomes for high genetic material containment and high biocompatibility of both, NDs and niosomes, here we propose a promising novel gene therapy strategy combining their attractive features in order to burst a powerful nanoplatform with high transfection efficiency and biocompatibility. In particular, we elaborated the named as nanodiasomes integrating NDs into cationic niosomes composed of DOTMA as cationic lipid and polysorbate 20 as non-ionic surfactant.

In a first step, we optimized, in terms of physicochemical and biological properties, a nanodiasome formulation employing different ND/DOTMA mass ratios (Supporting Information, figure S1 and figure S2). Interestingly, the more amount of DOTMA in the formulation, the smaller was the nanodiasome size and, consequently, it caused a slight increase of zeta potential.⁴⁷ This decrease of nanoparticle size could be explained by the electrostatic interactions between the positive charge of the cationic lipid and the negative charge of NDs where the physic and chemical properties of NDs would promote an increasing degree of compaction of the nanoparticle. Thus, the more cationic lipid, the higher electrostatic interactions with NDs, reducing the final size of the nanoparticle. In this sense, some studies have observed that different doses of NDs, might adsorb to the surface of the lipid membrane of liposomes without affecting the packing of the bilayer.⁴⁵ Hence, it could be suggested that the cationic lipid amount in the formulation is the responsible of the physicochemical changes in the nanodiasome. Even though the increase of cationic lipids can promote cell death due to the positive charge that it confers to the vector, the amount of DOTMA -from 1.1 to 3.7 mM- used in these formulations presented good biocompatibility in all cases. In general terms, cell viability values were around 95% at 2/1 and 5/1 lipid/DNA ratios, while slight progressive cytotoxicity was observed at 10/1 and 15/1 ratios

diminishing cell viability to 85% (Figure S1). We found an optimum balance between biocompatibility and transfection efficiency employing NDT12 at 5/1 lipid/DNA ratios, so further studies were carried out with this nanodiasome formulation.

To explore the influence of NDs integrated as a helper component into niosomes, additional physicochemical, transfection, biocompatibility and intracellular trafficking analysis were carried out with NDT12 nanodiasome compared to the same formulation devoid of NDs. Concerning the physicochemical parameters (Figure 2), nanodiasomes and nanodiaplexes presented nearly a 30% higher particle size than niosomes and nioplexes due to the NDs content, maintaining in all cases mean diameter sizes below 200 nm. As expected, sizes increased when complexing the formulations with the plasmid genetic material, while zeta potential decreased due to the neutralization of positive and negative charges.⁴⁸ Some mean dispersity values showed to be slightly high, as is the case of niosomes/nioplexes and nanodiaplexes at 5/1 ratio (Figure 2B), which could be due to the presence of few aggregates in the sample, denoted by the presence of a high peak in the particle size distribution intensity at micrometer scale (Figure 2C, D). Overall, mean dispersity values were lower in nanodiasomes and nanodiaplexes, pointing out to a better homogeneity of this formulation compared to niosomes. In fact, TEM captures revealed a clear spherical morphology of nanodiasomes with no aggregations (Figure 3A), where ND particles are integrated in the lipid layer of this non-viral vector (Figure 3B, C). Therefore, although both formulations showed suitable characteristics for gene therapy purposes they presented some physicochemical variations among them.

After physicochemical characterization, *in vitro* transfection studies were carried out in HEK-293 cell line, which is considered a good model for transfection. Transfection efficiency of nanodiaplexes was much greater to that of nioplexes at all lipid/DNA ratios, overall at 5/1 ratio where 75% increment was observed when compared to its counterpart niosomes devoid of NDs (Figure 5). Of note, this higher transfection efficiency was also accompanied by higher cell viability values around 90%. In this regard, the 1.25 mg/ml concentration of NDs employed in the present study, is higher than the described in other works -ranging from 0.01 to 1 mg/ml- for maintaining a suitable biocompatibility.⁴⁹ Hence, these observations highlight the benefits of combining a high biocompatible material presenting high adsorption properties, such as NDs, with other high biocompatible, stable and high loading capacity vector such as cationic niosomes.

Cellular uptake is one of the most decisive criteria to be considered when evaluating the delivery of the cargo into cells. The 25% increase in the cellular uptake of nanodiaplexes vs nioplexes could be considered as one of the potential factors that enhanced their transfection efficiency (Figure 6), in accordance with previous reports where NDs increased the cellular uptake of zwitterionic liposomes for drug delivery purposes.⁴⁵ In this regard, relevant physicochemical parameters of non-viral vectors, such as size, zeta potential, shape and rigidity seem to affect the internalization process and posterior intracellular pathway followed by the nanoparticle and the genetic material. In fact, rigid structures along with small size and positive zeta potential values may be the most favorable features to enhance cellular uptake.⁵⁰ In this sense, and taking into account that nanodiaplexes are bigger and slightly more positive than nioplexes, the physical and chemical properties of NDs could be contributing to the rigidity of the vector and therefore promoting the cell internalization of nanodiaplexes.

Additionally, the internalization pathway followed by the vector and its DNA can be critical to its intracellular fate. Most of the nanoparticles, including the lipid based vectors, are internalized by pinocytosis, principally through receptor-mediated endocytosis.⁵⁰ In this work we did not observe a predominant endocytic pathway when using nanodiaplexes or nioplexes but our data suggested that the first ones trafficked more by CME than nioplexes (Figure 7 A,B). In the case of specific endocytic pathway inhibition studies, our data revealed that when nanodiaplexes were administered to HEK-293 cells, endocytosis mediated by caveolae was the most efficient endocytic pathway to transfect cells, since when this pathway was inhibited by genistein, percentage of cells expressing EGFP plasmid decreased to around 30% value (Figure 7C). Consequently, the transfection performance of NDs integrated into niosome formulation as non-viral vectors could be promoted by the addition of chemical components that induce CvME pathway.⁵¹ However, the inhibition of CME, and macropinocytosis only decreased transfection efficiency values to around 90% values. In the case of transfection efficiency mediated by nioplexes, the percentage of transfected cells decreased only to around 80-70% values with the use of the three cellular uptake inhibitors, which suggest that probably other endocytic pathways could be playing a more relevant role in the complex transfection process.^{52, 53}

Further trafficking studies extending to the late endosomal compartment were carried out. It was observed that nanodiaplexes co-localized more with lysosomes than nioplexes (Figure 8 A,B), pointing out that NDs might promote CME pathway, the internalized vesicle would lose the clathrin coat obtaining an early endosome that turns into a late endosome which becomes a lysosome.⁵⁴ These results go in accordance with a previous but more basic intracellular trafficking study of fluorescent NDs which reported their internalization in early endosomes followed by lysosomal localization. Interestingly, authors explained the lysosomal compartment as a previous step for the exocytosis of these fluorescent NDs via lysosomal degradation pathway.⁵⁵ Of note, the artificial anionic micelles of PS developed in the present research work to mimic this late endosomal compartment (Figure 8C) revealed that nanodiasomes had better endosomal escape properties than niosomes. After subtracting the % of control SC DNA signal observed in lane 4 (26.38%, nanodiaplexes) and 5 (6.81%, nioplexes) from the % of SC DNA signal observed in lanes 2 and 3 (58.63%, nanodiaplexes and 29.44%, nioplexes, respectively, co-incubated with PS vesicles), the obtained value was 32.26% for nanodiaplexes and 22.63% for nioplexes. Such results suggest that the presence of NDs into the formulation increase 1.43-fold (around 30%) the endosomal escape property in HEK-293 cells than the formulation without NDs. Among the mechanisms by which nanodiaplexes could escape the endosomes, the most likely one consists of the direct fusion of the nanoparticles with the endosome membrane, as shown by their co-localization with lysosomes, along with the creation of pores in the endosome surface caused by the induction of stress and internal tension in the membrane, as evidenced by the great DNA released from this kind of compartments.⁵⁶ Taken all together, our data suggest that the enhanced transfection efficiency of nanodiaplexes over nioplexes might be attributed mainly to the higher cellular uptake, probably due to the rigidity that NDs confer to nanodiaplexes, and to the lysosomal escape properties promoted by NDs.

Additional gene delivery studies in primary CNS cells from cerebral and retinal source were carried out with nanodiaplexes at 5/1 lipid/DNA ratio in order to move on a more realistic and translational microenvironment of an *in vivo* model. Immunocytochemistry showed GFP signal in both primary cell cultures (Figure 9A and 9C), pointing out to the capacity of nanodiaplexes to successfully deliver genetic material to CNS cells. Since CNS diseases constitute an area where the development of new therapeutic strategies represents a burning need,⁵⁷ the

emerging role of NDs into niosomes for gene delivery applications represents a major finding. In addition, presumably NDs and not other carbon-based nanomaterials would possess excellent compatibility with biological systems, resulting in an encouraging candidate for biomedical applications.⁴⁹ In this sense, it has been described the non toxicity of NDs after their *in vivo* administration by intratracheal instillation, which is a decisive route when analyzing the potential toxic effect of nanocarriers on respiratory system.⁴² Although promising, these results represent a proof of concept and further studies in animal models would be required for corroborating the observed potential of nanodiasomes for gene delivery.

CONCLUSION

The main findings are the following ones: (1) NDs can be integrated into niosome formulation as helper component, maintaining suitable physicochemical characteristics for gene delivery; (2) niosomes with NDs represent a novel non-viral vector that binds, releases and protects the genetic material from degradation; (3) niosomes containing NDs present higher biocompatibility and transfection efficiency *in vitro* than those devoid of NDs, mainly explained by the higher cellular uptake promoted by NDs; (4) NDs integrated into niosomes are involved in lysosomal escape; (5) these nanodiasomes can deliver genetic material to primary central nervous system cells. Hence, NDs integrated into niosomes emerges as a powerful nanoplatform for gene therapy purposes, specially for CNS disorders, and may constitute a promising and safe non-viral strategy with potential biomedical applications.

ASSOCIATED CONTENT

Supporting information

Additional experimental details and results, including multimedia content. Biophysical screening of the nanodiasome formulations. Tomogram reconstruction and volumetric representation.

AUTHOR INFORMATION

Corresponding authors

José Luis Pedraz

NanoBioCel Research Group, Laboratory of Pharmacy and Pharmaceutical Technology. Faculty of Pharmacy, University of the Basque Country (UPV/EHU), Paseo de la Universidad 7, 01006 Vitoria-Gasteiz, Spain; Networking Research Centre of Bioengineering, Biomaterials and Nanomedicine (CIBER-BBN), Institute of Health Carlos III, 28029 Madrid, Spain; Bioaraba, NanoBioCel Research Group, 01009 Vitoria-Gasteiz, Spain; E-mail: joseluis.pedraz@ehu.eus

Gustavo Puras

NanoBioCel Research Group, Laboratory of Pharmacy and Pharmaceutical Technology. Faculty of Pharmacy, University of the Basque Country (UPV/EHU), Paseo de la Universidad 7, 01006 Vitoria-Gasteiz, Spain; Networking Research Centre of Bioengineering, Biomaterials and Nanomedicine (CIBER-BBN), Institute of Health Carlos III, 28029 Madrid, Spain; Bioaraba, NanoBioCel Research Group, 01009 Vitoria-Gasteiz, Spain; E-mail: gustavo.puras@ehu.eus

Authors**Nuseibah AL Qtaish**

NanoBioCel Research Group, Laboratory of Pharmacy and Pharmaceutical Technology. Faculty of Pharmacy, University of the Basque Country (UPV/EHU), Paseo de la Universidad 7, 01006 Vitoria-Gasteiz, Spain; Networking Research Centre of Bioengineering, Biomaterials and Nanomedicine (CIBER-BBN), Institute of Health Carlos III, 28029 Madrid, Spain.

Idoia Gallego

NanoBioCel Research Group, Laboratory of Pharmacy and Pharmaceutical Technology. Faculty of Pharmacy, University of the Basque Country (UPV/EHU), Paseo de la Universidad 7, 01006 Vitoria-Gasteiz, Spain; Networking Research Centre of Bioengineering, Biomaterials and Nanomedicine (CIBER-BBN), Institute of Health Carlos III, 28029 Madrid, Spain; Bioaraba, NanoBioCel Research Group, 01009 Vitoria-Gasteiz, Spain.

Alejandro J. Paredes

Research and Development Unit in Pharmaceutical Technology (UNITEFA), CONICET and Department of Pharmaceutical Sciences, Chemistry Sciences Faculty, National University of Córdoba. Haya de la Torre y Medina Allende, X5000XHUA, Córdoba, Argentina; School of Pharmacy, Queen's University Belfast, Medical Biology Centre, 97 Lisburn Road, Belfast, BT9 7BL, Northern Ireland, UK.

Ilia Villate-Beitia

NanoBioCel Research Group, Laboratory of Pharmacy and Pharmaceutical Technology. Faculty of Pharmacy, University of the Basque Country (UPV/EHU), Paseo de la Universidad 7, 01006 Vitoria-Gasteiz, Spain; Networking Research Centre of Bioengineering, Biomaterials and Nanomedicine (CIBER-BBN), Institute of Health Carlos III, 28029 Madrid, Spain; Bioaraba, NanoBioCel Research Group, 01009 Vitoria-Gasteiz, Spain.

Cristina Soto-Sánchez

Neuroprosthesis and Neuroengineering Research Group, Institute of Bioengineering, Miguel Hernández University, Avenida de la Universidad, 03202 Elche, Spain; Networking Research Centre of Bioengineering, Biomaterials and Nanomedicine (CIBER-BBN), Institute of Health Carlos III, 28029 Madrid, Spain.

Gema Martínez-Navarrete

Neuroprosthesis and Neuroengineering Research Group, Institute of Bioengineering, Miguel Hernández University, Avenida de la Universidad, 03202 Elche, Spain; Networking Research Centre of Bioengineering, Biomaterials and Nanomedicine (CIBER-BBN), Institute of Health Carlos III, 28029 Madrid, Spain.

Myriam Sainz-Ramos

NanoBioCel Research Group, Laboratory of Pharmacy and Pharmaceutical Technology. Faculty of Pharmacy, University of the Basque Country (UPV/EHU), Paseo de la Universidad 7, 01006 Vitoria-Gasteiz, Spain; Networking Research Centre of Bioengineering, Biomaterials and Nanomedicine (CIBER-BBN), Institute of Health Carlos III, 28029 Madrid, Spain; Bioaraba, NanoBioCel Research Group, 01009 Vitoria-Gasteiz, Spain.

Tania B. Lopez-Mendez

NanoBioCel Research Group, Laboratory of Pharmacy and Pharmaceutical Technology. Faculty of Pharmacy, University of the Basque Country (UPV/EHU), Paseo de la Universidad 7, 01006 Vitoria-Gasteiz, Spain; Networking Research Centre of Bioengineering, Biomaterials and Nanomedicine (CIBER-BBN), Institute of Health Carlos III, 28029 Madrid, Spain; Bioaraba, NanoBioCel Research Group, 01009 Vitoria-Gasteiz, Spain.

Eduardo Fernández

Neuroprosthesis and Neuroengineering Research Group, Institute of Bioengineering, Miguel Hernández University, Avenida de la Universidad, 03202 Elche, Spain; Networking Research

Centre of Bioengineering, Biomaterials and Nanomedicine (CIBER-BBN), Institute of Health Carlos III, 28029 Madrid, Spain.

Author Contributions

J.L.P., G.P.: Conceived the project. N.A.Q., I.G., A.J.P., C.S.S, G.M.N, M.S.R, T.B.L.M: Performed the experiments. N.A.Q., I.G., I.V.B.: Analyzed the results. N.A.Q., I.G.: Wrote the paper. N.A.Q., I.G, A.J.P., I.V.B., C.S.S, G.M.N.: Visualization. All authors: Reviewed-edited. J.L.P., G.P., E.F.: Supervision and project administration. J.L.P.: Funding acquisition. All authors have given approval to the final version of the manuscript. ‡These authors contributed equally

Funding Sources

This work was supported by the Basque Country Government (IT907-16). Additional funding was provided by the CIBER of Bioengineering, Biomaterials and Nanomedicine (CIBER-BBN), an initiative of the Carlos III Health Institute (ISCIII). I.V.B. and M.S.R. thank the University of the Basque Country (UPV/EHU) for the granted postdoctoral fellowship (ESPDOC19/47) and the granted pre-doctoral fellowship (PIF17/79), respectively.

Notes

The authors declare no competing financial interest.

ACKNOWLEDGMENTS

Authors wish to thank the intellectual and technical assistance from the Drug Formulation Unit (U10) of the ICTS “NANBIOSIS” from the CIBER in Bioengineering, Biomaterials and Nanomedicine (CIBER-BBN) at the University of Basque Country (UPV/EHU). Technical and human support provided by SGIKER (UPV/EHU) is also gratefully acknowledged. I.V.B. and M.S.R. thank the University of the Basque Country (UPV/EHU) for the granted postdoctoral fellowship (ESPDOC19/47) and the granted pre-doctoral fellowship (PIF17/79), respectively. We acknowledge Rocio Arranz, Noelia Zamareño and Francisco Javier Chichón access to the cryoEM CNB-CSIC facility in the context of the CRIOMECCORR project (ESFRI-2019-01-CSIC-16).

ABBREVIATIONS

CCF, cross-correlation function; CME, clathrin mediated endocytosis; CNS, central nervous system; CvME, caveolae mediated endocytosis; *D*, dispersity index; DCM, dichloromethane; EMEM, Minimal Essential Medium; DOTMA, 1,2-di-O-octadecenyl-3-trimethylammonium propane chloride salt; EGFP, enhanced green fluorescent protein; FBS, fetal bovine serum; FITC,

fluorescein isothiocyanate; HEK-293, human embryonic kidney cells; MFI, mean fluorescence intensity; ND, nanodiamond; NDT, ND/DOTMA mass ratio; PBS, *phosphate buffered saline*; PS, phosphatidylserine; RT, room temperature; SDS, sodium dodecyl sulfate; TEM, transmission electron microscopy.

REFERENCES

- (1) Dunbar, C. E.; High, K. A.; Joung, J. K.; Kohn, D. B.; Ozawa, K.; Sadelain, M. Gene Therapy Comes of Age. *Science* **2018**, *359*, 10.1126/science.aan4672, DOI: ean4672 [pii].
- (2) Pezzoli, D.; Chiesa, R.; De Nardo, L.; Candiani, G. We Still Have a Long Way to Go to Effectively Deliver Genes! *J. Appl. Biomater. Funct. Mater.* **2012**, *10*, 82-91, DOI: 10.5301/JABFM.2012.9707 [doi].
- (3) Escors, D.; Breckpot, K. Lentiviral Vectors in Gene Therapy: Their Current Status and Future Potential. *Arch. Immunol. Ther. Exp. (Warsz)* **2010**, *58*, 107-119, DOI: 10.1007/s00005-010-0063-4 [doi].
- (4) Sun, Y.; Lv, X.; Ding, P.; Wang, L.; Sun, Y.; Li, S.; Zhang, H.; Gao, Z. Exploring the Functions of Polymers in Adenovirus-Mediated Gene Delivery: Evading Immune Response and Redirecting Tropism. *Acta Biomater.* **2019**, *97*, 93-104, DOI: S1742-7061(19)30547-1 [pii].
- (5) Li, C.; Samulski, R. J. Engineering Adeno-Associated Virus Vectors for Gene Therapy. *Nat. Rev. Genet.* **2020**, *21*, 255-272, DOI: 10.1038/s41576-019-0205-4 [doi].
- (6) Mingozzi, F.; High, K. A. Therapeutic In Vivo Gene Transfer for Genetic Disease Using AAV: Progress and Challenges. *Nat. Rev. Genet.* **2011**, *12*, 341-355, DOI: 10.1038/nrg2988 [doi].
- (7) Yin, H.; Kanasty, R. L.; Eltoukhy, A. A.; Vegas, A. J.; Dorkin, J. R.; Anderson, D. G. Non-Viral Vectors for Gene-Based Therapy. *Nat. Rev. Genet.* **2014**, *15*, 541-555, DOI: 10.1038/nrg3763 [doi].
- (8) Charbel Issa, P.; MacLaren, R. E. Non-Viral Retinal Gene Therapy: a Review. *Clin. Exp. Ophthalmol.* **2012**, *40*, 39-47, DOI: 10.1111/j.1442-9071.2011.02649.x [doi].
- (9) Mohan, N.; Chen, C. S.; Hsieh, H. H.; Wu, Y. C.; Chang, H. C. In Vivo Imaging and Toxicity Assessments of Fluorescent Nanodiamonds in *Caenorhabditis Elegans*. *Nano Lett.* **2010**, *10*, 3692-3699, DOI: 10.1021/nl1021909 [doi].
- (10) Mochalin, V. N.; Shenderova, O.; Ho, D.; Gogotsi, Y. The Properties and Applications of Nanodiamonds. *Nat. Nanotechnol* **2011**, *7*, 11-23, DOI: 10.1038/nnano.2011.209 [doi].
- (11) Zhang, X. Q.; Chen, M.; Lam, R.; Xu, X.; Osawa, E.; Ho, D. Polymer-Functionalized Nanodiamond Platforms as Vehicles for Gene Delivery. *ACS Nano* **2009**, *3*, 2609-2616, DOI: 10.1021/nn900865g [doi].
- (12) Zhao, L.; Nakae, Y.; Qin, H.; Ito, T.; Kimura, T.; Kojima, H.; Chan, L.; Komatsu, N. Polyglycerol-Functionalized Nanodiamond as a Platform for Gene Delivery: Derivatization, Characterization, and Hybridization with DNA. *Beilstein J. Org. Chem.* **2014**, *10*, 707-713, DOI: 10.3762/bjoc.10.64 [doi].

- (13) Kim, H.; Man, H. B.; Saha, B.; Kopacz, A. M.; Lee, O. S.; Schatz, G. C.; Ho, D.; Liu, W. K. Multiscale Simulation as a Framework for the Enhanced Design of Nanodiamond-Polyethylenimine-based Gene Delivery. *J. Phys. Chem. Lett.* **2012**, *3*, 3791-3797, DOI: 10.1021/jz301756e [doi].
- (14) Alhaddad, A.; Adam, M. P.; Botsoa, J.; Dantelle, G.; Perruchas, S.; Gacoin, T.; Mansuy, C.; Lavielle, S.; Malvy, C.; Treussart, F.; Bertrand, J. R. Nanodiamond as a vector for siRNA delivery to Ewing sarcoma cells. *Small* **2011**, *7*, 3087-3095, DOI: 10.1002/sml.201101193 [doi].
- (15) Alwani, S.; Kaur, R.; Michel, D.; Chitanda, J. M.; Verrall, R. E.; Karunakaran, C.; Badea, I. Lysine-Functionalized Nanodiamonds as Gene Carriers: Development of Stable Colloidal Dispersion for In Vitro Cellular Uptake Studies and siRNA Delivery Application. *Int. J. Nanomedicine* **2016**, *11*, 687-702, DOI: 10.2147/IJN.S92218 [doi].
- (16) Edgington, R.; Spillane, K. M.; Papageorgiou, G.; Wray, W.; Ishiwata, H.; Labarca, M.; Leal-Ortiz, S.; Reid, G.; Webb, M.; Foord, J.; Melosh, N.; Schaefer, A. T. Functionalisation of Detonation Nanodiamond for Monodispersed, Soluble DNA-Nanodiamond Conjugates Using Mixed Silane Bead-Assisted Sonication Disintegration. *Sci. Rep.* **2018**, *8*, 728-017-18601-6, DOI: 10.1038/s41598-017-18601-6 [doi].
- (17) Lim, D. G.; Rajasekaran, N.; Lee, D.; Kim, N. A.; Jung, H. S.; Hong, S.; Shin, Y. K.; Kang, E.; Jeong, S. H. Polyamidoamine-Decorated Nanodiamonds as a Hybrid Gene Delivery Vector and siRNA Structural Characterization at the Charged Interfaces. *ACS Appl. Mater. Interfaces* **2017**, *9*, 31543-31556, DOI: 10.1021/acsami.7b09624 [doi].
- (18) Bi, Y.; Zhang, Y.; Cui, C.; Ren, L.; Jiang, X. Gene-Silencing Effects of Anti-Survivin siRNA Delivered by RGDV-Functionalized Nanodiamond Carrier in the Breast Carcinoma Cell Line MCF-7. *Int. J. Nanomedicine* **2016**, *11*, 5771-5787, DOI: 10.2147/IJN.S117611 [doi].
- (19) Mahale, N. B.; Thakkar, P. D.; Mali, R. G.; Walunj, D. R.; Chaudhari, S. R. Niosomes: Novel Sustained Release Nonionic Stable Vesicular Systems--an Overview. *Adv. Colloid Interface Sci.* **2012**, *183-184*, 46-54, DOI: 10.1016/j.cis.2012.08.002 [doi].
- (20) Grijalvo, S.; Puras, G.; Zarate, J.; Sainz-Ramos, M.; Qtaish, N. A. L.; Lopez, T.; Mashal, M.; Attia, N.; Diaz, D.; Pons, R.; Fernandez, E.; Pedraz, J. L.; Eritja, R. Cationic Niosomes as Non-Viral Vehicles for Nucleic Acids: Challenges and Opportunities in Gene Delivery. *Pharmaceutics* **2019**, *11*, 10.3390/pharmaceutics11020050, DOI: E50 [pii].
- (21) Mashal, M.; Attia, N.; Soto-Sanchez, C.; Martinez-Navarrete, G.; Fernandez, E.; Puras, G.; Pedraz, J. L. Non-Viral Vectors Based on Cationic Niosomes as Efficient Gene Delivery Vehicles to Central Nervous System Cells into the Brain. *Int. J. Pharm.* **2018**, *552*, 48-55, DOI: S0378-5173(18)30689-6 [pii].
- (22) Karmali, P. P.; Chaudhuri, A. Cationic Liposomes as Non-Viral Carriers of Gene Medicines: Resolved Issues, Open Questions, and Future Promises. *Med. Res. Rev.* **2007**, *27*, 696-722, DOI: 10.1002/med.20090 [doi].
- (23) Liu, F.; Yang, J.; Huang, L.; Liu, D. Effect of Non-Ionic Surfactants on the Formation of DNA/Emulsion Complexes and Emulsion-Mediated Gene Transfer. *Pharm. Res.* **1996**, *13*, 1642-1646, DOI: 10.1023/a:1016480421204 [doi].

- (24) Mochizuki, S.; Kanegae, N.; Nishina, K.; Kamikawa, Y.; Koiwai, K.; Masunaga, H.; Sakurai, K. The Role of the Helper Lipid Dioleoylphosphatidylethanolamine (DOPE) for DNA Transfection Cooperating with a Cationic Lipid Bearing Ethylenediamine. *Biochim. Biophys. Acta* **2013**, *1828*, 412-418, DOI: 10.1016/j.bbame.2012.10.017 [doi].
- (25) Ojeda, E.; Puras, G.; Agirre, M.; Zarate, J.; Grijalvo, S.; Eritja, R.; DiGiacomo, L.; Caracciolo, G.; Pedraz, J. L. The Role of Helper Lipids in the Intracellular Disposition and Transfection Efficiency of Niosome Formulations for Gene Delivery to Retinal Pigment Epithelial Cells. *Int. J. Pharm.* **2016**, *503*, 115-126, DOI: 10.1016/j.ijpharm.2016.02.043 [doi].
- (26) Al Qtaish, N.; Gallego, I.; Villate-Beitia, I.; Sainz-Ramos, M.; Lopez-Mendez, T. B.; Grijalvo, S.; Eritja, R.; Soto-Sanchez, C.; Martinez-Navarrete, G.; Fernandez, E.; Puras, G.; Pedraz, J. L. Niosome-Based Approach for In Situ Gene Delivery to Retina and Brain Cortex as Immune-Privileged Tissues. *Pharmaceutics* **2020**, *12*, 10.3390/pharmaceutics12030198, DOI: E198 [pii].
- (27) Ojeda, E.; Puras, G.; Agirre, M.; Zarate, J.; Grijalvo, S.; Eritja, R.; Martinez-Navarrete, G.; Soto-Sanchez, C.; Diaz-Tahoces, A.; Aviles-Trigueros, M.; Fernandez, E.; Pedraz, J. L. The Influence of the Polar Head-Group of Synthetic Cationic Lipids on the Transfection Efficiency Mediated by Niosomes in Rat Retina and Brain. *Biomaterials* **2016**, *77*, 267-279, DOI: 10.1016/j.biomaterials.2015.11.017 [doi].
- (28) Hagen, W. J. H.; Wan, W.; Briggs, J. A. G. Implementation of a Cryo-Electron Tomography Tilt-Scheme Optimized for High Resolution Subtomogram Averaging. *J. Struct. Biol.* **2017**, *197*, 191-198, DOI: S1047-8477(16)30113-7 [pii].
- (29) Kremer, J. R.; Mastrorade, D. N.; McIntosh, J. R. Computer Visualization of Three-Dimensional Image Data Using IMOD. *J. Struct. Biol.* **1996**, *116*, 71-76, DOI: S1047-8477(96)90013-1 [pii].
- (30) Agulleiro, J. I.; Fernandez, J. J. Fast Tomographic Reconstruction on Multicore Computers. *Bioinformatics* **2011**, *27*, 582-583, DOI: 10.1093/bioinformatics/btq692 [doi].
- (31) Collins, T. J. ImageJ for Microscopy. *BioTechniques* **2007**, *43*, 25-30, DOI: 000112517 [pii].
- (32) Schneider, C. A.; Rasband, W. S.; Eliceiri, K. W. NIH Image to ImageJ: 25 Years of Image Analysis. *Nat. Methods* **2012**, *9*, 671-675, DOI: 10.1038/nmeth.2089 [doi].
- (33) Pettersen, E. F.; Goddard, T. D.; Huang, C. C.; Couch, G. S.; Greenblatt, D. M.; Meng, E. C.; Ferrin, T. E. UCSF Chimera--a Visualization System for Exploratory Research and Analysis. *J. Comput. Chem.* **2004**, *25*, 1605-1612, DOI: 10.1002/jcc.20084 [doi].
- (34) van Steensel, B.; van Binnendijk, E. P.; Hornsby, C. D.; van der Voort, H. T.; Krozowski, Z. S.; de Kloet, E. R.; van Driel, R. Partial Colocalization of Glucocorticoid and Mineralocorticoid Receptors in Discrete Compartments in Nuclei of Rat Hippocampus Neurons. *J. Cell. Sci.* **1996**, *109 (Pt 4)*, 787-792.
- (35) Villate-Beitia, I.; Gallego, I.; Martinez-Navarrete, G.; Zarate, J.; Lopez-Mendez, T.; Soto-Sanchez, C.; Santos-Vizcaino, E.; Puras, G.; Fernandez, E.; Pedraz, J. L. Polysorbate 20 Non-Ionic Surfactant Enhances Retinal Gene Delivery Efficiency of Cationic Niosomes After Intravitreal and Subretinal Administration. *Int. J. Pharm.* **2018**, *550*, 388-397, DOI: S0378-5173(18)30508-8 [pii].

- (36) Villate-Beitia, I.; Puras, G.; Soto-Sanchez, C.; Agirre, M.; Ojeda, E.; Zarate, J.; Fernandez, E.; Pedraz, J. L. Non-Viral Vectors Based on Magnetoplexes, Lipoplexes and Polyplexes for VEGF Gene Delivery into Central Nervous System Cells. *Int. J. Pharm.* **2017**, *521*, 130-140, DOI: S0378-5173(17)30097-2 [pii].
- (37) Gallego, I.; Villate-Beitia, I.; Martinez-Navarrete, G.; Menendez, M.; Lopez-Mendez, T.; Soto-Sanchez, C.; Zarate, J.; Puras, G.; Fernandez, E.; Pedraz, J. L. Non-Viral Vectors Based on Cationic Niosomes and Minicircle DNA Technology Enhance Gene Delivery Efficiency for Biomedical Applications in Retinal Disorders. *Nanomedicine* **2019**, *17*, 308-318, DOI: S1549-9634(19)30034-6 [pii].
- (38) Middaugh, C. R.; Evans, R. K.; Montgomery, D. L.; Casimiro, D. R. Analysis of Plasmid DNA from a Pharmaceutical Perspective. *J. Pharm. Sci.* **1998**, *87*, 130-146, DOI: 10.1021/js970367a [doi].
- (39) Remaut, K.; Sanders, N. N.; Fayazpour, F.; Demeester, J.; De Smedt, S. C. Influence of Plasmid DNA Topology on the Transfection Properties of DOTAP/DOPE Lipoplexes. *J. Control. Release* **2006**, *115*, 335-343, DOI: S0168-3659(06)00399-3 [pii].
- (40) Ho, D.; Wang, C. H.; Chow, E. K. Nanodiamonds: The Intersection of Nanotechnology, Drug Development, and Personalized Medicine. *Sci. Adv.* **2015**, *1*, e1500439, DOI: 10.1126/sciadv.1500439 [doi].
- (41) Chauhan, S.; Jain, N.; Nagaich, U. Nanodiamonds with Powerful Ability for Drug Delivery and Biomedical Applications: Recent Updates on In Vivo Study and Patents. *J. Pharm. Anal.* **2020**, *10*, 1-12, DOI: 10.1016/j.jpha.2019.09.003 [doi].
- (42) Zhu, Y.; Li, J.; Li, W.; Zhang, Y.; Yang, X.; Chen, N.; Sun, Y.; Zhao, Y.; Fan, C.; Huang, Q. The Biocompatibility of Nanodiamonds and Their Application in Drug Delivery Systems. *Theranostics* **2012**, *2*, 302-312, DOI: 10.7150/thno.3627 [doi].
- (43) Karami, P.; Salkhi Khasraghi, S.; Hashemi, M.; Rabiei, S.; Shojaei, A. Polymer/Nanodiamond Composites - a Comprehensive Review from Synthesis and Fabrication to Properties and Applications. *Adv. Colloid Interface Sci.* **2019**, *269*, 122-151, DOI: S0001-8686(18)30394-4 [pii].
- (44) Zhang, Z.; Niu, B.; Chen, J.; He, X.; Bao, X.; Zhu, J.; Yu, H.; Li, Y. The Use of Lipid-Coated Nanodiamond to Improve Bioavailability and Efficacy of Sorafenib in Resisting Metastasis of Gastric Cancer. *Biomaterials* **2014**, *35*, 4565-4572, DOI: 10.1016/j.biomaterials.2014.02.024 [doi].
- (45) Wang, F.; Liu, J. Nanodiamond Decorated Liposomes as Highly Biocompatible Delivery Vehicles and a Comparison with Carbon Nanotubes and Graphene oxide. *Nanoscale* **2013**, *5*, 12375-12382, DOI: 10.1039/c3nr04143c [doi].
- (46) Bartelds, R.; Nematollahi, M. H.; Pols, T.; Stuart, M. C. A.; Pardakhty, A.; Asadikaram, G.; Poolman, B. Niosomes, an Alternative for Liposomal Delivery. *PLoS One* **2018**, *13*, e0194179, DOI: 10.1371/journal.pone.0194179 [doi].
- (47) Wissing, S. A.; Kayser, O.; Muller, R. H. Solid Lipid Nanoparticles for Parenteral Drug Delivery. *Adv. Drug Deliv. Rev.* **2004**, *56*, 1257-1272, DOI: 10.1016/j.addr.2003.12.002 [doi].

- (48) Hosseinkhani, H.; Tabata, Y. Self Assembly of DNA Nanoparticles with Polycations for the Delivery of Genetic Materials into Cells. *J. Nanosci Nanotechnol* **2006**, *6*, 2320-2328, DOI: 10.1166/jnn.2006.507 [doi].
- (49) Chipaux, M.; van der Laan, K. J.; Hemelaar, S. R.; Hasani, M.; Zheng, T.; Schirhagl, R. Nanodiamonds and Their Applications in Cells. *Small* **2018**, *14*, e1704263, DOI: 10.1002/sml.201704263 [doi].
- (50) Manzanares, D.; Cena, V. Endocytosis: The Nanoparticle and Submicron Nanocompounds Gateway into the Cell. *Pharmaceutics* **2020**, *12*, 10.3390/pharmaceutics12040371, DOI: E371 [pii].
- (51) Delgado, D.; del Pozo-Rodriguez, A.; Solinis, M. A.; Rodriguez-Gascon, A. Understanding the Mechanism of Protamine in Solid Lipid Nanoparticle-Based Lipofection: the Importance of the Entry Pathway. *Eur. J. Pharm. Biopharm.* **2011**, *79*, 495-502, DOI: 10.1016/j.ejpb.2011.06.005 [doi].
- (52) Ruiz de Garibay, A. P.; Solinis Aspiazua, M. A.; Rodriguez Gascon, A.; Ganjian, H.; Fuchs, R. Role of Endocytic Uptake in Transfection Efficiency of Solid Lipid Nanoparticles-Based Nonviral Vectors. *J. Gene Med.* **2013**, *15*, 427-440, DOI: 10.1002/jgm.2749 [doi].
- (53) El-Sayed, A.; Harashima, H. Endocytosis of Gene Delivery Vectors: from Clathrin-Dependent to Lipid Raft-Mediated Endocytosis. *Mol. Ther.* **2013**, *21*, 1118-1130, DOI: 10.1038/mt.2013.54 [doi].
- (54) Popova, N. V.; Deyev, I. E.; Petrenko, A. G. Clathrin-Mediated Endocytosis and Adaptor Proteins. *Acta Naturae* **2013**, *5*, 62-73.
- (55) Prabhakar, N.; Khan, M. H.; Peurla, M.; Chang, H. C.; Hanninen, P. E.; Rosenholm, J. M. Intracellular Trafficking of Fluorescent Nanodiamonds and Regulation of Their Cellular Toxicity. *ACS Omega* **2017**, *2*, 2689-2693, DOI: 10.1021/acsomega.7b00339 [doi].
- (56) Varkouhi, A. K.; Scholte, M.; Storm, G.; Haisma, H. J. Endosomal Escape Pathways for Delivery of Biologicals. *J. Control. Release* **2011**, *151*, 220-228, DOI: 10.1016/j.jconrel.2010.11.004 [doi].
- (57) Kimura, S.; Harashima, H. Current Status and Challenges Associated with CNS-Targeted Gene Delivery across the BBB. *Pharmaceutics* **2020**, *12*, 10.3390/pharmaceutics12121216, DOI: E1216 [pii].

Supporting Information

1. Biophysical screening of the nanodiasome formulations composed of niosomes with nanodiamonds as helper component

EXPERIMENTAL SECTION

All the formulations were elaborated by the oil in water technique. The components employed for the study of the best balance NDs/DOTMA for the development of a suitable nanodiasome formulation for gene therapy purposes were: 250 μ l of NDs (10 mg/ml in H₂O) ultrasonicated for 30 minutes and mixed with 2 ml of 0.5% Tween 20 and 1.75 ml of MilliQ water, as the aqueous phase. For the organic phase 1.25, 2.5 or 5 mg of the cationic lipid DOTMA were accurately weighted to obtain 1/0.5, 1/1 and 1/2 ND/DOTMA mass ratios, respectively. The DOTMA was diluted in 1 ml of dichloromethane (DCM). The organic phase was added upon the aqueous phase and immediately sonicated for 30 minutes at 50 W. DCM was evaporated for 2 h at room temperature under magnetic stirring obtaining formulations named as nanodiasomes NDT10, NDT11 and NDT12, for ND/DOTMA at 1/0.5, 1/1 and 1/2 mass ratios, respectively.

RESULTS

Physicochemical characterization of nanodiasomes at different ND/DOTMA mass ratios

The average particle size of ND alone was 89 nm (Figure S1 A-C, white bar). This value increased when ND were integrated as helper component into niosomes to obtain nanodiasomes, which presented size values below 200 nm in all cases (Figure S1A-C, grey bars). The quantity of DOTMA in nanodiasomes had a faint influence on particle size, decreasing around 30% along with the increasing amounts of DOTMA in the formulations (NDT10: 187 nm; NDT11: 121 nm; NDT12: 140 nm) (Figure S1 A-C, grey bars). In general terms, when complexing with DNA, average particle size peaked at 5/1 ratio reaching 228 nm for NDT10, 264 nm for NDT11 and 194 nm for NDT12, which corresponded to 1.2-fold, 2.2-fold and 1.4-fold increase compared with their respective nanodiasomes. Then, the nanodiaplexes size decreased gradually at 10/1 and 15/1 cationic lipid/DNA mass ratio. Zeta potential of ND alone was -23 mV (Figure S1 A-C, white dot) while it turned into positive to values between +38 mV and +48 mV when ND were integrated into the niosomes as helper component (Figure S1 A-C, grey dots). In particular, zeta potential

values increased gradually with the increasing amounts of cationic lipid in the formulation. Upon the addition of pEGFP to nanodiasomes, zeta potential values decreased at 2/1 cationic lipid/DNA mass ratio and increased gradually with the increasing ratios. In all cases, zeta potential of nanodiaplexes remained positive between +15 mV and +37 mV. Mean dispersity values obtained for nanodiasomes remained stable in all cases, between 0.18 and 0.21, and were lower than the ones corresponding to ND alone (0.28) (Figure S1D). Complexation of nanodiasomes with DNA conducted to slight changes in this parameter, presenting values below 0.4 in all cases.

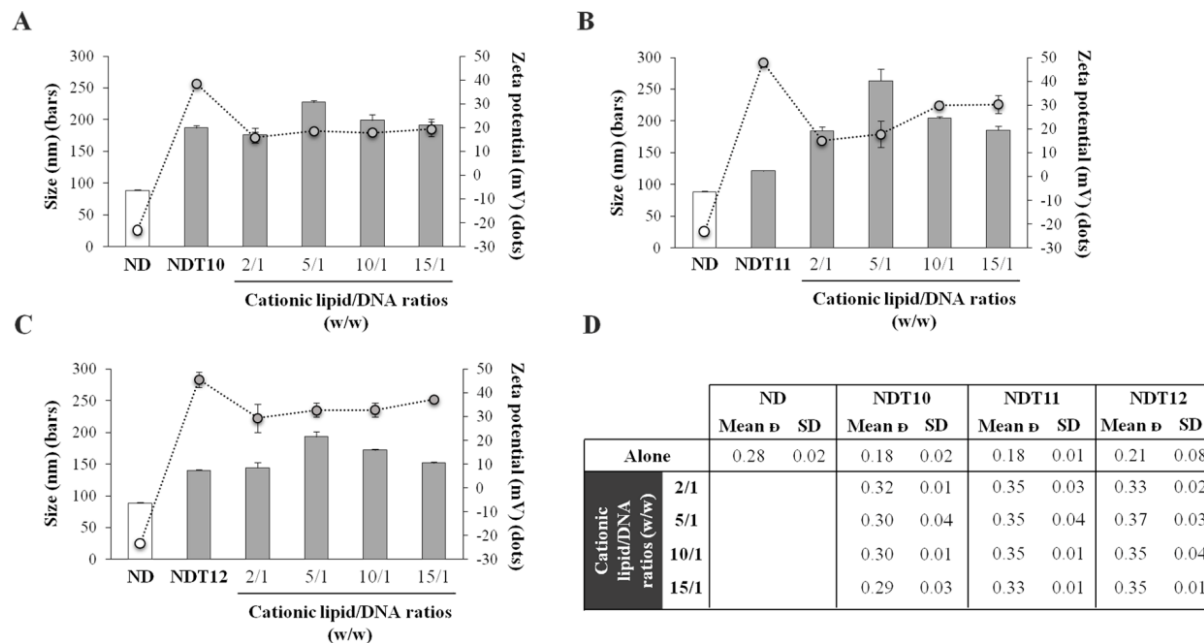


Figure S1: Physicochemical characterization of nanodiasome formulations, elaborated with ND as helper component at different ND/DOTMA mass ratios (1/0.5, named NDT10; 1/1, named NDT11 and 1/2, named NDT12), and nanodiaplexes at different DOTMA/DNA mass ratios (2/1, 5/1, 10/1 and 15/1). **A-C.** Size (bars) and zeta potential (dots) for (A) NDT10 and corresponding nanodiaplexes (B) NDT11 and corresponding nanodiaplexes, and (C) NDT12 and corresponding nanodiaplexes. **D.** Dispersity and SD values of nanodiamonds, nanodiasomes and nanodiaplexes. Each value represents the mean \pm standard deviation of three measurements. ND, means nanodiamonds; \bar{D} , means dispersity.

Transfection efficiency of nanodiasomes at different ND/DOTMA mass ratios

Analysis of EGFP expression in living cells, after transfecting with the complexes based on the three nanodiasome formulations, clearly showed a high transfection efficiency employing

NDT12 formulation at 5/1 cationic lipid/DNA mass ratio (Figure S2, bars). In particular, for NDT10 the maximum value obtained was around 20% of EGFP expression at 10/1 and 15/1 ratios (Figure S2 A, bars); for NDT11 this parameter doubled to 40% at 10/1 ratio (Figure S2 B, bars) and in the case of NDT12 it doubled over again the transfection efficiency presenting more than 85% of living cells expressing EGFP at 5/1 ratio (Figure S2 C, bars). Additionally, the biocompatibility of NDT12 was higher and remained constant at all cationic lipid/DNA mass ratios, compared with NDT10 and NDT11 (Figure S2, dots). In general terms, cell viability for NDT10 and NDT11 was around 95% at 2/1 ratio but declined progressively by 12% at 15/1 ratio (Figure S2 A and B, respectively, dots), while in the case of NDT12 cell viability was around 95% at all ratios (Figure S2 C, dots). Lipofectamine at 2/1 ratio was employed as a positive control for transfection, which presented a 43% of EGFP expression in live cells and 81% of cell viability (data not shown). Transfection data were normalized in regard to this transfection value.

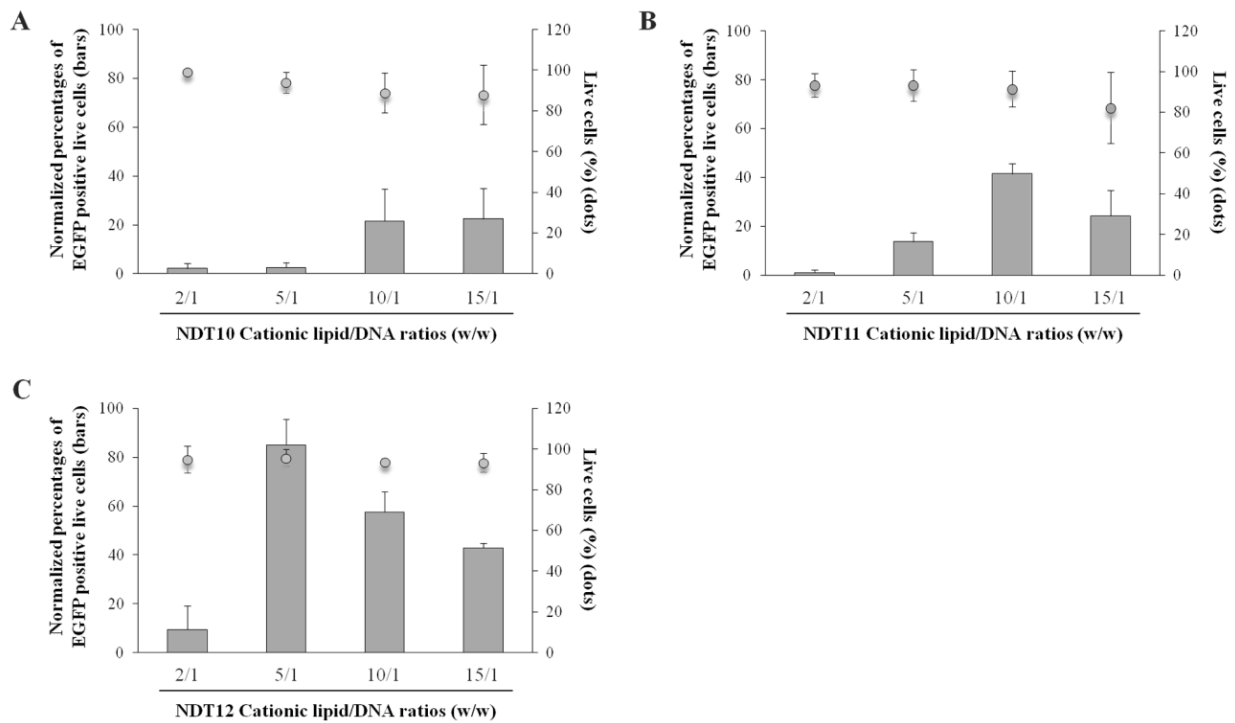


Figure S2: Normalized percentages of EGFP positive live cells (bars) and cell viability (dots) in HEK-293 cell line 48 hours post-transfection with nanodiaplexes. **A.** NDT10 nanodiaplexes **B.** NDT11 nanodiaplexes. **C.** NDT12 nanodiaplexes. Each value represents the mean \pm standard deviation of $n \geq 4$.

Therefore, from this biophysical screening to analyze the ideal ND/DOTMA balance for the development of a good gene therapy vector, NDT12 met the best conditions as it presented suitable physicochemical properties for gene delivery purposes and showed promising high values of transfection efficiency accompanied by great biocompatibility in HEK-293 cell line.

2. Additional multimedia supporting information



OK_2021_12_02_290_tomo_11_3DS30_rec-1.mrc kept stack.avi (Línea de comandos)

Video S1: Tomogram reconstruction showing the enclosed nano-diamonds. Scale bar represent 100 nm.



OK_tomo2_movie.mp4

Video S2: Volumetric representation of the tomograms. Higher densities of the tomogram (more electron-dense material) corresponds to gold nanoparticles added to the sample for tilt series alignment (yellow). Medium densities are labeled in cyan and are linked to nanodiamonds (turquoise blue).

Appendix 4

Long-term biophysical stability of nanodiamonds combined with lipid nanocarriers for non-viral gene delivery to the retina

Long-term biophysical stability of nanodiamonds combined with lipid nanocarriers for non-viral gene delivery to the retina

Nuseibah H. AL Qtaish^{a,b,1}, Ilia Villate-Beitia^{a,b,c,1}, Idoia Gallego^{a,b,c}, Gema Martínez-Navarrete^{b,f}, Cristina Soto-Sánchez^{b,f}, Myriam Sainz-Ramos^{a,b,c}, Tania B Lopez-Mendez^{a,b,c}, Alejandro J. Paredes^{d,e}, Francisco Javier Chichón^g, Noelia Z. Fernandez^g, Eduardo Fernández^{b,f}, Gustavo Puras^{a,b,c,*}, and José Luis Pedraz^{a,b,c,*}

- ^a NanoBioCel Research Group, Laboratory of Pharmacy and Pharmaceutical Technology. Faculty of Pharmacy, University of the Basque Country (UPV/EHU), Paseo de la Universidad 7, 01006 Vitoria-Gasteiz, Spain.
- ^b Networking Research Centre of Bioengineering, Biomaterials and Nanomedicine (CIBER-BBN), Institute of Health Carlos III, Paseo de la Universidad 7, 01006 Vitoria-Gasteiz, Spain.
- ^c Bioaraba, NanoBioCel Research Group, 01009 Vitoria-Gasteiz, Spain.
- ^d Research and Development Unit in Pharmaceutical Technology (UNITEFA), CONICET and Department of Pharmaceutical Sciences, Chemistry Sciences Faculty, National University of Córdoba, Haya de la Torre y Medina Allende, X5000XHUA Córdoba, Argentina.
- ^e School of Pharmacy, Queen's University Belfast, Medical Biology Centre, 97 Lisburn Road, Belfast, BT9 7BL Northern Ireland, UK.
- ^f Neuroprosthesis and Neuroengineering Research Group, Institute of Bioengineering, Miguel Hernández University, Avenida de la Universidad, 03202 Elche, Spain.
- ^g CryoEM CSIC Facility. Centro Nacional de Biotecnología (CNB-CSIC). Structure of macromolecules Department. Calle Darwin n°3, 28049 Madrid, Spain.

* Corresponding authors:

José Luis Pedraz, Ph.D. Laboratory of Pharmacy and Pharmaceutical Technology, School of Pharmacy, University of the Basque Country UPV/EHU), Paseo de la Universidad 7, 01006, Vitoria-Gasteiz, Spain.

E-mail address: joseluis.pedraz@ehu.es. Phone: + (34)-945013091. Fax number: + (34)-945013040

Gustavo Puras, Ph.D. Laboratory of Pharmacy and Pharmaceutical Technology, School of Pharmacy, University of the Basque Country (UPV/EHU), Paseo de la Universidad 7, 01006 Vitoria-Gasteiz, Spain.

E-mail address: gustavo.puras@ehu.eus. Phone number: + (34)-945014536. Fax number: + (34)-945013040

¹ These authors contributed equally to this work.

Abstract: In the present work, we combined nanodiamonds with niosome non-viral vectors, and the resulting formulations were named as nanodiasomes. The effect of such nanomaterial was evaluated over time in terms of physicochemical features, cellular internalization, cell viability and transfection efficiency both *in vitro* and *in vivo* in mouse retina. All these parameters were analysed at different storage temperatures and time points over 30 days. The main findings revealed that the incorporation of nanodiamonds into niosome formulations resulted in a 4-fold increase of transfection efficiency, and this difference was maintained over time. In addition, both formulations were more stable at lower (4°C) temperatures and nanodiasomes maintained their physicochemical properties more constant than niosomes. Finally, nanodiasomes were able to achieve high transgene expression levels in mouse retina after subretinal and intravitreal administration, both when injecting nanodiasome formulations freshly prepared and after 30 days of storage at 4°C.

Key words: nanodiamond; niosome; non-viral; gene delivery; stability; retina.

Introduction

The pharmaceutical science has directed considerable efforts towards discovering and developing safe and efficient vectors for gene therapy purposes. While most studies focus on overcoming specific issues related to conventional gene delivery platforms, such as unpredictability, incompatibility with biological systems or low efficiency, few studies conduct an exhaustive assessment of the storage stability of gene carriers, a critical quality to achieve both large-scale production and clinical application (Suzuki et al., 2015). Nowadays, few gene therapy drugs have been marketed globally, and most of these products are based on viral vectors (Al Qtaish et al., 2020; Shahryari et al., 2019). However, because of specific issues associated to viral gene carriers, including low DNA packing capacity, high costs and complex production, non-viral vectors are gaining increasing interest (Do et al., 2019; Ibraheem et al., 2014; Ginn et al., 2017). In addition to overcoming these specific challenges, non-viral vectors offer high versatility due to the wide variety of available nanomaterials that can be used to produce gene delivery systems (Grijalvo et al., 2019; Riley and Vermerris. 2014). Among these, niosomes have been reported in repeated occasions as efficient vehicles for gene delivery to brain (Mashal et al., 2018) and retina (Puras et al., 2015), among others. Niosomes are cationic lipid nanoparticles with a bilayer distribution similar to liposomes, but, additionally, niosomes can also contain a “helper”

component and a non-ionic surfactant to obtain more stable colloidal dispersions. All these mentioned components, provide niosomes superior chemical and storage stability than liposomes (Bartelds et al., 2018; Ojeda et al., 2016). All the components of niosome formulations influence on their biocompatibility and transfection efficiency. In particular, the characteristics of the “helper” component influence directly on relevant biological processes, such as the cellular uptake and the subsequent intracellular disposition, which are critical factors that determine successful gene delivery efficiency (Ojeda et al., 2016). Among the most studied “helper” components, lipid-based ones such as lycopene, cholesterol, squalane, squalene and sphingolipids (Al Qtaish et al., 2021; Mashal et al., 2017; Ojeda et al., 2016) have been the most employed to date, but also non-lipid ones such as chloroquine are gaining interest with encouraging results (Mashal et al., 2019).

Recently, nanodiamonds (NDs) have emerged as an interesting material to elaborate non-viral vectors for gene delivery applications. The high biocompatibility, low toxicity, along with their versatile surface chemistry (Lim et al., 2016), which allows multiple combination forms as “helper” components with other nanomaterials such as polymers or lipids have captured the interest of scientifics. NDs are allotropes of carbon that contain a core diamond crystalline structure and present unique physicochemical properties, such as almost spherical shape, low size polydispersity and high specific area. Additionally, NDs can be easily functionalized with many chemical compounds (Chauhan et al., 2020). In previous research for gene therapy purposes, authors combined NDs with hydrophilic cationic polymers such as polyethylenimine 800 (PEI 800) (Alhaddad et al., 2011); Chen et al., 2021; Zhang et al., 2009) and polyallylamine hydrochloride (PAH) (Alhaddad et al., 2011), or with cationic monomer such as lysine (Alwani et al., 2016) by electrostatic interactions. On the other hand, covalent derivatization of NDs has been performed with silane-NH₂ groups (Edgington et al., 2018; Zhang et al., 2009) and polyamidoamine (PANAM) (Lim et al., 2017). In other study, Bi et al designed and synthesized a complex structure of ND-CONH(CH₂)₂NH-VDGR/survivin-siRNA with antitumoral effect (Bi et al., 2016). Finally, our research group combined NDs with niosomes, demonstrating their superiority in enhancing the transfection efficiency of these non-viral vectors (Al Qtaish et al., 2022). However, to the best of our knowledge, the combination of NDs with niosomes to evaluate their stability along with their retinal gene delivery efficiency has not been explored yet.

In this work, we prepared and comparatively evaluated the transfection efficiency and long-term stability at different storage temperatures of two niosome-based formulations that only differed on the use or not of NDs as “helper” components. Formulations were based on cationic lipid N-[1-(2,3dioleoyloxy)propyl]-N,N,N-trimethylammonium chloride (DOTMA) and non-ionic surfactant polysorbate 20. NDs were added as “helper” components to one of the two formulations. Resulting formulations were named as niosomes and nanodiasomes depending on their ND content and were incubated with pCMS-EGFP plasmid in order to obtain nanocomplexes, named as nioplexes and nanodiaplexes, respectively. Formulations were evaluated in terms of physicochemical properties, including size distribution, superficial charge and polydispersity index at different periods of time (0, 15 and 30 days) and storage temperatures (4°C and 25°C). In addition, *in vitro* biological studies were performed to evaluate the toxicity of the formulations along with their cellular uptake and gene delivery efficiency over time at different storage temperatures in HEK-293 cells. Further assays were carried out in primary retinal cells and in mice after both intravitreal and subretinal administration of the formulations in order to determine the effect of NDs as “helper” components on the gene delivery efficiency and long-term storage of the formulations.

1. Materials and Methods

1.1. Preparation of nanodiasome and niosome formulations

For the preparation of the nanodiasome formulations, the water in oil emulsion technique was used as previously described. Briefly, 250 µL of NDs (10 mg/ml in H₂O, Sigma-Aldrich Madrid, Spain, product ID: 900180) were ultrasonicated for 30 minutes and mixed with an aqueous phase composed of 2 mL of 0.5% polysorbate 20 (Sigma-Aldrich Madrid, Spain) plus 1.75 mL of MilliQ water. On the other hand, 5 mg of DOTMA (Avanti Polar Lipids, Inc., Alabama, USA) were accurately weighted and diluted in 1 mL of the organic solvent dichloromethane (DCM) (Panreac, Barcelona). This oil phase was incorporated into the aqueous phase and sonicated for 30 seconds at 50 W (Branson Sonifier 250, Danbury). The emulsion was maintained under magnetic stirring for 2 h at room temperature (RT) until evaporation of DCM to obtain the nanodiasome formulation. The preparation of the niosome formulation followed the same procedure, but the aqueous phase did not contain NDs. Figure 1 summarizes the main components and their disposition in both formulations.


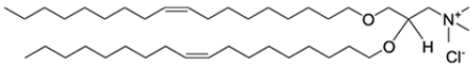

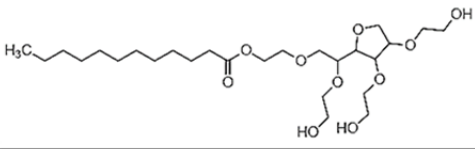

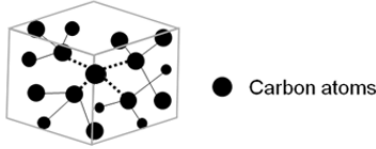
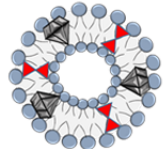
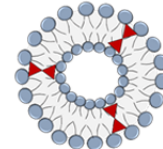
Components	Chemical structure	General scheme	
		Nanodiasomes	Niosomes
 Cationic lipid: DOTMA		✓	✓
 Non-ionic surfactant: Polysorbate 20		✓	✓
 Helper component: Monodispersed nanodiamond particles		✓	—
			

Figure 1. Overview of formulations and their components.

1.2. Preparation of the nanocomplexes

Nanocomplexes were obtained by incubating both niosomes and nanodiasomes with the previously propagated pEGFP plasmid, as described elsewhere (Ojeda et al., 2016), to obtain complexes (nioplexes and nanodiaplexes, respectively) at 5/1 cationic lipid/DNA ratio (w/w).

1.3. Physicochemical studies

Niosomes, nanodiasomes, and their corresponding complexes were physicochemically characterized by means of mean particle size, dispersity index (\mathfrak{D}) and zeta potential, following previously reported methodology (Mashal et al., 2017). Microscopy studies were carried out to determine the morphology and the disposition of NDs in the nanodiasomes, by Cryo-electron tomogram, as previously described (Al Qtaish et al., 2022).

1.4. Biophysical stability studies of formulations

Stability studies were performed with all formulations by means of physicochemical characterization and biological performance. For that purpose, particle size, dispersity, zeta potential, cell viability and transfection were evaluated at 0, 15 and 30 days with stored formulations at 4°C and 25°C. Cellular uptake, transfection in primary retinal cell cultures, along

with *in vivo* retinal assays were performed with freshly prepared formulations and with formulations stored at 4°C for 30 days.

1.5. *Transfection studies*

To perform transfection experiments, human embryonic kidney 293 cell line (HEK-293; ATCC® CRL1573™) was cultured and maintained as previously described (Ojeda et al., 2016). For this, HEK-293 cells were seeded at 20×10^4 cells per well in 24 well plates and incubated to reach 70% of confluence the next day. After discarding the medium from the wells, cells were transfected using OptiMEM (Gibco, San Diego, CA, USA) transfection medium, for 4 h with nioplexes and nanodioplexes, freshly prepared and stored for 15 and 30 days at 4°C and 25°C, at the cationic lipid/DNA mass ratio 5/1, as previously reported (Al Qtaish et al., 2022). Positive control of transfection consisted in cells transfected with Lipofectamine 2000™ (Invitrogen, Carlsbad, CA, USA), while negative control were non-treated cells but in OptiMEM for 4 h. Each condition was carried out in triplicate.

1.6. *EGFP expression and cell viability assays*

The efficiency of the transfection process was assessed both qualitative and quantitatively 48 h after the transfection assay. Qualitative determination of EGFP signal was performed using an inverted fluorescence microscope (Eclipse TE2000-S, Nikon). Quantitative studies of plasmid expression, cell viability and mean fluorescence intensity (MFI) were carried out by flow cytometry using a FACSCalibur system (Becton Dickinson Bioscience, San Jose, USA), as reported previously (Al Qtaish et al., 2022).

1.7. *Cellular uptake*

To analyse the cellular internalization process of nioplexes and nanodioplexes, using freshly prepared and stored for 30 days at 4°C formulations, niosomes and nanodiasomes were condensed with FITC- labelled pEGFP plasmid. Fluorescence microscopy and flow cytometry equipment were used to elaborate cellular uptake process in a qualitative and quantitative way, respectively (Al Qtaish et al., 2022).

1.8. *Animals and anesthetics*

Procedures were performed following the RD 53/2013 Spanish and 2010/63/EU European Union regulations, as well as the Association for Research in Vision and Ophthalmology (ARVO),

once obtained the approval of the Miguel Hernandez University Standing Committee for Animal Use in the Laboratory.

1.9. Transfection studies in rat primary central nervous system cell cultures and immunocytochemistry assays

E17-E18 rat embryos (Sprague Dawley) were employed for the extraction of primary central nervous system (CNS) cells, from the brain cortex and retinal tissue. Cells were removed and cultured onto pre-coated glass coverslips in 24 well plates. Cortical and retinal cells were transfected with freshly and 30 days stored nanodiaplexes. Lipofectamine™ 2000 (ThermoFisher Scientific) was used as a positive control. Transfections experiments were repeated three times for each condition and GFP expression was analyzed at 96 hours after transfection. Cell fixation was carried out with 4% paraformaldehyde for 25 minutes and permeabilized using 0.5% Triton X-100 during 5 min. After blocking with a solution of 10% BSA (v/v) in PBS for 1 hour at RT, cells were incubated with primary antibody chicken anti-EGFP (ThermoFisher Scientific) overnight at 4°C. Secondary antibody Alexa Fluor 555 goat anti-chicken IgG (ThermoFisher Scientific) and Hoechst 33342 (Sigma-Aldrich, Spain) were applied for 1 hour at 4°C. Coverslips were analyzed by a Zeiss AxioObserver Z1 (Carl Zeiss) microscope equipped with an ApoTome system and Leica TCS SPE spectral confocal microscope (Leica Microsystems GmbH, Wetzlar, Germany).

1.10. Intravitreal and subretinal administration of formulations

In vivo transfections were carried in C57BL/6J mice with freshly prepared (n=10) and 30 days stored nanodiaplexes (n=10). Animals were anesthetized, and intravitreal (n=5) or subretinal (n=5) injections were administered under microscope (Zeiss OPMI® pico; Carl Zeiss Meditec GmbH, Jena, Germany) using a Hamilton microsyringe with a blunt 34-gauge needle (Hamilton Co., Reno, NV). The nanodiaplexes solution injected was 0.5 µL which contained 100 ng of EGFP plasmid. As negative controls, the untreated right eyes were used.

EGFP expression was analyzed qualitatively one week after the injection of freshly or 30 days stored nanodiaplexes in frozen sections of the retina, as previously described (Mashal et al., 2017). Cryosections were incubated with the primary antibodies chicken anti-EGFP (ThermoFisher Scientific) and rabbit anti-Iba1 (Abcam) overnight at 4°C. Secondary antibodies Alexa Fluor 488 donkey anti-rabbit and Alexa Fluor 555 goat anti-chicken (both ThermoFisher Scientific) were applied for 1 hour at 4°C. Nuclei were stained with Hoechst 33,342 (Thermo Fisher Scientific).

The samples were analyzed and photographed using a Leica TCS SPE spectral confocal microscope (Leica Microsystems GmbH, Wetzlar, Germany).

1.11. Statistical analysis

Data were analyzed using SPSS 15.0 software. Normality and homogeneity of variances were evaluated with the Shapiro-Wilk test and the Levene test, respectively. Student's t test or ANOVA followed by post-hoc HSD Tukey test were employed under parametric conditions. On the contrary, Kruskal-Wallis test and/or Mann-Whitney U test were used under non-parametric conditions. In all cases, P value ≤ 0.05 was considered statistically significant. Data were represented as mean \pm standard deviation (SD).

2. Results

2.1. Physicochemical characterization of formulations

In general, formulations containing NDs presented higher mean particle size values than their counterparts in all conditions (Figure 2A). At day 0, freshly prepared nanodiosome formulations showed a mean particle size of 128.7 ± 4.2 nm, which maintained stable over time and was significantly increased ($P < 0.05$) only after 30 days of storage at 25°C . Regarding the niosome formulation, the mean particle size at day 0 was 90.5 ± 10.3 nm and presented significant oscillations ($P < 0.05$) at day 15 of storage at 25°C and at day 30 of storage at 4°C . The measurement of zeta potential of nanodiosomes and niosomes at different days and temperatures of storage revealed more oscillations in the case of niosome formulations than their counterparts (Figure 2B). The mean zeta potential value of freshly prepared nanodiosomes at day 0 was 35.2 ± 0.3 mV and presented a statistically relevant increase ($P < 0.05$) after 30 days of storage at both 4°C and 25°C . On the other hand, niosome formulations showed a mean zeta potential value of 20.2 ± 2.5 mV at day 0, which significantly increased after 15 days of storage at 25°C ($P < 0.05$) and decreased after 30 days of storage at 4°C ($P < 0.05$) and 25°C ($P < 0.01$). Dispersity values of nanodiosomes were lower than niosomes and remained stable with little oscillations at all conditions tested, while niosome formulations showed higher values and more variations, especially after being stored during 15 days at 25°C (Figure 2C). Nanodiosomes under cryo-TEM (Figure 2D) showed a spherical shape, with the NDs integrated in the lipid layer (Figure 2D, white arrow).

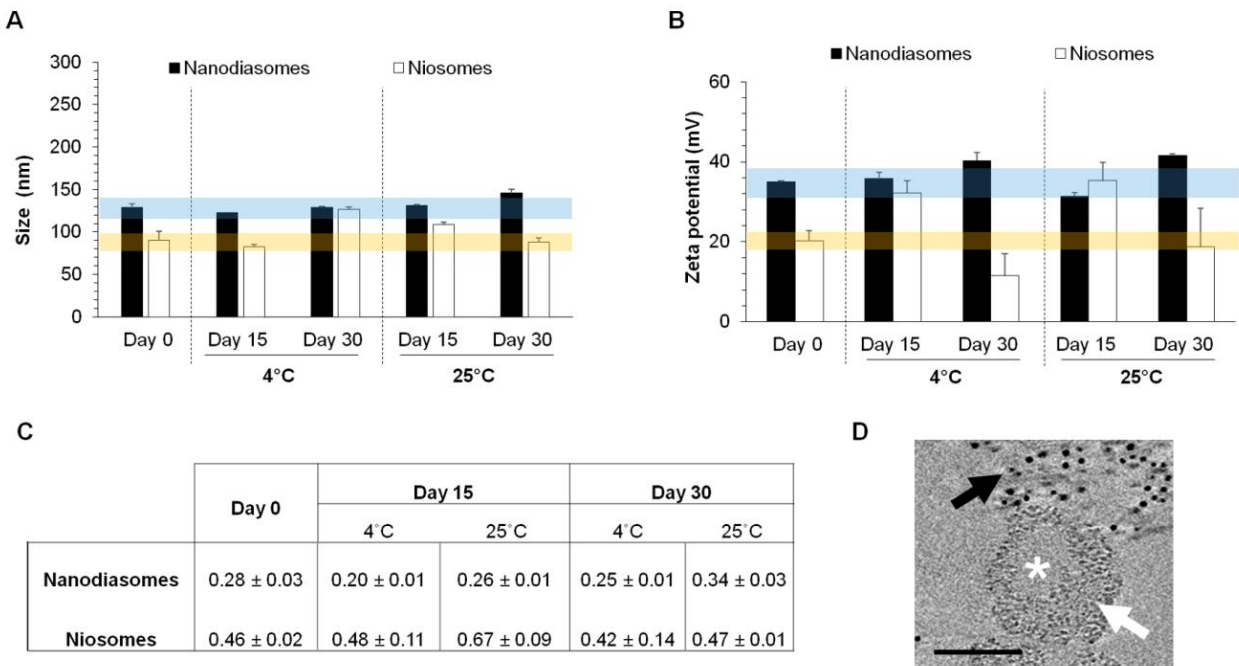


Figure 2. Physicochemical characterization and stability of formulations at different days and storage temperature. **A.** Mean particle size. **B.** Zeta potential. **C.** Dispersity. Each value shows the mean \pm SD of 3 readings. Blue and orange stripes represent $\pm 10\%$ deviation respect to nanodiasomes and niosomes parameters at day 0, respectively. **D.** Cryo-electron tomogram slice of a nanodiasome; asterisk indicates the aqueous phase; white arrow indicates the lipid layer of the nanodiasome with nanodiamonds integrated in the lipid structure; black arrow indicates higher densities of the tomogram (more electron-dense material), which correspond to gold nanoparticles added to the sample for tilt series alignment. Scale bar: 100 nm.

2.2. Gene delivery efficiency and toxicity of nioplexes and nanodiaplexes

The comparative evaluation of cell viability and gene delivery efficiency in cells between nanodiaplexes and nioplexes at different days and storage temperature showed that nanodiaplexes were better tolerated by cells and achieved significantly higher transfection rates at all conditions. The mean percentage of live cells exposed to freshly prepared nanodiaplexes was $90.79 \pm 2.5\%$, while this value was significantly lower ($P < 0.001$) for nioplexes which presented a mean percentage of live cells of $78.8 \pm 5.8\%$ (Figure 3A, lines). These values remained relatively stable over time and different storage temperatures, with little oscillations but no statistically relevant differences compared to the values of day 0 in both formulations. Regarding transfection efficiency, the percentage of EGFP expressing live cells exposed to freshly prepared nanodiaplexes

and nioplexes were, respectively, $89.8 \pm 3.4\%$ and $23.3 \pm 1.1\%$ (Figure 3A, bars). These values remained stable for both formulations over time and storage conditions, always maintaining significantly higher transfection percentages in cells treated with nanodioplexes than with nioplexes ($P < 0.001$).

In addition, the MFI data (Figure 3B) corroborated the advantage of nanodioplexes over nioplexes, with significantly higher MFI values obtained in cells exposed to nanodioplexes at all days and storage conditions tested ($P < 0.001$). Figures 3C and 3D show representative fluorescence microscopy images of HEK-239 cells transfected with both formulations at day 0 and after 30 days of storage at 4°C , respectively.

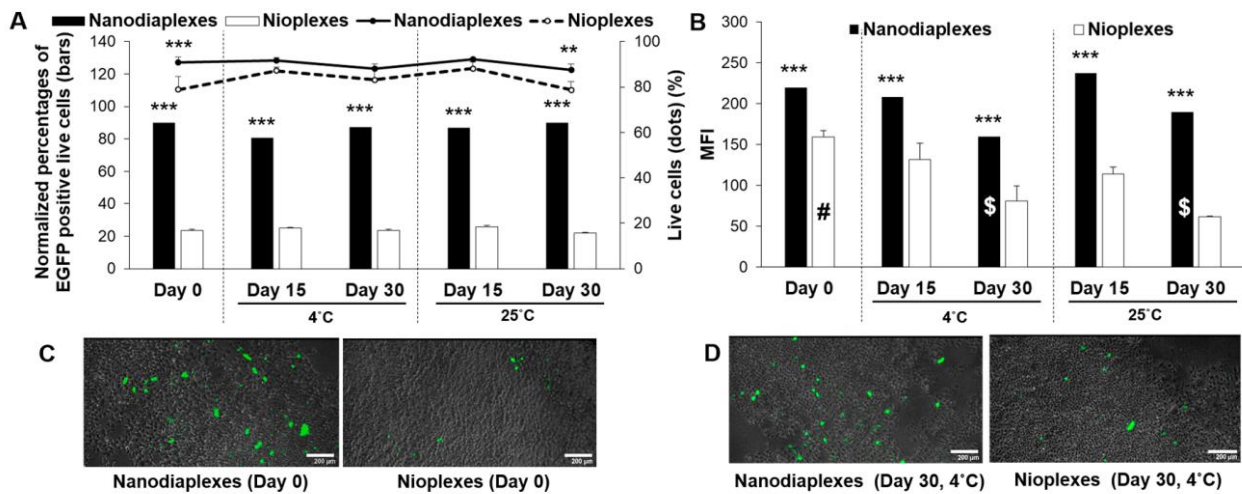


Figure 3. Gene delivery efficiency and toxicity of formulations in HEK-293 cells 48 hours after transfection with nanodioplexes and nioplexes at 5/1 cationic lipid/DNA ratio (w/w) over time at 4°C and 25°C . **A.** Normalized percentages of EGFP positive live cells (bars) and cell viability (dots). **B.** Mean fluorescence intensity values. Each value represents the mean \pm SD of 3 measurements. **C-D.** Merged images showing EGFP signal in HEK-293 cells transfected with both complexes at 5/1 lipid/DNA ratio (w/w) at day 0 (C) and after 30 days of storage at 4°C (D). Scale bars: $200\ \mu\text{m}$. *** $P < 0.001$; ** $P < 0.01$ for nanodioplexes vs nioplexes, no negative significant differences in term of live cells (%) for nioplexes between day 0 and the rest of days and temperatures; # $P < 0.05$ for nioplexes between day 0 and the rest of days, and temperatures; \$ $P < 0.05$ for nanodioplexes at day 30 compared with the rest of days and temperatures.

2.3. Cellular uptake of nioplexes and nanodiaplexes

The analysis of cellular uptake in HEK-293 cells 4 hours after exposure to freshly prepared and 30 days at 4°C stored nanodiaplexes and nioplexes revealed significantly higher ($P < 0.05$) cell internalization percentages for ND based formulations, both at day 0 and after 30 days being stored at 4°C (Figure 4A). These cell uptake percentages remained stable over time for both formulations, with statistically relevant differences. Figure 4B shows representative images of cellular uptake in HEK-293 cells exposed to both formulations at days 0 and 30.

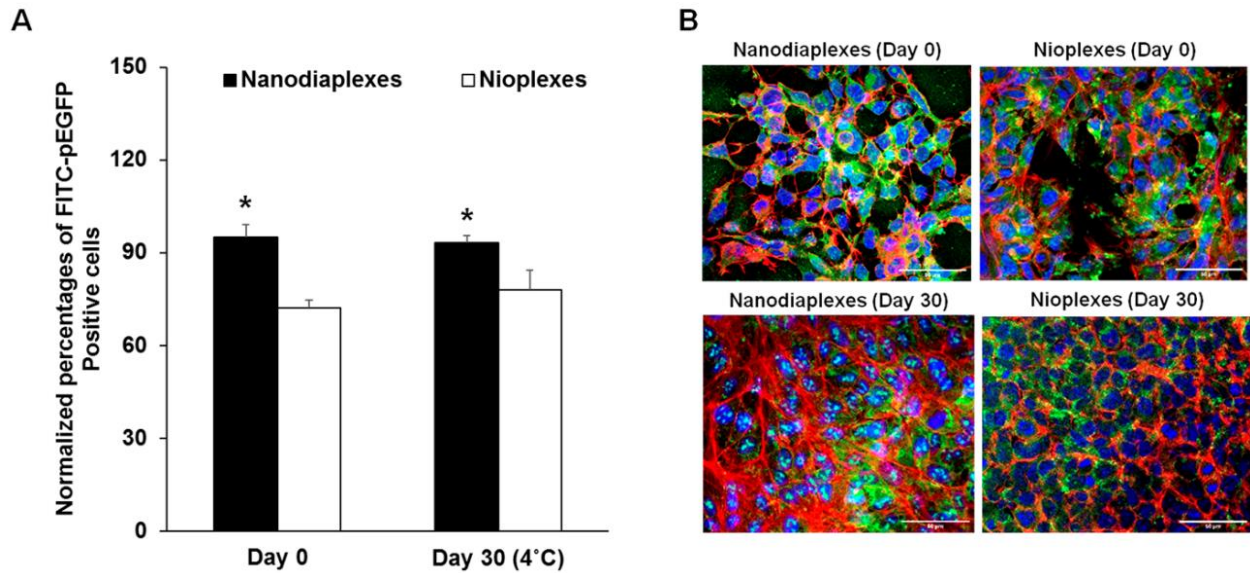


Figure 4. Cellular uptake in HEK-293 cells 4 h after exposure to nanodiaplexes and nioplexes at 5/1 lipid/DNA ratio (w/w) at day 0 and after 30 days of storage at 4°C. **A.** Normalized percentages of FITC-pEGFP positive live cells after the exposure to these complexes. Each value represents the mean \pm SD of 3 measurements. **B.** Confocal microscopy images. Cell nuclei were colored in blue (DAPI); F-actin in red (Phalloidin); nanodiaplexes and nioplexes in green (FITC). Scale bars: 50 μ m.* $P < 0.05$ for nanodiaplexes vs nioplexes.

2.4. Gene delivery efficiency of nanodiaplexes in rat primary cell cultures

The transfection assay in rat primary retinal cells with freshly prepared (Figure 5A) and 30 days stored nanodiaplexes at 4°C (Figure 5B) showed similar EGFP expression, indicating that the transfection efficiency of that formulation maintained stable over a month. Additionally, the transfection efficiency of fresh and 30 days stored nanodiasomes was also evaluated in another CNS cell type, specifically in rat primary neuronal cell culture, which clearly corroborated the high

gene delivery capacity, by means of EGFP expression, of stored formulations over a month and even 3 months (Supplementary Figure S1).

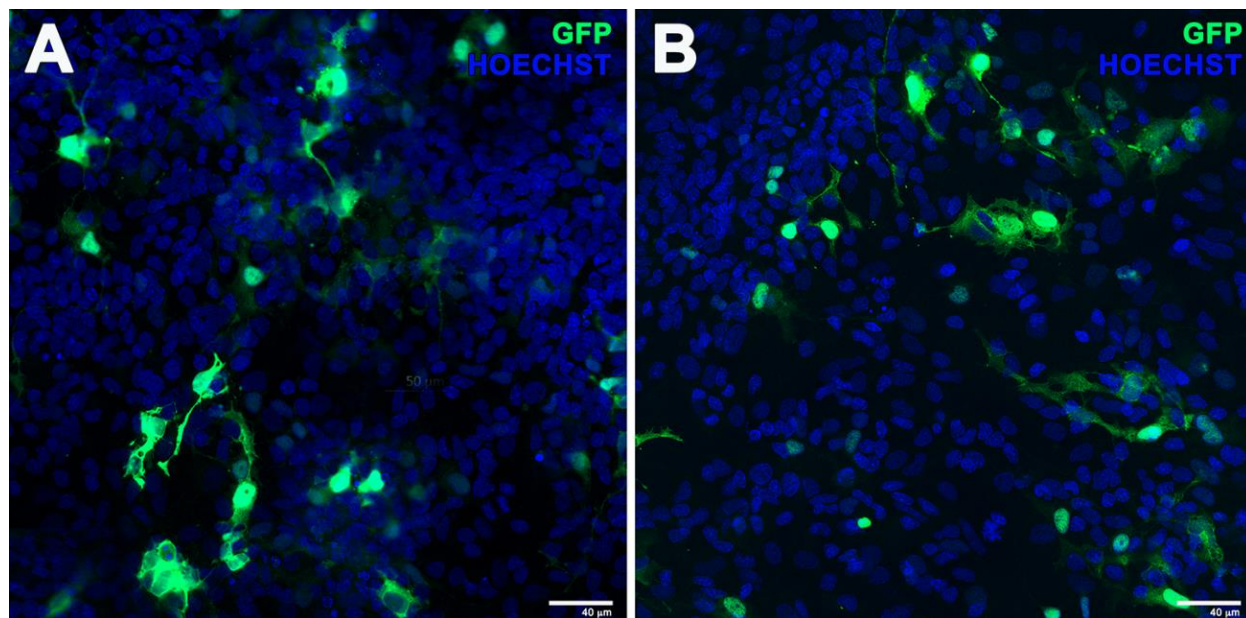


Figure 5. EGFP signal in primary culture of rat retinal cells transfected with freshly prepared (A) and 30 days stored at 4 °C (B) nanodiasomes at 5/1 lipid/DNA ratio (w/w). Scale bar: 40 μm. Blue: Hoechst 33,342 (cell nuclei); Green: EGFP. Scale bars: 40 μm.

2.5. *In vivo* transfection efficiency of nanodiaplexes

Freshly and stored nanodiaplexes were administered to the mouse eye through intravitreal (Figure 6A and 6C) and subretinal injections (Figure 6B and 6D), and fluorescence signal was detected in different retinal cell layers after one week. Both subretinally and intravitreally administered nanodiaplexes showed that EGFP expression colocalized mainly with microglial marker Iba-1 and was also located in the ganglion cell layer (GCL), as well as in the inner nuclear layer (INL) with some diffused fluorescence signal in the outer nuclear layer (ONL), and even the retinal pigment epithelial cell layer (RPE) after subretinal injections (Figure 6B and 6D). Results also showed that the intensity of the fluorescence signal was comparable in both transfections with freshly prepared and 30 days stored formulations. Additionally, mouse retinal cells tolerated well the exposition to nanodiaplexes, in terms of cell viability, considering the results reported in the qualitative analysis.

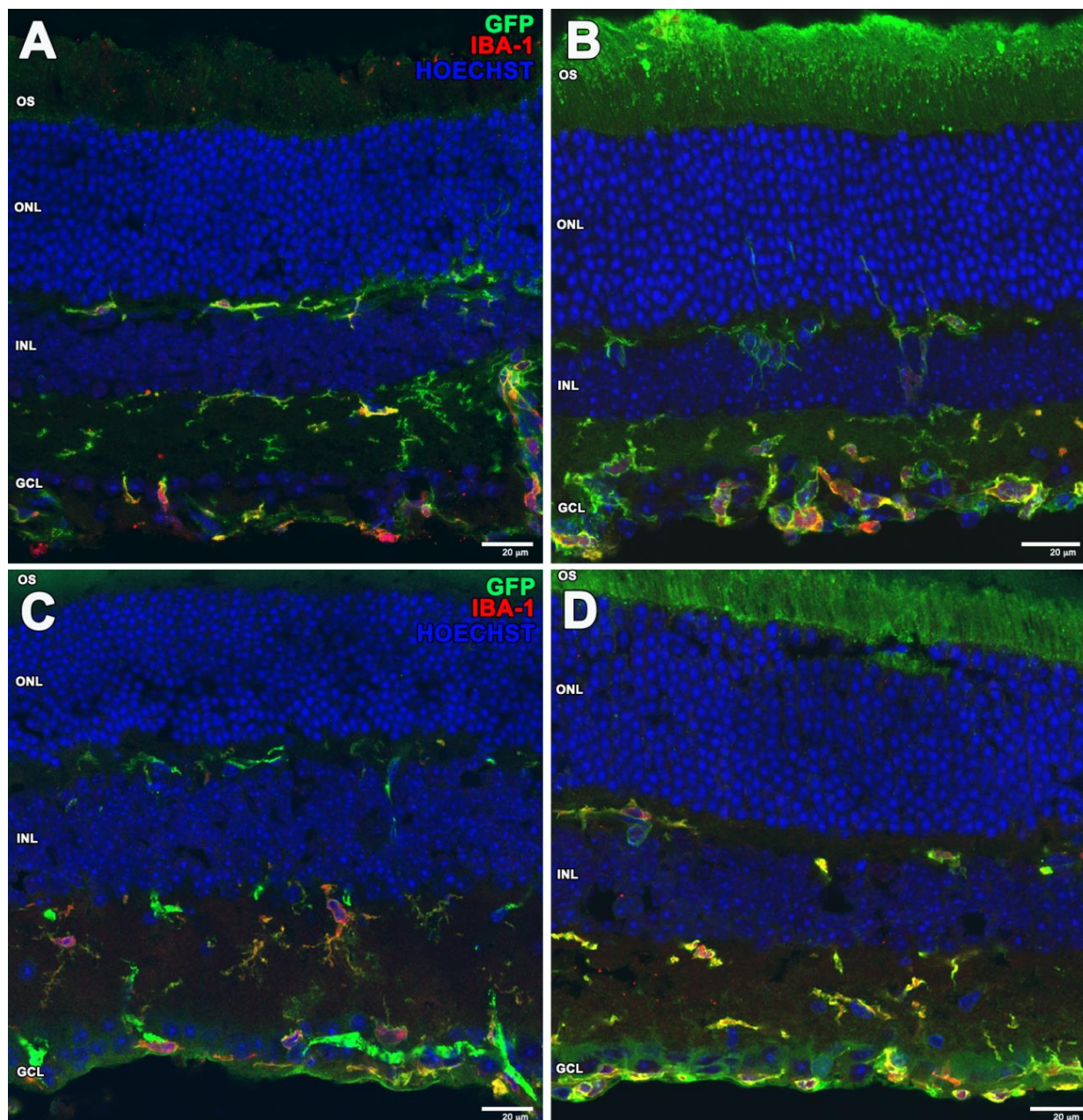


Figure 6. *In vivo* assays showing EGFP signal in rat retina after intravitreal (IV) (**A-C**) and subretinal (SR) (**B-D**) administration of freshly prepared (**A-B**) and 30 days stored (**C-D**) nanodiaplexes vectoring EGFP plasmid at 5/1 lipid/DNA ratio (w/w). Blue: Hoechst 33,342 (cell nuclei); Green: EGFP; Red: Iba-1. OS: outer segments; ONL: outer nuclear layer; INL; inner nuclear layer; GCL: ganglion cell layer. Scale bar: 20 μ m.

3. Discussion

The high versatility of non-viral vectors relies on the large variety of available nanomaterials and preparation methods that can be employed. Among the wide plethora, NDs have been recognized as powerful tools to increase the transfection efficiency of many non-viral vector systems due to their unique physicochemical properties, including versatile surface chemistry and ease of functionalization, together with their high biocompatibility and low toxicity (Al Qtaish et al., 2022). In addition, NDs show a favourable particle distribution, being almost spherical in shape. Interestingly, they can also be easily functionalized with many chemical compounds, show a high surface area-to-volume ratio, and their production process can be easily scalable (Krüger et al., 2006; Liu et al., 2007). As NDs present low stability in suspension, their combination with niosome formulations could be necessary to provide enhanced stability, which is necessary for gene delivery applications. Therefore, in this work we combined NDs with a niosome formulation, based on a cationic lipid and non-ionic surfactant, obtaining a final formulation named nanodiasome in order to assess over time at several storage temperatures the stability of nanodiasomes compared with niosomes devoid of NDs. To evaluate the stability of the formulations, relevant physicochemical parameters that affect to the transfection process, along with biocompatibility and transfection efficiency studies were performed in *in vitro* and *in vivo* conditions.

The physicochemical characteristics constitute key parameters that determine the biological behaviour of the formulations, including their cellular internalization process, gene delivery efficiency and biocompatibility. In the present work, nanodiasomes showed a slightly higher mean particle size than niosomes at day 0, probably due to the incorporation of NDs as additional elements, which might have affected to the packing of the formulation. The lower dispersity values observed with nanodiasomes, indicated a more homogeneous particle size distribution for that formulation compared to the niosome formulation. Both formulations presented statistically relevant oscillations in their physicochemical parameters, especially after 30 days being stored at 25°C, suggesting that these parameters are better preserved if formulations are kept at 4°C rather than at higher temperatures. Hence, in general terms, it can be said that nanodiasomes are physicochemically more stable over time than niosomes. Therefore, NDs integration in the lipid structure of niosomes is involved in supplying higher stability to the formulation, probably

providing more rigidity, by affecting the arrangement of the lipid membrane and modifying the rheological and packing behaviour of the formulation (Sainz-Ramos et al., 2021).

After the evaluation of physicochemical properties, biological *in vitro* transfection studies were performed in HEK-293 cells. We found that cells transfected with nanodiaplexes presented higher cell viability values than the ones transfected with nioplexes, which suggests that the formulations based on nanodiasomes are better tolerated by these cells. These results are in accordance with the previously reported high biocompatibility and low toxicity of NDs (Krüger et al., 2006; Liu et al., 2007; Zhang et al., 2009). In addition, the gene delivery efficiency of nanodiaplexes was approximately 4-fold superior than the one of nioplexes, and this difference was maintained over time. The MFI values refer to the quantity of the expressed GFP protein, and also indicated a higher transfection capacity of nanodiaplexes over nioplexes. In this sense, it is noteworthy that the number of DNA copies per cell decreased progressively for nioplexes from day 15, while nanodiaplexes did not suffer any alteration in this parameter until day 30. Taken all together, this could suggest that the combination of NDs with niosomes enhances the stability of the formulation, achieving more consistent and successful transfection results over time. To better understand the differences observed between both formulations, we studied their cellular uptake at 0 and 30 days after being stored at 4°C. We found statistically relevant differences in the percentage of cellular uptake between both formulations, obtaining almost 100% of uptake with nanodiasomes and around 70% with nioplexes at both storage conditions, which could support the idea that NDs increase the rigidity of the niosome formulation, enhancing the cellular entry (Manzanares and Cena. 2020). This higher cellular uptake could in part explain the differences in transfection efficiency between the two formulations, but further aspects need also to be taken into account. Traditionally, cellular endocytosis of non-viral vectors is mediated through the endosomal pathway, which eventually leads to endosomal vesicles with an acidic environment and digestive enzymes (Agirre et al., 2015). In these vesicles, the DNA risks of being degraded before reaching the nucleus. Therefore, DNA endosomal escape becomes a key step in order to achieve successful gene delivery. In this sense, it has been reported that NDs are able to escape the endosome confinement by rupturing the vesicle membrane shortly after their cellular uptake (Chu et al., 2015), which would also contribute to justify the higher gene delivery efficiency of nanodiaplexes compared to nioplexes counterparts. In addition, further transfection assays in CNS cells, both

retinal and neuronal primary cells, confirmed effective transgene expression after transfection with both freshly prepared and 30 days stored nanodiaplexes.

Therefore, based on these results, we performed an *in vivo* assay in order to determine the gene delivery efficiency of fresh and 30 days stored nanodiaplexes in rat retina. Formulations were injected through intravitreal and subretinal routes, which are widely used into the clinic for the treatment of genetically based retinal disorders (Conley and Naash. 2010). In most cases, after intravitreal injection, ganglion cell layer of the retina shows high transgene expression levels (Farjo et al., 2006), which, for instance, could be interesting for the treatment of glaucoma, a highly prevalent inherited retinal disorder that causes blindness (Almasieh et al., 2012; Kachi et al., 2005). On the other hand, the more invasive subretinal route is useful for transfecting the outer layer of the retina (Almasieh et al., 2012; Kachi et al., 2005), which would be interesting to face retinal diseases related to mutations at the photoreceptors and the retinal pigment epithelium level, such as Leber's congenital amaurosis, Stargardt's disease or retinitis pigmentosa (Lipinski et al., 2013). In the present study, EGFP signal was found mainly in microglial cells. Such expression was also located in both, the inner and outer layers of the retina both after intravitreal and subretinal injection of nanodiaplexes, which suggest that this formulation is able to efficiently diffuse along the different retinal layers achieving high transgene expression at different levels, which would be relevant from the therapeutic point of view. In addition, results revealed high EGFP expression *in vivo* after the administration of 30 days stored formulation, indicating that the storage of the formulation at 4°C for 30 days does not affect its transfection efficiency.

4. Conclusions

Taken together, the main conclusions of the present work are that (i) nanodiasomes present higher mean particle size, lower dispersity and higher zeta potential values than niosomes, (ii) nanodiasomes preserve more constant their physicochemical parameters over time than niosomes and both formulations prefer low temperatures for storage, (iii) nanodiaplexes present an around 4-fold superior transfection efficiency than nioplexes, in terms of percentage of live transfected cells, although both maintain their transfection efficiency over time, (iv) nanodiaplexes are more efficiently uptaken by HEK-293 cells than nioplexes, (v) high gene delivery efficiency of nanodiaplexes is maintained over time in rat central nervous primary cell cultures and (vi) also *in vivo* after subretinal and intravitreal injection of nanodiaplexes in rat retina.

CRedit authorship contribution statement

Nuseibah AL Qtaish: Investigation, Methodology, Visualization, Writing- Original draft preparation. **Ilia Villate-Beitia:** Formal analysis, Visualization, Writing- Original draft preparation. **Idoia Gallego:** Formal analysis, Visualization, Writing- Review & Editing. **Gema Martínez-Navarrete:** Investigation, Visualization, Writing- Review & Editing. **Cristina Soto-Sánchez:** Investigation, Visualization, Writing- Review & Editing. **Myriam Sainz-Ramos:** Investigation, Writing- Review & Editing. **Eduardo Fernández:** Supervision, Writing- Review & Editing. **Gustavo Puras:** Conceptualization, Supervision, Project administration, Writing- Review & Editing. **José Luis Pedraz:** Conceptualization, Supervision, Project administration, Writing- Review & Editing, Funding acquisition

Declaration of competing interest

The authors declare no conflicts of interest.

Acknowledgements

This work was supported by the Basque Country Government (Consolidated Groups, IT1448-22 and by CIBER -Consortio Centro de Investigación Biomédica en Red- CB06/01/1028, Instituto de Salud Carlos III, Ministerio de Ciencia e Innovación. Authors wish to thank: ICTS “NANBIOSIS”, specifically the Drug Formulation Unit (U10) of the CIBER in Bioengineering, Biomaterials and Nanomedicine (CIBER-BBN) for the intellectual and technical assistance. Authors also thank SGIker (UPV/EHU) for technical and human support. Authors acknowledge Rocio Arranz, access to the cryoEM CNB-CSIC facility in the context of the CRIOMECORR project (ESFRI-2019-01-CSIC-16). I.V.B. thanks the University of the Basque Country (UPV/EHU) for the granted postdoctoral fellowship (call for the Specialization of Doctor Researcher Personnel of the UPV/EHU, grant reference: ESPDOC19/47). M.S.R. thanks the University of the Basque Country (UPV/EHU) for the granted pre-doctoral fellowship (PIF17/79).

References

Agirre M, Ojeda E, Zarate J, Puras G, Grijalvo S, Eritja R, et al. New Insights into Gene Delivery to Human Neuronal Precursor NT2 Cells: A Comparative Study between Lipoplexes, Nioplexes, and Polyplexes. *Mol Pharm* 2015;12:4056-4066.

Al Qtaish N, Gallego I, Paredes AJ, Villate-Beitia I, Soto-Sanchez C, Martinez-Navarrete G, et al. Nanodiamond Integration into Niosomes as an Emerging and Efficient Gene Therapy NanoplatforM for Central Nervous System Diseases. *ACS Appl Mater Interfaces* 2022.

Al Qtaish N, Gallego I, Villate-Beitia I, Sainz-Ramos M, Lopez-Mendez TB, Grijalvo S, et al. Niosome-Based Approach for In Situ Gene Delivery to Retina and Brain Cortex as Immune-Privileged Tissues. *Pharmaceutics* 2020; 12:10.3390/ pharmaceutics 12030198.

Al Qtaish N, Gallego I, Villate-Beitia I, Sainz-Ramos M, Martinez-Navarrete G, Soto-Sanchez C, et al. Sphingolipid extracts enhance gene delivery of cationic lipid vesicles into retina and brain. *Eur J Pharm Biopharm* 2021;169:103-112.

Alhaddad A, Adam MP, Botsoa J, Dantelle G, Perruchas S, Gacoin T, et al. Nanodiamond as a vector for siRNA delivery to Ewing sarcoma cells. *Small* 2011;7:3087-3095.

Almasieh M, Wilson AM, Morquette B, Cueva Vargas JL, Di Polo A. The molecular basis of retinal ganglion cell death in glaucoma. *Prog Retin Eye Res* 2012;31:152-181.

Alwani S, Kaur R, Michel D, Chitanda JM, Verrall RE, Karunakaran C, et al. Lysine-functionalized nanodiamonds as gene carriers: development of stable colloidal dispersion for in vitro cellular uptake studies and siRNA delivery application. *Int J Nanomedicine* 2016;11:687-702.

Bartelds R, Nematollahi MH, Pols T, Stuart MCA, Pardakhty A, Asadikaram G, et al. Niosomes, an alternative for liposomal delivery. *PLoS One* 2018;13:e0194179.

Bi Y, Zhang Y, Cui C, Ren L, Jiang X. Gene-silencing effects of anti-survivin siRNA delivered by RGDV-functionalized nanodiamond carrier in the breast carcinoma cell line MCF-7. *Int J Nanomedicine* 2016;11:5771-5787.

Chauhan S, Jain N, Nagaich U. Nanodiamonds with powerful ability for drug delivery and biomedical applications: Recent updates on in vivo study and patents. *J Pharm Anal* 2020;10:1-12.

Chen M, Zhang X, Man H, Lam R, Chow E, Ho D. Nanodiamond Vectors Functionalized with Polyethylenimine for siRNA Delivery . *The journal of physical chemistry letters* 2021;1 (21):3167-3171.

Chu Z, Miu K, Lung P, Zhang S, Zhao S, Chang HC, et al. Rapid endosomal escape of prickly nanodiamonds: implications for gene delivery. *Sci Rep* 2015;5:11661.

Conley SM, Naash MI. Nanoparticles for retinal gene therapy. *Prog Retin Eye Res* 2010;29:376-397.

Do HD, Couillaud BM, Doan BT, Corvis Y, Mignet N. Advances on non-invasive physically triggered nucleic acid delivery from nanocarriers. *Adv Drug Deliv Rev* 2019;138:3-17.

Edgington R, Spillane KM, Papageorgiou G, Wray W, Ishiwata H, Labarca M, et al. Functionalisation of Detonation Nanodiamond for Monodispersed, Soluble DNA-Nanodiamond

Conjugates Using Mixed Silane Bead-Assisted Sonication Disintegration. *Sci Rep* 2018;8:728-017-18601-6.

Farjo R, Skaggs J, Quiambao AB, Cooper MJ, Naash MI. Efficient non-viral ocular gene transfer with compacted DNA nanoparticles. *PLoS One* 2006;1:e38.

Ginn SL, Amaya AK, Alexander IE, Edelstein M, Abedi MR. Gene therapy clinical trials worldwide to 2017: An update. *J Gene Med* 2018;20:e3015.

Grijalvo S, Puras G, Zarate J, Sainz-Ramos M, Qtaish NAL, Lopez T, et al. Cationic Niosomes as Non-Viral Vehicles for Nucleic Acids: Challenges and Opportunities in Gene Delivery. *Pharmaceutics* 2019;11:10.3390/pharmaceutics11020050.

Ibraheem D, Elaissari A, Fessi H. Gene therapy and DNA delivery systems. *Int J Pharm* 2014;459:70-83.

Kachi S, Oshima Y, Esumi N, Kachi M, Rogers B, Zack DJ, et al. Nonviral ocular gene transfer. *Gene Ther* 2005;12:843-851.

Krüger A, Liang Y, Jarrea G, Stegka J. Surface functionalisation of detonation diamond suitable for biological applications. *Journal of Materials Chemistry* 2006;16:2322-2328.

Lim DG, Prim RE, Kim KH, Kang E, Park K, Jeong SH. Combinatorial nanodiamond in pharmaceutical and biomedical applications. *Int J Pharm* 2016;514:41-51.

Lim DG, Rajasekaran N, Lee D, Kim NA, Jung HS, Hong S, et al. Polyamidoamine-Decorated Nanodiamonds as a Hybrid Gene Delivery Vector and siRNA Structural Characterization at the Charged Interfaces. *ACS Appl Mater Interfaces* 2017;9:31543-31556.

Lipinski DM, Thake M, MacLaren RE. Clinical applications of retinal gene therapy. *Prog Retin Eye Res* 2013;32:22-47.

Liu KK, Cheng CL, Chang CC, Chao JI. Biocompatible and detectable carboxylated nanodiamond on human cell. *Nanotechnology* 2007;18(32):325102.

Manzanares D, Cena V. Endocytosis: The Nanoparticle and Submicron Nanocompounds Gateway into the Cell. *Pharmaceutics* 2020;12:10.3390/pharmaceutics12040371.

Mashal M, Attia N, Martinez-Navarrete G, Soto-Sanchez C, Fernandez E, Grijalvo S, et al. Gene delivery to the rat retina by non-viral vectors based on chloroquine-containing cationic niosomes. *J Control Release* 2019;304:181-190.

Mashal M, Attia N, Puras G, Martinez-Navarrete G, Fernandez E, Pedraz JL. Retinal gene delivery enhancement by lycopene incorporation into cationic niosomes based on DOTMA and polysorbate 60. *J Control Release* 2017;254:55-64.

Mashal M, Attia N, Soto-Sanchez C, Martinez-Navarrete G, Fernandez E, Puras G, et al. Non-viral vectors based on cationic niosomes as efficient gene delivery vehicles to central nervous system cells into the brain. *Int J Pharm* 2018;552:48-55.

Ojeda E, Puras G, Agirre M, Zarate J, Grijalvo S, Eritja R, et al. The influence of the polar head-group of synthetic cationic lipids on the transfection efficiency mediated by niosomes in rat retina and brain. *Biomaterials* 2016;77:267-279.

Ojeda E, Puras G, Agirre M, Zarate J, Grijalvo S, Eritja R, et al. The role of helper lipids in the intracellular disposition and transfection efficiency of niosome formulations for gene delivery to retinal pigment epithelial cells. *Int J Pharm* 2016;503:115-126.

Puras G, Martinez-Navarrete G, Mashal M, Zarate J, Agirre M, Ojeda E, et al. Protamine/DNA/Niosome Ternary Nonviral Vectors for Gene Delivery to the Retina: The Role of Protamine. *Mol Pharm* 2015;12:3658-3671.

Riley MK, Vermerris W. Recent Advances in Nanomaterials for Gene Delivery-A Review. *Nanomaterials (Basel)* 2017;7:10.3390/nano7050094.

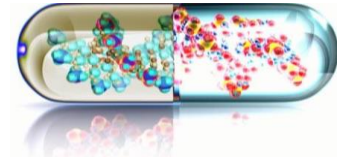
Sainz-Ramos M, Villate-Beitia I, Gallego I, Al Qtaish N, Menendez M, Lagartera L, et al. Correlation between Biophysical Properties of Niosomes Elaborated with Chloroquine and Different Tensioactives and Their Transfection Efficiency. *Pharmaceutics* 2021;13:10.3390/pharmaceutics13111787.

Shahryari A, Saghaeian Jazi M, Mohammadi S, Razavi Nikoo H, Nazari Z, Hosseini ES, et al. Development and Clinical Translation of Approved Gene Therapy Products for Genetic Disorders. *Front Genet* 2019;10:868.

Suzuki Y, Hyodo K, Tanaka Y, Ishihara H. siRNA-lipid nanoparticles with long-term storage stability facilitate potent gene-silencing in vivo. *J Control Release* 2015;220:44-50.

Zhang XQ, Chen M, Lam R, Xu X, Osawa E, Ho D. Polymer-functionalized nanodiamond platforms as vehicles for gene delivery. *ACS Nano* 2009;3:2609-2616.

Chapter 4



RESUMEN

La terapia génica comenzó en la década de 1980, debido al conocimiento de que la función de los organismos está controlada por la información transportada por los genes. La terapia génica es un procedimiento médico que tiene como objetivo agregar, eliminar o modificar genes para tratar enfermedades. De hecho, los defectos genéticos pueden producir enfermedades y cambiar los genes, cambia la forma en que una célula produce proteínas. En otras palabras, la terapia génica le da a la célula nuevo conjunto de instrucciones para cambiar la cantidad o el tipo de proteína que produce. Las categorías de terapia génica se pueden dividir en dos grupos: terapia génica de línea germinal; y terapia génica somática. La diferencia entre estas dos categorías es que los genes de terapia génica somática se insertan en células diana, pero el cambio no se transmite a la siguiente generación, en el tratamiento de los genes de terapia génica de línea germinal, se transmite su cambio a la próxima generación. Mediante el uso de la terapia génica, los científicos pueden hacer una de varias cosas, dependiendo del problema que se encuentra. La modificación genética puede incluir: adición, delección, reemplazamiento y reparación o regulación de un gen en una persona, con fines de alterar las propiedades biológicas de células vivas para su uso terapéutico.

La terapia génica se puede utilizar para modificar células dentro o fuera del cuerpo. Cuando esto se hace dentro del cuerpo, el médico inyecta el vector portador del gen directamente en la parte del cuerpo donde se encuentran las células defectuosas (*in vivo*), donde la edición de genes de las células del paciente se realiza mediante la introducción de genes terapéuticos directamente en el órgano defectuoso. La terapia génica, que se utiliza para modificar células fuera del cuerpo (*ex vivo*), implica la transferencia de genes a células viables que se remueven temporalmente del cuerpo, que luego se reintroducen en el cuerpo. Se puede obtener sangre, médula ósea u otros tejidos del paciente y se pueden aislar tipos específicos de células en un laboratorio. El vector que contiene el gen deseado se introduce en estas células, se permite que las células se multipliquen en el laboratorio y luego se vuelven a inyectar en el paciente para que continúen multiplicándose, produciendo finalmente el efecto deseado.

Para insertar nuevos genes directamente en las células, los científicos utilizan una herramienta conocida como vector diseñado para expresar el gen. Los vectores son responsables de asegurar la estabilidad de los genes y de superar todas las barreras biológicas hasta llegar a su destino: el núcleo de la célula, donde tiene lugar la regulación génica. Existen dos grandes grupos de vectores: virales y no virales. Los virus tienen la capacidad inherente de transferir genes a las

células, por lo que pueden usarse como vectores. Sin embargo, antes de que el virus pueda usarse para administrar terapia génica en células humanas, debe modificarse para eliminar su capacidad de causar enfermedades infecciosas. Debido a los riesgos que plantean los vectores virales, se han desarrollado otras estrategias. Los métodos fisicoquímicos no tienen limitaciones en el tamaño del transgén y no presentan riesgo biológico, aunque son menos efectivos. Sin embargo, el vector no viral más utilizado para el desarrollo de nuevas estrategias terapéuticas. Los vectores no virales utilizan métodos físicos o químicos para introducir material genético en las células. Los métodos comunes de transfección física incluyen electroforesis, hidroporación, ultrasonido, biotecnología, micro/nanoinyección y láser/optoinyección. Estos métodos suelen utilizar la fuerza física para cruzar la barrera de la membrana celular y así facilitar el transporte de ácidos nucleicos al interior de la célula. Los métodos químicos utilizan materiales naturales o sintéticos que son compatibles con el cuerpo humano, por lo que la capacidad de generar una respuesta inmunitaria es baja. Estos incluyen moléculas de lípidos, polímeros y nanopartículas.

Los sistemas de administración de genes deben ser capaces de superar las barreras biológicas para estar activos en el sitio de acción. Para los sistemas de administración de genes *ex vivo*, solo los obstáculos intracelulares pueden limitar su rendimiento final. Mientras que en el caso de la experimentación *in vivo*, el proceso de entrega al sitio de acción también puede verse afectado por barreras extracelulares adicionales. La vía de administración y el órgano a tratar pueden tener un gran impacto en la eficacia del tratamiento. Para que los vectores lleguen a su objetivo, deben superar los obstáculos de las barreras biológicas que se interponen en su camino. Las primeras barreras son extracelulares como aclaramientos rápidos, interacciones no específicas con proteínas y células y degradación por parte de enzimas. Por otra parte, las plaquetas tienen cargas superficiales negativas, lo que permite interacciones electrostáticas con vectores catiónicos. La activación del sistema inmunitario es otra barrera extracelular más a tener en cuenta. Aunque la activación inmunitaria se ha relacionado en común con los vectores virales, se ha demostrado que algunos vectores no virales también pueden producir una respuesta inmunológica. Además, el tiempo necesario para alcanzar concentraciones terapéuticas mediante el proceso de transfección puede ser aún más difícil si el objetivo es órgano inmunoprivilegiado como el cerebro o los ojos. Las nanopartículas deben cruzar de manera eficiente la barrera hematoencefálica y la barrera hematorretiniana para llegar a las células diana en el cerebro y el ojo, respectivamente.

Una vez se han cruzado las barreras extracelulares, las biomacromoléculas necesitan alcanzar a nivel citoplasmático o incluso nuclear. Las nanopartículas deben tener características biológicas y físicas apropiadas para mejorar la captación celular por las membranas citoplasmáticas. Durante la internalización celular, se pueden destacar cuatro vías principales: endocitosis mediada por clatrina (CME), endocitosis mediada por caveolas (CvME), macropinocitosis y fagocitosis. Después de la internalización celular, el escape endosomal es esencial, antes de la fusión de los endosomas con los lisosomas, para evitar la degradación de los vectores.

Comprender las unidades estructurales básicas de los niosomas puede ayudar a determinar qué sustancias pueden formar niosomas y cómo se pueden cargar los fármacos en los niosomas. Los niosomas son nanotransportadores vesiculares con capacidad de autoensamblaje y estructura en bicapa, las cabezas hidrofílicas están orientadas hacia una solución acuosa, mientras que las cabezas hidrofóbicas están orientadas hacia una solución orgánica, por lo tanto, las niosomas pueden administrar fármacos tanto hidrofóbicos como hidrofílicos. Los niosomas son una alternativa adecuada a los liposomas. La estructura química de los niosomas ofrece ventajas frente a los ampliamente utilizados liposomas, dando lugar a la generación de formulaciones más estables, menos citotóxicas y con menor coste de producción. Los niosomas están compuestos por tres componentes principales: un lípido catiónico, un surfactante no iónico y un componente auxiliary (Figura 1).

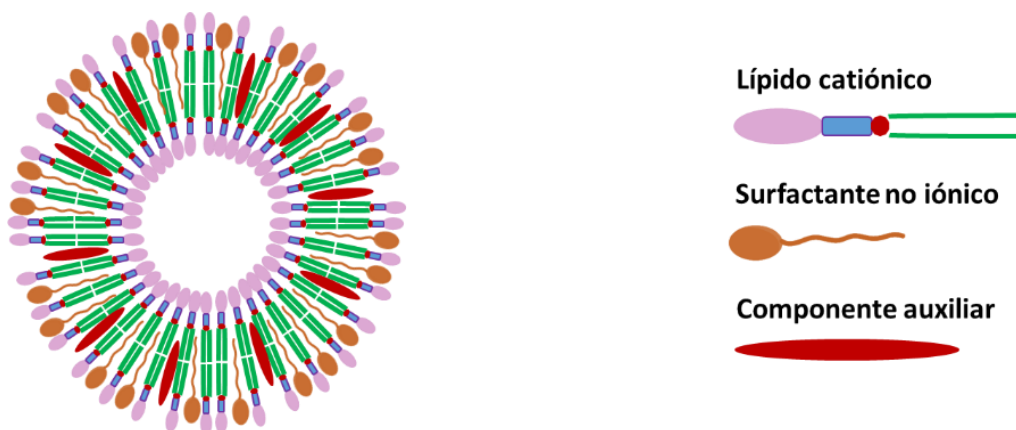


Figura 1. Esquema general de la estructura de los niosomas.

El lípido catiónico como el 1,2-di-O-octadecenil-3-trimetilamonio propano (DOTMA) es el responsable de las interacciones electrostáticas con las cargas negativas de los grupos fosfato

del material genético, lo que permite que los ácidos nucleicos formen complejos con los niosomas catiónicos. El surfactante no iónico como el polisorbato 20 es necesario para estabilizar las emulsiones, evitando la formación de agregados de partículas. Así, la sustitución de los fosfolípidos por surfactante no iónico en los niosomas, mejora notablemente su estabilidad, al mismo tiempo que reduce su citotoxicidad. Por último, la incorporación de un componente auxiliar como esfingolípidos o nanodiamantes, a la formulación de niosomas ha demostrado mejorar sus propiedades físico-químicas, aumentan la fluidez y la estabilidad de la membrana y promueven los procesos de transfección. Sin embargo, las diferentes modificaciones químicas de cada uno de los componentes influyen en las propiedades fisicoquímicas de los lípidos resultantes.

Los avances en nanomedicina ofrece nuevas oportunidades para el desarrollo y uso de vectores no virales, como los niosomas, para tratar enfermedades tanto de la retina como del cerebro. Teniendo en cuenta esta información, el objetivo principal de esta tesis doctoral es la incorporación de nuevos compuestos como componente "auxiliar" a las formulaciones y la selección del método más adecuado para la elaboración de niosomas, así como una extensa caracterización biofísica, *in vitro* e *in vivo*, lo que permite nuevas posibilidades y oportunidades para mejorar el tratamiento de diversas enfermedades mediante el uso de una estrategia de terapia génica. Para la elaboración de niosomas existen varios métodos. La técnica de emulsión aceite en agua (o/w) es uno de los métodos más utilizados.

Todas las formulaciones de niosomes en el presente trabajo se elaboraron a través de la técnica de emulsión de aceite en agua (o/w), posteriormente, evaporar el solvente orgánico y obtener las nanopartículas en solución acuosa. En esta tesis doctoral se utilizaron los siguientes reactivos químicos: El lípido catiónico empleado fue DOTMA, el cual se disolvió en la fase orgánica. Se eligió el polisorbato 20 como surfactante no iónico. Como componentes "auxiliares", utilizamos esfingolípidos y nanodiamantes en nuestras formulaciones. La composición de cada formulación en esta tesis se muestra en la tabla 1. El material genético utilizado en el estudio para obtener los complejos fue el plásmido reportero codificante para la proteína verde fluorescente (pEGFP).

Componentes Formulaciones	Lípido catiónico	Sufactante no iónico	Componentes "auxiliares"	
	DOTMA	Polisorbato 20	Esfingolípidos	Nanodiamantes
Niosomas	✓	✓		
Niosfingosomas	✓	✓	✓	
Nanodiasomas	✓	✓		✓

Tabla 1: Resumen de los componentes de las formulaciones empleados en los estudios experimentales.

En el primer trabajo experimental comparamos dos formulaciones de vectores compuestos por el mismo lípido catiónico y surfactante no iónico, pero con o sin esfingolípidos como componente "auxiliar", lo que dio como resultado niosfingosomas o niosomas, respectivamente. Es importante evaluar ambas formulaciones para determinar el efecto de la adición del componente "auxiliar" en el sistema de administración de genes. Tanto las formulaciones como los complejos correspondientes, obtenidos mediante la adición del plásmido reportero pEGFP, fueron caracterizadas y evaluadas. En comparación con las niosomas, las niosfingosomas y los complejos correspondientes disminuyeron el tamaño de las partículas y aumentaron la carga superficial. Aunque no hubo diferencias significativas en la captación celular, la viabilidad celular y la eficiencia de transfección aumentaron cuando las células ARPE-19 se expusieron a niosfingoplexes. La endocitosis vía caveolas disminuyó en el caso de los niosfingoplexes, que mostraron una mayor colocalización con el compartimento lisosomal y propiedades de escape endosomal. Además, los niosfingoplexes transfectaron no solo células primarias del sistema nervioso central, sino también diferentes células en la retina del ratón y la corteza cerebral. Estos resultados preliminares sugieren que los nioesfingosomas representan una formulación de vector no viral prometedora destinada al tratamiento de enfermedades tanto de la retina como del cerebro.

En el segundo experimento, se incorporaron nanodiamantes como componente "auxiliar" en formulaciones de niosomas para evaluar sus capacidades biofísicas como sistema de administración de genes para aplicaciones terapéuticas en enfermedades del sistema nervioso central. Los nanodiamantes son materiales prometedores para la entrega de genes debido a sus características fisicoquímicas y biológicas únicas. Las dos formulaciones con o sin nanodiamantes como componente "auxiliar", que dieron como resultado nanodiasomas o niosomas,

respectivamente fueron evaluadas. Los nanodiasomas, niosomas y sus correspondientes complejos, obtenidos tras la adición de material, se evaluaron en términos de propiedades fisicoquímicas, eficiencia de transfección en células HEK-293, captación celular, internalización celular y estudios en células primarias neuronales y retinales. Los nanodiasomas, niosomas y complejos cumplían las características fisicoquímicas para aplicaciones de terapia génica. Biológicamente, la incorporación de los nanodiamantes en los niosomas mejoró la eficiencia de transfección a valores superiores al 90 % de un 75 %, acompañada de una mayor captación celular. El análisis de internalización celular mostró una mayor endocitosis a través de clatrina en nanodiaplexes en comparación con nioplexes, seguida de una mayor colocación lisosomal, que coexistía con propiedades de escape endosomal, mientras que la endocitosis mediada por caveolas fue la vía más eficiente en el caso de nioplexes. Además, los estudios en células primarias revelaron que los nanodiaplexes transfectaron con éxito células primarias neuronales y retinales. Este estudio señala que la integración de los nanodiamantes en niosomas representa una nanoplataforma no viral para el tratamiento de enfermedades mediante terapia génica.

Por último, los nanodiasomas y los niosomas también se utilizaron en el tercer trabajo experimental para estudiar su estabilidad durante el tiempo. Se evaluó el efecto de la incorporación de nanodiamantes en formulaciones de niosomas a lo largo del tiempo (0, 15 y 30 días) y a diferentes temperaturas de almacenamiento (4°C y 25°C). Las formulaciones y los compuestos fueron evaluadas a lo largo del tiempo en términos de características fisicoquímicas, internalización celular, viabilidad celular y eficiencia de transfección tanto *in vitro* como *in vivo*. Todos estos parámetros se analizaron a diferentes temperaturas de almacenamiento durante 30 días. Los principales descubrimientos revelaron que la incorporación de nanodiamantes en las formulaciones de niosomas resultó en un aumento de 4 veces en la eficiencia de la transfección *in vitro* y que esta diferencia se mantuvo a lo largo del tiempo. Además, los nanodiasomas mantuvieron sus parámetros fisicoquímicos más constantes que los niosomas. Ambas formulaciones fueron más estables a bajas temperaturas de almacenamiento. Finalmente, los nanodiasomas pudieron alcanzar altos niveles de expresión transgénica en células primarias e *in vivo*. La eficiencia de los nanodiaplexes se mantuvo a lo largo del tiempo en cultivos de células del sistema nervioso central de rata y también *in vivo* después de la inyección subretiniana e intravítrea de nanodiaplexes en retina de ratón.

En resumen, el desarrollo de la nanomedicina ha abierto oportunidades para el desarrollo y mejora de vectores no virales como los niosomas, para el tratamiento de varias enfermedades, utilizando el método basado en la terapia génica. La incorporación de nuevos compuestos a las formulaciones y seleccionar el método más adecuado para la elaboración de niosomas, con una extensa caracterización biofísica y su evaluación *in vitro* e *in vivo*, pueden abrir nuevas posibilidades y oportunidades para mejorar el tratamiento de diversas enfermedades mediante el uso de una estrategia de terapia génica.